ELIN MARIA SOARES DE FIGUEIREDO

A STUDY ON METALLURGY AND CORROSION OF ANCIENT COPPER-BASED ARTEFACTS FROM THE PORTUGUESE TERRITORY

LISBOA
2010

nº de arquivo
“copyright”

ELIN MARIA SOARES DE FIGUEIREDO

A STUDY ON METALLURGY AND CORROSION OF ANCIENT COPPER-BASED ARTEFACTS FROM THE PORTUGUESE TERRITORY

Dissertação apresentada para a obtenção do Grau de Doutor em Conservação e Restauro, especialidade Ciências da Conservação, pela Universidade Nova de Lisboa, Faculdade de Ciências e Tecnologia

LISBOA
2010

Acknowledgments

I would like to express my gratitude and sincere thanks to my supervisors M. Fátima Araújo (*Instituto Tecnológico e Nuclear*, ITN) and Rui J.C. Silva (*Faculdade de Ciências e Tecnologia – Universidade Nova de Lisboa*, FCT-UNL) for giving me the opportunity to be involved in the study of ancient metals, particularly to participate in the project Metallurgy and Society in Late Bronze Age Central Portugal (METABRONZE), as well as for the general supervision of my PhD project. I'm also grateful to João C. Senna-Martinez (*Faculdade de Letras – Universidade de Lisboa*, FL-UL), the METABRONZE project coordinator.

Thanks are also due to all the people and institutions that provided items for study and guided me thought the contextual interpretation of them, namely: João C. Senna-Martinez (UNIARQ-FL-UL and *Associação Terras Quentes*) for the *Fraga dos Corvos* artefacts; João C. Senna-Martinez and João L. Inês Vaz (*Universidade Católica*) for the *Baiões/Santa Luzia* cultural group artefacts; Ana A. Melo, Luís Raposo and Ana Isabel Santos (*Museu Nacional de Arqueologia*) for the *Pragança* artefacts; Raquel Vilaça (*Faculdade de Letras – Universidade de Coimbra*) for the *Medronhal* artefacts; Mário V. Gomes (*Faculdade de Ciências Sociais e Humanas* – UNL) for the *Escoural* artefacts; and Miguel Pessoa (*Museu da Villa Romana do Rabaçal*) for the *Penela* spear-head.

I would also like to thank all my colleagues from ITN, CENIMAT/I3N-FCT-UNL and DCR-FCT-UNL, for all the exchange of ideas, knowledge and interesting discussions, which contributed to the development of this work. Special thanks are to Pedro Valério, M. João Furtado, António M. Monge Soares and Francisco M. Braz Fernandes, with whom I worked in close collaboration numerous times.

Special thanks are also due to my family and close friends, for all the support and companionship.

Finally, I'm grateful for the following financial supports:

- PhD grant (SFRH/BD/27358/2006) awarded by the Portuguese Foundation for Science and Technology (FCT-MCTES) for the period of 2007-2010;
- METABRONZE grant (2006) and project funded by FCT-MCTES (POCTI/HAR/58678/2004) for the period of 2006-2009;
- International Conference Attending grant awarded by the *Fundação Calouste Gulbenkian* for the attendance of the conference "Archaeometallurgy in Europe" in 2007;
- and CENIMAT/I3N-FCT-UNL funding by FCT-MCTES for the attendance of the conference "V International Materials Symposium" in 2009.

Resumo

Nesta tese de doutoramento foram estudados artefactos metálicos de diversas tipologias e vários restos de produção metalúrgica provenientes de vários sítios arqueológicos do território Português, cobrindo um período cronológico de cerca de 3 milénios, desde o Calcolítico à Idade do Ferro. Grande parte dos materiais estudados provêm de colecções museológicas emblemáticas, tais como as do Castro de Pragança e de Baiões. Com este estudo pretendeu-se obter uma perspectiva geral da metalurgia antiga do território oeste peninsular, assim como informação pormenorizada da metalurgia em cada sítio arqueológico. Pretendeu-se também efectuar uma apreciação da corrosão dos metais arqueológicos, nomeadamente das ligas de bronze (Cu-Sn). Para tal foram efectuadas análises elementares e microestruturais utilizando vários métodos analíticos, tais como a espectrometria de fluorescência de raios X dispersiva de energias (FRX), micro-FRX, microscopia óptica e electrónica de varrimento.

Os principais resultados do estudo da corrosão demonstraram que a decuprificação é o principal fenómeno de corrosão dos bronzes arqueológicos, mas que o fenómeno inverso, o da destanificação, poderá ocorrer em casos particulares. Foi também verificado que estes fenómenos podem ter uma influência muito significativa nos resultados das análises elementares superficiais efectuadas por FRX, devido à espessura das camadas de corrosão, que podem atingir os 500 μm. Foi observado que a corrosão interna, nomeadamente a intergranular, pode ser muito pronunciada nos artefactos com uma microestrutura mais heterogénea, ou seja, naqueles menos sujeitos a trabalhos termo-mecânicos. Adicionalmente, foram relatadas particularidades da corrosão a longo prazo, como a corrosão selectiva das fases α ou δ e a presença de cobre metálico redepositado nas zonas de corrosão mais internas.

Os principais resultados do estudo arqueometalúrgico demonstraram que durante o período Calcolítico foram utilizados cobres bastante puros, com a excepção do elemento As, sendo que durante o Bronze Final o bronze binário com teores relativamente constantes de estanho (média de ~13% Sn) e com ocasionais impurezas de Pb, As e Sb se tenha tornado dominante, passando o cobre a ser utilizado esporadicamente em artefactos onde se pretenderia um aproveitamento das suas propriedades particulares. Ao contrário de outras regiões do ocidente Europeu, os bronzes ternários parecem surgir tardiamente, já durante a Idade do Ferro. A moldagem dos artefactos maiores e de formas mais complexas (p. ex. pontas de lança, machados, anéis fechados) seria feita em molde sendo aplicados apenas alguns trabalhos termo-mecânicos de acabamento, enquanto que os objectos mais pequenos (p. ex. cinzéis, punções, fíbulas simples, anéis abertos) seriam fabricados a partir de pré-formas obtidas em molde, como barras, através de trabalhos termo-mecânicos por vezes muito intensos.

Abstract

In the present thesis metallic artefacts of various typologies and diverse materials related to metallurgical operations were studied. The items are from various sites in the Portuguese territory, covering a period of circa 3 millennia, from Chalcolithic to Iron Age. A large part of the studied items belong to emblematic museum collections, as the *Castro de Pragança* and the *Baiões* ones. The aim of the present study is to provide a general view of the ancient metallurgy in the Western territory of the Iberian Peninsula, as well as detailed information on the metallurgy of each archaeological site. It was also aimed an evaluation of the corrosion of archaeological metals, namely bronzes (Cu-Sn alloys). Accordingly, elemental analysis and microstructural examinations were made, combining diverse analytical techniques as energy dispersive X-ray fluorescence spectrometry (EDXRF), micro-EDXRF, optical microscopy and scanning electron microscopy.

The main results of the corrosion study showed that decuprification is the main corrosion phenomena among the bronzes, but that destannification can also occur in particular cases. It was found that these phenomena can have a major influence in the results of superficial EDXRF elemental analysis, mainly due to the thickness of the corrosion layers that can reach 500 μm. It was also found that the most internal corrosion, namely the intergranular corrosion, can be very pronounced among the artefacts with a heterogeneous microstructure, i.e. mainly among those that were less subjected to thermo-mechanical processing. Additionally, particular long-term corrosion phenomena were described, as the preferential corrosion of α or δ phase and the presence of redeposited metallic copper in the most internal corrosion regions.

The main results of the archaeometallurgical study showed that during the Chalcolithic period relatively pure coppers were used (with exception for the presence of As), and that during Late Bronze Age binary bronze with relatively constant tin contents (average of ~13 wt.% Sn) and impurities as Pb, As and Sb was the main material used, being unalloyed copper only used sporadically to produce particular items where the properties of this metal were an advantage. Differing from other Western European regions, ternary bronzes seem to have a later appearance, i.e. during Iron Age. The shaping of large and more complex artefacts (e.g. spear heads, axes, closed rings) was done in the mould, being needed just some final thermo-mechanical processing. On the other hand, smaller and simpler items (e.g. chisels, awls, simple fibulae, open rings) were produced by shaping pre-defined forms, as cast bars, through thermo-mechanical processes that could be very intense, as those that include various cycles of deformation and annealing.

Symbols and Notations

BA	Bronze Age
BCS	British Chemical Standards
BF	Bright Field (in OM observations)
BSE	Backscattered secondary emission (in SEM-EDS analysis)
CA	Copper Age
CCB	Centro Cultural de Belém
CENIMAT	Centro de Investigação em Materiais
CSG	Castro de Nossa Senhora da Guia de Baiões
CSR	Crasto de São Romão
DAS	(Secondary) Dendritic Arm Spacing
DCM	Departamento de Ciências dos Materiais
DCR	Departamento de Conservação e Restauro
DF	Dark Field (in OM observations)
EBA	Early Bronze Age
EIA	Early Iron Age
ESC	Povoado do Escoural
EDXRF	Energy Dispersive X-Ray Fluorescence
FC	Fraga dos Corvos
FCT	Faculdade de Ciências e Tecnologia
FCT-MCTES	Fundação para a Ciência e Tecnologia – Ministério da Ciência, Tecnologia e Ensino Superior
FD	Figueiredo das Donas
I3N	Instituto de Nanoestruturas, Nanomodelação e Nanofabricação
IA	Iron Age
IP	Iberian Peninsula
IPA	Instituto Português de Arqueologia
IUPAC	International Union of Pure and Applied Chemistry
ITN	Instituto Tecnológico e Nuclear
LBA	Late Bronze Age
MBA	Middle Bronze Age
MED	Medronhal
METABRONZE	Metallurgy and Society in Late Bronze Age Central Portugal (project)
MNA	Museu Nacional de Arqueologia
OM	Optical Microscopy
Pol	Polarized (in respect to OM observations)
PR	Castro de Pragança

QAA	Grupo de Química Analítica e Ambiental (ITN)
RH	Relative Humidity
SAM	Studien zu den Anfängen der Metallurgie (project)
SE	Secondary Electron (in SEM-EDS analysis)
SEM-EDS	Scanning Electron Microscopy – Energy Dispersive Spectroscopy
SL	Santa Luzia
UNL	Universidade Nova de Lisboa
VHN	Vickers Hardness Number
VNSP	Vila Nova de São Pedro
XRD	X-Ray Diffraction
ZAF	(Z) atomic number, (A) absorption and (F) fluorescence matrix effects (in SEM-EDS elemental analysis)

Index of contents

Index of figures

Chapter 1 – Materials and Methods

Chapter 2 – Corrosion Study

Chapter 3 – Archaeometallurgical Study

Postscript – Promoting Science&Heritage

Appendix

Index of tables

Chapter 1 – Materials and Methods

Chapter 2 – Corrosion Study

Chapter 3 – Archaeometallurgical Study

Appendix

Preamble

Part of this thesis was carried out in the framework of the project METABRONZE (Metallurgy and Society in Late Bronze Age Central Portugal, POCTI/HAR/58678/2004) financed by the Portuguese Science Foundation (FCT-MCTES). The main goals associated with that project were (1) the study and evaluation of the metallurgy and society of the Late Bronze Age period in Central and Northern Portugal, through elemental and microstructural characterisation of artefacts and metallurgical remains, (2) the re-enforcement of the scientific and technical quality of human resources in the archaeometric field in Portugal, through the realization of PhD and other investigation programs, and (3) the promotion of cooperation among various national institutions and international personalities. The studies presented in this work on the *Baiões/Santa Luzia* cultural group, *Pragança* and *Fraga dos Corvos* sites are part of this project. Studies on metals and metallurgical remains from other Portuguese sites, as *Escoural*, *Medronhal* and *Penela* are part of the archaeometallurgical studies that ITN and CENIMAT/I3N have conducted in close relationship with various archaeologists and national institutions.

All the work presented in this thesis has been developed in the following research centres:

- *Grupo de Química Analítica e Ambiental* (QAA), *Instituto Tecnológico e Nuclear* (ITN), Estrada Nacional 10, 2686-953 Sacavém, Portugal;
- *Centro de Investigação em Materiais/Instituto de Nanoestruturas, Nanomodelação e Nanofabricação* (CENIMAT/I3N) and *Departamento de Ciências dos Materiais* (DCM), *Faculdade de Ciências e Tecnologia*, *Universidade Nova de Lisboa*, 2829-516 Caparica, Portugal;
- *Departamento de Conservação e Restauro* (DCR), *Faculdade de Ciências e Tecnologia*, *Universidade Nova de Lisboa*, 2829-516 Caparica, Portugal.

List of published work

Part of the content of this thesis has been published and presented in scientific meetings.

Peer-reviewed papers (in ISI Web of Knowledge):

- E. Figueiredo, R.J.C. Silva, F.M.B. Fernandes, M.F. Araújo **(2010)** Some long term corrosion patterns in archaeological metal artefacts. *Materials Science Forum* 636-637, 1030-1035.
- E. Figueiredo, R.J.C. Silva, J.C. Senna-Martinez, M.F. Araújo, F.M.B. Fernandes, J.L. Inês Vaz **(2010)** Smelting and recycling evidences from the Late Bronze Age habitat site of Baiões (Viseu, Portugal). *Journal of Archaeological Science* 37, 1623-1634.
- E. Figueiredo, R.J.C. Silva, M.F. Araújo, J.C. Senna-Martinez **(2010)** Identification of ancient gilding technology and Late Bronze Age metallurgy by EDXRF, Micro-EDXRF, SEM-EDS and metallographic techniques. *Microchimica Acta* 168, 283-291.
- E. Figueiredo, J.C. Senna-Martinez, R.J.C. Silva, M.F. Araújo **(2009)** Orientalizing Artifacts from Fraga dos Corvos Rock Shelter in North Portugal. *Materials and Manufacturing Processes* 24, 949-954.
- A.A. Melo, E. Figueiredo, M.F. Araújo, J.C. Senna-Martinez **(2009)** Fibulae from an Iron Age site in Portugal. *Materials and Manufacturing Processes* 24, 955-959.
- R.J.C. Silva, E. Figueiredo, M.F. Araújo, F. Pereira, F.M. Braz Fernandes **(2008)** Microstructure Interpretation of Copper and Bronze Archaeological Artefacts from Portugal. *Materials Science Forum* 587-588, 365-369.
- E. Figueiredo, P. Valério, M.F. Araújo, J.C. Senna-Martinez **(2007)** Micro-EDXRF surface analyses of a bronze spear head: Lead content in metal and corrosion layers. *Nuclear Instruments and Methods in Physics A* 580, 725-727.
- E. Figueiredo, M. F. Araújo, R. Silva, F. M. Braz Fernandes, J. C. Senna-Martinez, J. L. Inês Vaz **(2006)** Metallographic studies of copper based scraps from the Late Bronze Age Santa Luzia archaeological site (Viseu, Portugal). In: R. Fort, M.Alvarez de Buergo, M. Gomez-Heras, C. Vazquez-Calvo (Eds.), *Heritage, Weathering and Conservation*, Taylor and Francis, London, Vol. I, pp. 143-149 (ISBN 978-0-415-40150-0).

Others:

- E. Figueiredo, M.F. Araújo, R.J.C. Silva, A ponta de lança da gruta da nascente do Algarinho (Penela) no contexto da metalurgia do Bronze Final. In: Proceedings of the International Meeting on the Application of Science and New Technologies to Archaeology in the Roman Villa of Rabaçal, Penela, Portugal (July 2009), ***in press.***

- E. Figueiredo, P. Valério, M.F. Araújo, R.J.C. Silva, M.V. Gomes **(2010)** Estudo analítico de vestígios metalúrgicos do povoado do Escoural (Évora, Portugal). In: J.A. Pérez Macias and E. Romero Bomba (Eds.), IV Encontro de Arqueologia del Suroeste Peninsular, *Collectanea* 145, Universidad de Huelva Publicaciones, Spain (CD-ROM) (ISBN 978-84-92679-59-1).
- E. Figueiredo, M.F. Araújo, R.J.C. Silva, J.C. Senna-Martinez (**2007**) Corrosion of bronze alloy with some lead content: implications in the archaeometallurgical study of Late Bronze Age metal artefacts from "Fraga dos Corvos" (North Portugal). In: C. Degrigny, R. van Langh, I. Joosten, B. Ankersmit (Eds.), *METAL 07 (ICOM-CC) Proceedings*, Amsterdam (Set 2007), Vol. I, pp. 61-66.
- E. Figueiredo, A.A. Melo, M.F. Araújo, Micro-EDXRF study of four Iron Age fibulae from Castro de Pragança (Portugal): use of bronze and iron in different components. Poster presented in TECHNART (Lisbon) **2007.**
- F. Geirinhas, M.Gaspar, J.C. Senna-Martinez, E. Figueiredo, M.F. Araújo, R.J.C. Silva, Copper isotopes on artifacts from Fraga dos Corvos First Bronze Age habitat site and nearby Cu occurrences: an approach on metal provenance. In: Proceedings V Congresso Internacional - Mineração e Metalurgia Históricas no Sudoeste Europeu, León, Spain (Jun 2008), ***in press.***

In the works where I appear as first author I had the main responsibility of the scientific planning, execution (including analysis and interpretation), evaluation, and writing. As co-author, I had an active participation on different parts of the scientific work, their discussion and writing. All the activities were performed in close collaboration with my PhD supervisors.

General Introduction

Once metal was recognised as a new material in pre-historical times metallic artefacts began to be produced at an increasing rate and the metallurgical skills started to develop. In the Old World, the early use of metals is such important evidence that chronological periods have been named after the main metal that was being processed: “Copper Age”, “Bronze Age” and “Iron Age”.

The study of ancient metallurgy (archaeometallurgy) has proven to be an important tool in the study of past spheres of interaction, as well as in the construction of a history of technology. The first archaeometallurgical studies involving Portuguese materials were made by the end of the 19th century, to prove the use of copper before bronze. Posterior studies were only performed half a century later to study the type of metal recovered in the Chalcolithic site of *Vila Nova de São Pedro* (VNSP) (Paço, 1955). It was not until the 1960´s and 70’s in the framework of the project *Studien zu den Anfängen der Metallurgie* (SAM) developed by researchers of the Stuttgart University on early metals of the European territory, that a large number of elemental analyses were performed on Chalcolithic and Early Bronze Age (3rd and first half of the 2nd millennium BC) artefacts from various Portuguese sites, giving a first global approach on early metallurgy (Junghans et al., 1960, 1964, 1974). In this large-scale project more than 22000 elemental analyses by optical emission spectroscopy (atomic emission spectroscopy) were produced and published, of which nearly 1700 from the Iberian Peninsula, and about 1000 from Southern and Central Portugal. The main goal of the project was to trace sources and trade routes based on the trace element pattern in the artefacts that should be kept unchanged from ore to metal during the extraction process. This goal was not completely achieved, in part due to the complexity in metallurgical extraction processes that can influence the trace element contents and in part due to the complexities of ores, that can show disperse trace patterns even among a small geographical area. Additionally, the possibility of recycling would create more difficulties in distinguishing clear trace element patterns. Despite these problems, the published data constitutes one of the most important data bases on ancient metals in Europe, and is still able to provide general trends in trace element patterns among different European regions. During the 1960´s and 70´s, with the rapid development of electronics that allowed the development of new analytical techniques for elemental analysis based on physical interactions, non-destructive analysis became available for application in the heritage field. The introduction of such analytical techniques, namely energy dispersive X-ray fluorescence spectrometry (EDXRF) in some Portuguese research institutions during the 1970’s and 80’s, marked a new stage with sporadic elemental analyses being performed by diverse national researchers on various artefacts, comprising a larger time span – from pre-historical to historical times (e.g. Araújo et al., 1993; Cabral et al., 1979; Gil et al., 1989; Seruya and Carreira, 1994; Soares et al., 1994).

Despite the extending data on elemental composition of ancient artefacts from the Portuguese territory, metallographic studies were very rare (e.g. Paço, 1955; Soares et al. 1996), contrasting with the

numerous studies that were performed in the neighbouring Spanish territory in the framework of the project *Arqueometalurgia de la Península Ibérica* (going on since the 1980's) which has given a vital contribution for the study of ancient Iberian manufacturing techniques (e.g. Rovira and Gómez Ramos, 2003).

Systematic elemental and metallographic studies on ancient metals from the Portuguese territory have only begun very recently, from 2000 onwards, with the emergence of a working group composed by researchers and students of national institutions, namely the *Instituto Tecnológico e Nuclear* (ITN), *Centro de Investigação em Materiais*, *Faculdade de Ciências e Tecnologia*, *Universidade Nova de Lisboa* (CENIMAT/I3N-FCT-UNL) and *Departamento de Conservação e Restauro*, *Faculdade de Ciências e Tecnologia*, *Universidade Nova de Lisboa* (DCR-FCT-UNL). The formation of such a group has relied on various joint factors. The emergence of a higher degree in Conservation and Restoration at the FCT-UNL by the end of the 1990´s (i.e. 1998) has shown to be a key factor for the union of different speciality researchers around heritage studies, and an investment in early formation on both science and history fields. This has provided adequate synergies between diverse researchers and also a national availability of students with adequate scientific background and cultural sensitivities to perform scientific studies involving cultural heritage. By 2000, a protocol *Investigação em Arqueometria* between the Portuguese Archaeological Institute (*Instituto Português de Arqueologia*, IPA) and ITN gave rise to the development of joint archaeometric studies, providing a link between archaeologists and analytical researchers. Among these, various archaeometallurgical studies were performed in the framework of the sub-area *Caracterização de metais e ligas metálicas Pré-históricas* (responsible researcher: M.F. Araújo), namely: *A Metalurgia do Penedo do Lexim na Plataforma Litoral a Norte da Serra de Sintra* (responsible archaeologist: A.C. Sousa); *Indígenas e Fenícios no Almaraz* (responsible archaeologist: L. de Barros); *Caracterização de um conjunto de artefactos metálicos do Castro de Pragança* (responsible archaeologist: A.A. Melo); and *Caracterização das produções metalúrgicas do grupo Baiões/Santa Luzia (Bronze Final)* (responsible archaeologists: J.C. Senna Martinez and J.L. Inês Vaz). The last project gave rise to the METABRONZE project (2006-2010), the first archaeometallurgical project totally financed by the Portuguese Science Foundation involving the working group previously introduced. Generally, since 2000, the group dedicated to archaeometallurgical issues has been growing, as well as studies and publications on ancient metals from the Portuguese territory, hoping to provide a solid and long-lasting platform on ancient metallurgical studies in the Portuguese territory.

Besides providing relevant information on ancient technologies, the study of ancient metallurgy is an perfect opportunity to provide detailed information on corrosion processes. Besides sharing many experimental methodologies, corrosion and archaeometallurgical studies find many contact points, as the study and interpretation of one helps in the other. In its turn, the study of corrosion can provide relevant information to the conservation field, as it can offer a better understanding of the state of conservation of the objects, providing useful guide lines to proper conservation conducts.

In fact, the close contact among Conservation Science and Archaeometallurgy has recently been outlined by the Metal Working Group of ICOM-CC (International Council of Museums – Conservation Committee) with the creation of a sub-working group BAC: Bridging Archaeometry and Conservation (Degrigny, 2007). To prove its adequacy, the Metal WG 2007 Meeting (in Amsterdam) had as first theme "When archaeometry and conservation meet", which experienced large attendance, predicting regular and profitable works linking the two fields.

In the present work, elemental and microstructural characterisation of ancient metallic artefacts is the main axis for the study of ancient technological features and for the study of long-term corrosion of archaeological metals. A more in-depth understanding of these materials and their long-term degradation will in turn enable a better approach to cultural heritage, namely to the understanding of ancient technologies and to the conservation of ancient metals. In this work an evaluation of metallurgical techniques carried out over a period of circa 3 millennia was performed, to attain the metal composition over time, the thermo-mechanical operations involved in the production of various artefacts, and to provide some highlights on ancient metallurgical extraction techniques. Also, an evaluation on the long-term corrosion of ancient copper-based metals was performed to attain the state of preservation of the artefacts, study some specificities of long-term corrosion on copper based artefacts, evaluate the implications of the corrosion on the general artefact composition, and better adjust the experimental methodologies.

As a result, the present thesis has been organised into two main sections: the Archaeometallurgical Study and the Corrosion Study. Before these two sections a brief chapter introducing the materials studied and the analytical procedures will be presented, Chapter 1 – Materials and Methods. Next, the study on the long-term corrosion is going to be presented first, Chapter 2 – Corrosion Study, since it has strong influence in the interpretation of the analytical results and in the archaeometallurgical study. Here, the main results on long-term corrosion features are going to be presented, as well as a discussion of the influence of corrosion in the analytical study aided by some selected case-studies. The last and following chapter, Chapter 3 – Archaeometallurgical Study, is the longest and has been organized following the artefacts provenance (Portuguese regions and archaeological sites) as a consequence of the diversity of materials collected in each site, the large number of sites, and their different chronologies. Here, elemental and microstructural specificities of the artefacts in each site are being presented, and particularities are discussed in order of appearance. Both main chapters (Chapter 2 and 3) begin with a specific introduction and finish with a converging discussion where the principal conclusions are presented. At the end of the thesis a general conclusion of the study is presented, with some suggestions for future research.

Chapter 1 - Materials and Methods

1.1 Materials – brief introduction to the artefacts and sites

A general introduction to the artefacts and provenance sites is presented here to introduce the type of metallurgical remains and the chronological periods involved in the present study. In Chapter 3 – Archaeometallurgical Study, the various sites and artefacts are presented individually in more detail, and previous studies on some of the collections are also reported.

For the present work circa 200 items from various sites in the Portuguese territory (**Fig. 1.1**) were subjected to analysis. The items include metallic artefacts and fragments, and other metallurgical remains as crucibles, vitrified fragments, slags, moulds, etc. (**Table 1.1**). Most of the metallic artefacts are fragments of artefacts, such as bars and other leftovers, which were chosen for analysis due to their lower display value in museums, which allowed the dislocation for study during longer periods of time and facilitated the application of some invasive analytical procedures (this subject is further developed in the next section 1.2.1 – Introduction and experimental design). Also, fragments of artefacts and other leftovers can reveal different stages of metallurgical processes that are not evident in the study of finished artefacts. Additionally, regarding corrosion studies it is not significant if the studied items are finished artefacts or metal scraps.

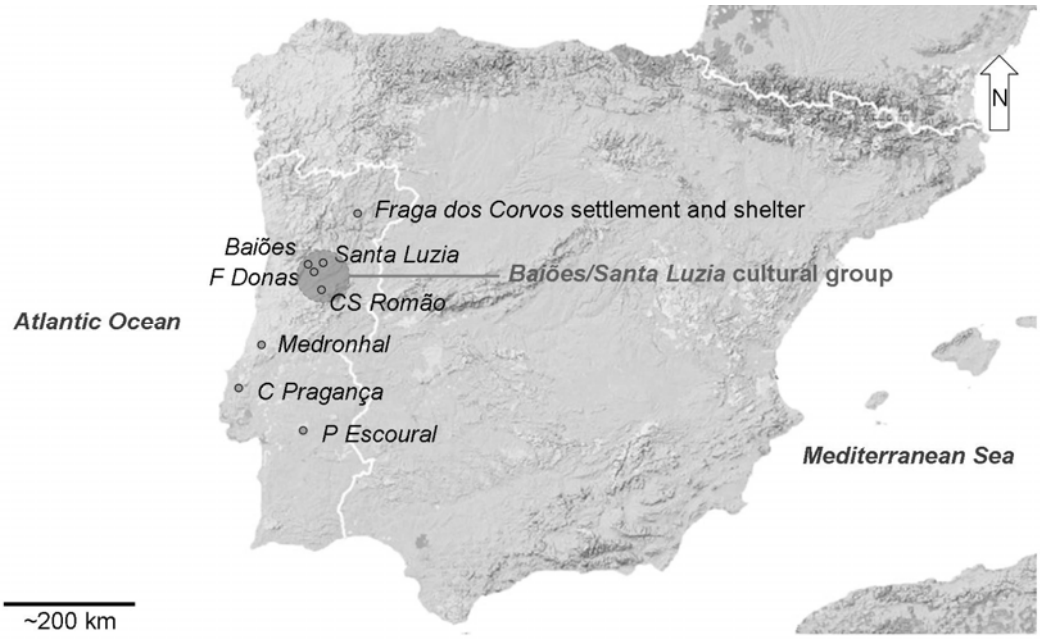

Fig. 1.1 Iberian Peninsula with approximate location of the main sites studied in this work (Portuguese territory outlined in white).

The sites from which the studied items were collected are representative of various chronological periods, ranging from Chalcolithic to Iron Age (**Table 1.2**). Most of them have metals and metallurgical remains from only one period, except for *Castro de Pragança*, which has metals and metallurgical remains covering a very large time span, from Chalcolithic to the Roman period.

Table 1.1 Number and type of items studied in the present work

Sites		Metallic artefacts	Metallic nodules	Slag fragments	Crucible fragments	Moulds	Others	**Total**
ESC	*Povoado do Escoural*	1	1	1	7		~10	**~20**
PR	*Castro de Pragança*	52	9	(9)	1		9	**71**
MED	*Medronhal*	37						**37**
CSG	*Baiões*	19	12	1				**32**
SL	*Santa Luzia*	10						**10**
FD	*Figueiredo das Donas*	8						**8**
CSR	*Crasto de São Romão*	4			1		1	**6**
FC	*Fraga dos Corvos* (settlement)	5	3		2		~20	**~30**
FC	*Fraga dos Corvos* (shelter)	12	1					**13**
	Others	7				1		**7**
	Total	**155**	**26**	**2**	**11**	**1**	**~30**	**225**

Table 1.2 Period and chronological occupation of the sites from which the artefacts were collected. Since duration of different periods can vary accordingly to regional cultural spheres, the table presents an simple organization with estimated chronologies

Sites		CA (~3000-2000 BC)	1st BA(EBA+MBA)* (~2000-1250 BC)	LBA+1st IA** (~1250-550 BC)	2nd IA (~5th c. BC onwards)
ESC	*Povoado do Escoural*				
PR	*Castro de Pragança*				
MED	*Medronhal*				
CSG	*Baiões*				
SL	*Santa Luzia*				
FD	*Figueiredo das Donas*				
CSR	*Crasto de São Romão*				
FC	*Fraga dos Corvos* (settlement)				
FC	*Fraga dos Corvos* (shelter)				

CA – Copper Age; BA – Bronze Age; EBA – Early Bronze Age; MBA – Middle Bronze Age; LBA – Late Bronze Age; IA – Iron Age
* The term 1st Bronze Age has been adopted due to the cultural continuity that is observed in the archaeographic record in Central and Northern Portuguese territory during the periods that correspond to EBA and MBA in other regions.
** The transition from Late Bronze Age to Iron Age happens first in the south of the Iberian Peninsula with the beginning of the Orientalising period – a consequence of the presence of Phoenicians in the southern coasts. In the Northern Iberian regions the Orientalising influences are not as evident as in the South; therefore, in the North the LBA continues until the mid-first millennium BC and after that the region enters directly to the 2nd Iron Age.

Generally, most of the studied artefacts are related to the Late Bronze Age (LBA) period and are from the Central and Northern Portuguese territories. This chronological period has not been studied in the framework of the SAM project, and posterior national investigations have shown that by LBA these regions seem to have had a flourishing and characteristic metallurgy that is worth investigating.

1.2 Methods

1.2.1 Introduction and experimental design

Multidisciplinary studies involving chemical and physical analytical techniques applied to cultural objects are one of the most significant happenings in the last century that has contributed enormously to the understanding of past societies, ancient technologies, the use of early materials and their degradation processes. Fields as archaeometry and conservation science are a product of such happening and are continuously growing.

Various analytical techniques are being applied to very different cultural materials (e.g. Creagh, 2005), and among them, non-invasive and non-destructive analyses, in the sense that no sample is taken and that most inorganic specimens are not altered by the analytical procedure, are frequently favoured (e.g. Adriens, 2005; Mantler and Schreiner, 2001). Nevertheless, due to specific characteristics of some analytical techniques, e.g. surface analyses in energy dispersive X-ray fluorescence spectrometry (EDXRF) or particle induced X-ray emission (PIXE) (Guerra, 1995), and due to the chemical

alteration of the surface in many cultural objects (e.g. most metals) and general heterogeneous composition in some artefacts, surface preparation or sampling is often needed to provide reliable quantitative data.

Amongst the wide variety of modern analytical techniques that are employed in the study of metals (some examples in Artioli, 2007; De Ryck et al., 2003; Doménech-Carbó et al., 2008; Grolimund et al., 2004; Thornton et al., 2002), EDXRF and scanning electron microscopy with energy dispersive analysis (SEM-EDS) for elemental analyses, and SEM and optical microscopy (OM) for microstructural studies, are well established techniques (some examples in Ferrer Eres et al., 2008; Gimeno Adelantado et al., 2003; Giumlia-Mair, 2005; Ingo et al., 2006; Kienlin et al., 2006). Both EDXRF, either in its conventional form or as micro-EDXRF, and SEM-EDS can be described as non-destructive (i.e. respecting the physical integrity of the material/object) or micro-invasive (i.e. in the sense that sampling or cleaning of a small surface is frequently required), multielemental, relatively fast and versatile, allowing average compositional information but also local information of small areas (Janssens et al., 2000). The SEM-EDS and OM are able to provide a wide range of information on metallurgical features and conservation state of the objects, and the metallographic approach can be considered easy to apply, not expensive, a flexible and adaptable research tool (Pinasco et al., 2007).

In this work, due to the cultural and historic significance of the studied artefacts, their complex structures and frequent altered state, the selection of analytical techniques and experimental procedures was done cautiously, balancing the type of information provided and the minimum physical and chemical alteration on the objects. Also, the analytical techniques were chosen considering their regular availability, their facility in use, their “low cost” (to be able to perform a high number of analyses), and their complementary character to provide relevant data.

In general, the experimental methodology employed in the present study followed a 3 stage procedure:
[1] primary elemental evaluation by EDXRF without any previous surface preparation;
[2] determination of metal composition through micro-EDXRF in prepared areas;
[3] and a microstructural study by OM in prepared areas.

Some items were also studied by SEM-EDS to evaluate inclusions, intermetallic compounds, corrosion, and other special features. A slag fragment was also analysed by X-ray diffraction (XRD). Digital X-ray radiography was also performed in some artefacts that were not submitted to invasive analyses to aid the study of the manufacturing techniques. In **Fig. 1.2**, a scheme of the analytical design is shown.

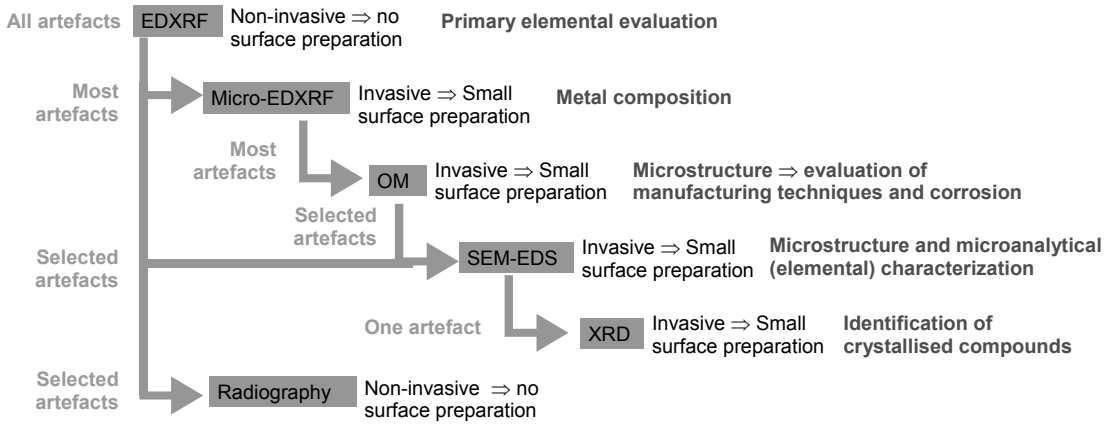

Fig. 1.2 Analytical design employed in the study of the artefacts.

1.2.2 EDXRF

Conventional EDXRF analyses were performed, at a first stage, on all the items over two different areas, whenever possible. These analyses were done with no surface preparation. Regarding the metallic items the analysis allowed an evaluation of the type of metal (e.g. identification of alloying elements and impurities), and allowed the identification of any special features such as the presence of composite objects (e.g. the gilded copper nail CSR-3000 from *Crasto de São Romão*, section 3.3.3.4). In the case of other metallurgical related items, such as crucibles, moulds and vitrified fragments, it allowed an evaluation of their use in ancient metallurgical operations through the presence of specific elements related with ancient metallurgy.

The analyses were conducted in a Kevex 771 spectrometer installed at ITN, that is composed by a rhodium anode X-ray tube with six secondary targets and filters that can be selected to optimize the primary photon beam, and a liquid nitrogen cooled Si(Li) detector with a resolution of 175 eV at 5.9 keV (Mn-Kα). The equipment has a chamber with a rotating 16-position sample tray (**Fig. 1.3**) and also a fix tray that allows analyses in relatively large size items. The spot size of the analysed area can reach up to ~7 cm^2. Artefacts were irradiated using two different monochromatic X-ray beams, generated by a Gd secondary target (using a tube voltage of 57 kV and 1 mA current intensity) and a Ag secondary target (using a tube voltage of 35 kV and 0.5 mA current intensity), both during 300 s, to detect a variety of characteristic X-ray peaks of the metallic elements (e.g. K lines of Fe, Cu and As, and L lines of Au and Pb with the Ag secondary target, and K lines of Sn and Sb with the Gd secondary target). Due to the characteristics of the EDXRF analysis elements with an atomic number <12 (Mg) are not detected.

Elemental concentrations were determined through the EXACT computer program, based upon a fundamental parameter method that uses calibration coefficients and accounts for matrix effects (Van Grieken and Markowicz, 1993). Calibration was performed with the certified reference material Phosphor Bronze 551 Spectrographic Standard from British Chemical Standards (BCS), using a single calibration coefficient for each element.

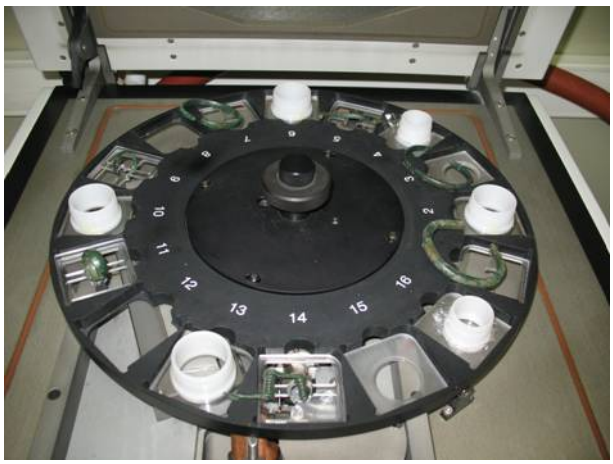

Fig. 1.3 Kevex 771 chamber (EDXRF) with artefacts from *Medronhal* placed in the rotating 16-position sample tray.

To determine the accuracy of the analytical technique another certified reference material (Phosphor Bronze 553 from BCS) was analysed. The results are shown in **Table 1.3**, being the accuracy generally better than 5% for major and minor elements. The quantification limits were also determined according to the International Union of Pure and Applied Chemistry (IUPAC, 1978) and are presented in **Table 1.4**. Due to the frequent presence of Pb and As in ancient metals and due to the interference between the strongest lines of Pb (Lα) and As (Kα), the quantification limit calculated for Pb (0.10%) was adopted as the quantification limit for As.

Table 1.3 EDXRF analysis of Phosphor Bronze 553 from BCS (accuracy calculated as ((certificated content–obtained content)/certificated content) ×100)

wt. %	Cu	Sn	Pb	Zn	Fe	Ni
Certified	87.0	10.8	0.47	0.49	0.056	0.44
Obtained	88.7	11.0	0.46	0.50	0.059	0.46
Accuracy	2.0	1.6	2.1	2.0	5.4	4.5

Table 1.4 Quantification limits for EDXRF analysis (calculated as 10×(background)½ /sensitivity)

Cu	Sn	Pb	As	Sb	Fe	Ni
0.04%	0.02%	0.10%	0.10%	0.02%	0.05%	0.07%

Since the analyses were made directly over the irregular, heterogeneous corroded surfaces of artefacts, the results were interpreted as semi-quantitative. This issue is going to be discussed in more detail in section 2.3 – Influence of corrosion in the analytical study.

1.2.3 Micro-EDXRF

Micro-EDXRF analyses were performed in most metal artefacts to determine the alloy composition. According to the characteristics of each object, analyses were performed either in sampled sections (few cases) or in a small cleaned area free from the superficial corrosion layers (most cases). These areas were afterwards metallographically prepared for microstructural examination by OM or SEM-EDS (see next sections 1.2.4 and 1.2.5).

The micro-EDXRF analyses were performed in an ArtTAX Pro spectrometer installed at DCR-FCT-UNL (**Fig. 1.4**), which comprises: a low-power X-ray tube with a molybdenum anode; a set of polycapillary lens that generate a microspot of ~70 µm in diameter of primary radiation; an integrated CCD camera and three beam-crossing diodes that provide the control over the exact position on the sample to be analysed; and a silicon drift electro-thermally cooled detector with a resolution of 160 eV at Mn-Kα (Bronk et al., 2001). Artefacts were analysed using 40 kV, 0.5 mA and 100 s of tube voltage, current intensity and live time respectively, and three analyses were made on different spots of each prepared area being considered the average value.

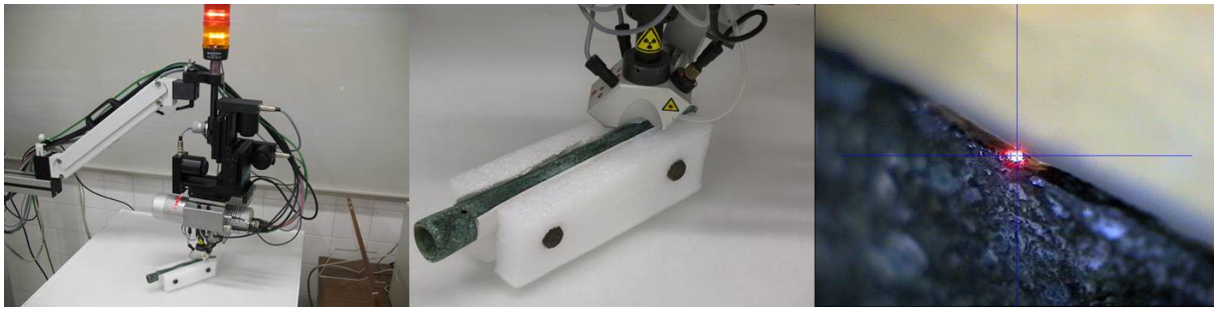

Fig. 1.4 Analysis of the *Penela* spear-head in the ArtTAX Pro spectrometer (micro-EDXRF).

Quantitative analysis was made using the WinAxil software that uses the fundamental parameter method and experimental calibration factors that were calculated with the certified reference material Phosphor Bronze 551 Spectrographic Standard from BCS.

To determine the accuracy of the analytical technique another certified reference material (Phosphor Bronze 553 from BCS) was analysed. The results are shown in **Table 1.5**, being the accuracy better than 5% for the major elements and better than 20% for minor elements. The quantification limits were also determined according to IUPAC (1978) and are presented in **Table 1.6**. Due to the frequent presence of Pb and As in ancient metals and due to the interference between the strongest lines of Pb (Lα) and As (Kα), the quantification limit adopted for As (0.10%) was (under)estimated as similar to the quantification limit determined for Pb.

Table 1.5 Micro-EDXRF analysis of Phosphor Bronze 553 from BCS (average± one standard deviation for 3 spot analyses) (accuracy calculated as ((certificated content–obtained content)/certificated content) ×100)

wt. %	Cu	Sn	Pb	Zn	Fe	Ni
Certified	87.0	10.8	0.47	0.49	0.056	0.44
Obtained	87.73±0.06	10.53±0.06	0.56±0.07	0.58±0.01	0.050±0.001	0.51±0.01
Accuracy	0.8	2.5	19.1	18.4	10.2	15.9

Table 1.6 Quantification limits for micro-EDXRF analysis (calculated as 10×(background)½ /sensitivity)

Cu	Sn	Pb	As	Fe	Ni
0.04%	0.5%	0.10%	0.10%	0.05%	0.07%

1.2.4 OM and Metallographic preparation

Microstructural observations by optical microscopy (OM) were performed in most of the metallic artefacts (exceptions are mainly the *Pragança* and the *Figueiredo das Donas* collections). The examinations were conducted in the previous sampled sections or in the small cleaned areas free of corrosion.

Most of the sampled artefacts were small bars, which were sampled so that their cross-section could be analysed. Samples were cold-mounted in a mould with a metallographic preparation resin that allows the recovery of the samples after the study. All the mounted samples were first ground with SiC abrasive paper from 240 to the 2400 grit size and then polished with a diamond suspension in a rotary polishing wheel until one-quarter micron diamond size.

All the small cleaned areas were metallographically prepared by a manual polish with diamond suspension in a cotton swab until 1 micron diamond size (**Fig. 1.5**). This procedure allowed the observation of the microstructure on selected superficial areas of complex shaped and aesthetical significant artefacts, with a minimum invasive procedure.

Fig. 1.5 Preparation of surfaces in the *Penela* spear-head for micro-EDXRF analysis and microstructural observation by OM.

The OM observations were conducted in a Leica DMI5000M microscope installed at CENIMAT/I3N-FCT-UNL. This microscope is coupled to a computer with the LAS V2.6 software which allows the collection of digital images at different z-positions that can be combined into one single sharp composite image that effectively extends the depth-of-focus of the image. This feature helped the observation of the small manually polished areas which have varying levels of roughness. Additionally, since the microscope has inverted lenses, it allowed the examination of large size artefacts without the need of sampling (**Fig. 1.6**).

The microstructure examinations were made in bright field (BF), dark field (DF) and polarized light (Pol) with the surface in as-polished state. The DF observations had the particularity of revealing topographical details, such as pores, and the Pol observations allowed a first approach in the identification of some corrosion compounds due to their specific vivid colours under this type of observation (see Appendix VI – Some properties of elements and compounds). After these observations, etching of the surfaces was performed with an aqueous ferric chloride solution to reveal microstructural features as grain boundaries, annealing twins and slip bands among the grains.

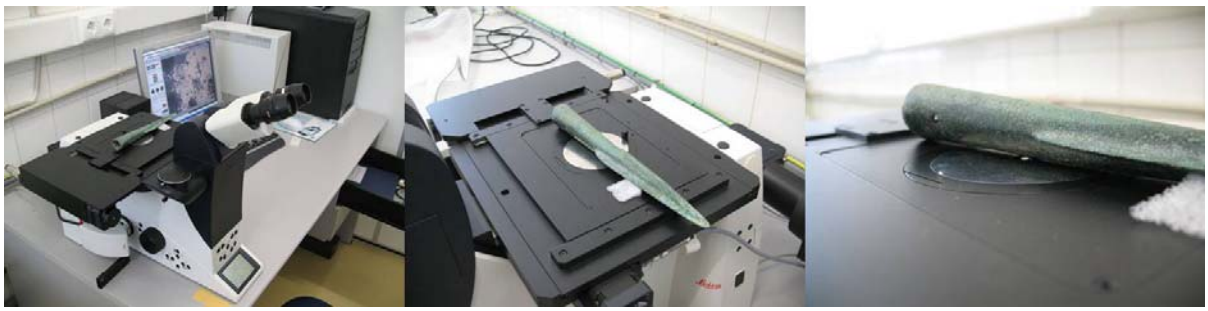

Fig. 1.6 Microstructure observation of prepared surfaces in the *Penela* spear-head by OM (Leica equipment).

1.2.5 SEM-EDS

SEM-EDS analyses were performed on some selected items to aid the identification of common phases and inclusions in the beginning of the study, and later to study particular features of some microstructures.

The SEM analyses were performed in a Zeiss model DSM 962 equipment installed at CENIMAT/I3N-FCT-UNL, which has backscattered electrons (BSE) and secondary electrons (SE) imaging modes and an energy dispersive spectrometer (EDS) from Oxford Instruments model INCAx-sight with an ultra-thin window able to detect low atomic number elements as oxygen and carbon. Semi-quantifications were made using a ZAF correction procedure.

Mounted samples were analysed with a gold coating or with a carbon tape bridge. Examination of non-mounted items (CSG-315; CSG-327; CSR-3000; MED-03; MED-30) was made with only a contact of copper and/or carbon conductive tape from one extreme of the prepared surface to the ground, which also ensured the right positioning of the items (**Fig. 1.7**). Experimental conditions were regularly: 20 kV of voltage; approximately 3 A of filament current; 25 mm of work distance; and 70 μA of emission current.

Fig. 1.7 Preparation of a bracelet fragment from *Medronhal* for SEM-EDS analysis and its placement in the Zeiss model DSM 962 equipment chamber.

1.2.6 XRD

XRD analyses were performed on a slag fragment (CSG-315) to support SEM-EDS observations and supply complementary crystalline phase identification.

The XRD analysis was conducted in a Siemens D5000 diffractometer, with Cu (Kα) radiation, installed at CENIMAT/I3N-FCT-UNL. For this analysis the fragment was positioned in such a way that the cut cross-section could be analysed, without any previous preparation (**Fig. 1.8**).

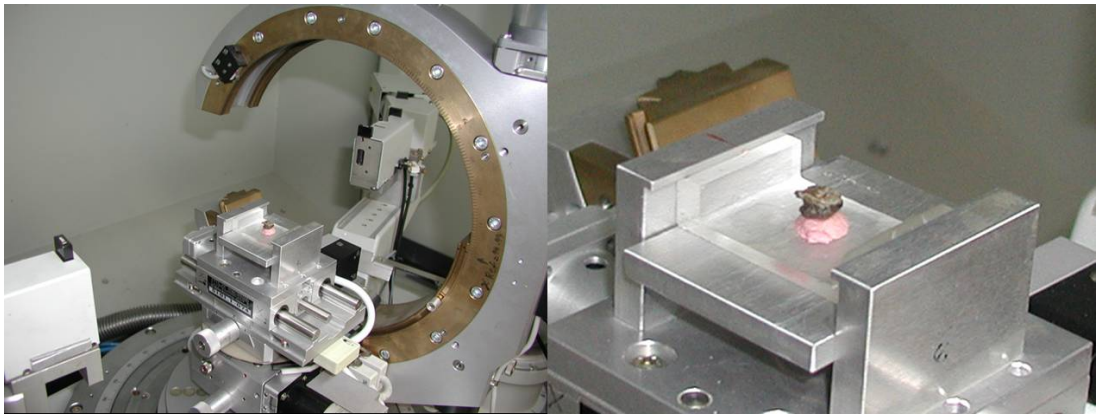

Fig. 1.8 Analysis of the slag fragment (**CSG-315**) in the XRD equipment (Siemens D5000).

1.2.7 Digital X-ray Radiography

Digital X-ray radiography was applied in some occasions to artefacts that were not submitted to invasive analyses. The investigation of metal heterogeneities could aid the study of the manufacturing techniques, namely the joining of metallic elements (e.g. nails from *Figueiredo das Donas*, section 3.3.3.3).

The radiographic investigation was conducted with a digital X-ray system, ArtXRay, SEZ Series, manufactured by NTB GmbH (Dickel, Germany), installed at the DCR-FCT-UNL. The parameters used were a maximum voltage of 130kV and current intensity of 3.7 mA, with the focus-detector distance of 1.40 m, and the artefacts positioned within a distance of circa 20 cm from the detector. The image processing involved the iX-Pect software.

Chapter 2 – Corrosion Study

2.1 Introduction

Archaeological metallic artefacts can be considered perfect guides to long-term corrosion. Since many corrosion processes are not easily reproduced in laboratorial controlled tests, exhaustive descriptions of corrosion in archaeological artefacts are essential to construct a reliable prediction of long-term corrosion, which in turn can benefit a long-term conservation of the artefacts (Degrigny, 2007).

The first descriptions of corrosion on ancient copper-based artefacts, namely tin bronzes (Cu-Sn alloys), date to the early XIX century (e.g. Davy, 1826). Although the first studies were sporadic, from the 1950's onwards increasing and more regular contributions in specialized journals began to appear (e.g. Gettens, 1951; Organ, 1963; Scott, 1985). Generally, for tin bronzes (from now on bronzes) a decuprification phenomenon has been described to be the main corrosion phenomenon, involving copper dissolution and copper ion migration outwards, together with tin dissolution followed by *in situ* precipitation (Robbiola et al., 1998). Although tin is a more active metal than copper (as shown by the relative potentials in the galvanic series, see Appendix III – Standard reduction potentials), tin compounds as cassiterite (SnO_2) and its hydrated forms are chemically inert and stable over a large pH domain, when compared to the corresponding copper compounds (as shown by the Pourbaix diagrams, see Appendix IV – Potential-pH diagrams). As a result of the insolubility of cassiterite (SnO_2) and its hydrated forms, the permanence of this element *in situ* is favoured, leading to tin-rich corrosion surfaces on archaeological artefacts.

For corrosion of single α-phase archaeological bronzes, a very detailed study has been published by Robbiola et al. (1998), showing that two classes of corrosion structures can be defined, Type I and Type II, designations that are going to be adopted in the present work. Generally, the first one is a more passivating mechanism, with artefacts exhibiting a more "even" surface, and the second one is a more severe attack associated to the presence of chlorides, with the artefacts exhibiting a "coarser" surface (exhibiting pitting and a general uneven surface) (note that both types can exist in one artefact). In **Fig. 2.1** a detailed description of the different corrosion layers among the two types of corrosion is shown. In both types, a more internal layer(s) with Cu[I] and a more external/outer layer(s) with Cu[II] compounds is present. Depending on the burial environment, the copper [II] salts are frequently basic copper carbonates (as malachite, $Cu_2(CO_3)(OH)_2$) and trihydroxyclorides (as atacamite and paratacamite, $Cu_2(OH)_3Cl$) in Type II corrosion, and the Cu[I] species are frequently copper oxides (as cuprite, Cu_2O) and cuprous chloride (as nantokite, CuCl) in Type II corrosion (for other common compounds see Appendix VII – Some common corrosion products). Under OM observations these can be easily distinguished due to different colours under BF, Pol and DF modes (see Appendix VI – Some properties of elements and compounds).

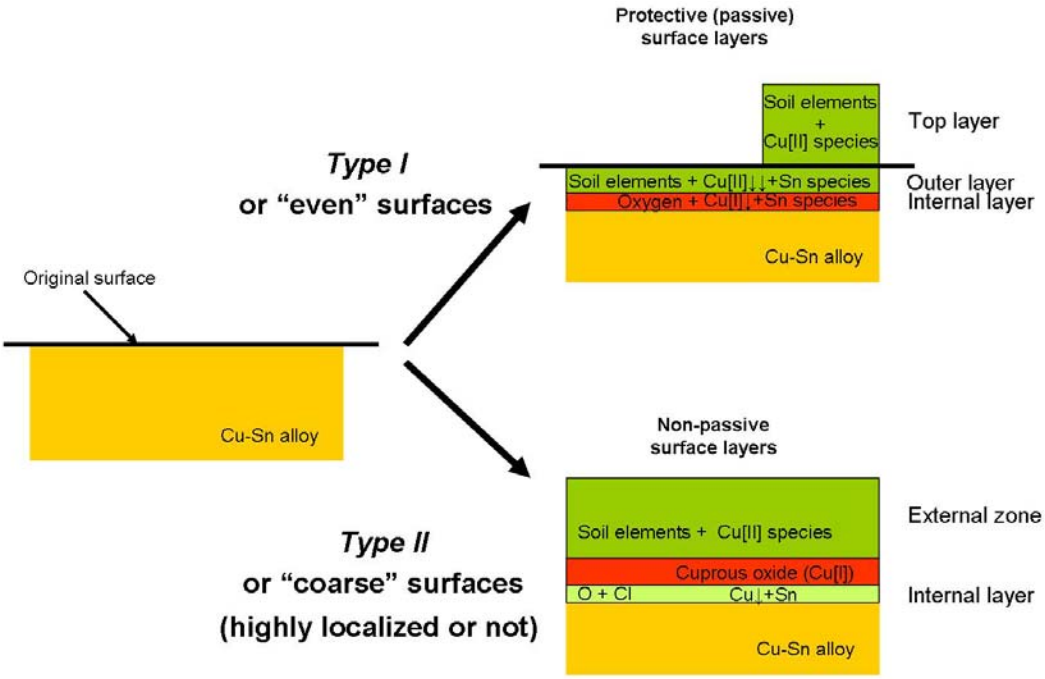

Fig. 2.1 Scheme with the two types of corrosion found in archaeological Cu-Sn artefacts based on Robbiola et al. (1998) with further additions in Piccardo et al. (2007).

According to Robbiola et al. (1998), for an artefact corroded in a moderately aggressive context (i.e. soil, urban atmosphere, lake water, etc.), a copper dissolution factor (f_{Cu}) is expected to be around 0.94±0.04 in the outer passivated layer of corrosion Type I. This means that for every 100 atoms of Cu initially present in the metal only 2-10 atoms remain in the outer corrosion layer considering that no tin is lost (f_{Cu}=1 means total dissolution of Cu and f_{Cu}=0 means no loss of Cu) (for details on the equation see Appendix V – Some reactions and mechanisms of corrosion formation).

The nearly constant Cu/Sn ratio determined in corrosion of various artefacts despite their different Cu/Sn ratio in the alloy does also indicate the formation of distinct copper and tin compounds rather than well-defined mixed copper-tin compounds (such as $CuSn(OH)_6$ or $CuSnO_3.3H_2O$) (Robbiola et al., 1998). The formation of distinct copper and tin compounds has also been reported for the most internal layer of Type II corrosion (Piccardo et al., 2007).

Next, some of the most significant corrosion patterns observed among the studied bronze artefacts from the Portuguese territory will be described. Generally, the cases refer to Type I corrosion except when depicted, since this was the most frequent corrosion type found. In relation to the previous works on corrosion, a special attention is made to specificities of two-phase (α+δ) bronzes (since these were common among the artefacts analysed) and on the pattern of internal corrosion layer and its relation with microstructure specificities in cast or wrought items. After, the influence of corrosion in the analytical study is going to be presented aided by some case-studies. Here, the influence of corrosion in the superficial elemental analysis is discussed, as well as the influence of corrosion thicknesses, and also the influence of mass loss due to corrosion in a metrical study. Type II corrosion is going to be discussed in a specific case-study in one of the last sections.

2.2 Specificities on long-term corrosion[1]

2.2.1 Top, outer and internal layers

The burial of metal artefacts under long periods of time favours the development and permanence of a thick corrosion layer (patina) when compared to atmosphere exposed metals, where a regular loss of patina due to dynamic environmental factors (i.e. rain, wind or other abrasion actions) is more significant. The OM examinations made on various artefacts revealed an outer corrosion layer, of green colour under the DF and Pol modes, which could frequently reach 500 μm of thickness (**Fig. 2.2**). This layer has the Cu in the highest oxidation state, Cu[II], and its common greenish colour is given by the copper compounds, as copper carbonates. In some artefacts that had not been subjected to a strong mechanical cleaning, a top layer could also be observed, frequently with a dark brown colour. This top layer can be understood as a kind of aggregate composed by particles from the soil involving the artefact during burial and precipitated species which were leached from the metal artefact (a detailed case-study is shown in the Archaeometallurgical Study, section 3.3.3.4 – *Crasto de São Romão*, in the study of the gilded copper nail CSR-3000).

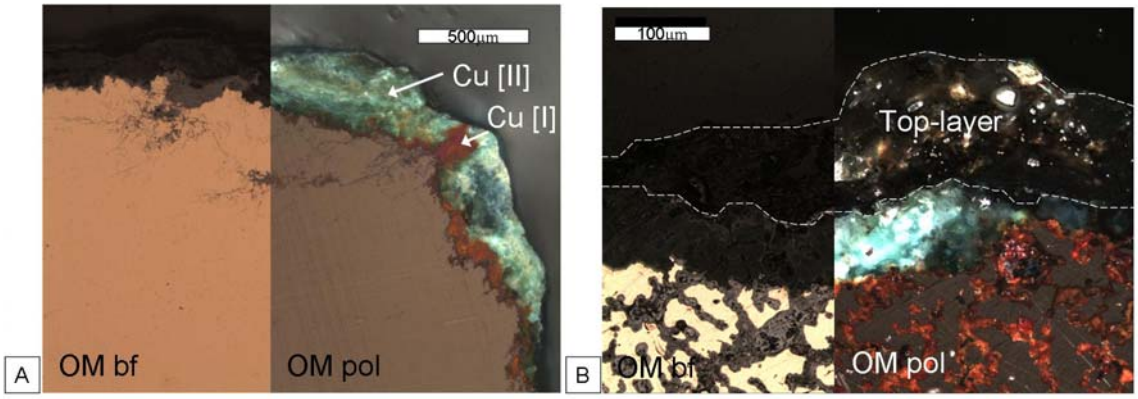

Fig. 2.2 OM images related to different corrosion layers: (A) Cu[II] green outer layer and Cu[I] red internal layer (CSR-3169 bronze awl,~9 wt.% Sn); (B) dark top layer formed by soil particles and Cu[II] species placed over the Cu[II] green outer layer (FC-474 leaded bronze nodule, ~5 wt.% Sn and ~6 wt.% Pb).

Below these two layers an internal layer of reddish colour under DF and Pol modes could also be observed. This layer has the Cu in the lowest oxidation state, Cu[I], and its reddish colour is given by the copper compound cuprite (Cu_2O). In relation to the outer layer, the internal layer has a higher content of copper and lower content in oxygen, as clearly visible in a SEM-EDS elemental line scan

[1] The content of this section has adaptations from the following published works:

- E. Figueiredo, R.J.C. Silva, F.M. Braz Fernandes and M.F. Araújo (2010) Some long term corrosion patterns in archaeological metal artefacts. *Materials Science Forum* 636-637, 1030-1035;
- R.J.C. Silva, E. Figueiredo, M.F. Araújo, F. Pereira, F.M. Braz Fernandes (2008) Microstructure interpretation of copper and bronze artefacts from Portugal. *Materials Science Forum* 587-588, 365-369;
- E. Figueiredo, M.F. Araújo, R. Silva, F.M. Braz Fernades, J.C. Senna-Martinez, J.L. Inês Vaz (2006) Metallographic studies of copper based scraps from the Late Bronze Age Santa Luzia archaeological site (Viseu, Portugal). In: R. Fort, M. Alvarez de Buergo, M. Gomez-Heras, C. Vazquez-Calvo (Eds.), *Heritage, Weathering and Conservation*, Taylor and Francis, London, Vol. I, 143-149.

shown in **Fig. 2.3**. Also, in this line scan, the tin-rich outer layer as a result of decuprification phenomena is clearly perceptible.

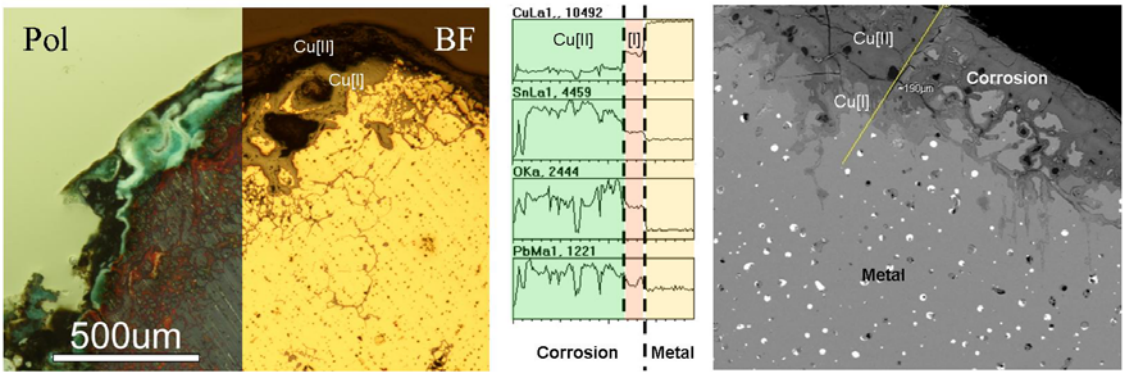

Fig. 2.3 (from left to right) OM image, SEM-EDS line scan and BSE image over the external and internal corrosion layers as well as over unaltered metal (FC-206) (note that white inclusions on right image are Pb rich globules that are aligned according to the dendritic structure formed during solidification of the metal).

The internal corrosion layer can take many forms, which are going to be discussed in more detail in the next section.

2.2.2 Internal corrosion – intergranular and transgranular patterns

An internal corrosion layer of reddish colour (under DF and Pol modes in OM) due to the presence of cuprite (Cu[I]) was present in most artefacts. This corrosion could be present as a relatively uniform layer, or it could show a very irregular shape extending to the interior of the artefact along the grain boundaries – intergranular corrosion (see left images in **Fig. 2.4**, see also **Fig. 2.2**B in last section for a dendritic structure). Consequently, the sizes and shapes of grains were frequently revealed without etching.

The depth of the internal corrosion layer, in the form of intergranular corrosion, was very variable. Generally, it was found that the less homogenized microstructures, i.e. those composed by cored dendrites with the presence of eutectoid and large pores, were more affected by deep internal corrosion than wrought items, i.e. those composed by recrystallized single phase grains. The described pattern is a result of the progression of corrosion along the paths with higher internal energies, such as grain boundaries with impurities or crystallographic defects. In artefacts that had suffered a mechanical deformation during the final shaping or a surface finishing operation (e.g. forging or a final mechanical surface polishing), transgranular corrosion along crystallographic planes could also be observed (see right images in **Fig. 2.4**). Since forging or even a final mechanical surface polishing causes plastic deformations in the metallic grains (Wang and Ottaway, 2004), i.e. increasing dislocation density along slip planes, corrosion do also follows this path. As a result, in these artefacts, a final mechanical operation could frequently be predicted without metal etching.

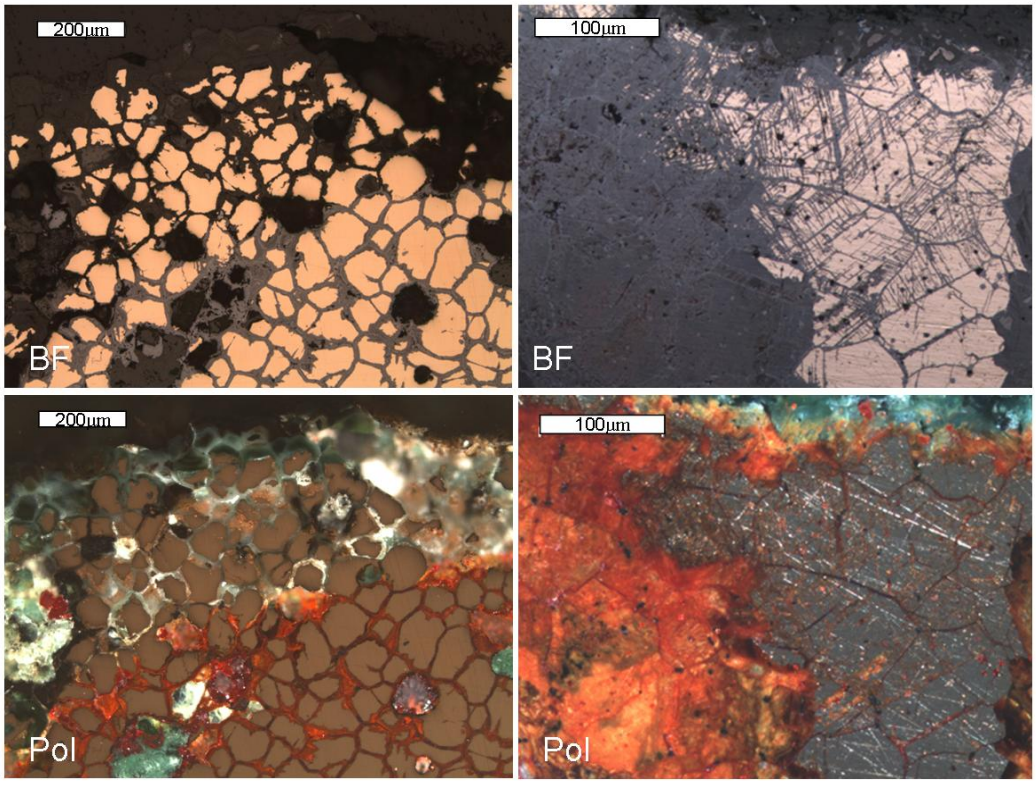

Fig. 2.4 OM images of intergranular corrosion at left (FC-660 bronze nodule) and transgranular corrosion at right (CSG-330 bronze spatula) (note that in the bottom right image the internal corrosion of reddish colour bears the morphology of the grains – pseudomorphic replacement; note also that copper sulphides – dark spots – do also remain unaltered in place).

In the case of sampled bar fragments with different microstructures, it was possible to evaluate the corrosion on different symmetry planes. It was found that the internal corrosion besides developing from (i) the outer surface to the internal regions (i.e. perpendicular to the surface plane), could also develop (ii) along the length of the bars, either in regions not far from the surface, as a consequence of grain deformation patterns, or at the centre of the bar, probably as a result of a higher concentration of pores and impurities due to normal segregation (the most internal region is the last region to solidify). In the latest corrosion form (centre of the bar), it is the contact area with surface at the top of the bars that allows the development of corrosion. Some OM observations of the areas affected by this corrosion suggest a higher degree of material loss, frequently resulting in empty spaces. This phenomenon can be related to a crevice corrosion mechanism, which is associated to a stagnant solution on a micro-environmental level, leading to the formation of a rather aggressive acidic micro-environment resulting in faster dissolution.

Among the corrosion along different symmetry planes the former (i) was more significant among the less mechanical processed items, and the latest (ii) was more significant among the more mechanical processed items. This tendency can be explained by the strong anisotropic deformation in the more worked items. In **Fig. 2.5** some representative cases are shown with a brief explanation in the caption.

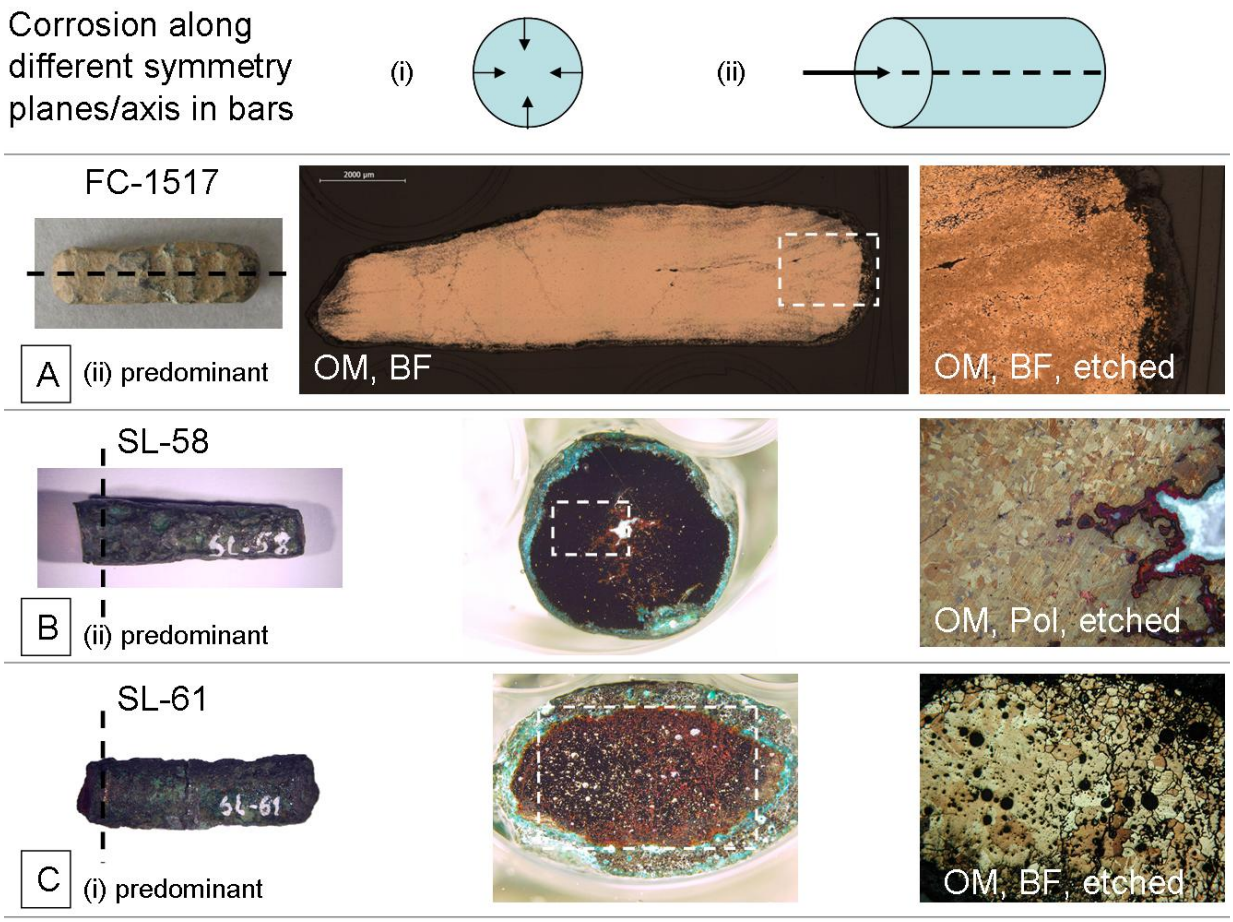

Fig. 2.5 Details of bar sections along different symmetry planes/axis: (A) section along the length in a worked bar (microstructure composed by equiaxed twinned grains) showing intergranular corrosion along the length, mainly in the areas near to surface, but also at the central areas; (B) cross-section of a worked bar (microstructure composed by equiaxed twinned grains) showing the development of corrosion along the length, in the central axis; (C) cross-section of a slightly worked bar (in the microstructure note the large pores) with strong intergranular corrosion from the surface to the centre of the metal.

Detailed SEM-EDS analysis of intergranular corrosion showed that this corrosion was rarely homogeneous at a microscopic level. An intergranular corrosion that is composed by a two layer strata, one at contact with the unaltered metal grains (1st layer) and another at the central region (2nd layer) is shown in **Fig. 2.6**, in a bronze with some Pb rich inclusions (FC-206). It can be observed that decuprification phenomena begins in the grain boundaries (see EDS mapping at bottom of **Fig. 2.6**) and that a "corridor" of metals as Sn and Pb plus oxygen develops. The decuprification in the grain boundaries can somehow be compared to the more macroscopic observation of the superficial layers in Type I corrosion that have suffered from copper loss (see **Fig. 2.3** in section 2.2.1). In the present case, intergranular corrosion is also responsible for the leaching of Pb from the globules and for the filling of previous empty spaces (also pores) with Cu-O, likely cuprite as indicated by the reddish colour under Pol and DF modes in OM.

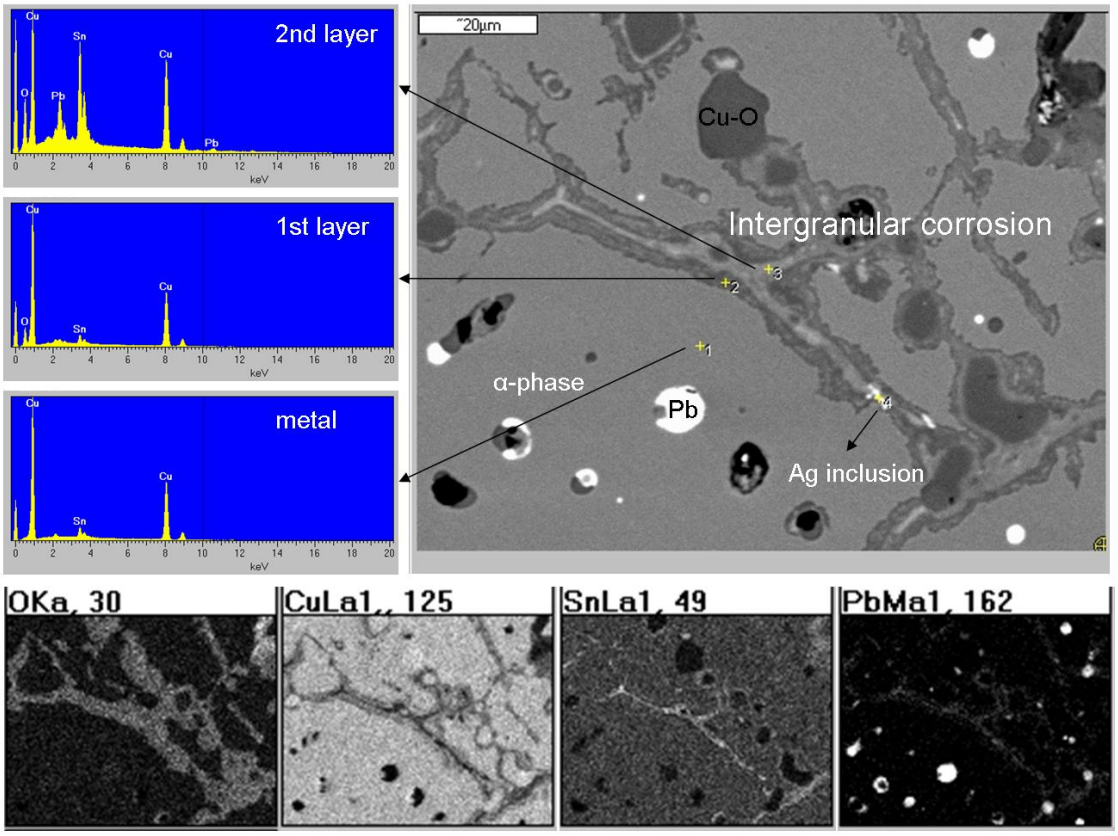

Fig. 2.6 Detailed SEM-EDS analysis of intergranular corrosion in a bronze bar with some Pb globules (FC-206) showing intergranular compositional heterogeneities at a microscopic level.

The low "mobility" of tin species (i.e. tin oxidises in its initial position and does not diffuse long distances) in the basis of the decuprification phenomena, is clearly demonstrated next. In **Fig. 2.7** an image is shown with corrosion developing in an internal large hollow space of a bar fragment (SL-68) and thus not perturbed by physical exterior factors that could constrain crystal growth. It is observed that within the Cu[I] zone, the Sn presence/absence marks the original metal/hollow interface. In this particular case this interface is among a Cu[I] layer as a result of the oxygen restriction inside the bar; if this corrosion was developing on a more superficial (aerated) region it would probably be among a Cu[II] zone (see **Fig. 2.1** in section 2.1 – Corrosion introduction). Also, in the SEM-BSE and SE images it can be observed that in the empty space copper carbonates grew freely as acicular crystals. Malachite growing in this form has previously been reported by Scott (1994) for a vacuole in a bronze. These crystals probably grew as carbonates and are thus not cuprite transformed into carbonate since cuprite does not seems to take the acicular form (Zhou and Yang, 2003). When cuprite forms in hollow spaces it normally grows as cubic crystals, as observed in **Fig. 2.8** and reported in other studies (e.g. Gettens, 1951).

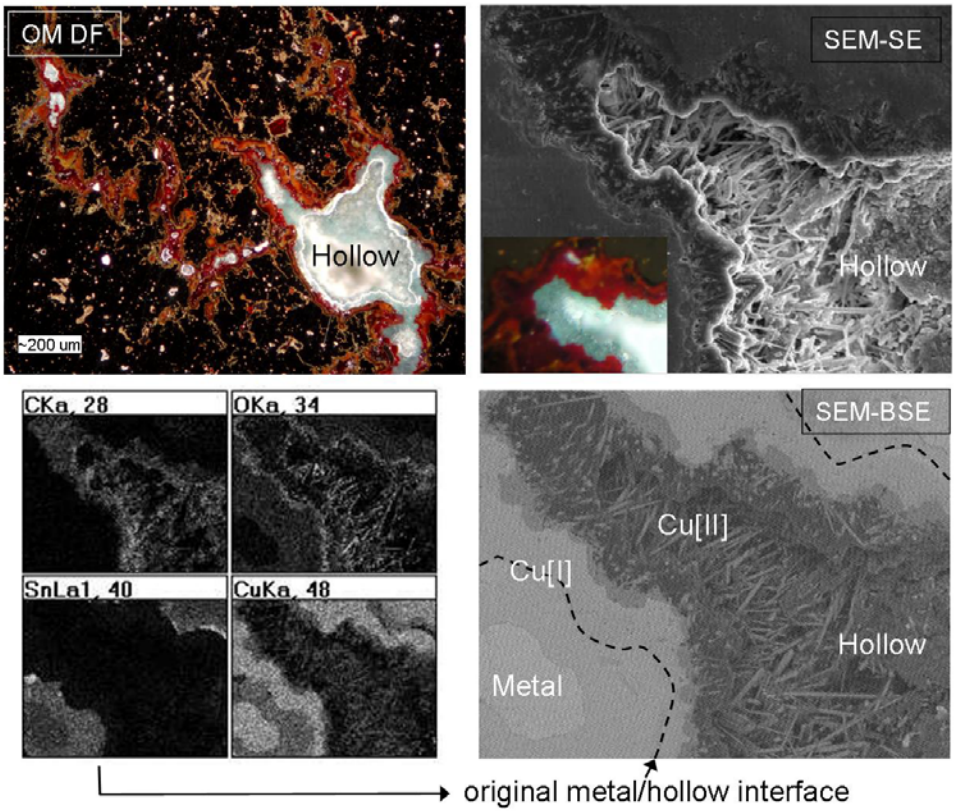

Fig. 2.7 Detailed OM and SEM-EDS images of the central zone of a bronze bar fragment (SL-58) with a hollow space (extending along the bars length) where migration and precipitation of copper species are clearly observed.

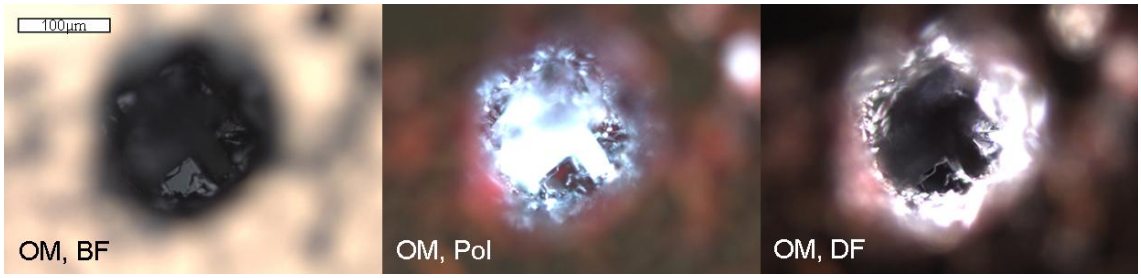

Fig. 2.8 Cubic crystals of cuprite inside a hollow space (pore) (CSG-153).

In some specific cases it was possible to easily detect corrosion Type II during the investigations. Although not being the most common corrosion type found among the studied items, either due to its scarcity or due to its localized character, this type of corrosion was very significant among the items from *Medronhal*. A study on this type of corrosion that results in different internal corrosion patterns is presented in section 2.3.4 – Type II corrosion – the *Medronhal* case-study. Here, its influence in the analytical study as well as OM observations, SEM-EDS and micro-EDXRF analysis to different corrosion layers is discussed.

2.2.3 Selective corrosion among α and δ phases

Many of the bronze artefacts studied have a microstructure composed by two phases: α, copper rich; and δ (comparatively) tin rich, product of γ eutectoid decomposition (see metastable phase diagrams

for Cu-Sn system in Appendix II). Different corrosion behaviours were observed among these two phases, regarding the depth of corrosion.

In the most external regions, those frequently composed by the outer thick corrosion layer, it was observed a preferential corrosion of α phase (both α-primary and α-eutectoid). In these areas, δ phase frequently remained among all the corrosion products, assisting in the interpretation of the original microstructure of the bronze (**Fig. 2.9**A). On the contrary, in the most internal regions of some items it was observed a preferential corrosion of the δ phase, which turned into a very dark colour under BF observations in the OM (**Fig. 2.9**B).

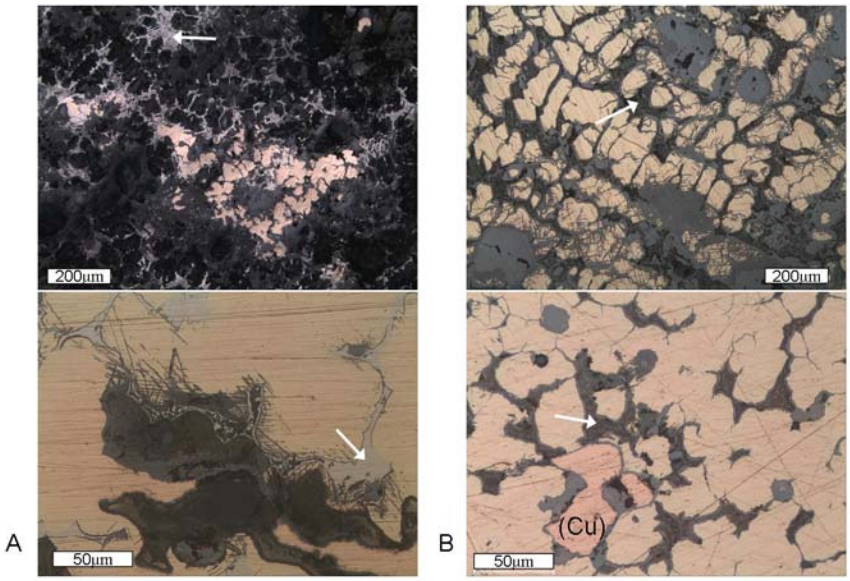

Fig. 2.9 Some OM (BF) images showing the (A) passivation of the δ-eutectoid and (B) preferential corrosion of δ-eutectoid (δ is depicted with arrows) (images are from SL-596, MED-04, MED-05 and CSG-187, from top left to bottom right) (note that on bottom right image the pink unalloyed copper formation is going to be mentioned in the next section).

Taylor and MacLeod (1985) have already observed opposite selective corrosion of these two bronze phases in marine environments regarding the partial pressure of oxygen. They found that when exposed to well-oxygenated conditions the α phase was preferably corroded, and when exposed to less oxygenated conditions the δ phase was preferably corroded. Probably, as for the underwater observations, the reason for the coexistence of these two opposite phenomena in buried archaeological items does rely in the oxygen content, which is different among the outer and internal regions (see again **Fig. 2.3** in section 2.2.1). Although copper is a more noble metal than tin, tin has the property of producing a strong passive oxide layer (SnO_2) at certain oxidizing conditions, which protects the metal from further corrosion. Taylor and MacLeod (1985) have suggested that the difference in corrosion may rely in the nature of the corrosion products, and describe that for the bronzes that were in the less oxygenated conditions the valence of tin corrosion products was more commonly II than IV. Possibly, under very low oxygen potential levels Sn[II] corrosion products (as stannous oxide SnO, romarchite) are preferably formed instead of the SnO_2 (cassiterite) based products.

A SEM-EDS study of the selective corrosion of eutectoid in the most internal corrosion regions is shown in **Fig. 2.10**. It is observed that the corroded δ phase suffers selective loss of copper while Sn remains oxidized in-situ (both stannous and stannic oxide are relatively insoluble). A two layer strata is also observed in the intergranular corrosion (remember **Fig. 2.6** in section 2.2.2), composed by a tin rich layer in contact with the unaltered grain (presenting copper loss) and a central region composed mainly by copper species. Again, and here regarding both corrosions of α and δ phases, the high diffusion of copper species compared to tin ones is demonstrated.

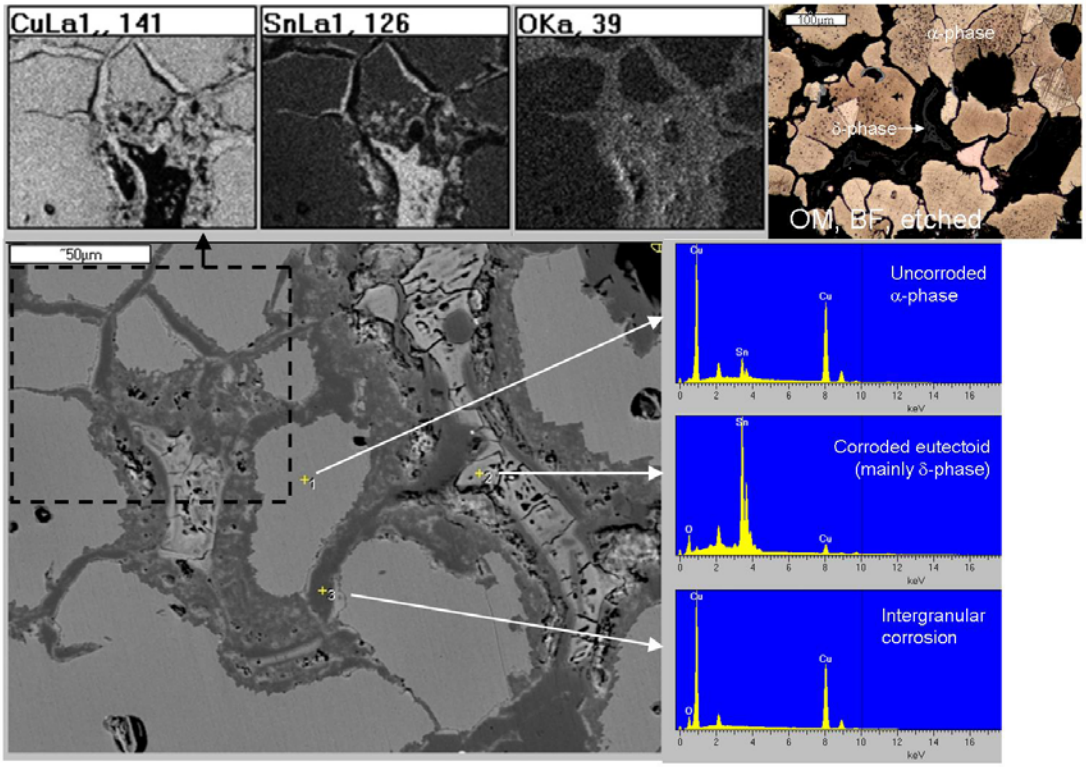

Fig. 2.10 SEM-EDS images with the study of selective corrosion of δ phase. At top right an OM image. All images are from the same artefact (FC-781).

2.2.4 Redeposited copper

In the most internal corrosion regions it was often observed the presence of a pink microconstituent (in BF, OM) of unalloyed copper, that could be present in various forms: in irregular or round shapes filling previous empty spaces as pores; or in long and thin shapes among the intergranular corrosion alternating its presence with cuprite (reddish colour in Pol and DF, OM) (**Fig. 2.11,** see also right bottom image in **Fig. 2.9** section 2.2.4). The presence of metallic copper among corrosion products of ancient bronzes has been reported numerous times, and has been subject of some dedicated studies, as Bosi et al. (2002) and Wang and Merkel (2001). Generally referred as redeposited copper, its mechanism of formation has taken various interpretations regarding its shape/morphologie, proximity to other metallic phases, as eutectoid, or even proximity to Cu-S inclusions.

As one of the suggestions made by Bosi et al. (2002), redeposited copper can be a result of a reduction of previous formed cuprite, due to the decrease in oxygen content that can happen during burial as the external corrosion layers become thicker and more protective and the item is accommodated to more anaerobic burial environments (along time older soil layers are accommodated deeper in soil). In respect to the present study, this would explain their presence in shapes similar to the ones taken frequently by cuprite in voids (as pores) (cf. **Fig. 2.8** in section 2.2.2 and **Fig. 2.11**B in this section).

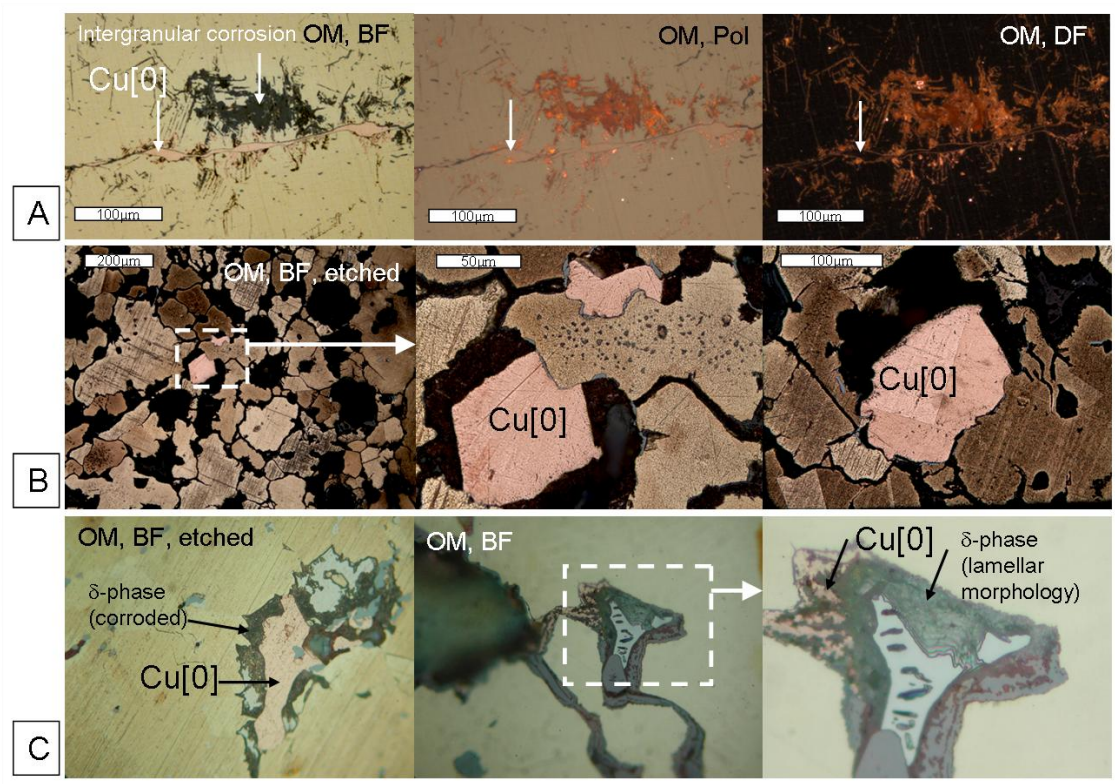

Fig. 2.11 OM images showing the presence of unalloyed copper in the internal corrosion regions: (A) among intergranular corrosion in single phase bronze (CSR-3169); (B) among previous empty spaces (pores) in two phase bronze (FC-781); (C) near eutectoid in two phase bronze (SL-58 left and SL-259-II centre and right).

In two-phase bronzes, redeposited copper can also be understood as a result of the selective corrosion of δ phase, as suggested by Wang and Merkel (2001) for Chinese bronzes. As shown in **Fig. 2.10** in the previous section, during the corrosion of δ phase under low oxygen potential levels a loss in copper occurs. Most probably, as tin oxidizes, the metallic bonds that existed with copper are broken, leaving copper cations free to redeposit as metallic copper in a nearby place, or to be more oxidized, depending on the amount of oxygen present (examples in **Fig. 2.11**C).

Only the suggestion made by Bosi et al. (2002) for redeposited copper in spherical morphologies surrounded by Cu-S as a result from liquid phases immiscibility does not seem to be appropriate, since it is based only in the Cu-S binary diagram. For bronzes, a ternary system has to be considered. Thus, taking also into account the Cu-Sn phase diagram (see Appendix II), it is observed that Sn is highly soluble in α-Cu, resulting in a copper and tin solid solution. Another explanation for this morphology

would simply rely in the filling of a pore by Cu species, since Cu-S inclusions are frequently present around pores (inclusions and impurities are normally concentrated towards the last parts to solidify; their common presence around the pores is illustrated in **Fig. 2.11** (B), where grey Cu-S inclusions are observed in the periphery of the pores). A figure exemplifying this formation is going to be presented later, in section 2.4 – Corrosion final discussion and conclusions.

2.3 Influence of corrosion in the analytical study

2.3.1 Superficial analysis – *Pragança* fibula and *Escoural* fragment case-studies[2]

Since EDXRF analysis with no surface treatment has been employed as a rule to all artefacts previously to other methodologies, and this technique performs a superficial analysis, variable contributions from the corrosion layer and from the metal are expected. Thus, an evaluation of the elemental content obtained by this method and the elemental content obtained by micro-EDXRF in a small prepared surface free of corrosion – and thus representing the uncorroded metal – is of great importance.

In a preliminary study performed over a bronze spear-head from *Sernancelhe* (see also section 3.3.4), micro-EDXRF analysis performed in a region free of the superficial corrosion layers were compared with past analysis obtained by EDXRF (Senna-Martinez et al., 2004) over the corroded surface, showing that Sn and Pb could easily reach four times higher contents (wt.%) in the EDXRF analyses when compared to the metal.

Later, a bronze fibula from *Pragança* (2005.10.77, section 3.3.1) with an even and dark corrosion surface was analysed by EDXRF over the corroded surface, as the normal first stage procedure described before, and by micro-EDXRF over (1) a small area with metal exposed and (2) the corrosion surface. The results are presented in **Table 2.1**, and are compared in a graphical way in **Fig. 2.12**.

Table 2.1 Summary of the experimental results on the bronze fibulae 2005.10.77 from *Pragança* (micro-EDXRF results are an average of five spot analyses ± one standard deviation)

		Composition wt.% (normalized)						
		Cu	Sn	Pb	As	Sb	Fe	Ni
EDXRF	Over corrosion	57.3	33.9	7.9	n.d.	1.1	- *	<0.5
Micro-EDXRF	Over corrosion	50.4±21.7	40.5±18.0	8.4±4.0	n.d.	-	0.5±0.1	0.5±0.1
Micro-EDXRF	Over metallic surface	86.8±2.4	10.3±2.3	2.3±0.2	n.d.	-	0.2±0.1	<0.5

* Not considered due to interference of an iron axle in the analyses (see details in section 3.3.1).

[2] Part of the content of this section has been published or presented in the following works:

- E. Figueiredo, P. Valério, M.F. Araújo, J.C. Senna-Martinez (2007) Micro-EDXRF surface analyses of a bronze spear head: lead content in metal and corrosion layers. *Nuclear Instruments and Methods in Physics A* 580, 725-727;
- E. Figueiredo, A.A. Melo, M.F. Araújo, Micro-EDXRF study of four Iron Age fibulae from Castro de Pragança (Portugal): use of bronze and iron in different components. Poster presented in TECHNART (Lisbon) 2007.

The results show that the fibula has a bronze composition of ~10%Sn and ~2%Pb, and that both EDXRF and micro-EDXRF analyses made over the corrosion resulted in higher Sn and Pb values, that can be in the order of four times higher than those obtained in the metal surface, and thus comparable to the previous results of the *Sernancelhe* spear-head study.

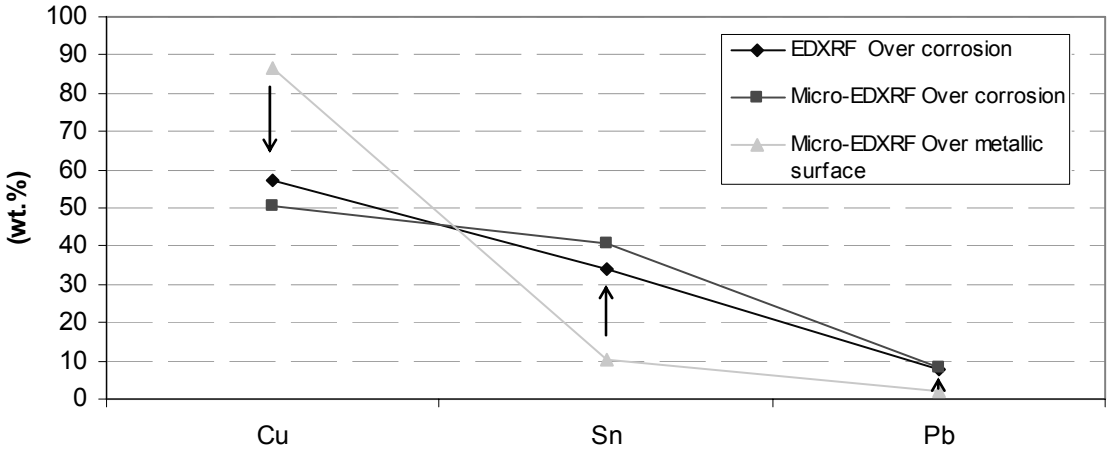

Fig. 2.12 Plot of EDXRF and micro-EDXRF analysis performed over corrosion and metal of the 2005.10.77 fibula from *Pragança*. A decrease in Cu and an increase in Sn and Pb are evident from metallic surface to corrosion.

These results indicate that Pb, in resemblance to Sn and differing from Cu, was not significantly leached from the corrosion surface, probably as a result of the environmental burial conditions. The resistance of lead under non-aggressive soil conditions has already been highlighted by Tylecote (1983), where lead can be oxidized to a fairly dense insoluble film of lead oxide (PbO) and lead carbonate ($PbCO_3$).

Comparing the micro-EDXRF analysis performed over metallic surface and corrosion, it is observed that the analysis performed over corrosion show a higher standard deviation. This is probably due to heterogeneities in corrosion composition and distribution. Comparing the results obtained by EDXRF and micro-EDXRF over corrosion, it is observed that the micro-EDXRF analysis show an average higher Sn content than the EDXRF analysis. This is most likely due to differences in depths of analyses performed by the two equipments. The use of the high energy Sn K characteristic lines in the EDXRF analysis contrasts with the low energy L lines used in the micro-EDXRF analyses (for Pb, L characteristic lines were used on both procedures). This means that the Sn content determined by EDXRF is more likely to have a greater influence from metal (that is behind corrosion), than the micro-EDXRF results (see **Table 2.2** for an approach in depth of analysis). This subject is going to be discussed further in the next section 2.3.2 – Thickness of corrosion.

Table 2.2 Calculation of 99% of total attenuation of the characteristic radiation emitted by Sn (Kα) and Sn (Lα) in a metal or corrosion matrix (see Appendix VIII for details of the Lambert-Beer equation used for the calculation)

	Metal Cu-10Sn (wt.%)	Corrosion layer*
K_α(Sn) ≈ 25.2 keV	~ 306 µm	~ 1161 µm
L_α(Sn) ≈ 3.44 keV	~ 9.5 µm	~ 25.8 µm

* Based on corrosion Type I it is considered that from 100 Cu atoms initially present in the alloy 6 remain in the corrosion layers, and that all Sn atoms present in the alloy remain in corrosion layers. Then, for a bronze Cu-10Sn (wt.%) (≈Cu-6Sn (at.%)) the corrosion should have ≈Cu-52Sn (wt.%). For the sake of simplicity, it is considered that half of the copper is in the form of cuprite (Cu_2O) and the other half in the form of malachite ($CuCO_3.Cu(OH)_2$), and all tin is present as oxide.

Due to the regular presence of As in early copper artefacts (this subject is developed in Chapter 3 – Archaeometallurgical Study) a brief comparison of As contents determined by (1) EDXRF analysis performed over corrosion and (2) micro-EDXRF analysis performed over the metal bulk (in a cross-section) of an copper artefact with As is also presented. In **Table 2.3** a summary of the elemental results of *Escoural* metal fragment ESC-M-Q3 are presented. It can be observed that As content is relatively enriched in the corrosion layers when compared to the metal bulk. However, it does not reach values as high as those previously determined for Sn and Pb elements in bronze artefacts. This can be due to the formation of arsenic oxides that comparing with tin and lead oxides (the latest in particular environments) are more soluble, and thus less stable among the corrosion layers. The analysis of this copper fragment also shows the relatively high values in which Fe can be present in the superficial corrosion layers as a consequence of incorporation from the surrounding soil during burial.

Table 2.3 Summary of the experimental results on the copper fragment ESC-M-Q3 from *Escoural* (EDXRF is a result of an average of 2 analysis and micro-EDXRF results are an average of three spot analyses ± one standard deviation)

		Composition wt.% (normalized)		
		Cu	As	Fe
EDXRF	Over corrosion	93.4	2.5	4.12
Micro-EDXRF	Over metal	98.0±0.6	1.9±0.6	<0.05

2.3.2 Thickness of corrosion – *Fraga dos Corvos* case-study[3]

The previous case-study of the *Pragança* fibula showed that corrosion can have a high influence in the superficial EDXRF analysis, with a significant increase of Sn and Pb contents when compared to the bronze composition below the corrosion. In the present case-study the influence that the thickness of corrosion can have in the EDXRF results is going to be evaluated.

[3] Part of the content of this section has been published in the following work:

- E. Figueiredo, M.F. Araújo, R.J.C. Silva, J.C. Senna-Martinez (2007) Corrosion of bronze alloy with some lead content: implications in the archaeometallurgical study of Late Bronze Age metal artefacts from "Fraga dos Corvos" (North Portugal). In: C. Degrigny, R. van Langh, I. Joosten, B. Ankersmit (Eds.), *METAL 07 (ICOM-CC) Proceedings*, Amsterdam (Set 2007), Vol I, pp. 61-66.

Four items from *Fraga dos Corvos* shelter were analysed by EDXRF over corrosion and by micro-EDXRF over sampled cross-sections, representing the bronze composition. The four items were also examined by OM to evaluate the thickness of corrosion. Results are presented in **Table 2.4**. In one of these items SEM-EDS analysis was also performed and the main results have been shown previously in section 2.2.2 – Internal corrosion.

Table 2.4 Summary of the experimental results on four bronze items from *Fraga dos Corvos* shelter (micro-EDXRF results are an average of three spot analyses ± one standard deviation)

			Composition wt.% (normalized)							Corrosion thickness (μm)
			Cu	Sn	Pb	As	Sb	Fe	Ni	
FC-206	EDXRF	Over corrosion	60.1	26.1	11.6	n.d.	0.11	2.05	n.d.	~125
	Micro-EDXRF	Over metal	89.2±0.5	8.6±0.5	2.0±0.3	n.d.	-	<0.05	n.d.	
FC-208	EDXRF	Over corrosion	33.0	51.9	10.8	n.d.	0.12	4.29	n.d.	~500
	Micro-EDXRF	Over metal	88.4±0.4	10.1±0.5	1.3±0.1	<0.1	-	0.05	n.d.	
FC-120	EDXRF	Over corrosion	60.6	33.5	4.0	n.d.	0.11	1.94	n.d.	~100
	Micro-EDXRF	Over metal	87.1±0.5	11.8±0.5	0.86±0.22	<0.1	-	0.05		
FC-215	EDXRF	Over corrosion	42.4	39.2	15.4	n.d.	0.28	2.48	0.18	~200
	Micro-EDXRF	Over metal	89.7±0.6	8.1±0.2	1.7±0.64	<0.1	-	<0.05	n.d.	

The results show that Sn and Pb are always in higher contents in the EDXRF analysis made over corrosion than in the micro-EDXRF analysis made over metal. This is in agreement with the previous study of the *Pragança* fibula, which in turn is in conformity with the decuprification corrosion phenomena for binary bronzes and with a general resistance of lead under common burial conditions.

Although the similarities in metal composition of the analysed items (8-12% Sn and 0.8-2.0% Pb) there is a general dispersion on the Sn and Pb contents obtained in the EDXRF analysis over corrosion (26-51% Sn and 4-15% Pb). This dispersion can be a reflection of variable contributions of metal and corrosion in the EDXRF analysis, as a result of different corrosion thicknesses.

In **Fig. 2.13** the ratios of Sn and Pb elements obtained in the EDXRF analysis and in the micro-EDXRF analysis (representing metal) are shown, in relation to an increasing corrosion thickness measured for each item. Generally, it can be observed that higher Sn ratios are also followed by higher Pb ratios, and that an increase in both is related to thicker corrosions: for thin corrosion layers (~100 μm) an increase of ~5 times (wt.%) Pb and of ~3 times (wt.%) Sn are expected in the EDXRF analysis compared to the metal composition; and for thicker corrosion layers (200-500 μm) up to ~9 times and ~5 times, respectively.

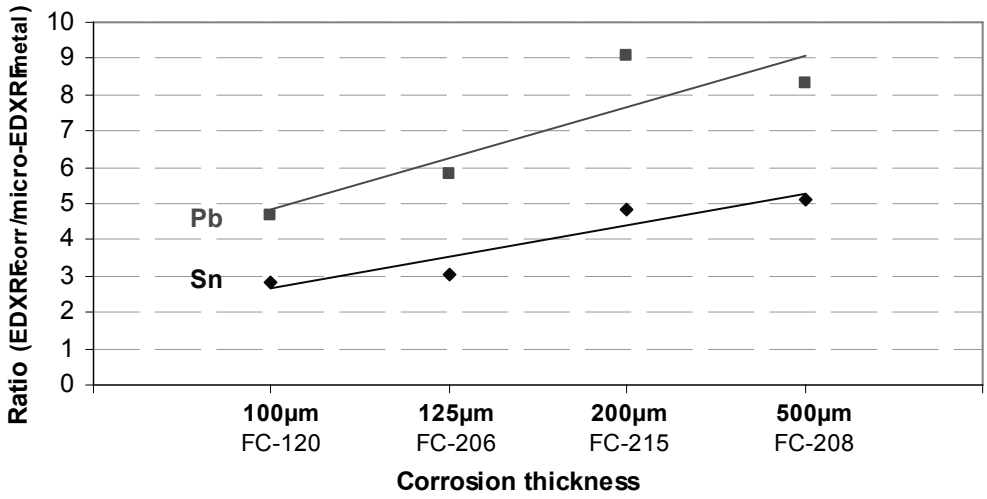

Fig. 2.13 Plot of Pb and Sn ratios obtained by EDXRF and micro-EDXRF analysis performed over corrosion and metal of four items from *Fraga dos Corvos* shelter.

Additionally, it is demonstrated that regardless the corrosion thickness, Pb ratios show higher values than Sn ratios. This can be explained by the use of the less energetic x-ray characteristic lines of Pb (L) than Sn (K) in the EDXRF analysis, having as consequence different depths of analysis among the two elements. Thus, it is expected a larger contribution of metallic bulk composition in the Sn characteristic lines than in the Pb (L) lines.

2.3.3 Type II corrosion – the *Medronhal* case-study

The EDXRF analysis made on the *Medronhal* items revealed a general different feature from the other collections. Around 1/3 of the items had relatively low Sn contents (<20 wt.%) (**Fig. 2.14**) differing from the usual higher Sn contents (>30 wt.%) obtained by this superficial technique when performed over the corroded surfaces of common Cu-~10Sn bronzes without any previous preparation (see e.g. sections 2.3.1 and 2.3.2).

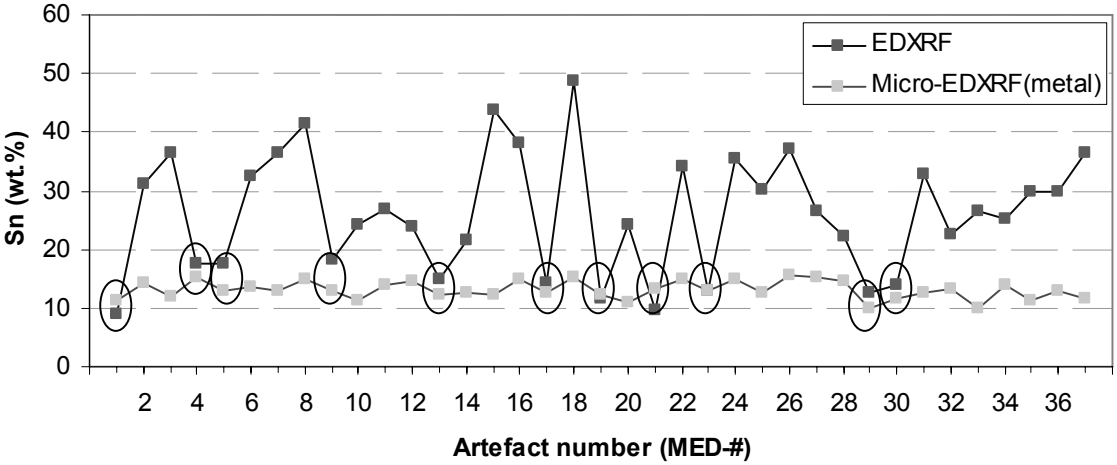

Fig. 2.14 Sn contents (average) of the Medronhal items determined by EDXRF and micro-EDXRF analysis. EDXRF results with <20 wt.% Sn and respective micro-EDXRF result are depicted by a circle.

In three cases the Sn contents determined by EDXRF were even lower than the contents determined in the metal by micro-EDXRF (MED-01, MED-19 and MED-21), excluding a simple explanation that would rely in a very thin corrosion layer.

As previously introduced in section 2.2.2 – Internal corrosion, OM observations in prepared surfaces pointed out to the presence of a different type of corrosion, the Type II, which is characterised by a significant presence of chlorides, of a yellow-greenish colour (Pol, OM), in contact with unaltered metal. The corrosion of bronzes due to the presence of chloride has been historically called *bronze disease*, due to the high reactivity of cuprous chloride (Cu[I]Cl) in the presence of moisture and air (generally RH>55%), resulting in light green, powdery, voluminous basic chlorides of copper (as atacamite and paratacamite, both with Cu[II]) which disrupt the surface and may disfigure the object (Scott, 1990).

At the present study, in a prepared surface of the bracelet MED-30 (representative of a cross-section), micro-EDXRF and SEM-EDS analysis were performed over the metallic bulk and corrosion products. In **Fig. 2.15** some OM images, and micro-EDXRF and SEM-EDS results are presented. OM images show the presence of a greenish corrosion layer (Pol, OM) all around the artefact that at the right side seems to be in direct contact with the unaltered metal, and a large amount of more internal corrosion of red and dark colour (Pol, OM) at the left side (between unaltered metal and the outer greenish layer). Micro-EDXRF analysis performed in (a) metal, (b) external greenish corrosion, (c) red corrosion and (d) dark corrosion show clear compositional differences, revealing that the outer greenish corrosion layer is very poor in Sn, and that the two most internal corrosion of red and dark colours have very different Sn contents: the red is very Cu rich and the dark is Sn rich. Detailed SEM-EDS analysis confirm the previous observations and analysis, and give further details, as the heterogeneity of the corrosion at a microscopic level, and the presence of a thin internal layer in contact with metal rich in Cl (**Fig. 2.15**, EDS spectra (5)).

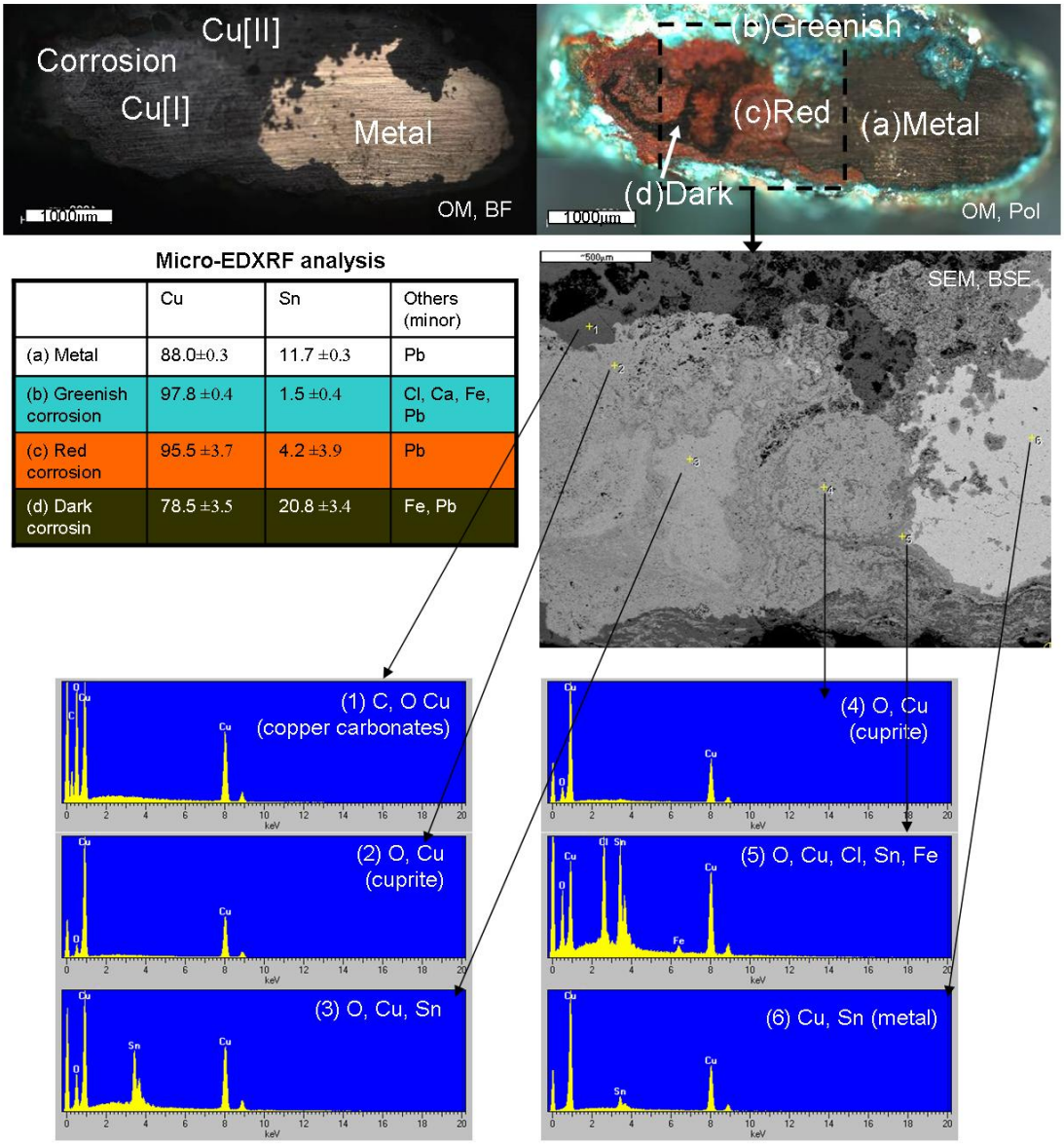

	Cu	Sn	Others (minor)
(a) Metal	88.0±0.3	11.7 ±0.3	Pb
(b) Greenish corrosion	97.8 ±0.4	1.5 ±0.4	Cl, Ca, Fe, Pb
(c) Red corrosion	95.5 ±3.7	4.2 ±3.9	Pb
(d) Dark corrosin	78.5 ±3.5	20.8 ±3.4	Fe, Pb

Fig. 2.15 (top) OM images of the MED-30 item with Type II corrosion; (middle left) micro-EDXRF results of analysis performed over different corrosion layers and metallic bulk (metal); (middle right) SEM (BSE) image of a central area of cross section and (bottom) some EDS spectra of different corrosion layers and metallic bulk (metal).

The corrosion layers shown in **Fig. 2.15** do not follow perfectly the strata for Type II corrosion shown in the scheme of **Fig. 2.1** (section 2.1 – Corrosion Introduction). This, however, does not bear surprises since corrosion Type II does frequently have a very heterogeneous structure, as reported by Scott (1990). Nevertheless, the three main corrosion layers can be easily identified: the external zone with Cu[II] species (see EDS spectra (1)); the cuprous oxide layer (see EDS spectrum (2) and (4); this layer is the (c) red internal layer observed in OM (Pol) and is a typical product of corrosion involving Cl ions, see Appendix V); and the most internal layer, that has a strong presence of Cl (see EDS spectra (5)). This latest besides having the presence of Cl, has a Sn/Cu ratio higher than in the bulk alloy, and has the presence of Fe which can be explained as a soil element contamination, all common features in this internal corrosion layer (Robbiola et al., 1998). The distinct dark corrosion (Pol, OM),

relatively tin-rich (micro-EDXRF results), can be interpreted as the most internal layer of a region where metal has been totally oxidised.

In a general way, the detailed analysis of the corrosion layers of this artefact do support the low Sn contents detected in the superficial EDXRF analysis performed as first stage of the analytical study: the external greenish corrosion layer and the more internal red corrosion have very low Sn contents (lower than in metal), easily explaining the relatively low Sn contents obtained by the superficial EDXRF analysis.

The preferential dissolution of tin (destannification) is a feature that has been described for some archaeological bronzes as a process that occurs similarly as dezincification of brass, i.e. temporary corrosion of both constituents of a binary alloy and the subsequent reduction and redeposition of the nobler constituent at the cost of further oxidation and dissolution of the less noble (Tylecote, 1979). This implies that while a preferential deposition of copper products on the alloy surface or in internal defects occurs, tin goes into solution and is dispersed. Since tin oxide is very insoluble and is the main Sn corrosion product for the general archaeological burial environments, the destannification process has to imply very specific conditions. Possibly, the presence of high amounts of chloride ions can be responsible for the destannification process, favouring the formation of tin chloride species instead of oxide ones, which are water soluble and thus readily removed from the corrosion layers.

Since objects that have the presence of chlorine species can be considered as metastable[4] (Scott, 1990), the sealing of the small surfaces that were prepared for the study was of major importance. Thus, after the present study, the small cleaned surfaces were stabilised and sealed by a conventional conservation treatment[5] (Williamson and Nickens, 2000).

This methodology was also adopted as a preventive conservation procedure to the items of the other collections before handling them back to the institutions where they were stored.

[4] Unreacted cuprous chloride might still be present at some depth of corrosion, meaning that the uncover of the most superficial and protective corrosion layers leaves the internal corrosion layers (as cuprite and curprous chloride) to be in contact with moisture of air, reactivating the autocatalytic process typical of the bronze disease (see Appendix V – Some reactions and mechanisms of corrosion formation).

[5] The conservation treatment consisted in the local application of (1) an corrosion inhibitor, benzotriazol (BTAH) ($C_6H_5N_3$) dissolved in ethanol (3% m/v), (2) an acrylic protector, Paraloid B-72 dissolved in acetone (5% m/v), (3) pigments with a coloration reproducing the surrounding patina dissolved in the previous prepared Paraloid solution, and (4) microcrystalline wax dissolved in the paraffin-derived "white spirit".

2.3.4 Loss of mass – the LBA weights case-study

The present case-study regards to a rather different topic than those presented in the last three sections. Since it covers ancient measurement systems, a rather unusual topic, a particular introduction to the theme and a contextual discussion is also presented in this section, which in turn might serve as a launch to the next main chapter, the Archaeometallurgical Study (Chapter 3).

The use of measurement systems can be regarded as one of the early stages towards civilization. The study of ancient metrology offers the possibility to connect information about different pre-monetary economies, as for everyday exchange operations or for "international" commercial transactions (Ascalone and Peyronel, 2006).

Most of ancient weight metrological studies are based on analysis of ancient administrative documents in literate cultures, masses of various metallic artefacts (e.g. bronze, gold and silver items) in illiterate cultures (e.g. Galán and Ruiz-Gálvez, 1996; Ruiz-Gálvez, 2000, 2003; Spratling, 1980), rather than in the actual weighing tools (Alberti et al., 2006). However, balance weights can be regarded as the most accessible and reliable witness for investigations into early cultural metrics, since an artefact may or might not have been metrically configured, and administrative texts are not always explicit (Petruso, 1978).

One indication of the external relationships that the Late Bronze Age (LBA) Iberian communities had, and of major importance, is the earliest recognisable balance weights, all of small geometrical shapes and made of metal, which have been found in Western IP (Vilaça, 2003). Most of them have been included in the present work, namely: 15 weights from *Castro de Pragança*, 1 weight from *Santa Luzia* and 2 weights from *Baiões* (**Fig. 2.16**). All were analysed by EDXRF and the 2 weights from *Baiões* were also analysed by micro-EDXRF, and microstructure examination was performed by OM in a small prepared area of the weights surface. The results are presented in detail in sections 3.3.1, 3.3.3.1 and 3.3.3.2 of the Chapter 3 – Archaeometallurgical Study. In the main, it was observed that all the weights are made of binary bronze, and that in the case of the *Baiões* weights the alloy has ~11-12 wt.% Sn and impurities of Pb, As and Sb (note that this composition is consistent with the LBA metallurgy of the Portuguese territory that has been studied in this work, see section 3.5 – Archaeometallurgical final discussion and conclusions).

Since the weights are made of metal and are of small size, the loss of mass due to corrosion can affect greatly the attribution of individual pieces in a system. Thus, a simple approach to the loss of mass in the studied weights is presented, to aid the correct attribution to an ancient measuring system.

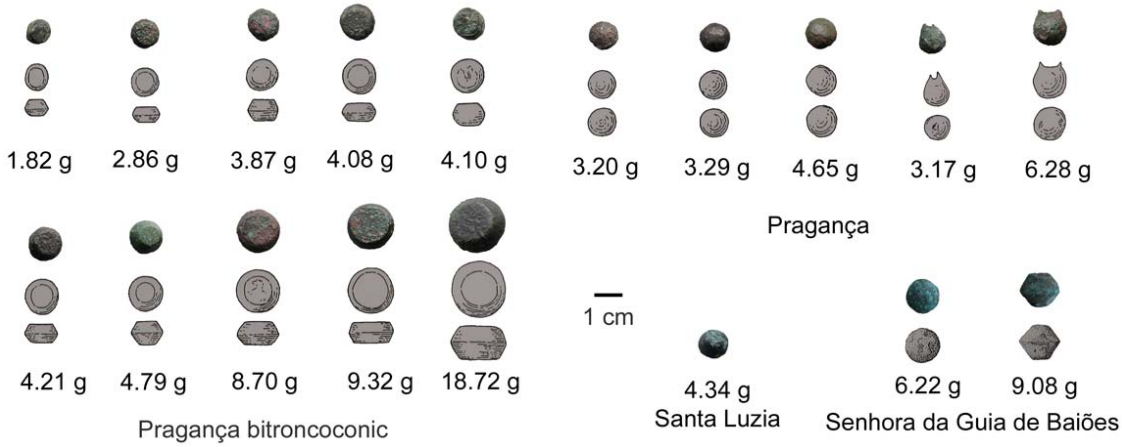

Fig. 2.16 Photos and drawings of the studied weights (drawings are based on Vilaça (2003) and references there).

Corrosion of Cu-Sn alloy involve differentiated loss of the metallic elements into the surrounding soil, and incorporation of others, such as oxygen, carbon, calcium, sulphur, phosphorous and iron into the corrosion layers. The work of Robbiola et al. (1998) illustrates very well what happens in the most common corrosion scenarios (corrosion Type I), showing that the loss of tin in the corrosion layer can be neglected compared to the loss of copper, which reaches 90 to 98 atoms lost for every 100 atoms originally present (this matter has been presented in section 2.1 – Corrosion Introduction).

The density of a typical Cu-10Sn bronze is about 8.7 g/cm^3 and the density of the expected corrosion products, composed by cuprite, malachite and tin oxide, taking into consideration copper loss, can be roughly around 5 g/cm^3 (decuprification considered, corrosion composed by ~50 wt.% tin oxide and ~50 wt.% copper species). Due to the presence of heterogeneities among the corrosion products, as porosities, the real density may in many cases be even lower.

The copper and tin species such as copper carbonates, tin and copper oxides, do not show a significant increase in volume when compared to the original bronze. This means that the mass lost in the volume transformed into corrosion can be around 5/8.7 of the mass of bronze previously there. In **Table 2.5** the loss of mass in a weight with a spherical shape of 1 cm ∅ (close to the *Santa Luzia* sphere weight) made of Cu-10Sn, and thus originally weighting 4.56 g, is shown (calculations have been made for corrosion thicknesses ranging 50-500 μm, as previously demonstrated to be common among the studied artefacts, see section 2.2.1 and 2.3.2). Beside the conversion of metal into corrosion, there is another process that can change the mass of a metallic object: commonly, the original surface is lost, meaning that part of the outer layer is no longer present. Thus, higher losses in mass can be reached than those calculated just for decuprification and oxidation phenomena (i.e. >>11.6%).

Regarding the same weight shape, it is expected the smallest weights to lose relatively more mass than the larger weights that have a smaller specific area. Similarly, among different shapes but with the same mass, as the bitroncoconic and the sphere weights, it is expected the bitroncononic ones to loss more mass due to a larger specific area.

Table 2.5 Evaluation of the loss of mass due to transformation of metal into corrosion (see text for estimation of corrosion composition)

	Initial mass	Thickness of corrosion (mainly composed by outer corrosion layer)	Loss of mass (g)	%	Final mass (g)	Final mass with loss of original surface (g)	%
Sphere shape	4.56 g	50 µm	0.06	1.3	4.50	<<4.50	>>1.3
1 cm ∅		250 µm	0.28	7.5	4.28	<<4.28	>>7.5
(Cu-10Sn)		500 µm	0.53	11.6	4.03	<<4.03	>>11.6

Since the precision of ancient measuring systems has been proposed to be in the range of +/-5% (Rahmstorf, 2006), one can expect a higher contribution from corrosion than ancient technological imprecision to differences in mass among a same weight unit, especially when dealing with relative small size weights. Thus, for the search of a mathematical relationship among the weights, different states of preservation should be taken into consideration.

In order to search for a system unit and a mathematical design the exceptional set of 10 bitroncoconic weights from *Castro de Pragança* were analysed alone at a first stage. This was useful to minimize interferences of weights from other sites or shapes that could easier be part of other weighting systems.

Within this set the presence of one standard unit based on a mass of ~9.5 g is intuitive, as well as the fractional and multiple units of 1/5, 1/3, 1/2 and 2 (**Fig. 2.17**). The variation in mass of the weights corresponding to the 1/2 fraction (from 4.79 to 3.87 g) can be mainly due to different corrosion degrees, explaining the tendency to lower masses. As demonstrated previously, the 3.87 g weight (with the lowest mass) may perfectly well represent an original mass of ~4.75 g considering some loss of superficial material (~18% loss of mass). Visual examination does also support this, as the 3.87 g weight is the one that shows the heaviest corrosion with relatively significant superficial material loss, contrasting with the 4.79 g weight (with the highest mass) that is the one that shows the best preserved surface.

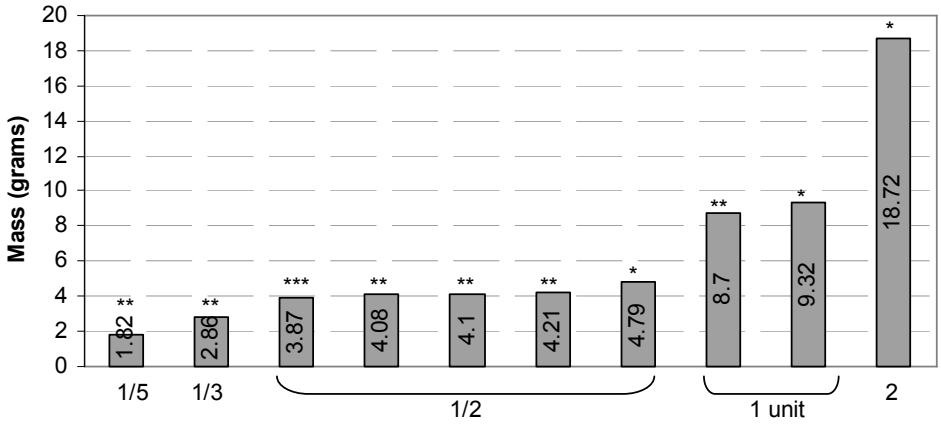

Fig. 2.17 *Pragança* bitroncoconic weights ordered by mass with the conservation state of the surface annotated: * surface with edges well preserved; ** surface with some visible material loss; *** surface with heavy corrosion and significant material loss in the edges.

The bitroncoconic shaped weight from *Baiões* (9.08 g) fit well into the system established for the *Pragança* weights, with the weight representing a 1 unit mass of a ~9.5 g standard.

The three sphere weights from *Pragança* (3.20 g, 3.29 g and 4.65 g) and the sphere weight from *Santa Luzia* (4.34 g) can probably represent 1/2 of the standard unit established before for the bitroncoconic weights. The low masses of 3.20 g and 3.29 g *Pragança* weights might well be explained by a significant loss of superficial material (constituting a variation in mass of ~36%), as observed by the similar sizes but different states of conservation of the surfaces (**Fig. 2.18**).

Fig. 2.18 Image of the three sphere weights from *Pragança* with similar sizes but with different states of surface conservation (those of lower mass are depicted ↓).

The 6.22 g sphere weight from *Baiões* seems to introduce a new mass that is not present within the bitroncoconic shape weights. That mass could represent 2/3 of the standard unit ~9.5 g, i.e. ~6.3 g, or it could represent a unit of some other system.

The attribution of the *Pragança* spheres with a suspension hole (?) (3.17 g and 6.26 g) as weights can be dubious if one considers what Alberti et al. (2006) mentions for Eastern Mediterranean contexts: in light weights (as the ones studied here) there shouldn't be any suspension hole since they were surely used on two-pan scales. However, if they are weights, they would have had a significantly larger mass since the top part of the suspension is missing. Thus, although the resemblance of the 6.26 g weight with the sphere weight from *Baiões* (6.22 g) they would probably be part of another system.

In **Table 2.6** all the weights, except for the spheres with a suspension hole (?), are organized under a 9.5 g unit system and the maximum loss in mass for each fraction or multiple is shown.

Table 2.6 Tentative denomination in a 9.5(±5%) g unit based system of the bitroncoconic and sphere weights (mass in grams)

Tentative denomination	Original mass (precision ±5%)	*Pragança*	*Santa Luzia*	*Baiões*	Loss of mass[+]
2	19.0±0.95	18.72**			<6%
1	9.5±0.48	9.32*		9.1	<13%
		8.70**			
2/3	6.33±0.32			(s)6.2	<7%
1/2	4.75±0.24	4.79*	(s)4.34		<22% (bitroncoconic) <36% (sphere)
		(s)4.65			
		4.21**			
		4.10**			
		4.08**			
		3.87***			
		(s)3.29↓			
		(s)3.20↓			
1/3	3.17±0.16	2.86**			<14%
1/5	1.9±0.10	1.82**			<9%

Pragança bitroncoconic weights: (*) Surface with corrosion but edges well preserved; (**) surface with corrosion with some visible material loss; (***) surface with heavy corrosion and significant material loss in the edges.

(s) Sphere weights.

(↓) Surface evidencing a higher material loss in *Pragança* sphere weights.

([+]) Calculated as [(max. original mass - min. weight mass) / max. original mass] × 100.

A weight system based in an absolute mass unit of ~9.5 g is not unknown among the Ancient World. It was one of the most popular units used in the Eastern Mediterranean during the late 2nd millennium BC, as early demonstrated by Petruso (1984) for the LBA stone balance weights from Enkomi, Ayia Irini, Idalion and the Cape Gelidonya shipwreck (ca. 1200 BC). It was commonly used along the Syro-Palestinian coast (especially in the north), on Cyprus and in Cilia (actual Greece) (Pulak, 2000) and during the New Kingdom it also became the prevailing standard in Egypt (Rahmstorf, 2006). Also, studies of the well-preserved weights of the Uluburun shipwreck (ca. 1300 BC) mostly of stone showed the prevalence of sets with a standard unit of circa 9.3 g, and few others possibly with circa 7.4 g and 8.3 g standard units. The weights from the Uluburun shipwreck have shown a concentration of 1/6, 1/3, 1/2, 2/3 fractions and 2, 3, 5, 10, 20, 30, 50 and 100 multiples, with a differentiated distribution of the shapes of the weights among the denominations, with just the sphendonoids representing the lower fractions and the domed the highest multiples (Pulak, 2000). Egyptian LBA weights from Museum of Cairo have showed a concentration of 1/5, 1/3, 1/2 and 2/3 fractions and 2, 3, 5, 10 and 20 multiples (Larssen, 2000; Petruso, 2006).

Resemblances among the studied Western Iberian system and the ~9.5 g Eastern measurement systems are quite remarkable. A pre-colonial contact between peoples of the Iberian Peninsula and peoples of the Eastern Mediterranean territories (i.e. before Phoenician colonisation of the coast lines of Iberian Peninsula which happened at the end of the IX century BC, Barros and Soares, 2004) is an actual theme of discussion (e.g. Celestino et al., 2008). Nevertheless, while the weight standard unit and the mathematical model was certainly imported, the prevalence of small masses, bitroncoconic shapes (that are absent in Eastern Mediterranean) and the manufacture of the weights in binary bronze

indicates that these weights were most likely local (i.e. Western Iberian) productions, adapted for an inter-regional Iberian trade. The materials that were being weighted are not known, however, these must have been "precious" and were circulating in small quantities (large LBA weights have not been recognized yet in the Western IP archaeographic records). As described by Rahmstorf (2006), while many objects can be counted (animals) or measured by volume (grain), amorphous objects such as metals and precious stones cannot. So, it might come to no surprise that weight metrology developed when intensive exchange of these materials started. As a consequence, it might not be inappropriate to propose the presence of weights in the inner-land Western Iberian regions as possibly being related with the local exploration of cassiterite and gold, resources that were at constant demand by LBA (about this theme see sections 3.1 – Archaeometallurgical Introduction and 3.3.3 – *Baiões/Santa Luzia* – a pertinent LBA cultural group).

2.4 Final discussion and conclusions

The corrosion study has provided a general picture of the various corrosion patterns that ancient buried copper-based metals, particularly bronzes, can show. Generally, the various patterns presented and their interpretations are a result of the high number of artefacts observed using the same analytical approach, leading to an intrinsic experience on the most common and the most uncommon features, as well as on the awareness of patterns of distribution of some particular features.

The study has provided detailed information on some particular patterns, as in the selective corrosion of different phases in two phase bronzes, and on the development of internal corrosion through different symmetry planes in cast and wrought bars. A clear distinction among top, outer and internal layers was possible through SEM-EDS analysis and these can be clearly distinguished in OM observations through their characteristic colours under Pol and DF modes. Among these, the internal and the outer layers define the passage of Cu [I] to Cu [II] regions. It was found that the outer corrosion layer could frequently reach large thicknesses, as 500 μm, and the internal corrosion could develop to very deep regions under the form of intergranular corrosion. It was also found that items with less homogenized microstructures, as cast items, have a higher tendency to deeper corrosion. In the case of small items, as bars, the intergranular corrosion could comprise the entire cross-section. Also, it was observed that the development of cuprite and malachite in hollow spaces allowed the growth of well defined crystals. It was found that in the most common Type I corrosion, the presence/absence of Sn species may mark the original surface of the item (if still existent). Also, it was found that decuprification phenomena starts at the grain boundaries, as previously suggested in Piccardo et al. (2007).

As part of the final discussion, the formation of redeposited copper and the selective corrosion of either α or δ phase among two-phase bronzes were selected to be presented in more detail due to a scarce and frequently contradictory explanations of formation in literature, and the absence of previous reports on the coexistence of both types of selective phase corrosion among buried artefacts regarding the depth of corrosion. In **Fig. 2.19**, a scheme with an interpretation of their mechanism of formation

is presented. The figure does also uses as example a wrought bar, where the formation of corrosion along specific symmetry planes (as a consequence of grain morphology and heterogeneities among the alloy) is represented.

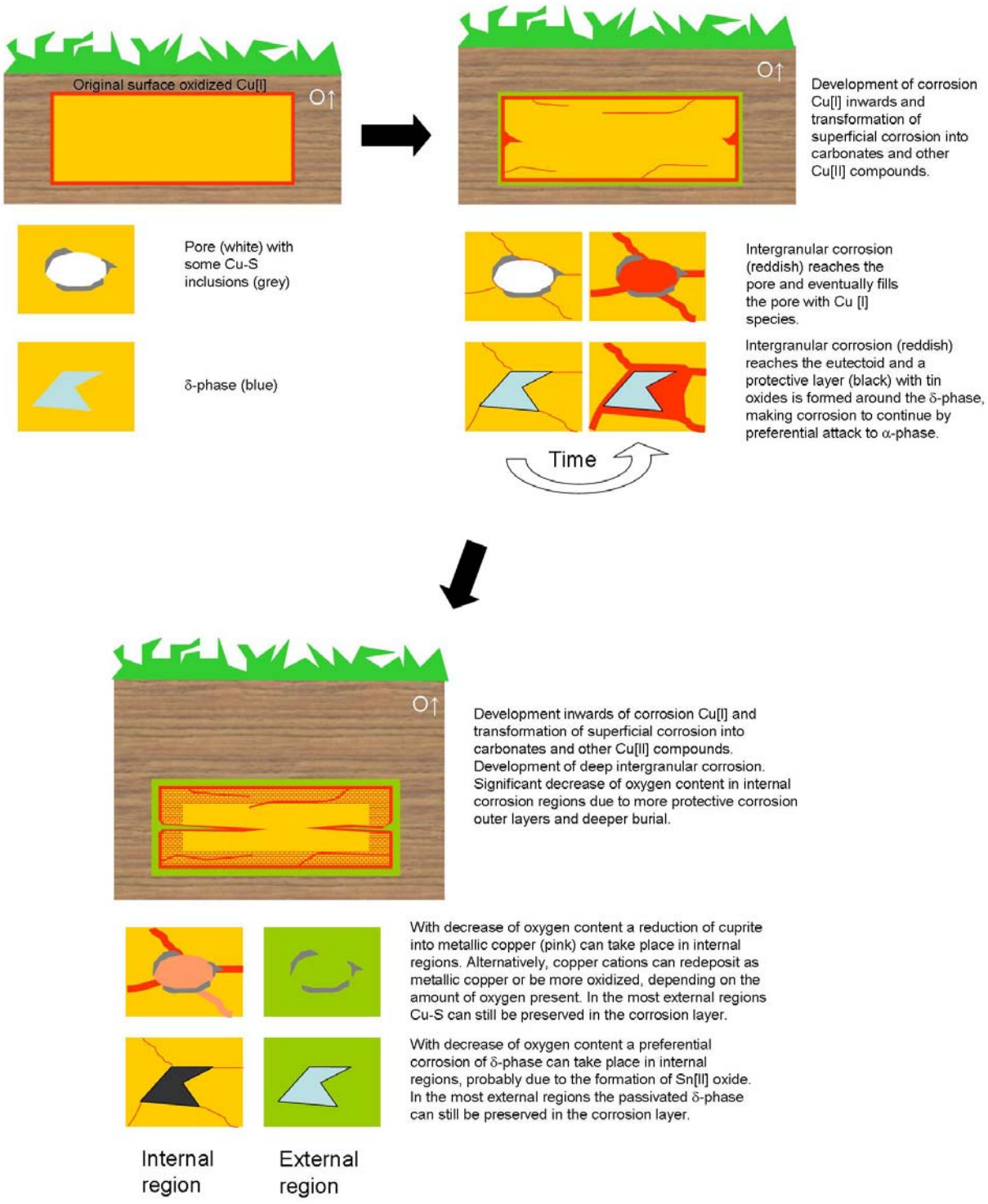

Fig. 2.19 Scheme with some specific features of corrosion development during burial.

Additionally, the corrosion study has provided general information on the influence of corrosion in the analytical study, which in turn will aid the archaeometallurgical study. It was found that due to the thickness of corrosion, which can frequently reach ~500 μm, the superficial analysis made by EDXRF

can be greatly affected by the corrosion composition. Generally, in respect to the metal bulk composition it can be expected to find: higher Sn and Pb values on analysis made over corrosion layers, regardless the method used (EDXRF or micro-EDXRF); relatively higher Pb "enrichments" than Sn "enrichments" among EDXRF analysis when compared to micro-EDXRF analysis made over corrosion due to different Sn characterisitc X-ray lines used in the analysis; and more dispersed Sn and Pb values on micro-EDXRF analysis made over corrosion layers, as a reflection of heterogeneities in corrosion products and/or thicknesses. As a guide line, Sn and Pb contents (wt.%) in corrosion can be expected to be up to 5 and 9 times higher than in the unaltered metal. This meets the loss in copper previously calculated by Robbiola et al. (1998) for Type I corrosion[6], and it also means that similarly to Sn, the loss of Pb in corrosion layers seems to be much less than the loss in copper (decuprification) for the most common burials among the various Portuguese regions.

On the other hand, a particular corrosion phenomenon was also identified, the one of destannification, which does not meet the above descriptions. This phenomenon could be detected by the preliminary EDXRF superficial analysis, by very low Sn contents, which could reach values lower than the content in the alloy. This particular corrosion was found among the *Medronhal* collection, associated with corrosion Type II (characterised by a significant presence of chloride species) and has seldom been described for archaeological items. Although it was not possible to study further the *Medronhal* collection, the selective loss of Sn in respect to Cu can possibly be associated to particular conditions, as low pH and poor oxidizing conditions, which have favoured the formation of tin chlorides instead of oxides, which are very soluble. In turn, copper chlorides are relatively stable, facilitating the permanence of copper among the corrosion layers.

[6] If considered that from 100 Cu atoms initially present in the alloy a mean of 6 remain in the corrosion layers, and that all Sn atoms present in the alloy remain in corrosion layers, then, for a bronze Cu-10Sn (wt.%) (≈Cu-6Sn (at.%)) the corrosion should have ≈Cu-52Sn (wt.%). This represents about 5 times higher Sn content (wt.%) in corrosion than in unaltered metal.

Chapter 3 – Archaeometallurgical Study

3.1 Introduction

The first metallurgical evidences in the Iberian Peninsula (IP) date to the Neolithic period, as those found in the archaeological site of *Cerro de Virtud* (Almería, Spain) (first half of the 5th millennium BC) (Rovira, 2004), and possibly the shapeless and almost pure copper artefact found in *Atalaia do Peixoto* (Évora, Portugal) together with material attributed to the Late Neolithic (Soares et al., 1994).

At the end of the 4th and the beginning of the 3rd millennium BC numerous habitat sites with metallurgical evidences flourished in the IP. In the Portuguese territory some examples are: *Castanheiro do Vento* (Jorge et al., 2006-2007) and *Castelo Velho de Freixo Numão* in Trás-os-Montes region (North Portugal); *Vila Nova de São Pedro* (VNSP), *Pragança*, *Zambujal* and *Leceia* in Estremadura region (Central Portugal); *Porto Mourão*, *Castelo Velho de Safara*, *Três Moinhos*, *São Brás 1* (Soares et al., 1994), *Povoado de Perdigões* (Lago et al., 1997), *Porto das Carretas* (Valério et al., 2007b) and *Monte Novo dos Albardeiros* (Gonçalves et al., 2005) in Alentejo region (Centre-South Portugal); *Cerro do Castelo de Santa Justa* and *Cerro do Castelo de Corte João Marques* in Algarve region (South Portugal). All these evidences for copper metallurgy suggested an independent centre in the Iberian Peninsula of the more advanced lands of the Near East (Renfrew and Bahn, 1991) (**Fig. 3.1**).

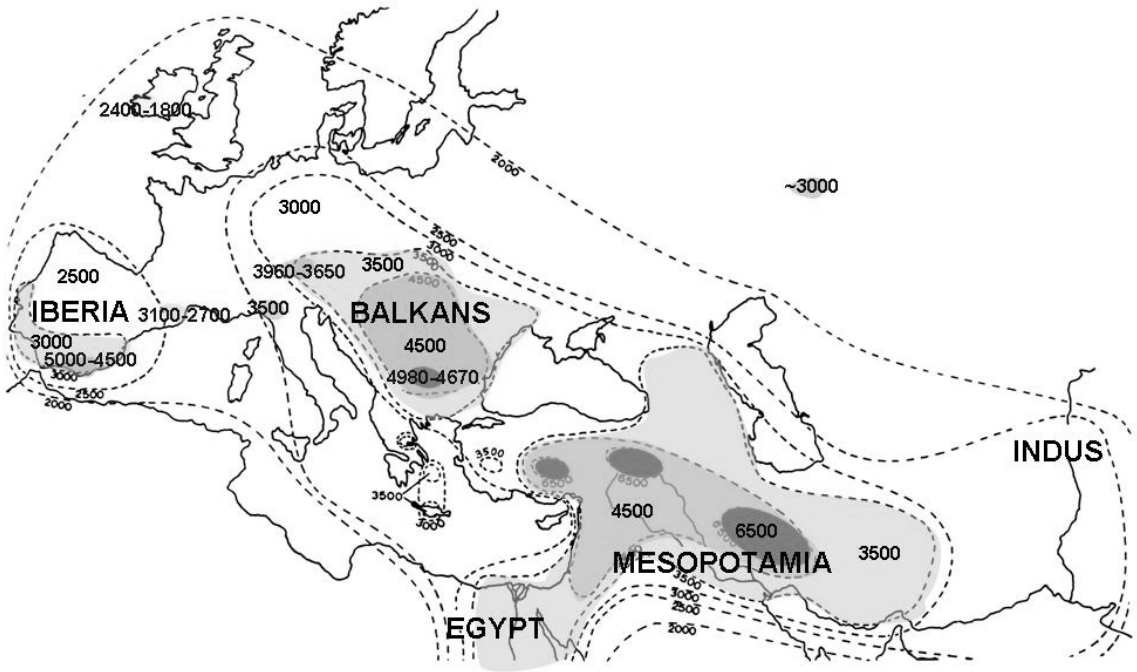

Fig. 3.1 Origins of European copper metallurgy after Renfrew and Bahn (1991) with new early evidences after Ottaway and Roberts (2008) that anticipate the beginnings of copper metallurgy in some regions, including the Iberian Peninsula.

The extensive SAM analysis on Chalcolithic (same as Copper Age, CA) artefacts fairly well documented the composition of early metals from the Portuguese territory (see also General Introduction). The artefacts from this period are generally made of a quite pure copper except for As, that can be regularly present probably as a trace of the ores smelted to produce the copper (Sangmeister, 2005). A tendency to the presence of As mostly in the artefacts from the latest chronologies (the Bell Beaker period), and the deliberated use of copper with higher As contents to manufacture specific typologies (e.g. Pamela points and tanged daggers in opposition to awls and flat axes), are subjects that are still under discussion (Soares, 2005; Müller and Pernicka, 2009).

Studies regarding the type of metallurgical operations performed in the various sites and their particularities are very scarce. One can account for the studies in the *Zambujal* site (Müller et al., 2007), VNSP site (Müller and Soares, 2008) and *Leceia* (Müller and Cardoso, 2008), where melting and smelting activities were probably performed in the first two, being the metals produced with minerals originating from the Ossa-Morena region (E Alentejo). In the Spanish territory numerous studies have been performed mainly in the framework of the project *Arqueometalurgia de la Península Ibérica*, accounting already for numerous sites where the smelting of metal was proven. Smelting of ores in crucibles or other vessels with large open shapes (Rovira, 2002), in a relatively weak reducing atmosphere, with the heat from above, seems to have been a common procedure among these early metallurgical populations. Exceptions are only found in the sites of *Cabezo Juré* and *Valencina de la Concepción*, which have metallurgical vestiges that point out to a more complex and large scale metallurgy, with a possible use of furnaces for smelting and crucibles for refining metal (Sáez et al., 2003; Nocete et al., 2008).

In the IP, the first evidences for copper alloyed with tin (bronze) happens among Bell Beaker contexts dated to the last half of the 3rd millennium BC (i.e. *Bauma del Serrat del Pont*, Gerona, NW Spain, and *Guidoiro Areoso*, Pontevedra, NE Spain), with slightly earlier chronologies than the most Western European areas (**Fig. 3.2**). Contrary to the first evidences of copper metallurgy, in the IP bronze seems to have spread from Northern to the Southern areas, which may indicate that it was introduced from the other side of the Pyrenees (Fernandez-Miranda et al. 1995; Rovira, 2004).

Despite the early evidences for bronze (at least in N IP) unalloyed copper continued to be the main metal used in the IP until the last quarter of the 2nd millennium BC. Analysis to the Middle Bronze Age (MBA) Argaric artefacts (S Spain) showed that only 1/5 were bronzes, and that these had variable tin contents, ranging between 2 and 15% (Rovira, 2004). This seems to be different from what happened in other Western European regions, as in the British Isles, where by the Early and MBA (~2300-1700 BC and onwards) almost all the artefacts were made of bronze with 8-14% Sn and <1% of impurities (Needham et al., 1989; Pare, 2000).

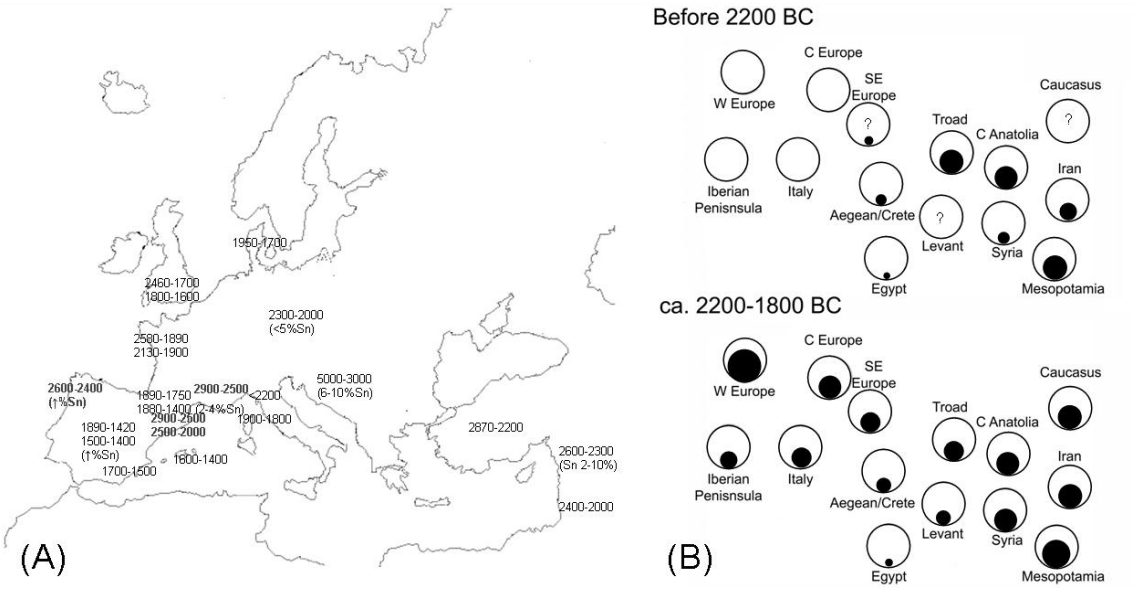

Fig. 3.2 (A) Map with chronologies (BC) attributed to the first evidences of bronze, based on Rosenfeld et al. (1997) (for regions in the Middle East – Israel, Syria and Lebanon), De Ryck et al. (2005) (for regions in the Middle East – Mesopotamia and Anatolia), Fernandez-Miranda et al. (1995) (for Europe, including the Iberian Peninsula) and Pare (2000) for new evidences in France and Iberian Peninsula (in bold). (B) Distribution of bronze before 2200 BC and between 2200-1800 BC in Europe and Middle East, adapted from Pare (2000) and references there (filled circles indicate the amount of bronze objects in total metal artefacts).

In other European areas, as Central and Northern Europe, the transition from using copper to using bronze was a slower process lasting some centuries. During the transition, in Central Europe a bronze alloy with about 10% Sn was the choice of the workshops making up the alloys (Liversage and Northover, 1998). In Western France, analyses to the axes of the *Tréboul* hoard, attributed to an early phase of MBA, has shown an average of 12% Sn and 2% Pb (Briard et al., 1998). In Denmark, both copper and bronze artefacts were imported, and the first alloys showed various tin contents (probably the alloy was diluted and lost through indiscriminate recycling with unalloyed copper) and only later, with the import of bronze from Central Europe, did a single level of tin prevail: 6, 10 or 12%, depending on time and space (Vandkilde, 1998; Liversage and Northover, 1998).

For the Portuguese territory it is consensus that bronze alloy began to be used sporadically during 1st Bronze Age (BA) (Senna-Martinez, 1994), being only by the last quarter of the 2nd millennium BC, with the beginning of Late Bronze Age (LBA), that it took over the previous role of copper.

By LBA (~1250-550 BC in many Western European areas) full adoption of bronze had already happened in most of the European regions and numerous metal artefacts and deposits dating to this period have been found all over Europe (Huth, 2000). In the IP, where a "traditional" metallurgy had persisted until then (both in the typological models as in the use of unalloyed copper), this period is also characterized by a significant diversification in artefacts typologies (Melo, 2000), which can frequently be linked to either Atlantic or Mediterranean influences (Coffyn, 1985; Giardino, 1995).

In many European regions changes in the bronze alloy did also happened during this period. A decrease in Sn and an increase in Pb can be traced for most areas. In many Atlantic regions leaded bronzes began to be used – Pb was incorporated in contents that could reach values up to 10% (mainly for socketed axes, winged axes and palstaves) (Rovira and Gómez-Ramos, 1998) – probably as a technological-cultural choice to improve the castability of the metal (Mohen, 1990) or as a "cheaper" substitute of tin, to confer weight or change the colour of copper (?). A map with general trends of bronze compositions during LBA is shown in **Fig. 3.3** (note that during this time many Eastern Mediterranean territories began to experience the Iron Age period).

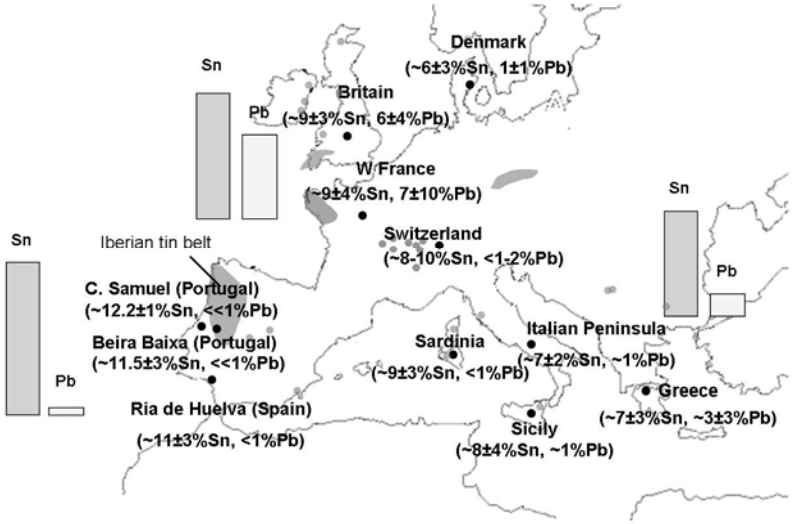

Fig. 3.3 Map with average bronze compositions during LBA in different regions of Europe (indicative of general trends) based on: Coffyn (1985) for *Coles de Samuel* (Portugal); Vilaça (1997) for Beira Baixa region (Portugal); Bauer and Northover (1998) for Switzerland; Liversage and Northover (1998) for Denmark; and Rovira and Gómez-Ramos (1998) for others. Location of tin deposits (grey areas) based on Merideth (1998).

When comparing the Iberian bronze composition with external Peninsular bronzes, a decrease in tin and an increase in lead content occur when moving from IP towards Atlantic and Mediterranean territories. Generally, the bronze used in the IP seems to be more similar to earlier bronzes used elsewhere in Western European regions, e.g. in the British Isles. This general trend can be a reflection of the exploitation of the local ores, namely tin ores (i.e. cassiterite) and thus a bronze metallurgy independent of the most Atlantic and Mediterranean areas, as suggested by Rovira and Gómez-Ramos (1998). If Iberian bronzes were made just by recycling imported bronzes lower contents in tin were to be expected since tin is lost preferentially to copper after some re-meltings (after several meltings the tin content can decrease to one third of the original value (Rovira and Montero, 2003) (see also **Fig. 3.4** for a simple scheme of metal use).

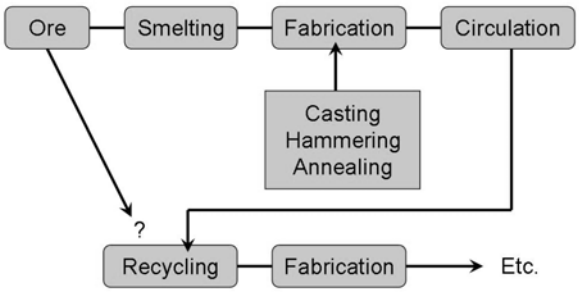

Fig. 3.4 Flow chart of metal use, based on Primas et al. (1998).

Despite the high number of bronze artefacts dating to LBA all over Europe, many aspects of prehistoric technologies for Cu-Sn production are so far unknown. Three hypotheses for bronze production have been proposed in literature (Coghan, 1975; Rovira, 2007): (1) smelting ores of tin and copper together, in a co-smelting operation; (2) adding one of the metals to the other still as ore, in a partial smelting operation; (3) smelting the ores separately and then alloying the metals in a melting operation.

Slags are a crucial evidence for the study of the technology involved in bronze production. Nevertheless, these are very scarce in Western European contexts, namely in the so called Atlantic areas (Craddock, 2007). Ancient tin slags have only been found in the French Finistère, dating to ~1390-1080 BC (end of MBA/beginning of LBA) (Giot and Lulzac, 1998) and in a burial at Caerloggas (Cornwall, SW England) dating to ca. 1500 BC (reference to Salter in Ottaway and Roberts, 2008; and Rovira, 2007). Most of the latest works on the topic are based on some copper-tin slags that have been found in a number of settlements in the IP, particularly in the Spanish territory, having the earliest ones (from CA to MBA) been found in North-Eastern regions, and later ones (dating to LBA and Early Iron Age) all over the Spanish territory (Gómez Ramos, 1999; Rovira, 2007). Studies on these slags and associated metallurgical debris (e.g. reduction vessels) has conducted to the proposal that bronze was initially obtained by (1) co-smelting, a technique that was still in use during LBA and Early Iron Age (EIA) in many settlements. There are also some possible evidences of (2) smelting cassiterite (tin oxide, as it appears in nature) with metallic copper during the transition from LBA to EIA, being the earliest evidences of (3) copper and tin alloying dated to VIII-VII century BC, probably as a result of Mediterranean contacts (Rovira, 2002b).

These studies suggest that in the IP, the adoption of bronze did not seem to change the extractive technology; bronze was obtained in a similar way as previously done in Chalcolithic times for copper, with a direct smelting of ores in reducing vessels (Gómez Ramos, 1999). Such primitive smelting process involved a very simple infrastructure, as those composed by a small pit excavated in the soil where a vessel containing the ores was placed, with charcoal, being heated from above. The resulting smelt was completely fragmented to recover the metallic lumps and prills (also called smelting droplets) leaving scarce evidences (e.g. slags) in the archaeological record (Hauptmann, 2007). The employ of a primitive and simple method for smelting for such a long period of time in the IP (about 3 millennia) has been related to its adequacy to the kind of minerals being worked – rich minerals, such

as copper carbonates, achieving acceptable efficient rates of metal recovery – and to the social adequacy – serving the metal requirements of the immediate local communities (Rovira, 2002b). A recent experimental co-smelting operation by Rovira et al. (2009) demonstrated that bronze could easily be obtained by this method, and that the resulting products were very similar to the ones found in the Spanish BA sites with metallurgical vestiges. The authors therefore suggest that working with copper and tin ores did not imply drastic technological changes in obtaining metal, being thus perfectly adequate to the pre-historic IP communities.

A different reality existed in most Eastern regions, as in Central and Alpine regions of Europe, Eastern Mediterranean and Middle East, that experienced important developments in technological knowledge and skills between CA and LBA, i.e. a transition from simple primitive, crucible based, small scale domestic production to mass production involving slag heaps and complex furnaces, the existence of large smelting sites distributing ingots, sites specialized in producing copper and sites specialized in producing tin (Adriaens et al., 1999; Burger et al., 2007; Rothenberg, 1985). Also, for the Middle East it has been shown that the partitioning coefficient for different impurities between the produced metal and the resultant slag changed from EBA to Roman times, showing a generalized higher value for the latest (more extracted metal) due to the stronger reducing atmospheres of the later extraction processes (Hauptmman, 2007).

Significant changes in the extractive metallurgy in the IP seems to just have happened at the beginning of Iron Age (IA) (frequently called the Orientalising period, or 1st IA) in those regions better connected with the Eastern Mediterranean, as indicated by the content of iron in the copper-based metals. Analysis of artefacts from Western European to the Eastern Mediterranean territories have shown that the metals smelted by the more primitive processes have Fe contents around 0.03% (generally <0.05%), whereas roughly purified product of the more advanced processes typically contains about 0.3% Fe, i.e. about an order of magnitude higher (Craddock, 1995). In the IP, bronzes of the LBA cultures on the Spanish interior regions show mainly <0.05% (95% of 49 artefacts analysed), whereas bronzes from Phoenician settlements dating to the beginning of the 1st millennium BC show much higher iron contents (as *Tejada* with an average of 0.27% Fe) (Craddock, 1995). Similarly to the IP, the BA copper alloys from elsewhere in the Western Europe have low iron contents representative of the simple, poorly-reducing process until the early 1st millennium BC when the introduction of the smelting of iron itself took place (Craddock, 1995).

The beginning of IA in IP also seems to have brought some modifications in the composition of the metals used; a significant incorporation of Pb and higher variations in Sn contents in the bronzes became common (**Fig. 3.5**). In the study of circa 190 artefacts from SE Spain (Montero Ruiz, 2008), representing a chronological sequence from LBA to 1st IA, a tendency to lower tin contents in bronzes (that can decrease from an average of 11.9 to 5.3%, i.e. to half the content), an increase in unalloyed copper artefacts and leaded bronze artefacts (that can reach about one third of the total artefacts analysed) was clearly observed from the earlier to the later period.

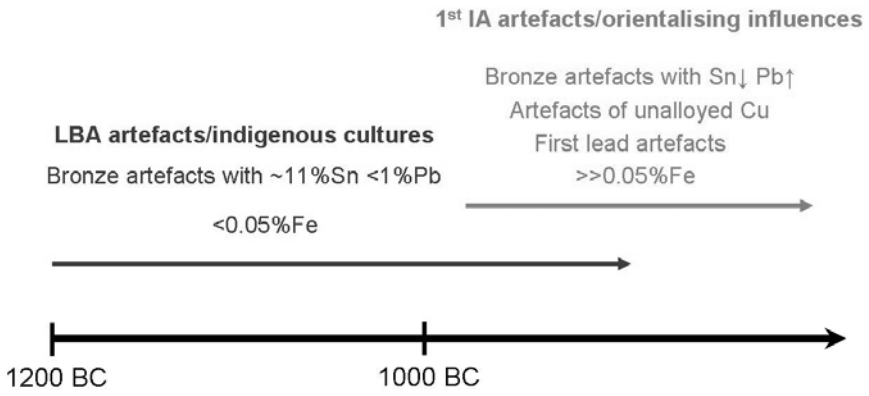

Fig. 3.5 Simple scheme with general compositional trends of copper-based Iberian artefacts from LBA and a posterior (or contemporary) IA metallurgical tradition (Fe wt.% based on Craddock, 1995).

Analyses of metallic items from the Phoenician site of *Almaraz* (W coast of Portugal) determined alloys with low Sn and variable Pb contents (Araújo et al. 2004), which can be easily distinguished from the previous alloys used during the LBA. Studies concerning the Orientalising sites of *El Palomar* and *Medellín* (Extremadura, W Spain), dated to the 7–6th century BC, determined mostly Cu–Sn alloys with <2% Pb, a small number of bronzes with a high amount of Pb (mainly large sized objects), and a few pieces of unalloyed copper (Rovira et al., 2005). Also, analyses of numerous metallic items from the Post-Orientalising site of *Cancho Roano* (SW Spain), dated to the middle of the 1st millennium BC (with a later chronology than *El Palomar* and *Medellín*) showed alloy compositions with highly variable concentrations of Sn and Pb and some lead artefacts (Montero Ruiz et al., 2003).

Iron was incorporated by the beginning of the 1st millennium BC in several places of the Mediterranean basin, and in its early appearance it seems to have been considered as "precious" material (Haarer, 2000). In the IP, the technology of iron manufacture has been traditionally linked with the Phoenician colonization. However, iron must have been known in earlier times since some iron artefacts have been found in LBA indigenous sites in the Beiras region (C Portugal) (Vilaça, 2006a), namely *Baiões*, possibly as a result of far-exchange contacts before Phoenician colonisation of the Iberian coasts (for indications of far-distance contacts see also section 2.3.4 – Loss of mass – the LBA weight case-study).

In respect to microstructural studies it has been shown by Rovira and Gómez Ramos (2003) that various thermo-mechanical operation chains have been performed by the ancient metallurgists to shape the metals (**Table 3.1**). During the CA most of the artefacts analysed by the authors were cold worked without annealing (nº. 2 in **Table 3.1**). With the advent of BA the type of works broadens, and by MBA the longer operation chains with sequential deformation and annealing were the most used (nº. 6 in **Table 3.1)** (Rovira, 2004). The broadening of the operations chain can be related to the development of the metallurgical skills, but also with the introduction of bronze. Adding tin to copper lowers the melting temperature of the metal (the liquidus temperature of a Cu-10Sn alloy is ~1000ºC, while unalloyed copper has a melting temperature of ~1200ºC) and allows a higher hardness after cold

work when compared to unalloyed copper (e.g. after 40% reduction a Cu-8Sn alloy increases its hardness from ~70 VHN to ~200 VHN, while unalloyed copper after the same reduction increases from ~70 VHN to ~120 VHN (Mohen, 1990)). According to the non-equilibrium binary phase diagram for copper-tin alloys (see Appendix II – Phase diagrams) with normal casting cooling rates, as attained in sand castings, bronzes with 8–12 wt.% Sn show a biphasic microstructure composed by α and δ phases. If a homogenizing heat treatment, as annealing, is performed, a monophasic (α phase) microstructure can be obtained in bronzes with Sn contents up to 15 wt.%. This heat treatment will improve the bronze mechanical properties since it results in the absence of the brittle δ phase in the final microstructure and in the transfer of Sn to the α solid solution. In the case of a mechanical work a posterior heat treatment will help to recover ductility, by promoting a recrystallization process. Thus, it seems reasonable that with the beginning of use of bronze more cycles of mechanical and thermal treatments where needed during shaping.

Table 3.1 Type of thermo-mechanical processing employed in pre and proto-historic artefacts. Due to the impossibility of distinguishing final deformations caused forging, use, or even a superficial finishing as polishing (even the latest can leave strain lines near to the surface (Wang and Ottaway, 2004) the last mechanical treatment includes all these possibilities. Also, the use of pre-heated moulds during LBA proposed by Rovira (2004) was included in the first thermal treatment

	Casting (C)	Heat treatment (T) (Homogenization annealing, mould pre-heated in LBA)	Plastic deformation (D) (Forging)	Heat treatment (T) (Recrystallization annealing)	Plastic deformation (D) (Forging, polishing or use)
(1) C					
(2) C+D					
(3) C+T					
(4) C+D+T		?			
(5) C+T+D					
(6) C+D+T+D		?			

Microstructural studies performed in various BA items from the British Isles (Allen et al., 1970) have also shown a large variety of thermo-mechanical cycles, which where performed in large size cast items as spear-heads and axes, possibly to improve the hardness of the blades and finish the surfaces.

Next, the studies on the metals and metallurgical related items from the various Portuguese sites are going to be presented. The Southern sites are presented first due to their earlier chronologies, followed by the sites in the Central region and at last the sites in the Northern region.

3.2 Southern Portugal – Alentejo region

3.2.1 *Povoado do Escoural* – A Chalcolithic metallurgy[7]

The Chalcolithic site of *Escoural* is located in Montemor-o-Novo, Évora district. It is a fortified habitat site, positioned over the cave of Escoural, famous for its human vestiges from the Palaeolithic

[7] The content of this section has adaptations from the following published work:

- E. Figueiredo, P. Valério, M.F. Araújo, R.J.C. Silva, M. Varela Gomes (2010) Estudo analítico de vestígios metalúrgicos do Povoado Cacolítico do Escoural (Évora, Portugal). In: J.A. Pérez Macias and E. Romero Bomba (Eds.), IV Encontro de Arqueologia del Suroeste Peninsular, *Collectanea* 145, Universidad de Huelva Publicaciones, Spain, (CD-ROM) (ISBN 978-84-92679-59-1).

until the end of the Neolithic period, and its rock art paintings and engravings. During the 1980's and 90's archaeological excavations were performed at the site, and an area related with metallurgical activities was discovered inside the walls (Gomes, 1991; Gomes et al., 1983, 1994). In this area two fire places were identified, and in their proximities seven crucible fragments and three metallic fragments were found (**Fig. 3.6**). Most of the crucibles show major vitrification in the borders in respect to the bottom indicating that the heating was made from above, in agreement with the most primitive metallurgical processes. Also, most of them show visible metallic inclusions in the borders and internal surfaces proving their use in ancient metallurgy. Among the metallic fragments one has an adhering slag (ESC-M-B5-L1 A). Additionally, numerous fragments of burned bones, iron minerals (with reddish and yellowish colours), fired clay and various fragments of vitrified material were collected in the area. The burned bone fragments had blue-grey colour (or purple hues), indicative of high temperature exposure in oxygen-poor environments (Walker et al., 2008). The relative abundance of this material, and its positioning near the fire places, lead the responsible members of the excavation to consider a relation of these bones with metallurgical activities (M.V. Gomes, personal communication).

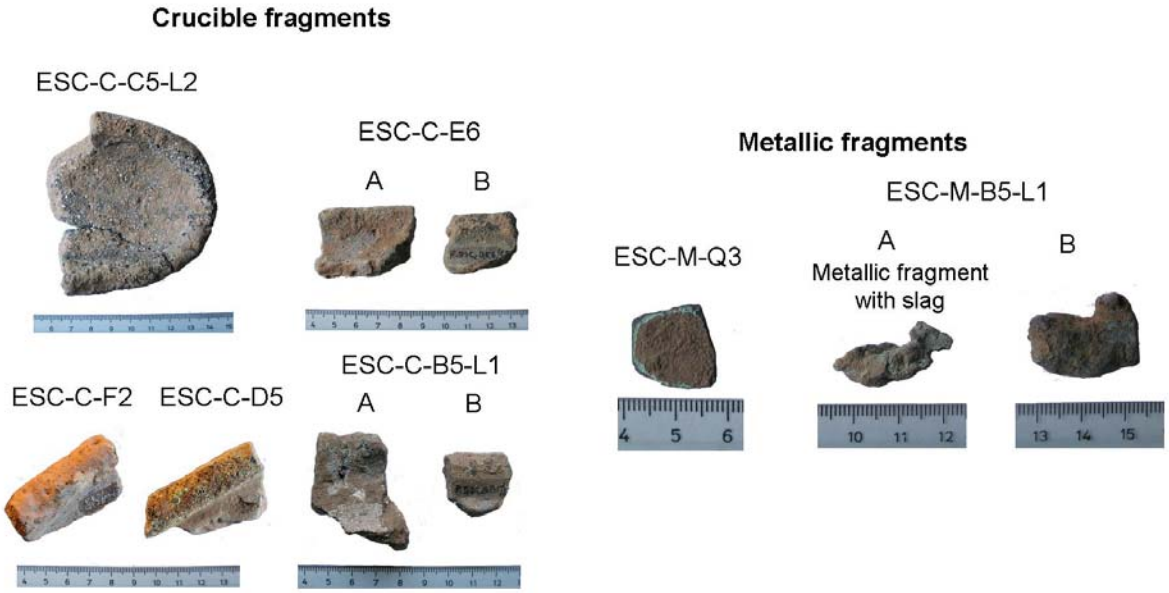

Fig. 3.6 Artefacts from *Escoural* related with metallurgy.

A fragment of bone collected in one of the fire places was Radiocarbon dated (ICEN 608 4120±100 BP), pointing out to an age of 2880-2570 (1σ) or 2920-2460 (2 σ) cal BC.[8] This indicates that the occupation of the site and its metallurgical activity date to the first half of the 3rd millennium BC.

The shapes of the fragments of crucibles show that crucibles with both flat and rounded bottoms with relatively short walls were used. The largest fragment indicate an elongated shape that bear similarities with other Chalcolithic crucibles found in Portuguese sites (e.g. in *Zambujal*, *Perdigões*, *Três*

[8] Acknowledgements are due to A.M. Monge Soares and J.M. Martins for the new radiocarbon calibration using the IntCal04 curve (Reimer et al., 2004) and the program OxCal v4.0.5 Bronk Ramsey 2007.

Moinhos, *S. Brás* and *Cerro de Santa Justa*) as well as in Southern and Northern Spanish sites (e.g. in the fortified settlement of *San Blas* (Cheles, Badajoz) or even in Chalcolithic sites of Zamora region (Delibes de Castro et al., 1998)). Two of the metal fragments (ESC-M-B5-L1-A and ESC-M-B5-L1-B) show irregular shapes, resembling unfinished products (of smelting operations?), and the metallic fragment ESC-M-Q3 shows a more regular shape – "sheet" like – resembling a fragment of a blade.

All the artefacts were submitted to EDXRF analysis. The crucibles were analysed on two different areas, one on the external side, representative of the crucible material composition, and another on the internal side and/or border, where metallic inclusions and metallurgical vestiges could be expected. Metallic inclusions that were clearly visible in five crucible fragments were analysed by micro-EDXRF without any surface preparation. Micro-EDXRF analyses were also performed on the metal bulk of the three metallic fragments after sampling. The samples were also submitted to microstructural study by OM and SEM-EDS (ESC-M-B5-L1 A and ESC-M-Q3).

EDXRF analyses were also made in the fired clay, on some of the vitrified materials and on some of the iron minerals. None of these materials showed vestiges related to Chalcolithic metallurgy, as Cu or As. Possibly, the fired clay and the vitrified fragments are remains of positive structures, being the latest related with fire structures, but clearly not a direct result of some metallurgical process (as slag). The presence of various iron minerals on the site (the site is positioned over marbles), can indicate that these were brought from nearby areas, since these minerals are abundant in the region. The relationship of these with a metallurgical activity is not evident; nevertheless one can suggest that they can be a result of the extraction of copper minerals in iron hats, being the beneficiation of the minerals made on the site. A stone with a shape resembling a mining hammer was found at the site (M.V. Gomes, personal communication), which can be an evidence of ore processing by the local community to conduct smelting activities. The presence of iron minerals associated with copper ores has previously been described for other Chalcolithic sites with metallurgical evidences from Southern and Central Portugal, as the fortified *Povoado do Porto das Carretas* (Mourão) (Valério et al., 2007b), *Castelo Velho de Safara* (Moura), *Povoado de Porto Mourão* (Moura) (Soares et al., 1994) and VNSP (Azambuja) (Müller and Soares, 2008).

The EDXRF analysis made on the crucibles show the presence of Cu in all the fragments, and variable amounts of As (**Fig. 3.7**) (As is absent only in the ESC-C-B5-L1-A and ESC-C-D5 fragments). Generally, these elements were identified with higher intensities in the analysis made over the internal and border side of the crucibles, being absent or identified with lower intensities on the analysis made over the external sides (**Fig. 3.8**). In all the crucible fragments Fe, Sr and Zr were identified in similar intensities in the two sides, indicating that they are part of the crucible clay. Only Ca was identified with higher intensities on the areas were also the Cu and As elements showed more intense peaks – the internal side and border areas.

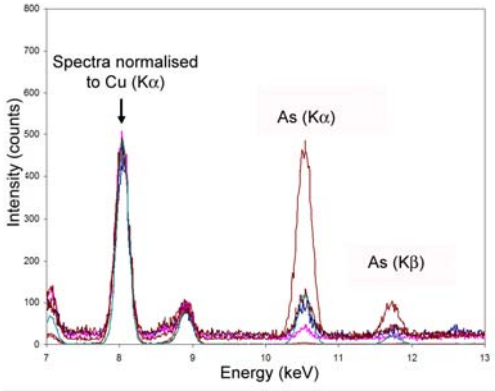

Fig. 3.7 EDXRF spectra of the seven crucibles from *Escoural* demonstrating the presence of Cu and As in variable contents.

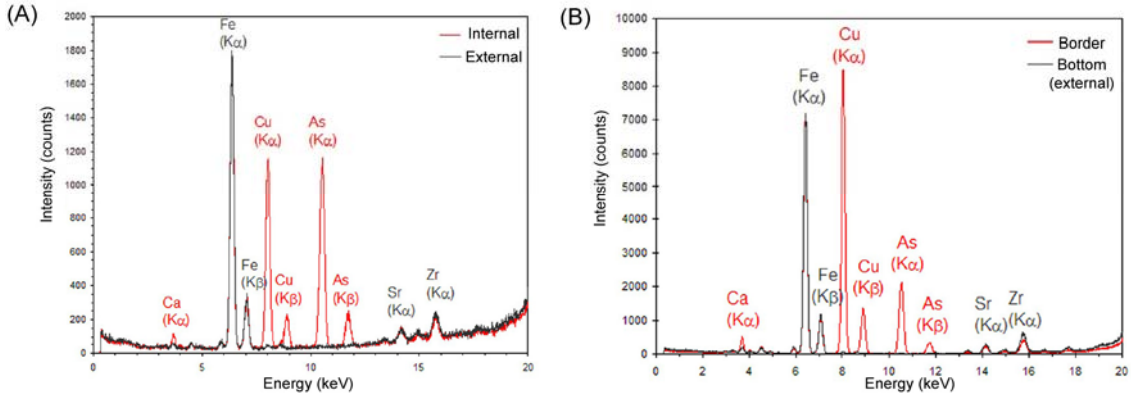

Fig. 3.8 EDXRF spectra of different areas in (A) ESC-C-B5-L1 B and (B) ESC-C-F2 crucibles from *Escoural*.

The presence of Ca does probably result from the charge used in the metallurgical process. Charcoal contains about 3 to 20% of ash (depending upon whether the charcoal is made from small branches with bark attached, the bark having a far higher proportion of ash than the wood itself) and ash can contain up to 60 wt.% of CaO (Tylecote, 1962). Some minerals with Ca associated to the ores could also be present, or materials Ca rich could be added as a fluxing agent, although intentional fluxing is not proven for this early period. On the other hand, taking into consideration the archaeographic data, bones do also contain Ca and their use as fuel has been proved for remote times. This material combined with ash could have benefits in a metallurgical operation as smelting: ash is important to lower the liquidus temperature of the slag; and a combination of bones and wood enables a significant increase in the duration of combustion – the higher the proportion of bone the longer the combustion lasts, regardless of the total mass of fuel (Théry-Parisot, 2002).

Although the crucibles were confirmed to have been used in metallurgical operations, the nature of them, as for melting or smelting, is not evident with this analysis. The presence of metallic inclusions in most of the crucible borders, as well as the presence of an intense vitrification of the ceramic material can, however, suggest that some (most?) were used in smelting processes.

The micro-EDXRF analysis made on some metallic inclusions of the crucibles confirm the presence or absence of As among the different fragments, and suggest that the As content varies within different inclusions in each crucible. The results show inclusions with variable As contents: from absent (n.d.) to ~4% (three analyses in each one of the five crucibles) (**Fig. 3.9**).

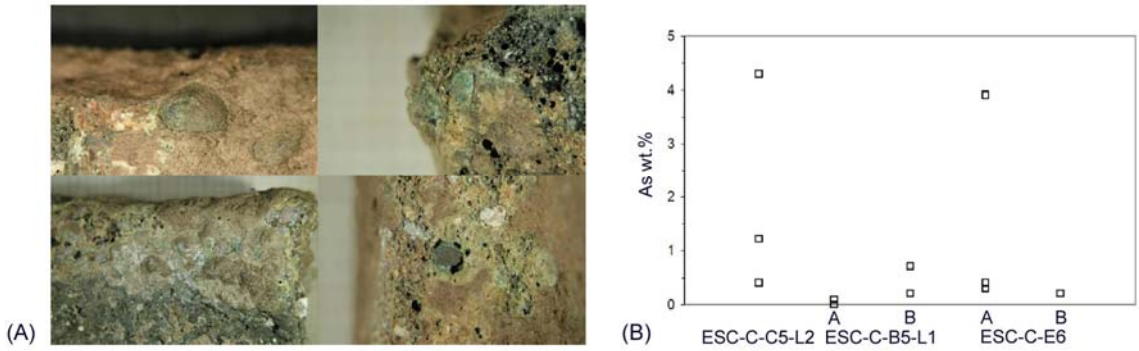

Fig. 3.9 (A) Pictures showing the metallic inclusions in the crucibles from *Escoural*; (B) Micro-EDXRF results of the As contents in metallic inclusions of crucibles.

The micro-EDXRF analysis made on the sampled metallic fragments show that all are made of copper, with variable (and relatively low) As contents, being thus in agreement with the composition of the crucible inclusions. The regular-shaped fragment ESC-M-Q3 is the one that shows the highest As content (~2%), having the irregular-shaped fragment ESC-M-B5-L1 A ~0.5% As, and the ESC-M-B5-L1 B fragment with adhering slag absence of As (**Table 3.2**).

Table 3.2 Results of the EDXRF and micro-EDXRF analysis made over the sampled metallic fragments from *Escoural* (EDXRF results are given in a semi-quantitative way; composition is given by average of three micro-EDXRF analyses ± one standard deviation)

Item	Type of analysis	Composition (wt.%)						
		Cu	Sn	As	Pb	Sb	Fe	Ni
ESC-M-Q3	EDXRF	+++	n.d.	+	n.d.	n.d.	+	n.d.
	Micro-EDXRF	98.0±0.6	n.d.	1.9±0.6	n.d.	-	<0.05	n.d.
ESC-M-B5-L1 B	EDXRF	+++	n.d.	vest.	n.d.	vest.	+	n.d.
	Micro-EDXRF	99.8±0.1	n.d.	0.2±0.1	n.d.	-	<0.05	n.d.
ESC-M-B5-L1 A	EDXRF	+++	n.d.	vest.	n.d.	n.d.	++	n.d.
	Micro-EDXRF	99.9±0.0	n.d.	n.d.	n.d.	-	<0.05	n.d.

+++ >50%; ++ 10-50%; + 1-10%; vest. (Vestiges) <1%; n.d. not detected

The absence of other impurities (as Pb, Sb, Ni) and the low Fe content is in agreement with other Chalcolithic artefacts from the Portuguese territory and neighbouring areas, being the low Fe content characteristic of primitive metallurgy, with poorly reducing conditions (the Fe + content in EDXRF analysis is a result of incorporation of Fe from burial soil in the corrosion (see section 2.3.1 – Superficial analysis – the *Pragança* and *Escoural* case-studies), and Fe ++ in ESC-M-B5-L1 A is a result of contribution from the adhering slag, as demonstrated further below).

The OM observations made on the three metallic fragments allowed a differentiation based on their microstructures: the regular shaped ESC-M-Q3 and the irregular shaped ESC-M-B5-L1 B fragments show a coarse grain microstructure; and the irregular shaped ESC-M-B5-L1 A fragment with adhering slag shows a dendritic structure.

The two first fragments have a microstructure composed by α-Cu grains, with numerous pores of spherical shape and various sizes (**Fig. 3.10**). The etching showed absence of twining and slip bands. These microstructures represent a solidification product, with absence of posterior thermo-mechanical treatments (as-cast structures).

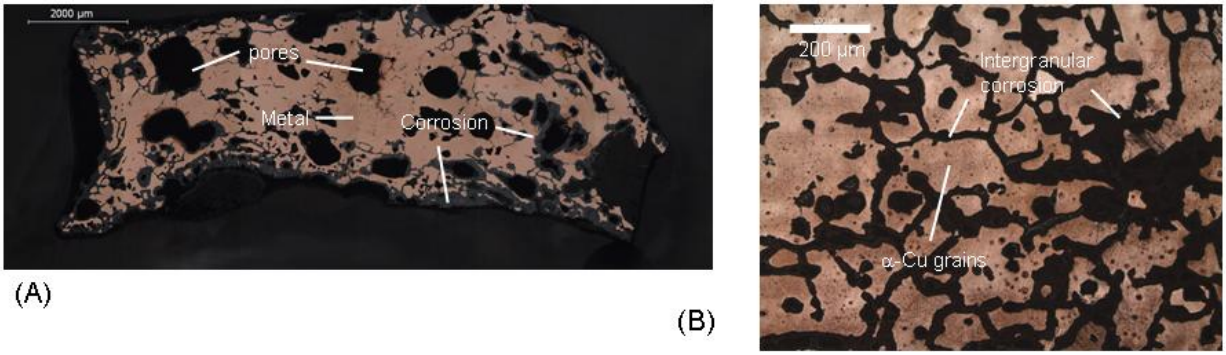

Fig. 3.10 OM images of the microstructures of (A) ESC-M-B5-L1 B irregular shaped fragment (not etched) and (B) ESC-M-Q3 regular shaped fragment (etched).

Detailed observation of the fragment ESC-M-Q3 in the SEM-EDS showed the presence of a Cu-O layer, most likely CuO (tenorite), that covers most of the surface of the fragment (**Fig. 3.11**). A tenorite layer is very fragile and is created under very specific conditions: by a direct oxidation of the metal in contact with air at high temperatures (**Fig. 3.12**). Its presence can be a result of casting, an annealing treatment, or an unintentional contact with fire. The shape of this fragment and its composition suggests rather that the tenorite was formed by the pouring of the metal to an open mould or a plain surface since: (1) copper would not necessary need a softening annealing treatment after casting and previous to any mechanical work; and (2) by Chalcolithic times one-piece open moulds were at use which would result in the oxidation of the surface during cooling (two-piece closed moulds seem to have appeared just by BA). Furthermore, the presence of the tenorite layer suggests that this item has not been significantly handled after solidification.

The irregular shaped ESC-M-B5-L1 B fragment has roundish forms that show similarities with unfinished metal products, as large nodules that result from a smelting operation. The large size grains, resulting from a slow solidification, and its high porosity, converge with this hypothesis.

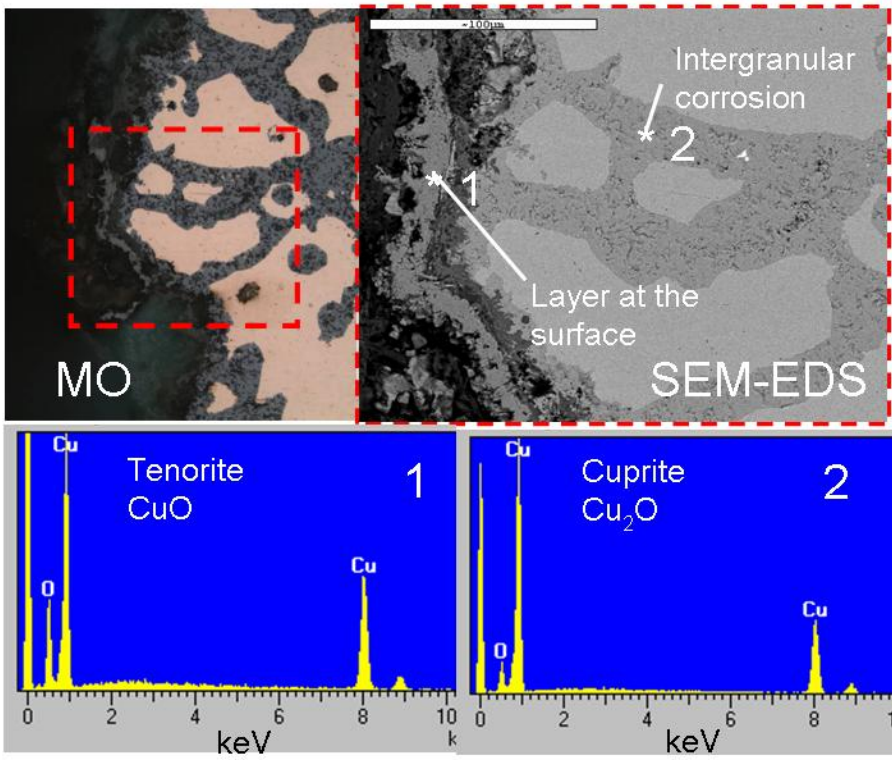

Fig. 3.11 OM observations and SEM-EDS analysis of the surface layer of tenorite in ESC-M-Q3 metallic fragment.

Fig. 3.12 Laboratorial experiments showing the formation of a surface layer of tenorite. At left, the annealing of copper-based metal bars and at right the pouring of metal to an open mould.

The ESC-M-B5-L1 A fragment has a different microstructure. The OM observations and SEM-EDS analysis identified the metallic part as being constituted by primary dendrites of cuprite (Cu_2O), in a eutectic matrix of α-Cu and Cu_2O (**Fig. 3.13**). The slag that encloses most of the metallic part is constituted by a vitreous matrix, with the following elements: O, Mg, Al, Si, Ca, Fe, Cu, and sometimes K (**Fig. 3.14**). The relative contents of each element vary, however Si is always present with the most intense peak. Within the alumino-silicate matrix inclusions of Si, small globules of metallic copper, magnetite and delafossite were observed. Also, globules of copper carbonate were observed which can be a result of corrosion through open fissures. Magnetite and delafossite have been found with relative frequency in primitive slags, namely Chalcolithic slags from the neighbouring Spanish territory. Their presence suggests that the conditions on the reaction vessel were

relatively oxidising and the particular presence of delafossite indicates that the fragment has been subject to temperatures >1100ºC (Rovira, 2004).

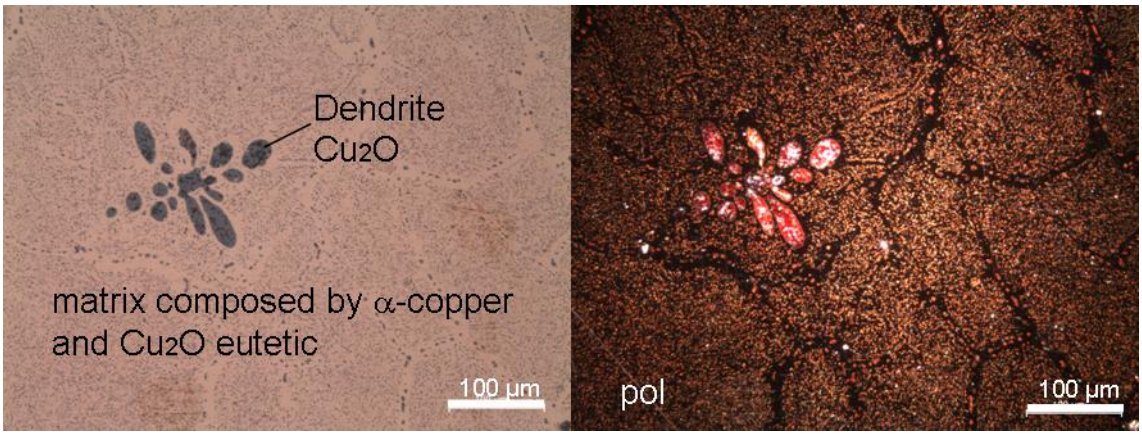

Fig. 3.13 OM images of the metallic part of the ESC-M-B5-L1 A fragment.

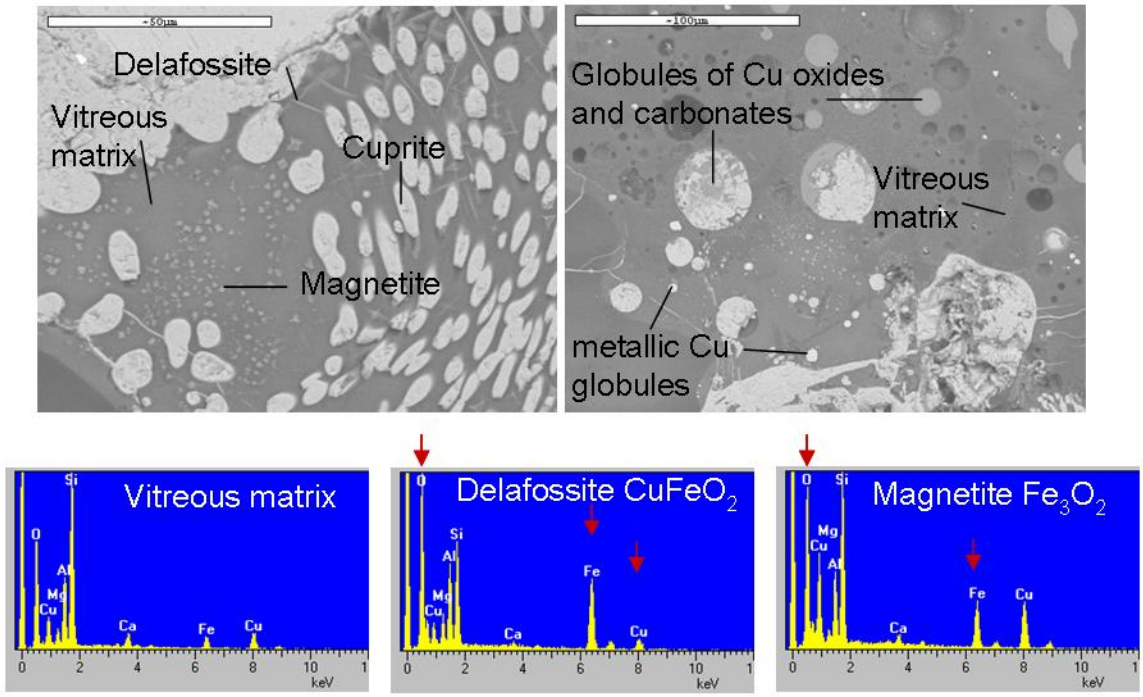

Fig. 3.14 SEM-EDS images of the slag part of the ESC-M-B5-L1 A fragment. On bottom some spectra that allowed the identification of delafossite and magnetite (by comparison with vitreous matrix).

The microstructure of the B5-L1 A fragment suggests that this fragment is a primary product of a metallurgical reaction, likely a crucible, and that the quantity of oxygen dissolved in the mixture was relatively high, resulting in a copper with ~0.5% O (based on Cu-O phase diagram, see Appendix II). The presence of Cu_2O eutectic in pure coppers is expected in respect to impure or alloyed coppers, since As and Sn act as deoxidizing elements, transferring the oxygen from the molten metal to the slag. In fact, in the ESC-M-B5-L1 B fragment that has 0.2% As the presence of Cu_2O is much scarcer, being only observable in some grain boundaries. The presence of Cu_2O eutectic in Chalcolithic items from the Portuguese territory has been demonstrated before, as in the case of a blade axe from VNSP (Silva et al., 2008).

In the main, the study on the *Escoural* collection suggests that metallurgical operations were performed at the site, involving copper with low impurity contents, being the main one As. The highly vitrified crucible fragments with prills entrapped, as well as the metallic fragment with adhering slag, are strong indications pointing out to local smelting operations. Possibly, local ores were explored and the beneficiation and extraction process was performed inside the settlement.

3.3 Central Portugal – Estremadura and Beiras regions

3.3.1 *Castro de Pragança* – a site with a long diachrony[9]

Castro de Pragança is located in Cadaval, Lisbon district, and has provided one of the largest Pre-historic metallic collections of the Portuguese territory. Most of the artefacts are currently in the *Museu Nacional de Arqueologia* (MNA), where they exceed half a thousand, including artefacts, fragments and metallurgical remains.

The artefacts cover a wide range of typologies and chronologies, from Chalcolithic to Roman times. Some of the Chalcolithic artefacts and a few BA artefacts (probably mainly from 1st BA period) were analysed in the SAM project: 53 artefacts, of which 42 of copper and 11 of bronze. Despite this first significant archaeometallurgical approach, there is a limit of usability of the data since the correspondence between the artefact analysed and the elemental results is not easily found: each analysis is only labelled by an internal SAM number and a word defining the general typology of the artefact. Also, even if the correspondence is found, some mistakes have been discovered, as in the case of the VNSP "cutler" (n.º 1184) that has been published as being a bronze but a more recent analysis by EDXRF have shown that it is in fact made by copper, as suggested by its colour and typological features (Figueiredo et al., 2007). Such mistakes, that can become frequent when dealing with such high number of analysis, can lead to misleading debates, as the present cutler that has been presented until very recently as being an exciting example of a Chalcolithic typology made of BA metal (e.g. Soares, 2005; Müller and Soares, 2008). Also, and in respect to the few bronze artefacts analysed by the SAM project, the Sn content is generally given by ~10% or >10%, thus, in a semi-quantitative way.

More recently, another approach over the *Pragança* collection has begun, conducted in collaboration with archaeologists and MNA in the framework of different projects. This approach has tried to focus not only in the earliest metals, but also on those of later chronologies, as LBA and IA. A first analytical work in selected items was made by the author in the framework of the 5th year degree in Conservation and Restoration, which showed that there is a significant number of artefacts dated to LBA that are composed by binary bronze (Figueiredo et al., 2007). Also, the typological study of the collection that is being made by A.A. Melo has shown that besides the artefacts previously known to

[9] Part of the content of this section has adaptations from the following published work:

- A.A. Melo, E. Figueiredo, M.F. Araújo, J.C. Senna-Martinez (2009) Fibulae from an Iron Age site in Portugal. *Materials and Manufacturing Processes* 24, 955-959.

the general public many metallurgical remains are part of the collection, giving the indication that metallurgical operations were performed at the site.

In the present work, due to the museological value of most items and the early stage of the study of the collection (taking into account the complexity of the collection), only non-invasive EDXRF analyses were performed to selected items (stage [1] in section 1.2.1). In the future, more detailed analysis, using other methodologies, should be applied to selected items.

The materials studied in this work include 52 metallic artefacts and fragments, 9 metallurgical remains that include one metallic nodule and vitrified fragments, one intact crucible, and some fragments of colanders (**Fig. 3.15-3.17**). These latest were also included since they have occasionally been related to metallurgical processes by finders (Hunt Ortiz, 2003). This study will allow a further approach over the variety of metal types present in the collection, an evaluation of the relationship of the vitrified fragments and colanders with metallurgy, and an evaluation of the use of the crucible. In respect to the previous studies, this work will provide a further knowledge of the variety of metals present in the collection, and present a first evaluation of the metallurgy that could have been practiced at the site.

Fig. 3.15 Items studied from *Pragança* (B-bronze; C-copper; I-iron; L-lead).

Fig. 3.16 Items studied from *Pragança* (B-bronze; C-copper).

Fig. 3.17 Items studied from *Pragança* (B-bronze; C-copper; LB-leaded bronze).

The EDXRF analysis clearly distinguished among the different types of metals used in the manufacture of the **artefacts and fragments**. Tables have been organized according to the type of metal identified: **Table 3.3** for copper artefacts; **Table 3.4** for bronze artefacts; **Table 3.5** for a lead artefact; and **Table 3.6** for composite artefacts involving iron components.

Table 3.3 EDXRF results of copper artefacts from *Pragança*

		Cu	Sn	Pb	As	Sb	Fe	Ni
983.299.165	Small axe(?)	+++	vest.	n.d.	+	n.d.	vest.	n.d.
983.299.201	Blade frag.(?)	+++	vest.	n.d.	+	n.d.	vest.	n.d.
983.299.202	Saw frag.	+++	n.d.	n.d.	+	n.d.	vest.	n.d.
983.299.207	Small axe(?)	+++	n.d.	n.d.	+	n.d.	vest.	n.d.
983.299.210	Blade/knife frag.(?)	+++	n.d.	n.d.	+	n.d.	vest.	n.d.
983.299.200	Axe blade frag.	+++	n.d.	n.d.	+	n.d.	vest.	n.d.
983.299.185	Awl	+++	n.d.	n.d.	vest.	n.d.	vest.	n.d.
983.299.187	Awl	+++	vest.	n.d.	vest.	n.d.	vest.	n.d.
986.119.28	Flat axe	+++	n.d.	n.d.	vest.	n.d.	vest.	n.d.
986.161.2115	Small axe(?)	+++	n.d.	n.d.	vest.	n.d.	n.d.	n.d.
983.299.182	Frag. of artefact	+++	vest.	n.d.	n.d.	n.d.	vest.	n.d.

+++ >50 wt.%; ++ 10-50 wt.%; + 1-10 wt.%; vest. (Vestiges) <1 wt.%; n.d. not detected

Table 3.4 EDXRF results of bronze artefacts from *Pragança* (the weights that have been object of a metrological study in section 2.3.4 are highlighted in dark grey)

		Cu	Sn	Pb	As	Sb	Fe	Ni
983.299.209	Blade/dagger frag.(?)	+++	++	vest.	vest.	vest.	+	n.d.
983.299.206	Dagger frag. with rivets	+++	++	+	n.d.	vest.	+	n.d.
983.299.205	Blade/dagger frag.(?)	+++	++	+	n.d.	n.d.	+	n.d.
983.299.208	Blade/dagger frag.(?)	+++	++	n.d.	vest.	vest.	+	n.d.
983.299.203	Blade/dagger frag.(?)	+++	++	vest.	vest.	vest.	+	n.d.
983.299.163	Rod with hole	+++	++	n.d.	vest.	vest.	vest.	n.d.
983.299.186	Awl/needlle(?)	+++	++	vest.	vest.	n.d.	vest.	n.d.
986.161.1098	Weight with a hole (9.73 g)	++	++	+++	n.d.	vest.	vest.	n.d.
986.119.27	Palstave	+++	++	vest.	vest.	vest.	vest.	n.d.
983.299.174	Weight bitroncoconic 18.72g	+++	++	vest.	vest.	vest.	vest.	n.d.
983.299.174	Weight bitroncoconic 9.32 g	+++	++	vest.	vest.	vest.	vest.	n.d.
983.299.174	Weight bitroncoconic 8.70 g	+++	++	vest.	vest.	vest.	vest.	n.d.
983.299.174	Weight bitroncoconic 4.79 g	+++	++	+	vest.	vest.	vest.	vest.
983.299.174	Weight bitroncoconic 4.21 g	+++	++	vest.	n.d.	vest.	vest.	vest.
983.299.174	Weight bitroncoconic 4.10 g	+++	++	+	n.d.	vest.	vest.	n.d.
983.299.174	Weight bitroncoconic 4.08 g	+++	++	vest.	vest.	vest.	vest.	n.d.
983.299.174	Weight bitroncoconic 3.87 g	+++	++	vest.	vest.	vest.	vest.	n.d.
983.299.174	Weight bitroncoconic 2.86 g	+++	++	vest.	vest.	n.d.	vest.	n.d.
983.299.174	Weight bitroncoconic 1.82 g	+++	++	vest.	vest.	vest.	vest.	n.d.
983.299.174	Weight sphere with hang(?) 6.26 g	+++	++	vest.	vest.	vest.	vest.	n.d.
983.299.174	Weight sphere with hang(?) 3.17 g	+++	++	vest.	vest.	n.d.	vest.	n.d.
983.299.174	Weight sphere 4.65 g	+++	++	vest.	vest.	vest.	vest.	n.d.
983.299.174	Weight sphere 3.29 g	+++	++	+	vest.	vest.	vest.	n.d.
983.299.174	Weight sphere 3.20 g	+++	++	vest.	vest.	n.d.	vest.	n.d.
983.299.170	“Sheet” with two holes frag.	+++	++	n.d.	+	+	vest.	n.d.
986.161.2114	Nail from helmet(?)	+++	++	vest.	+	+	vest.	vest.
983.299.183	Ring (spiral)	+++	++	n.d.	n.d.	vest.	vest.	vest.
983.299.189	Ring frag.	+++	++	n.d.	n.d.	n.d.	vest.	n.d.
986.161.2111	Button from helmet(?)	+++	++	vest.	vest.	n.d.	+	n.d.
986.161.2112	Button (conic)	+++	++	n.d.	vest.	n.d.	vest.	n.d.
986.161.2113	Button (conic)	+++	++	vest.	vest.	n.d.	+	n.d.
2005.10.27	Fibula	+++	++	vest.	n.d.	n.d.	+	n.d.
983.299.180	Fibula	+++	++	vest.	n.d.	n.d.	vest.	n.d.
2005.10.75	Fibula	+++	++	+	n.d.	vest.	vest.	vest.
2005.10.76	Fibula	+++	++	+	n.d.	vest.	+	n.d.

+++ >50 wt.%; ++ 10-50 wt.%; + 1-10 wt.%; vest. (Vestiges) <1 wt.%; n.d. not detected

Table 3.5 EDXRF results of a lead artefact from *Pragança*

		Cu	Sn	Pb	As	Sb	Fe	Ni
983.299.177	Weight with a hole	vest.	vest.	+++	n.d.	n.d.	vest.	n.d.

+++ >50 wt.%; ++ 10-50 wt.%; + 1-10 wt.%; vest. (Vestiges) <1 wt.%; n.d. not detected

Table 3.6 EDXRF results of composite artefacts – bronze artefacts with iron components – from *Pragança* (the fibula 2005.10.77 has been subject of a more detailed study by micro-EDXRF in section 2.3.1)

		Cu	Sn	Pb	As	Sb	Fe	Ni
2005.10.26	Fibula	+++	++	+	n.d.	vest.	+	n.d.
2005.10.77	Fibula	+++	++	+	n.d.	+	++	n.d.
2005.10.79	Fibula	+++	++	+	n.d.	vest.	++	vest.
2005.10.80	Fibula	+++	++	+	n.d.	vest.	++	vest.
983.299.164	Fibula	+++	++	+	n.d.	vest.	++	n.d.

+++ >50 wt.%; ++ 10-50 wt.%; + 1-10 wt.%; vest. (Vestiges) <1 wt.%; n.d. not detected

The results have shown that most of the studied artefacts are made of bronze (67%), and among these, the majority (57 of 67%) has minor quantity of impurities (including Pb). The next group is composed by copper artefacts (21%), and the latest ones are composed by other metals, such as the composite artefacts that have iron components (10%) and the lead artefact (2%) (**Fig. 3.18**).

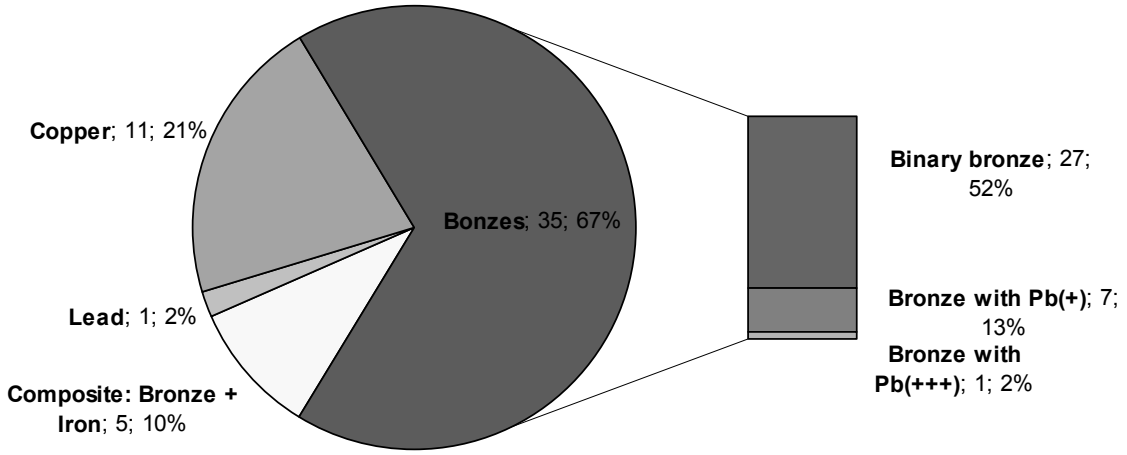

Fig. 3.18 Relative frequencies of metal type in the analysed metallic artefacts from *Pragança*.

Most of the copper artefacts have typological features which clearly relate them to the Chalcolithic period, i.e. simple shapes, namely blades, saws and awls. The copper is relatively pure, bearing similarities with the Chalcolithic metals studied from *Escoural* (section 3.2.1), with only As element being present in values >1% (+) in five artefacts. As described before, this feature is common among the Chalcolithic metals from the IP (Sangmeister, 2005), and the issue of intentionality in the fabrication of copper with relatively high As contents (arsenical coppers) is not going to be discussed here due to the small number of copper artefacts analysed and the lack of microstructural studies that could aid the interpretation. However, it can be worth mentioning that all the artefacts with As (+) have "blade/sheet" shapes (note that the same happens for the *Escoural* fragment ESQ-M-Q3), and that typologies as awls and plain axes do not show high As contents, which is in agreement with the argument of some authors for the use of coppers with higher As contents to produce some specific typologies (see section 3.1 – Archaeometallurgical Introduction).

The bronze artefacts show a higher typological diversity. Some show complex shapes (as the buttons, rings and nail) and may be attributed to LBA (see section 3.1 - Archaeometallurgical Introduction).

Others show more simple shapes, as the daggers, that bear similarities with copper ones, being possibly attributed to an earlier period (i.e. 1st BA).

The majority of the bronze artefacts (52% out of 67%) have a low impurity pattern, with vestiges of Pb, As and Sb. Ni is rarely detected, and the Fe contents are most probably due to soil contaminations in the corrosion layers (see Chapter 2 – Corrosion Study). In respect to the previous copper artefacts one can point out two differences: the presence of Pb and Sb and a generally lower content in As. These differences can be a result of different commercial routs of ore or metal supply; different types of ores used to smelt copper; the incorporation of additional impurities during bronze manufacturing due to the use of metallic tin or tin ores with these impurities; or they can even be a reflect of different extractive technologies. This theme is going to be discussed further along the work, when unalloyed copper artefacts from LBA sites are presented (section 3.3.3.1; section 3.3.3.4; section 3.4.1.1; section 3.4.1.2; and also section 3.5 – Archaeometallurgical final discussion and conclusions).

Some of the bronze artefacts show slightly higher Pb contents (represented as +), that can be interpreted as a result of thicker corrosion layers or slightly higer Pb contents in the alloy (e.g. ~1-2 %) (see Chapter 2 – Corrosion Study, section 2.3.2). Only one artefact, the weight with a hole (986.161.1098), shows a different composition, with much higher Pb content (+++). This artefact is most certainly a Cu-Sn-Pb alloy (leaded bronze), and its shape associates it to a later period than the other weights that are of binary bronze with minor impurities and are attributed to LBA (Vilaça, 2003) (see also the metrological study on the LBA weights that has been presented in section 2.3.4).

The single lead artefact, a weight, has Cu and Sn vestiges (Fe can be due to soil contamination in corrosion layers). The presence of lead artefacts becomes regular during the IA. Lead weights, with similar shapes, have been found in the Orientalising site of *Cancho Roano*, in a ca. V century BC context, suggesting that this weight can be from a similar period.

The nine fibulae from *Castro de Pragança* are a rather unusual finding for a settlement in the Portuguese Estremadura; ancient fibulae are prestige items, and for that reason they are normally recovered from burials. Since their typological features are often characteristic of a specific region and a short time span, they can frequently be attributed to specific periods and cultural contexts. According to their typological classification, the nine fibulae from *Pragança* seem to be Iberian productions, and can be attributed to a chronological time span that goes from IA through to the Roman Conquest – their typological and chronological attribution is shown in **Table 3.7**.

Table 3.7 Typological, chronological and regional classification of the fibulae, based on Ponte (2006a) with contributions of A.A Melo

Fibula number	Typological affinity	Chronological classification	Regional classification
2005.10.26 2005.10.27	Acebuchal type	8th-7th c. BC	Iberian Peninsula (mainly SE regions); Typology suggests Western Mediterranean influences
2005.10.77 (Cu-10Sn-2Pb) (section 2.3.1)	La Tène I	Developed 1st IA (7th c. BC) and fully spread in 2nd IA (through 3rd c. BC)	Fully widespread
2005.10.75 2005.10.76 983.299.180 2005.10.79 2005.10.80	Transmontano type (subtype of La Tène I)	Beginning 2nd IA (5th c. BC) until 1st c. AD	Widespread in Northern Iberian Peninsula (associated in NW with the "Castreja" culture)
983.299.164	La Tène III	3rd c. BC-1st c. AD	Widespread in Iberian Peninsula

Micro-EDXRF analyses were performed in the various components of the fibulae, with no surface preparation. Results showed that all the components are made of bronze except for the axis of 5 fibulae that are made of iron (**Fig. 3.19**) (the fibula 2005.10.77 has also been analysed in a small area without superficial corrosion, demonstrating that the bow is made of an bronze alloy with ~10 wt.% Sn and ~2 wt.% Pb, see section 2.3.1).

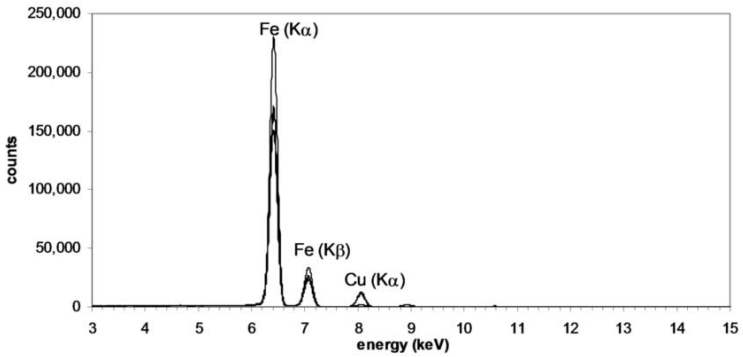

Fig. 3.19 Micro-EDXRF spectra of the iron axles of the fibulae from *Pragança* (2005.10.77, 2005.10.80, 2005.10.79 and 983.299.164).

The use of iron to make the axles can be understood as: (1) a substitution of the more valuable bronze by the less valuable iron to manufacture the less visible component (by the VII century BC onwards iron was no longer considered a "precious" material as it seems to have been in its earlier appearance); or as (2) a new technological feature, since the bronze axles were probable not as hard as iron and thus suffered deformation much easier. In the sociologic scope it seems to synchronise with a new social organization of the proto-historic communities, contributing to the specialization and division of the economic activities (Ponte, 2006b).

Within the **metallurgical remains**, EDXRF analyses have also provided valuable data (**Table 3.8**). All the metallurgical remains could clearly be associated to metallurgy, and were either related to binary bronze (56%) or to copper (44%) metallurgy (**Fig. 3.20**). These metallurgical remains can thus be attributed to a time span from Chalcolithic to LBA, or even IA, if we consider that bronze with minor impurities was still circulating at this time. Although the nature of the operations that produced

this items (smelting or melting) cannot be determined with the present analysis, the evidences show that both copper and bronze metallurgical activities were performed at the site.

Table 3.8 EDXRF results of metallurgical remains from *Pragança*

		Elements identified (high intensities in bold)	Related to metallurgy of
983.299.197	Metal/slag(?) (A)	Mn Fe **Cu** As **Sn**	Bronze
983.299.197	Slag (?) (B)	Mn Fe **Cu** As? Pb? **Sn**	Bronze
983.299.192	Slag (?)	Mn Fe (Ni) **Cu** (Zn) As(-) **Sn**	Bronze
983.299.198	Vitrified crucible/slag (?)	Ca Mn Fe **Cu** Zn	Copper
983.161.2117	Metal (A)	Ca Mn Fe **Cu** As? Pb **Sn**	Bronze
983.161.2117	Vitrified crucible(?) (B)	Ca Ti(-) Mn Fe **Cu** Zn (Rb Sr Y Zr)	Copper
983.161.2117	Slag (?) (C)	Ca Ti(-) Mn Fe **Cu** Zn? As? Pb? **Sn**	Bronze
983.161.2118	Metal	Ca Fe **Cu** As Pb?	Copper
983.161.2118	Metal nodule	Fe **Cu** As Pb?	Copper

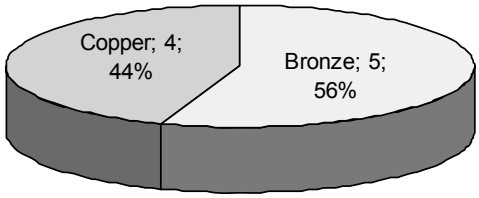

Fig. 3.20 Relative frequencies of the metal type related to the metallurgical remains from *Pragança*.

The analysis made over two areas of the crucible (internal and external sides) did not show any peaks associated with ancient metallurgy indicating that the crucible is in an unused state. This had previously been suggested by its particular good state of preservation (this is the only whole crucible that was studied), absence of secondary-firing evidences, absence of vitrified areas, and its relatively high mass, contrasting with other crucible fragments analysed in this work. The shape of the crucible shows similarities with Chalcolithic crucibles studied in this work, as the largest fragment form *Escoural*. The opening of the crucible in one end suggests that it would be used for melting, as for facilitating the pouring of the melt to a mould.

The analysis made over two areas of the colanders (internal and external sides) did neither show any peaks associated with ancient metallurgy. Thus, and similarly to what has been published by Hunt Ortiz (2003), so far there is no clear analytical evidence linking these objects with ancient metallurgical processes.

3.3.2 *Medronhal* – a LBA burial

Various metal artefacts have been found in the *Gruta do Medronhal* (Medronhal cave) (Condeixa-a-Nova, Beira Litoral) and are believed to belong to a burial. The collection is composed by 30 rings, 6 bracelets and a double-spring fibula (**Fig. 3.21**). These types of ornamental artefacts are frequently found in LBA/1st IA burials of the Iberian territory, as in *Qurénima* (SE Spain) (Lorrio, 2008) as well as in the *Medellín* necropolis (Extremadura, Spain) (Almagro-Gorbea, 2008). Similar artefacts have also been found in settlements of the Portuguese territory with occupations in the turn of the 2nd to the

1st millenium BC, as in *Baiões* (bracelets and rings; Valério et al., 2006) and *Castro dos Ratinhos* (rings and double-spring fibulae; Valério et al., 2010).

Fig. 3.21 Artefacts studied from *Medronhal*.

The rings from *Medronhal* can be divided into open or closed pieces. All are closed, except for MED-19 and MED-34, which are also the smallest rings in the collection. MED-19 has a near-circular cross-section and MED-34 has a flat cross-section. Among the closed rings, all show near-circular cross-sections except for the MED-35 and MED-36 rings which show a thin flat cross-section. Provided their shape and size, these two rings are the only ones that seem adequate to have been worn in the fingers (the others could have been clothing or hair accessories).

The bracelets are open pieces with near-rectangular cross-sections, sometimes with particularities, as MED-29 that shows two opposite flat sides and two opposite round sides.

The double-spring fibula MED-37 is almost complete (only missing the pin), and such type of fibula is commonly associated to a period that comprise already the 1st IA (in SW IP such fibula have been found in contexts dated to the VIII-VI century BC); the origin of this typology is much discussed, however, Almagro-Gorbea (2008) proposes that it can be a local adaptation of Sicilian and Italian models.

All the artefacts were analysed by EDXRF and by micro-EDXRF in a small prepared area. These small areas were also prepared for microstructural observation in the OM, and one of the rings (MED-

03) was analysed by SEM-EDS for the identification of inclusions. The main results on the elemental and microstructural analysis are exposed in **Table 3.9**.

Table 3.9 Summary of the experimental results on the bronze artefacts from *Medronhal* (EDXRF results are given in a semi-quantitative way; composition is given by average of three micro-EDXRF analyses ± one standard deviation)

No.	Item	Composition (wt.%)							Method of fabrication	Phases present
		Cu	Sn	Pb	As	Sb	Fe	Ni		
MED-01	Ring	+++	+	vest.	vest.	vest.	vest.	n.d.	C+D↓	α, δ
		88.6±2.3	11.3±2.3	n.d.	0.12±0.0	-	<0.05	n.d.		
MED-02	Ring	+++	++	vest.	vest.	vest.	vest.	n.d.	C+D+T+D	α, δ↓
		85.5±0.2	14.4±0.2	n.d.	0.13±0.0	-	<0.05	n.d.		
MED-03	Ring	+++	++	n.d.	n.d.	n.d.	vest.	n.d.	C+D+T+D↑	α
		88.1±0.9	11.9±0.9	n.d.	n.d.	-	<0.05	n.d.		
MED-04	Ring	+++	++	vest.	vest.	vest.	vest.	n.d.	C+D	α, δ
		84.4±2.9	15.4±2.9	n.d.	0.23±0.0	-	<0.05	n.d.		
MED-05	Ring	+++	++	vest.	vest.	vest.	+	n.d.	C+D	α, δ
		86.9±1.0	12.9±0.9	0.14±0.0	n.d.	-	<0.05	n.d.		
MED-06	Ring	+++	++	vest.	vest.	n.d.	vest.	n.d.	C+D+T+D	α
		86.2±2.3	13.6±2.3	0.17±0.0	n.d.	-	<0.05	n.d.		
MED-07	Ring	+++	++	vest.	vest.	n.d.	vest.	n.d.	C+D+T+D	α
		86.9±2.9	12.9±3.0	0.21±0.0	n.d.	-	<0.05	n.d.		
MED-08	Ring	+++	++	vest.	vest.	n.d.	+	n.d.	C	α, δ
		84.9±0.3	14.8±0.3	0.19±0.0	n.d.	-	<0.05	n.d.		
MED-09	Ring	+++	++	vest.	n.d.	n.d.	+	n.d.	C+D↓	α, δ
		86.6±2.5	12.9±2.5	0.49±0.2	n.d.	-	<0.05	n.d.		
MED-10	Ring	+++	++	vest.	vest.	n.d.	vest.	vest.	C+T+D	α, δ↓
		88.3±1.5	11.4±1.5	0.13±0.0	n.d.	-	<0.05	n.d.		
MED-11	Ring	+++	++	vest.	vest.	n.d.	vest.	vest.	C	α, δ
		85.8±2.9	14.0±2.8	n.d.	0.18±0.0	-	<0.05	n.d.		
MED-12	Ring	+++	++	vest.	vest.	n.d.	vest.	n.d.	C+D↓	α, δ
		85.2±0.9	14.7±0.9	n.d.	0.12±0.0	-	<0.05	n.d.		
MED-13	Ring	+++	++	n.d.	n.d.	n.d.	vest.	n.d.	C+D+T+D	α
		87.4±0.6	12.3±0.6	0.17±0.0	n.d.	-	<0.05	n.d.		
MED-14	Ring	+++	++	vest.	vest.	n.d.	vest.	n.d.	C+T+D	α
		87.1±4.2	12.7±4.2	n.d.	0.16±0.0	-	<0.05	n.d.		
MED-15	Ring	+++	++	+	+	n.d.	vest.	n.d.	C+D+T+D	α, δ↓
		86.6±0.6	12.1±0.5	0.61±0.1	0.54±0.0	-	<0.05	0.21±0.0		
MED-16	Ring	+++	++	vest.	n.d.	n.d.	vest.	n.d.	C+D↓+T+D↓	α, δ
		85.2±0.4	14.8±0.4	n.d.	n.d.	-	<0.05	n.d.		
MED-17	Ring	+++	++	vest.	vest.	vest.	+	n.d.	C+D↓+T↓	α, δ
		87.3±0.9	12.6±0.9	n.d.	0.15±0.0	-	<0.05	n.d.		
MED-18	Ring	+++	++	vest.	vest.	n.d.	vest.	n.d.	C+D+T+D	α, δ
		84.8±0.2	15.1±0.2	n.d.	0.15±0.0	-	<0.05	n.d.		
MED-19	Ring (open)	+++	++	n.d.	n.d.	n.d.	vest.	n.d.	C+D↑+T+D	α
		87.9±1.3	12.1±1.3	n.d.	n.d.	-	<0.05	n.d.		
MED-20	Ring	+++	++	vest.	vest.	n.d.	vest.	n.d.	C+D↓+T↓+D↓	α, δ↓
		88.5±0.6	11.1±0.6	0.3±0.0	n.d.	-	<0.05	n.d.		
MED-21	Ring	+++	+	n.d.	vest.	n.d.	vest.	n.d.	C+D	α, δ
		86.6±1.1	13.2±1.1	n.d.	0.17±0.0	-	<0.05	n.d.		
MED-22	Ring	+++	++	vest.	vest.	vest.	vest.	n.d.	C+D↓	α, δ↑
		85.1±1.2	14.8±1.1	n.d.	0.15±0.0	-	<0.05	n.d.		
MED-23	Ring	+++	++	vest.	vest.	vest.	+	n.d.	C+D	α, δ
		86.9±0.1	12.9±0.0	n.d.	0.16±0.0	-	<0.05	n.d.		

Table 3.9 (continued)

No.	Item	Composition (wt.%)							Method of fabrication	Phases present
		Cu	Sn	Pb	As	Sb	Fe	Ni		
MED-24	Ring	+++	++	vest.	n.d.	vest.	vest.	n.d.	C+D↓	α, δ
		85.0±2.9	14.8±2.9	0.16±0.0	n.d.	-	<0.05	n.d.		
MED-25	Ring	+++	++	vest.	n.d.	vest.	vest.	n.d.	C+D↓	α, δ
		87.5±0.8	12.5±0.9	n.d.	n.d.	-	<0.05	n.d.		
MED-26	Ring	+++	++	vest.	vest.	n.d.	vest.	n.d.	C+D+T+D↑	α, δ↓
		84.4±1.9	15.6±1.9	n.d.	n.d.	-	<0.05	n.d.		
MED-27	Ring	+++	++	vest.	n.d.	n.d.	vest.	n.d.	C+D↓+T↓+D↓ (?)	α, δ
		84.6±0.5	15.3±0.6	n.d.	n.d.	-	<0.05	n.d.		
MED-28	Ring	+++	++	vest.	vest.	vest.	vest.	n.d.	C+D+T+D	α
		85.1±5.5	14.6±5.0	n.d.	0.21±0.0	-	<0.05	n.d.		
MED-29	Bracelet	+++	++	vest.	n.d.	vest.	vest.	n.d.	C+D+T+D	α
		89.8±2.2	10.1±2.1	0.19±0.0	n.d.	-	<0.05	n.d.		
MED-30	Bracelet	+++	++	vest.	n.d.	n.d.	vest.	n.d.	C+D+T+D↓	α
		88.0±0.3	11.7±0.3	0.24±0.0	n.d.	-	<0.05	n.d.		
MED-31	Bracelet	+++	++	n.d.	vest.	n.d.	vest.	n.d.	C+D+T+D	α
		87.3±0.1	12.7±0.0	n.d.	n.d.	-	<0.05	n.d.		
MED-32	Bracelet	+++	++	vest.	vest.	vest.	+	n.d.	C+D↓+T+D	α
		86.7±1.5	13.1±1.5	n.d.	n.d.	-	<0.05	n.d.		
MED-33	Bracelet	+++	++	vest.	vest.	n.d.	vest.	n.d.	C+D+T+D	α
		89.8±0.2	10.1±0.2	n.d.	n.d.	-	<0.05	n.d.		
MED-34	Ring (open)	+++	++	n.d.	n.d.	n.d.	+	n.d.	C+D+T+D	α
		85.9	13.9	0.17	n.d.	-	<0.05	n.d.		
MED-35	Ring	+++	++	vest.	vest.	n.d.	vest.	n.d.	C+T↑+D	α, δ↓
		88.3±1.2	11.3±1.2	0.18±0.1	0.17±0.0	-	<0.05	n.d.		
MED-36	Ring*	+++	++	vest.	vest.	vest.	vest.	n.d.	C+T↑+D	α, δ↓
		87.1	12.9	n.d.	n.d.	-	<0.05	n.d.		
MED-37	Fíbula	+++	++	vest.	vest.	vest.	vest.	n.d.	C+D+T+D	α
		88.2±1.4	11.6±1.4	n.d.	0.12±0.0	-	<0.05	n.d.		

+++ >50%; ++ 10-50%; + 1-10%; vest. (Vestiges) <1%; n.d. not detected

C cast; D deformation/forged; T heat treatment/annealed; ↓ low amount; ↑ high amount

* Only one micro-EDXRF analysis was considered due to the small size of the cleaned area (constrained by the shape of the artefact).

The EDXRF analyses show that all the artefacts are made of bronze with As, Pb and Sb frequently present as impurities. The micro-EDXRF analysis show that the Sn content is not significantly different among the different typologies, with Sn contents in the range of 10 to 16 wt.%, although the fibula and the bracelets show a slightly tendency to be at the lower range (**Fig. 3.22**).

Analysis on similar artefacts as rings and bracelets from *Baiões* has shown that these were also manufactured in a binary bronze with a low impurity pattern (Sn contents were not determined, Valério et al., 2006). Analysis on rings and a double-spring fibula from *Castro dos Ratinhos* (Alentejo) have shown that the first ones were made of bronze with Sn contents in the range of ~8-14%, and the fibula was made in a slightly different alloy, with ~6% Sn (all with low impurity patterns, being ~10%Sn the average content of all the artefacts analysed in the site; Valério et al., 2010a). Another double-spring fibula from *El Palomar* (Extremadura, Spain) has ~13% Sn and ~0.25% Pb (Rovira et al., 2005), showing a Sn content more similar to the one studied here.

Generally, the composition of the *Medronhal* artefacts is very similar to other earlier and contemporaneous LBA bronzes from the Portuguese territory, e.g. from the *Baiões/Santa Luzia* group

(see next section 3.3.3). This can reflect a continuity in the use of this bronze composition from LBA to 1st IA, possibly as a result of the cultural continuity that is observed at the Central and Northern regions of the Portuguese territory at the ~1250-550 BC period (Senna-Martinez, 2000).

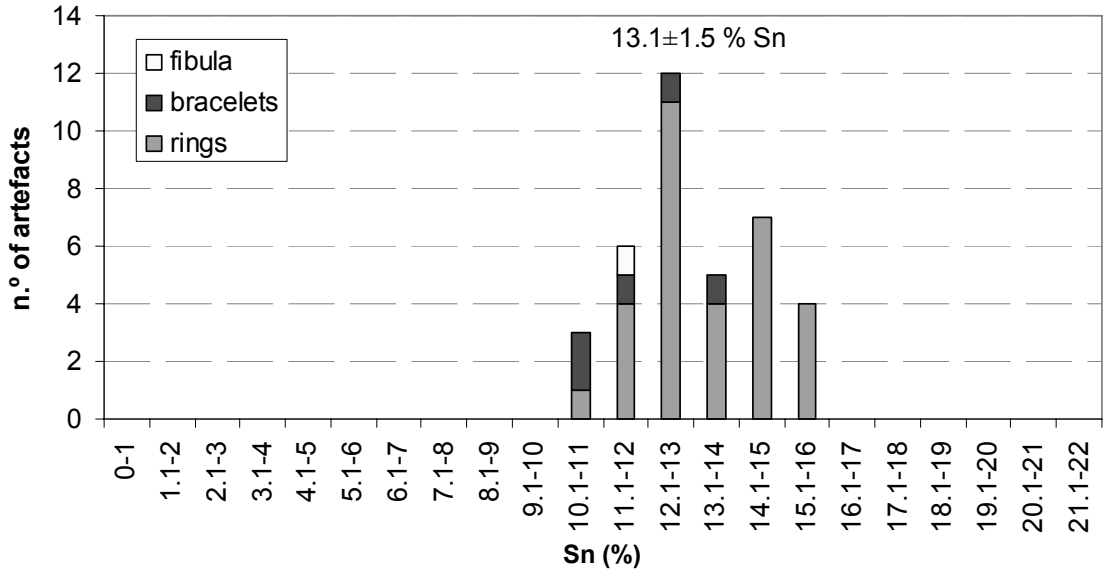

Fig. 3.22 Histogram of Sn content in the studied artefacts from *Medronhal* (average and one standard deviation annotated).

The OM observations showed that the artefacts have various microstructures, from cored dendrites (as-cast), to recrystallized grains, with or without slip bands (**Fig. 3.33-3.34**), and that all show Cu-S inclusions. The presence of Cu-S inclusions is very recurrent in the analysed copper and bronze artefacts dating to BA (see next sections), and according to the Cu-S phase diagram these are copper sulphides (Cu_2S). Their presence can indicate that sulphur rich mineralizations were used to produce the copper, as copper sulphides, or, that during the smelting operation other minerals rich in sulphur were in contact with the forming metal, making sulphur to be incorporated into the metal. These sulphur-rich minerals could be in the gangue, or, as has been shown for Iberian mineral outcrops, relatively pure copper carbonates can also have some dispersed iron carbonates and copper sulphates (Pérez et al., 2002).

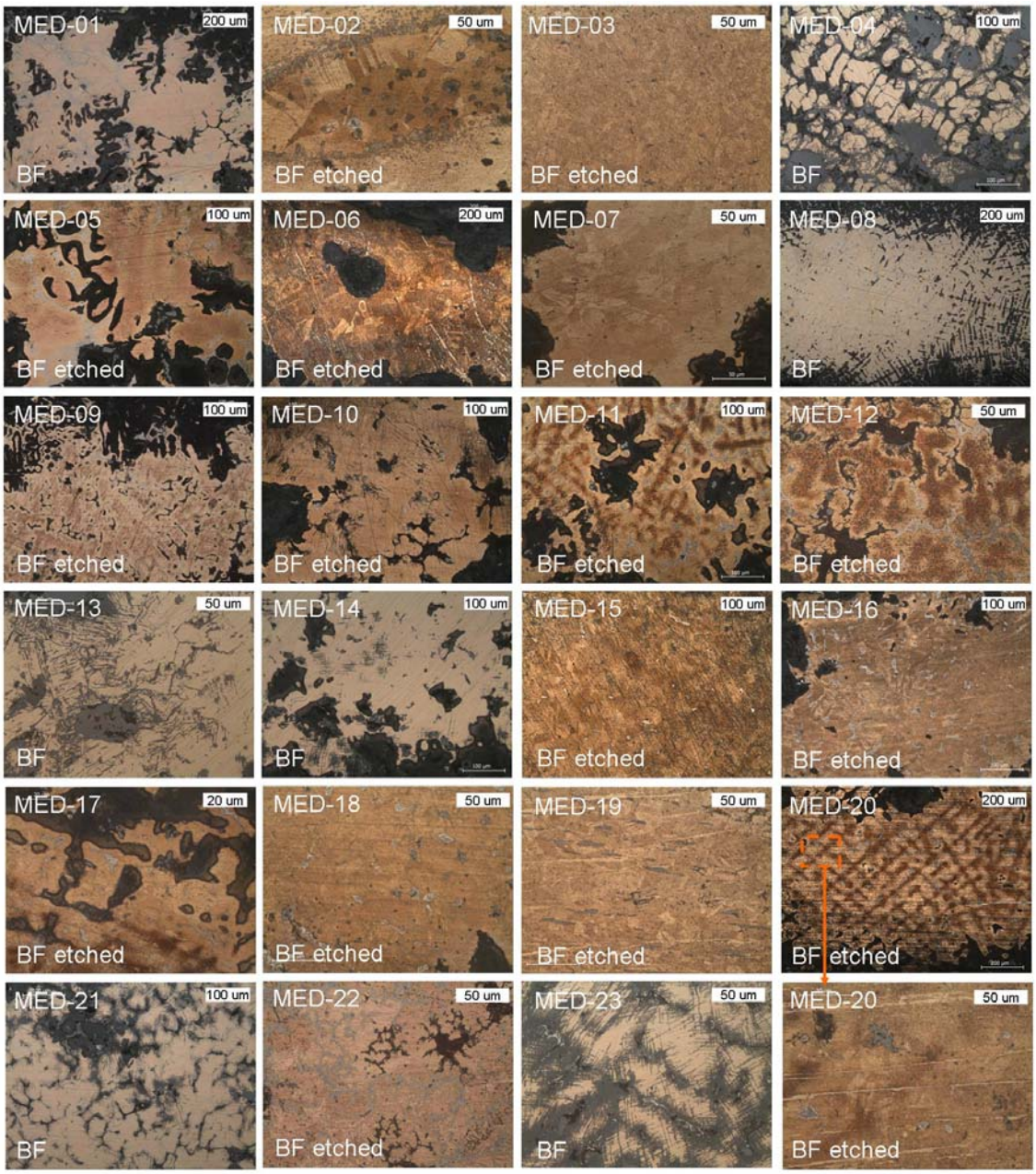

Fig. 3.33 Microstructures of the artefacts from *Medronhal*, from MED-01 to MED-23 (OM).

It was observed that some closed rings show as-cast microstructures (with or without some superficial deformations) (**Fig. 3.35**) confirming that they where shaped in a mould, being posterior minor corrections to the shape or surface performed by different kinds of thermo-mechanical sequences. Among these closed rings, the shape of the ring MED-22 is very interesting, since it has marks indicating that the artefact was produced in a two-piece mould (bivalve mould). These marks resulted from the default matching of one half of the mould on the other. Additionally, at opposite sides, the ring has an area with irregular surface, which suggests the placement of sprues. These two sprues were probably a feeder and a channel that allowed the metal to flow to the next section of the mould, possibly another ring (**Fig. 3.36**). This ring does still bear these imperfections since it was not subjected to accurate post-casting works, as also suggested by its microstructure, composed by dendrites with some slip bands, indicating that only some minor plastic deformation was performed

after casting, possibly to remove the seams and the sprues. Also, another ring, the MED-06, appears to have remnants of a casting seam all around the outer border pointing out to the production of the closed rings in bivalve moulds.

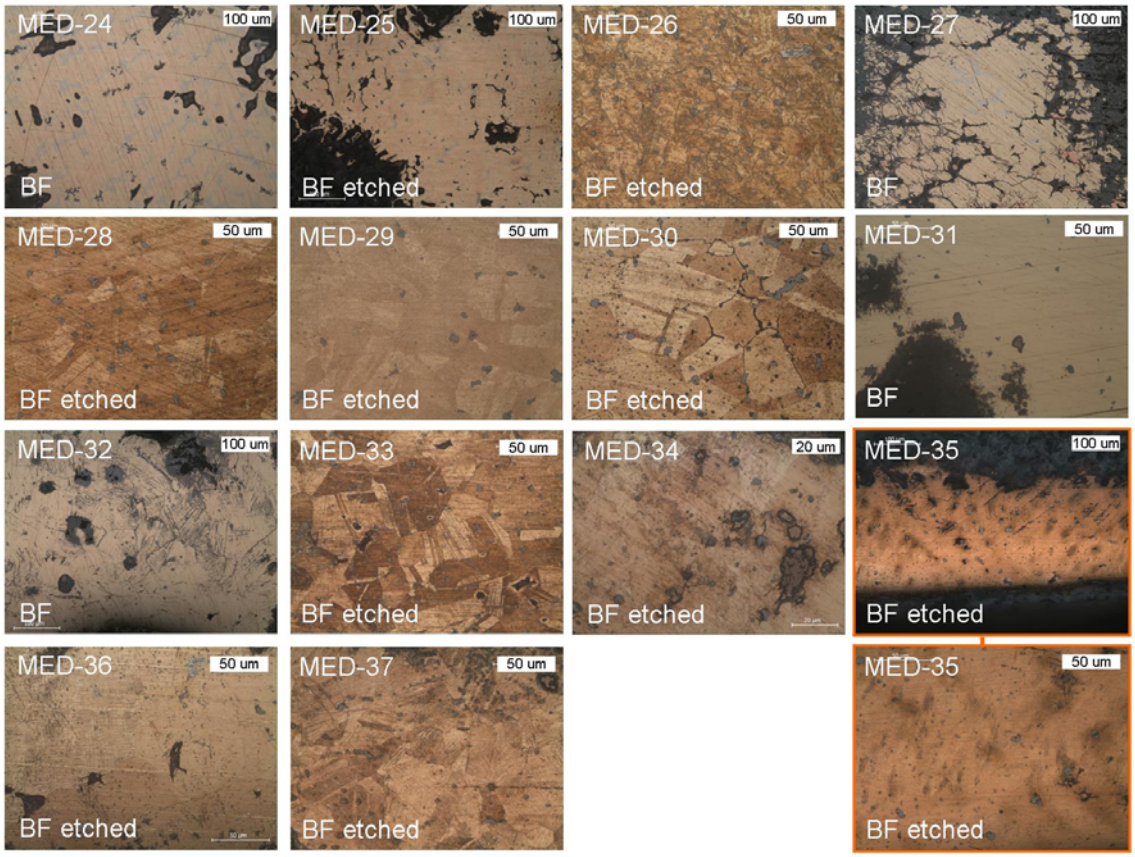

Fig. 3.34 Microstructures of the artefacts from *Medronhal*, from MED-24 to MED-37 (OM).

The manufacturing of these rings in bivalve (closed) moulds does also find support in the observation of some rings that show other casting defects. The ring MED-14 has a large pore near the surface that has allowed corrosion to penetrate deep and leave the hollow exposed (**Fig. 3.37**). Such a large pore was most likely produced during the solidification of metal as a consequence of gas trapping, a recurrent phenomena in closed moulds due to a difficultly of gas escaping.

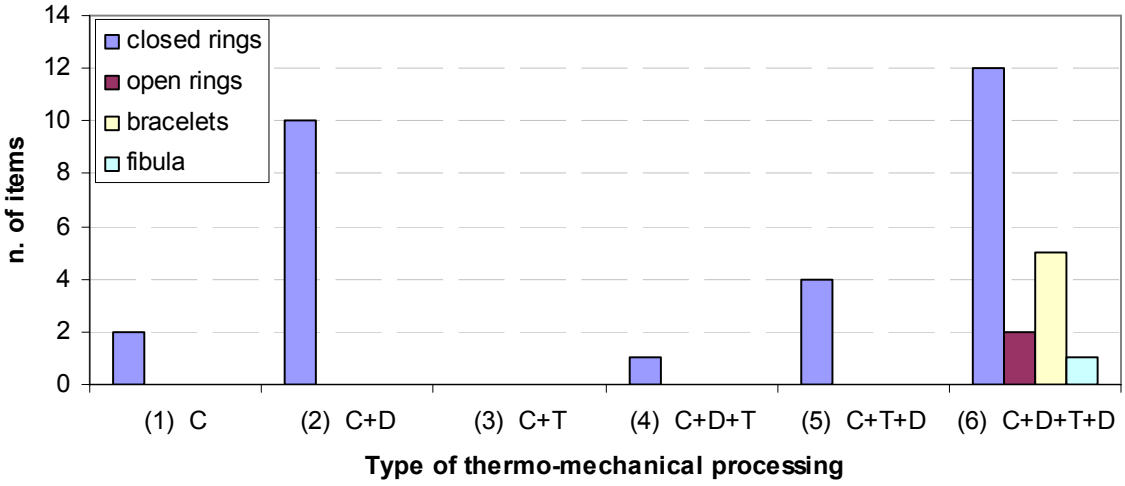

Fig. 3.35 Histogram with the type of thermo-mechanical processing performed in the artefacts from *Medronhal* (C – Cast; D – Plastic deformation; T – Heat treatment).

Fig. 3.36 Casting defects resulting from a bivalve mould. At left a scheme with the casting defects observed on the ring MED-22: (A) inadequate matching among the two halves and (B) irregular surfaces after casting sprue. At the centre a photograph of MED-22, with the positioning of the (B) defects depicted. At the right (C) a scheme representing the interpretation of a possible bivalve mould for casting various rings.

Fig. 3.37 Pictures showing some surface particularities of the rings: the large pore of MED-14; the even surface of MED-26; and the numerous pores of MED-32.

The ring MED-26 is the one that shows the highest tin content (~15.6% Sn). It is also the one that shows the most even, polished-like surface, resulting in a superficial shining appearance that bears some similarities with the pendant from *Fraga dos Corvos* shelter (FC-252) although the lighter colour of the latest (section 3.4.1.2). Its microstructure shows that the relative high Sn content did not prevent the ancient metallurgists to execute thermo-mechanical operations after casting, resulting in a general

homogenization of the metal. Additionally, the highly deformed grains indicate a large amount of final cold work, which can be related to works performed to even and polish the surface. Possibly, such homogenized microstructure has avoided deep corrosion (as through pores and areas with higher segregations) (see section 2.2.2) and the relatively high tin content helped in the development of a more protective corrosion layer. Among the other three artefacts with Sn contents around 15% (MED-04, MED-18 and MED-27), MED-18 do also show similar features (even, shining, polished-like surface) and is the only one that also has an intense worked microstructure. The others, despite the relative high Sn contents show deep intergranular corrosion due to a less homogenized microstructure.

The only two open rings (MED-19 and MED-34) show a recrystallized grain structure with slip bands, pointing out to the production of these rings by working a bar or other open-shaped object. The small ring MED-19 does even show very elongated Cu-S inclusions, as a result of its manufacture thought severe deformations.

The two closed rings MED-35 and MED-36 with a distinct thin flat cross-section have similar microstructures, composed by large annealed grains, still with the previous dendritic structure perceptible thought regular patterns of Cu-S inclusions and some eutectoid. This shows that any deformation to which they were subjected was not enough to disrupt the dendritic pattern. Their microstructure suggests that their intermediate shape must have been obtained in a mould, being a reduction/adjustment in the thickness performed afterwards. This adjustment was performed by minor mechanical deformations after annealing. This type of thermo-mechanical processing (nº 5, see section 3.1) is not the most usual, and was only observed in two other rings (MED-10 and MED-14). Nevertheless, a similar working sequence has also been observed in the bracelet from *Baiões* (CSG-408, section 3.3.3.1), and on two open rings from *Castro dos Ratinhos* (Valério et al., 2010a, 2010b), suggesting that an annealing after casting and before any mechanical work could be rather usual to prevent brittleness and improve ductility of the alloy.

All the 5 **bracelets** show the same type of microstructure, composed by recrystallized grains with some slip bands. Their shape and microstructure suggest that they were shaped from a cast bar through thermo-mechanical processes. One of the bracelets, the MED-32, shows a large amount of pores all over the surface (**Fig. 3.37**). Such casting defect is indicative of the use of a closed mould to cast the pre-form bar. The casting of bars in bivalve moulds, together with the production of other more complex shaped artefact, seems to have been a common practice in LBA times (see the mould presented in section 3.3.4). Thus, it can be perfectly possible that the bars to produce bracelets have been produced in such multi-artefact bivalve moulds.

The **fibula** MED-37 does also show a microstructure similar to the bracelets, suggesting that it was shaped from a cast bar though thermo-mechanical processes. The rather high deformation needed to produce the double spring of the fibula did not prevent the ancient metallurgists of manufacturing this item in a bronze with Sn contents similar to the others. The production of the spring, by bending the bronze bar numerous times, must have been done with the metal in an annealed state to avoid break.

Probably, numerous annealing operations were needed between deformations, to recover the metal to its most soft condition as possible.

The OM observations of the *Medronhal* microstructures did also reveal that many of the artefacts have a distinct dark inclusion inside the Cu-S grey inclusions. One of the artefacts (MED-03) was analysed in the SEM-EDS to investigate this feature, and the result shows that inside many of the Cu-S inclusions there is an Sn-O rich inclusion (**Fig. 3.38**). Such inclusions have been observed by Dungworth (2000) in investigational bronzes produced by the alloying of copper with tin in the metallic state, and has been explained as a result of the preferential oxidation of Sn in respect to Cu, having a relatively low melting temperature prevented the oxide inclusions to be transferred to the slag (Dungworth, 2000). Similar inclusions were also observed by Valério et al. (2010a) in a LBA knife with ~5% Sn (the lowest Sn content among the artefacts studied in that work) which can suggest that those are a result of the use of recycled bronze, since melting operations do also lead to the preferential oxidation of Sn and its partial loss. Since small amounts of Sn-O inclusions can be present in the alloy due to various factors, the presence of these oxides in the present case cannot be regarded as evidence for any specific metallurgical process; instead, it may only be an indication that the temperature was not sufficiently high to allow all the tin oxide to be incorporated in the slag.

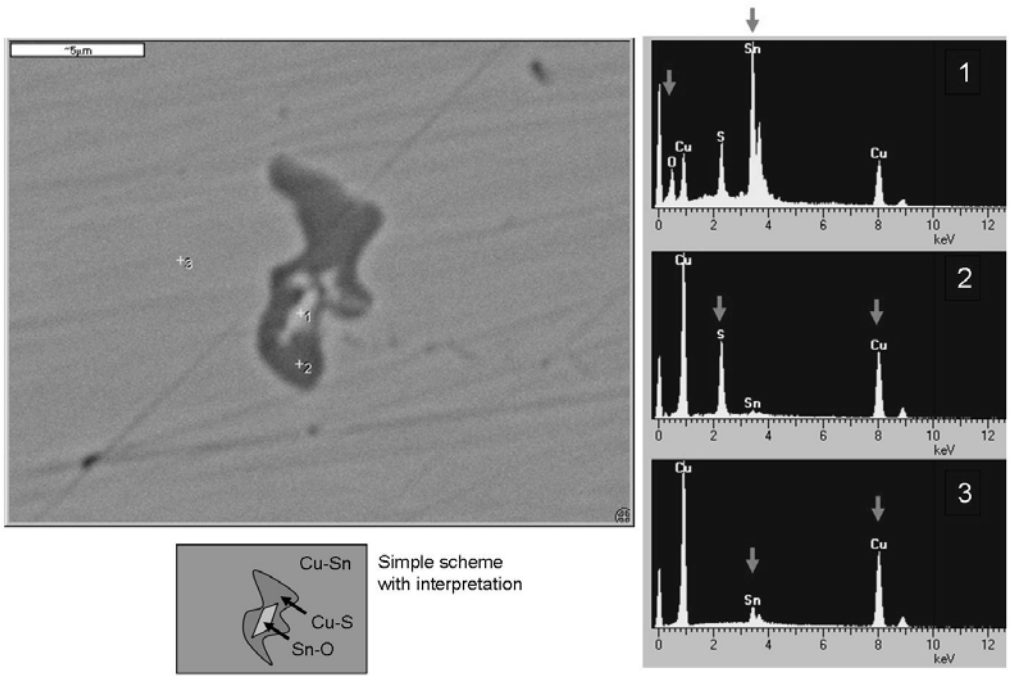

Fig. 3.38 SEM (BSE) image and spot EDS analysis (1-3) of the (1) Sn-O inclusion, (2) Cu-S inclusion and (3) bronze on the MED-03 artefact (note that due to the small size of the inclusions, the spot analysis made on the Sn-O inclusion has strong influence from the surrounding compounds). At bottom, a simplified scheme of the BSE image and elemental composition of inclusions.

3.3.3 *Baiões/Santa Luzia* – a pertinent LBA cultural group

During the last quarter of the 2nd millennium BC, with the advent of full adoption of bronze and the increase in metallic artefacts production, the Central Portuguese Beiras region witnessed an emergence of many sites positioned in places that confer a great domain over the involving landscape, and frequently in places without previous evidences of occupation. Archaeological works on many of those sites have uncovered various vestiges of metallurgical activities (e.g. bronze foundry leftovers, scrap, bits of wire and bars to forge, moulds in clay, stone and bronze together with brand new artefacts still with casting beams) (Senna-Martinez, 2000; Vilaça, 2004). Taking into consideration all these evidences, plus that the region has abundant tin and gold resources (Garcia, 1963), the emergence of these sites has been suggested to be related to the control and exploitation of gold and cassiterite (Senna-Martinez and Pedro, 2000), the latest an essential ore for bronze fabrication. Later, the collapse of most of those sites in the middle of the 1st millennium BC (Vilaça, 1995) has been explained as a possible result of the rupture on metal circulation, which happened with the crisis of the Phoenician settlements in Iberian coastal areas (Senna-Martinez, 1998).

Although the general lack of evidence for ancient mining activities in the Portuguese territory, to which many factors may contribute (from posterior mining works destroying the older ones to a difficulty in recognizing sparse evidences in the field), during the reopening of the ancient gallery of the *S. Martinho* mine (Orgens, Viseu) during the World War Two, a bronze dagger of "Porto de Mós" type was found at the bottom of the rubble which filled its shaft, proving its original opening and posterior infilling during the LBA probably for cassiterite exploration (Correia et al., 1979). Regarding copper exploration, one can report to the finding of a bronze palstave at a depth of 12 meters during the reopening of the ancient mining shaft of the *Quarta Feira* copper mine (Sabugal, Guarda) at the end of nineteenth century (Melo et al., 2002), proving the capability and interest, by LBA and within the region, in performing underground mining works.

In Beira Alta region (Beiras Plateau) there is a particular number of sites positioned in the Viseu district and surroundings, which have been called *Baiões/Santa Luzia* cultural group after the name of the largest sites (**Fig. 3.39**). Among the *Baiões/Santa Luzia* cultural group, artefacts with Atlantic typological features and others with Mediterranean typological features have been found, indicating distinct influences and contacts (Ambruster, 2004; Ruiz-Gálvez, 1993, 1998; Senna-Martinez, 1995). Of all the *Baiões/Santa Luzia* sites, the *Baiões* site is the most famous and its collection of artefacts has been reported in numerous studies, related with typological and production issues (Ambruster, 2004; Coffyn, 1985; Giardino, 1995; Senna-Martinez and Pedro, 2000; Ruiz-Gálvez, 1998).

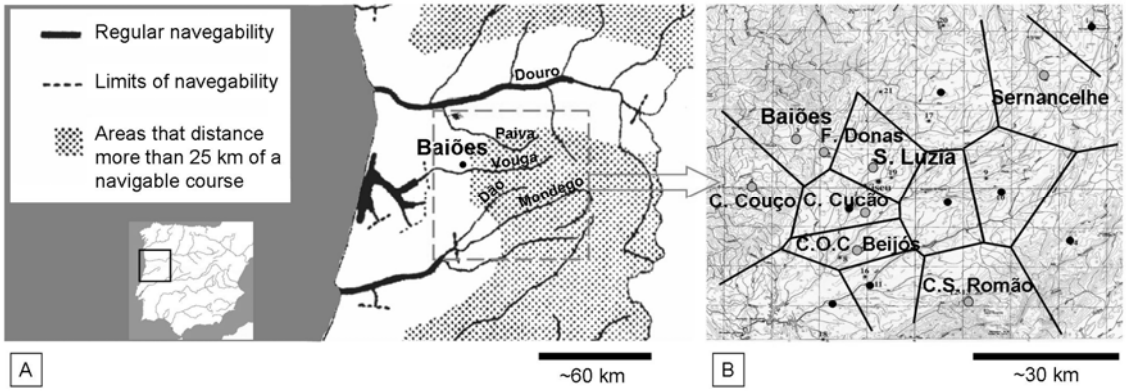

Fig. 3.39 (A) Location of *Baiões/Santa Luzia* cultural group in Iberian Peninsula with details of the navigability of nearby rivers (until middle of the XIX century) adapted from Blot (2002). (B) Settlement grid of the LBA *Baiões/Santa Luzia* cultural group after Senna-Martinez (2000) with annotated sites from where materials studied in this work where recovered.

In the present work, a significant number of artefacts and metallurgical remains from various sites belonging to the *Baiões/Santa Luzia* cultural group are going to be studied. The major collections (*Baiões*, *Santa Luzia*, *Figueiredo das Donas* and *Crasto de São Romão*) are presented in this section (3.3.3); some single finds are presented in the section 3.3.4 (Others) created to incorporate particular and isolated finds.

3.3.3.1 *Baiões*[10]

The *Castro de Nossa Senhora da Guia de Baiões* (CSG) site is placed on a granitic hilltop in the county of S. Pedro do Sul, Viseu. The site has a great domain over the involving landscape and controls the old road going West, alongside the Northern margin of the Vouga river (that was navigable just some 20 km ahead until middle of XIX century), allowing a good access to the Atlantic waters. Its pre-historic occupation is estimated to lay in between the 13th and the 8th centuries BC (Senna-Martinez, 2000; Senna-Martinez and Pedro, 2000).

The majority of the metal finds of *Baiões* comprise bronze foundry leftovers, scrap, bits of wire and bars to forge, as well as moulds in clay, stone and bronze together with brand new artefacts still with the casting seams. Despite the richness and importance of the collection, previous analytical studies are very scarce. The most significant investigation carried out until now were the EDXRF semi-quantitative analyses performed by Valério et al. (2006) over 54 bronze artefacts (complete or semi-complete), which showed that the items were made of bronze, occasionally with lead and arsenic as impurities.

For the present study other items were selected, most of them metallurgical debris. The items include one vitrified fragment, later recognized as a slag fragment, twelve minute roundish or irregular

[10] The content of this section has adaptations of the following published work:

- E. Figueiredo, R.J.C. Silva, J.C. Senna-Martinez, M.F. Araújo, F.M.B. Fernandes, J.L. Inês Vaz (2010) Smelting and recycling evidences from the Late Bronze Age habitat site of Baiões (Viseu, Portugal). *Journal of Archaeological Science* 37, 1623-1634.

fragments of metal named "metallic nodules" for the sake of simplicity (**Fig. 3.40**), and nineteen artefacts and fragments of artefact (**Fig. 3.41**). The metallic nodules were selected owing their high number amongst the collection and since their study could provide information about metallurgical operations. Among the selected artefact fragments, some showed partially heat-distorted areas. Accordingly, the microstructure examination could help in their classification as faulty castings or partial melted artefacts, as resulting from an incomplete recycling operation.

Fig. 3.40 Nodules and slag (CSG-315) studied from *Baiões*.

Fig. 3.41 Artefacts and fragments of artefacts studied from *Baiões*.

All the metallic artefacts were analysed by EDXRF and micro-EDXRF in prepared surfaces (CSG-349 was sampled) and microstructural observations by OM were performed. Additionally, XRD was performed in a cross-section of the slag (CSG-315) and SEM-EDS was performed in the slag and in one nodule (CSG-327). Next, the results are going to be presented and discussed according to the nature of the items. First, the slag fragment is going to be presented, followed by the nodules, and at last the artefacts and fragments of artefacts.

For the study of the **slag fragment**, the SEM-EDS analysis were essential to provide detailed information on morphological and elemental distribution of the various constituents of the slag. In **Fig. 3.42** are presented the main results of the analyses made on the cross-section. This revealed a heterogeneous structure, essentially composed by: a vitreous matrix (aluminium silicate) with the regular presence of O, Cu, Al, Si and irregular presences of K, Fe, Pb, Mg and Ti; large globular inclusions of malachite (surrounded by cuprite) (**Fig. 3.42**A), cuprite and metallic copper (surrounded by cuprite) (**Fig. 3.42**B); occasionally some small inclusions of metallic lead (**Fig. 3.42**B); cuprite in coarse dendrites (image embedded in **Fig. 3.42**A) or in small globular forms (**Fig. 3.42**B); and the presence of cassiterite, frequently in needle like crystals with a rombohedric form enclosing cuprite (**Fig. 3.42**C-E). The morphologies of the cassiterite and dendritic cuprite among the vitreous matrix indicates that they formed during the solidification process.

Many of these features have been described previously for BA and EIA slags from the neighbouring Spanish territory and regarding some particularities, they have been related with co-smelting processes, “cementation” of copper with cassiterite or an alloying of copper with metallic tin (in later times) (Rovira, 2007).

The XRD analyses of the slag showed peaks related to cassiterite, cuprite and magnetite (**Fig. 3.43**). The formation of magnetite (Fe[II]/[III]) instead of fayalite (Fe[II]) is a frequent feature in early Iberian smelting slags (before IA). This is a consequence of the smelting being normally conducted in open shape reaction vessels with heat from above (Rovira, 2004), producing very heterogeneous conditions inside the vessels, and thus frequently weak reducing atmospheres in many parts.

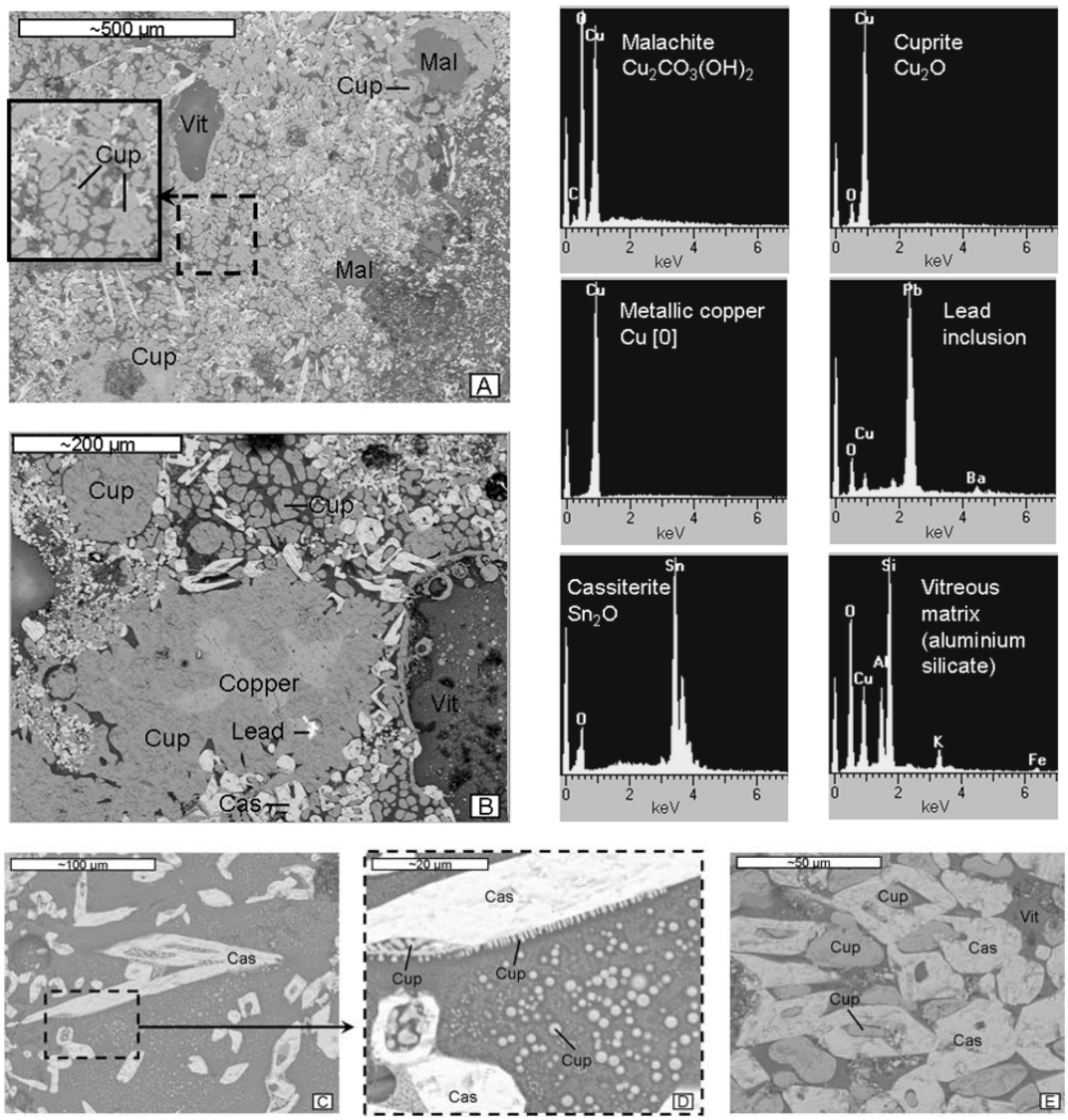

Fig. 3.42 SEM (BSE) images (A-E) of CSG-315 slag fragment and some representative examples of EDS spectra of different compounds present in the slag (Mal – malachite; Vit – vitreous matrix; Cup – cuprite; Cas – cassiterite).

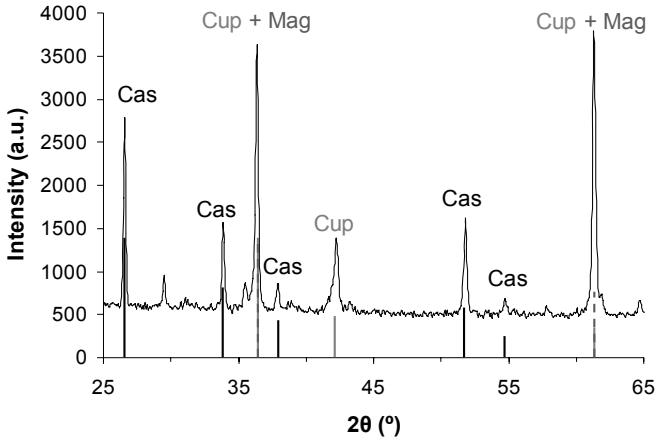

Fig. 3.43 XRD spectrum of CSG-315 slag fragment. The strongest peaks are related to cassiterite and cuprite. The relative intensities of the cuprite peaks corresponding to 2θ values close to 36.4 and 61.3º can be explained by the presence of magnetite.

The studied fragment is most likely only one small part of the whole product that resulted from a metallurgical operation. The weak reducing atmosphere that this particular fragment experienced, at least in the last stage before solidification, was only enough to keep some Cu in metallic form, but clearly not enough to allow Sn to exist in the metallic solid solution (Sn is preferentially oxidised in respect to Cu). The interpretation of such a microstructure is rather difficult, more over since we lack other vitrified fragments and any ceramic body that served as reaction vessel, which could give additional information. This fragment could be a result of an oxidation process, e.g. during a bronze recycling or an alloying of metallic copper and metallic tin, or it could be a result of an extractive operation, such as a smelting operation to reduce copper and tin ores. All these possibilities can be considered since ancient firing techniques, as using blow pipes, did not create constant or uniform conditions inside the reaction vessel (Hauptmann, 2007). Thus, this fragment does most probably not represent the thermodynamic conditions reached in other parts of the reaction vessel, sufficient to retain or produce bronze. It has been shown that in a recycling or alloying operation some oxidation could occur (e.g. Klein and Hauptmann, 1999) and in ancient smelting operations all the transitional stages between thermal decomposition of the original material up to the formation of proper melts can be present in the slag (e.g. Hauptmann 2007). These heterogeneities might even explain why this fragment stayed behind in the archaeographic record: it was probably recognized as "waste" part that enclosed no metallic bronze.

Regardless all the possibilities, some particularities in the microstructure may suggest that the fragment is a slag resulting from a reduction operation. The presence of malachite inclusions in areas without external corrosion evidences, as the malachite inclusion (Cu[II]) that is totally surrounded by cuprite (Cu[I]) (**Fig. 4**A top right) suggests that this malachite is not a secondary corrosion product. Most likely, it was originally present in the mixture, and was partially decomposed at some stage of the process into CuO, CO_2 and H_2O (decomposition of malachite can continue to temperatures greater than 600ºC; Simpson et al., 1964), and the resultant tenorite was reduced into cuprite.

Although copper may initially been present as ore, the initial state of tin is more difficult to accomplish. In the fragment, tin is only present as cassiterite that resulted from the slag's solidification process. Thus, it is impossible to determine if tin was added as metal or ore. Additionally, the lack of archaeological evidences of metallic tin items or cassiterite fragments in *Baiões* and other local LBA sites does not provide additional information on the subject – both can be very difficult to recognize in the archaeographic records, due to "tin pest" in the first case, and due to the not expressive colour of cassiterite when compared with copper ores in the second case. So, future studies on other materials and sites are needed to help answering this question.

In the study of the **nodules**, the EDXRF and micro-EDXRF analyses indicate that all are made of bronze with Sn in the range of 9.7-15.5% and Pb, As and Sb frequently present in low contents (**Table 3.10**).

Table 3.10 Summary of the experimental results on the bronze nodules from *Baiões* (EDXRF results are given in a semi-quantitative way; composition is given by average of three micro-EDXRF analyses ± one standard deviation)

No.	Composition (wt.%)							Phases
	Cu	Sn	Pb	As	Sb	Fe	Ni	present
CSG-153	+++	++	vest.	vest.	vest.	vest.	n.d.	α
	87.9±1.0	12.0±1.0	n.d.	<0.1	-	<0.05	n.d.	
CSG-154	+++	++	vest.	vest.	n.d.	vest.	n.d.	α
	86.8±1.3	12.9±1.2	n.d.	0.13±0.05	-	<0.05	n.d.	
CSG-159	++	+++	+	vest.	vest.	vest.	n.d.	α, δ
	85.7±0.8	13.6±0.6	0.44±0.21	0.21±0.02	-	<0.05	n.d.	
CSG-186	++	+++	vest.	vest.	vest.	vest.	n.d.	α, δ↓
	86.9±0.9	12.9±0.9	n.d.	0.18±0.02	-	<0.05	n.d.	
CSG-187	++	+++	vest.	vest.	n.d.	vest.	n.d.	α, δ
	88.9±0.6	10.9±0.6	0.11±0.08	<0.1	-	<0.05	n.d.	
CSG-210	+++	++	vest.	vest.	vest.	vest.	vest.	α, δ↑
	87.3±0.1	12.6±0.1	n.d.	<0.1	-	<0.05	n.d.	
CSG-227	+++	++	vest.	vest.	n.d.	vest.	n.d.	α, δ
	87.5±2.8	12.5±2.8	n.d.	<0.1	-	<0.05	n.d.	
CSG-317	++	+++	vest.	vest.	vest.	vest.	n.d.	α
	85.7±2.2	14.2±2.2	n.d.	0.10±0.01	-	0.08	n.d.	
CSG-320	++	+++	vest.	vest.	n.d.	vest.	n.d.	α
	90.2±0.2	9.7±0.2	n.d.	<0.1	-	<0.05	n.d.	
CSG-325	+++	++	vest.	vest.	vest.	vest.	vest.	α, δ
	85.6±2.8	14.3±2.8	<0.1	<0.1	-	0.05	n.d.	
CSG-327	+++	++	n.d.	vest.	n.d.	vest.	n.d.	α, δ, ε, η
	85.6±0.5	14.3±0.5	n.d.	n.d.	-	<0.05	n.d.	
CSG-329	++	+++	vest.	vest.	vest.	vest.	n.d.	α, δ↓
	84.3±4.6	15.5±4.6	n.d.	0.11±0.03	-	<0.05	n.d.	

+++ >50%; ++ 10-50%; + 1-10%; vest. (Vestiges) <1%; n.d. not detected

↓ low amount; ↑ high amount

In **Fig. 3.45** micrographs of the microstructures of the nodules are presented, with the exception of the nodule CSG- 327 that is described later in more detail. The microstructures of the nodules CSG-154, 186 and 320 (with Sn contents between 9.7 and 12.9%) are composed by twinned equiaxed grains, a result from a mechanical deformation followed by annealing, and exhibit deep intergranular corrosion. Among these, the CSG- 186 nodule shows the smallest recrystallized grains which are superimposed in an earlier dendritic structure, pictured by the corrosion along preferential paths. These paths are given by the interdendritic regions that show a concentration of Cu-S inclusions and (α+δ) eutectoid. Their microstructures suggest that they are probably remains of artefacts.

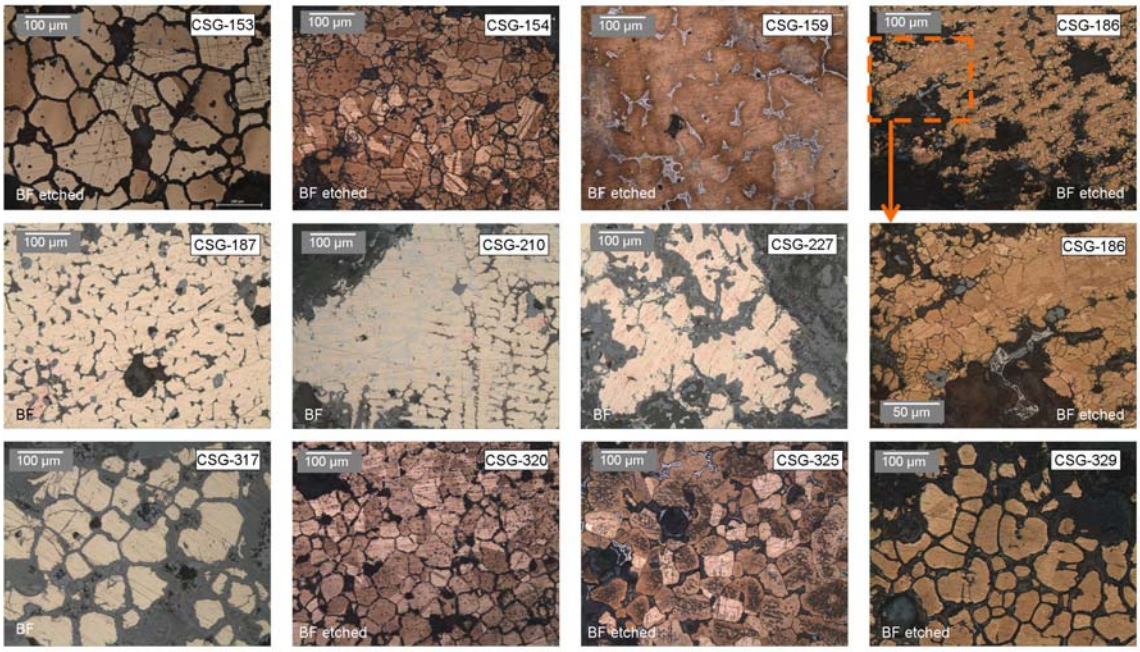

Fig. 3.45 Microstructures of the nodules from *Baiões* (OM).

The other nodules, show coarse microstructures with grain twinning absent or very low (CSG-153, 187, 317, 325 and 329) or cored dendrites with (α+δ) eutectoid in the interdendritic regions (CSG-159, 210 and 227), and Cu-S inclusions are frequently observed. The nodules with coarse microstructures suggest a very slow cooling rate or a heat treatment after solidification and the nodules with cored dendrites suggest faster cooling and absence of a heat treatment. It can be proposed that some of those with coarse (more homogenised) microstructures and rounded shapes (CSG-317, 325, 187, 327 and 329, with Sn contents between 10.9 and 15.5%) are smelting droplets. Smelting droplets are expected to show coarse microstructures due to the rather slow cooling of the smelt. Nevertheless, if this is so, one has to question their narrow range of Sn content, since dispersed Sn contents among lumps and prills recovered from a smelt are expected (Rodríguez Diaz et al., 2001; Rovira, 2007). Also, within those that show a faster cooling microstructure, the existence of some melting droplets, as suggested by Kalb (1995), cannot be rejected.

The CSG-327 nodule has a distinct microstructure of the previous ones and was therefore also analysed by SEM-EDS. The bulk is composed by primary α phase grains and (α+δ) eutectoid. Near to the nodule surface two clear layers of the intermetallic compounds δ and ε were observed, followed by an irregular outer layer of η phase which had small amounts of a tin rich constituent amongst it (**Fig. 3.46**). These features suggest two independent events: one at higher temperatures (>520ºC), to allow the formation of (α+δ) eutectoid from γ decomposition in the bronze bulk; and another, at lower temperatures (<415ºC), to allow a thermally activated solid interdiffusion of Sn from metallic tin and Cu from the pre-existing bronze bulk. For this last stage the system temperature should have been between 350 and 415ºC, since only at this temperature range, and according to the Cu-Sn equilibrium phase diagram, all the three monophasic layers (δ, ε, η) could coexist, without an (α+δ) eutectoid layer resulting from γ decomposition during cooling.

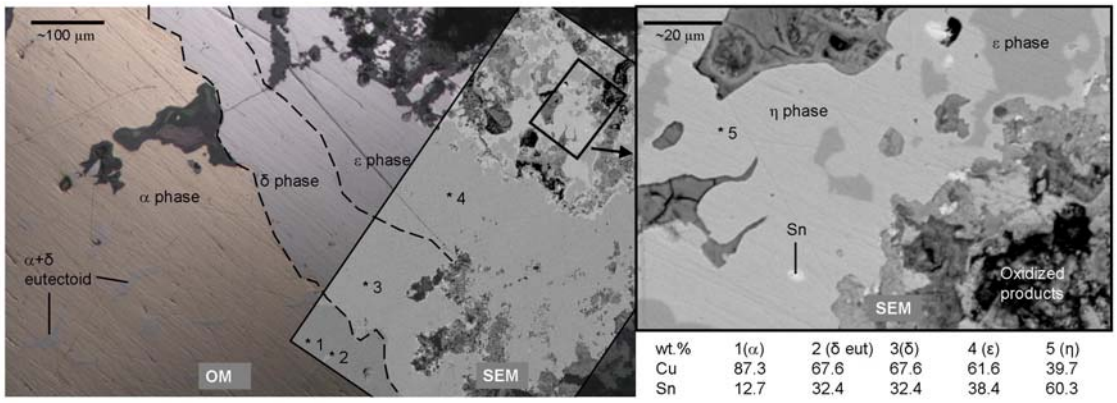

Fig. 3.46 OM (BF) (left) and SEM (BSE) (centre and right) images of CSG-327 nodule. The table shows the results of the EDS analyses on the different Cu-Sn intermetallic compounds.

The archaeometallurgical explanation of this nodule is not simple. The absence of conventional tinned artefacts during BA – tinned artefacts have a eutectoid or delta (Rovira, 2005) layer formed by in-situ cassiterite reduction or by inverse segregation during solidification (Meeks, 1986) – seems to rule out the possibility of this being a fragment of a tinned artefact. As a result, the nodule might have been formed during a smelting or alloying operation, where at a stage of cooling of the reaction vessel some metallic Sn (formed over strong reduction conditions if cassiterite was initially added), still in a liquid state, moved through fissures and cracks ending up in contact with a bronze nodule already in a solid state, starting the interdiffusion process. On the other hand, if this nodule is a result of some recycling operation, then one can only suppose that metallic tin or cassiterite was intentionally added to balance the loss in tin due to its preferential oxidation in respect to copper. Either way, the presence of metallic tin adds the information that the local metallurgists were capable of creating reducing conditions sufficient to preserve tin in a metallic state or reduce cassiterite into metallic tin in the course of their metallurgical operations. This should bear no surprise, since Timberlake (2007) was successful in reducing cassiterite to tin, by smelting high grade ores within small, low-temperature, poorly reducing open hearths, and thus in a comparable way as bronzes could have been produced in IP during LBA.

Among the metallic **artefacts and fragments** the EDXRF and micro-EDXRF analysis showed that all items were made of bronze except for one item of unalloyed copper, and a composite item made of copper and bronze components. Elements as Pb, As and Sb are frequently present, although in low contents, and the presence of Cu-S inclusions is also recurrent, similarly to the nodules. The main results on the artefacts and fragments elemental composition, microstructural features as well as possible thermo-mechanical treatments applied are summarized in **Table 3.11** for copper item, **Table 3.12** for bronze artefacts, and **Table 3.13** for the composite item.

Table 3.11 Summary of the experimental results on the copper artefact from *Baiões* (EDXRF results are given in a semi-quantitative way; composition is given by average of three micro-EDXRF analyses ± one standard deviation)

No.	Item	Composition (wt.%)							Method of fabrication	Phases present
		Cu	Sn	Pb	As	Sb	Fe	Ni		
CSG-293	Bar	+++	vest.	vest.	vest.	vest.	vest.	n.d.	C+D+T	α-copper
		99.8	n.d.	n.d.	0.16±0.02	-	<0.05	n.d.		

+++ >50%; ++ 10-50%; + 1-10%; vest. (Vestiges) <1%; n.d. not detected

C cast; D deformation/forged; T heat treatment/annealed

Table 3.12 Summary of the experimental results on the bronze artefacts and fragments of artefacts from *Baiões* (EDXRF results are given in a semi-quantitative way; composition is given by average of three micro-EDXRF analyses ± standard deviation)

No.	Item	Composition (wt.%)							Method of fabrication	Phases present
		Cu	Sn	Pb	As	Sb	Fe	Ni		
CSG-139	Socket frag	++	+++	vest.	vest.	vest.	vest.	vest.	C	α, δ↑
		82.3±1.7	17.1±1.8	<0.1	0.17±0.06	-	<0.05	0.24		
CSG-162	Pin head	+++	++	vest.	vest.	vest.	vest.	n.d.	C	α, δ↑
		81.0±2.2	18.8±2.1	n.d.	0.16±0.03	-	<0.05	n.d.		
CSG-179	Spatula frag	+++	++	vest.	vest.	vest.	vest.	n.d.	C+D+T	α
		89.0±0.1	10.9±0.1	n.d.	0.12±0.06	-	<0.05	n.d.		
CSG-308	Palstave butt	+++	++	vest.	vest.	vest.	vest.	n.d.	C+D↓?+T	α
	frag	86.2±1.7	13.6±1.7	n.d.	<0.1	-	<0.05	n.d.		
CSG-312	Amalgam of 4	+++	++	vest.	vest.	vest.	vest.	n.d.		
	bar frag	85.8±4.7	13.2±3.2	n.d.	0.12±0.04	-	<0.05	n.d.	C+T	α
		89.9±1.7	9.9±1.7	n.d.	0.11±0.01	-	<0.05	n.d.	C+D↓?+T	α
CSG-314	Frag of artefact	++	+++	vest.	vest.	vest.	vest.	vest.	C+D↓?	α, δ
		86.1±3.0	13.7±2.9	<0.1	0.13±0.01	-	<0.05	n.d.		
CSG-316	Frag of artefact	+++	++	vest.	vest.	vest.	vest.	n.d.	C+T↓	α, δ
		85.0±0.7	14.8±0.7	n.d.	0.18±0.01	-	<0.05	n.d.		
CSG-318	Blade frag part.	+++	++	n.d.	n.d.	n.d.	vest.	n.d.	C+D↓+T	α, δ↓
	remelted?	90.2±2.4	9.7±2.3	n.d.	n.d.	-	<0.05	n.d.		
CSG-330	Spatula frag	+++	++	vest.	n.d.	vest.	vest.	n.d.	C+D+T+D	α
		88.2±0.9	11.7±0.9	n.d.	<0.1	-	<0.05	n.d.		
CSG-335	Blade frag part.	+++	++	vest.	vest.	vest.	vest.	n.d.	C+D↓+T	α
	remelted?	88.8±0.6	11.1±0.6	n.d.	<0.1	-	<0.05	n.d.		
CSG-383	Double spatula	+++	++	n.d.	vest.	n.d.	vest.	n.d.	C+D+T+D↓?	α
		89.2±2.9	10.8±3.0	n.d.	<0.1	-	<0.05	n.d.		
CSG-346	Scabbard chape	++	+++	vest.	vest.	n.d.	vest.	vest.	C+T	α, δ↓
	fragment	84.3±1.0	15.4±1.0	<0.1	0.15±0.02	-	<0.05	n.d.		
CSG-400	Sickle frag part.	+++	++	vest.	vest.	vest.	vest.	n.d.	C+T	α, δ↓
	remelted?	85.4±2.0	14.4±2.0	n.d.	0.15±0.03	-	<0.05	n.d.		
CSG-407	Buckle element	+++	++	vest.	n.d.	vest.	vest.	n.d.	C+T+D	α
		90.4±1.7	9.6±1.7	n.d.	<0.1	-	<0.05	n.d.		
CSG-408	Bracelet frag	+++	++	vest.	vest.	vest.	vest.	vest.	C+T+D↓?	α
		89.3±0.6	10.6±0.7	n.d.	<0.1	-	<0.05	n.d.		
CSG-410	Weight 6.22 g	+++	++	vest.	vest.	vest.	vest.	n.d.	C+D+T+D↓?	α, δ
	(sphere)	88.8±1.1	11.1±1.0	0.1±0.0	<0.1	-	<0.05	n.d.		
CSG-411	Weight 9.08 g	+++	++	vest.	vest.	vest.	vest.	n.d.	C+D↓?	α, δ
	(bitroncoconic)	88.0±1.3	11.7±1.2	0.2±0.1	<0.1	-	<0.05	n.d.		

+++ >50%; ++ 10-50%; + 1-10%; vest. (Vestiges) <1%; n.d. not detected

C cast; D deformation/forged; T heat treatment/annealed; ↓ low amount; ↑ high amount

Table 3.13 Summary of the experimental results of composite artefact – bronze and copper – from *Baiões* (EDXRF results are given in a semi-quantitative way; composition is given by average of three micro-EDXRF analyses ± one standard deviation)

No.	Item	Composition (wt.%)							Method of fabrication	Phases present
		Cu	Sn	Pb	As	Sb	Fe	Ni		
CSG-349	Cauldron/vessel frag with rivet	+++	++	vest.	n.d.	n.d.	vest.	n.d.		
	copper	99.9±0.1	n.d.	n.d.	n.d.	-	<0.05	n.d.	C+D+T+D	α-copper
	bronze	86.6±0.4	11.4±0.3	n.d.	n.d.	-	<0.05	n.d.	C+D+T	α

+++ >50%; ++ 10-50%; + 1-10%; vest. (Vestiges) <1%; n.d. not detected

C cast; D deformation/forged; T heat treatment/annealed

In **Fig. 3.47** micrographs with the microstructures of all the artefacts and fragments are presented, with the exception of the composite CSG-349 item that is described later in more detail.

The **copper** bar CSG-293 has equiaxed twinned grains and numerous Cu-S inclusions. Its microstructure indicates that it has been shaped through thermo-mechanical processing to the final near-quadrangular section. The composition and typology of this artefact suggests that it might be a semi-finished product. It could have served to provide small amounts of metal, that were cut-off, to manufacture small simple copper items, such as rivets, cramps, etc., or to melt to produce more complex shaped copper artefacts. The thermo-mechanical processes detected can be explained as a result of shaping and softening it for easier transport, handling and posterior cutting. Another hypothesis could be that the copper bar was used for bronze production, to be joined to cassiterite (or metallic tin?), as a copper ingot. Some copper ingots attributed to LBA have been found in the Iberian territory. However, these are scarce, and a clear connection to metallurgical activities is lacking since most of them were found in hoards with finished palstaves and not among metallurgical debris (Gómez Ramos, 1993). Comparing to earlier copper artefacts analysed from *Pragança* and *Escoural* this bar has a larger impurity pattern. This can possibly be related to the copper that was circulating in later periods (i.e. LBA), where an increase in the impurities can be a result of more recycling/mixing of metals, different sources and/or types of ores extracted.

Among the **bronzes**, tin contents are in the range of 9.6-15.4%, except for two items: socket fragment CSG-139 and pin head CSG-162, which have >15% (17.1 and 18.8%, respectively). These two items show as-cast microstructures, with the formation of cored dendrites and a high amount of the hard and brittle interdendritic (α+δ) eutectoid. Therefore, it seems reasonable that these artefacts were not subjected to mechanical work. The manufacture of these two items with a higher Sn content could be intentional, to produce a more “silver like” colour, or, if unintentional, these artefacts could just be waiting for recycling.

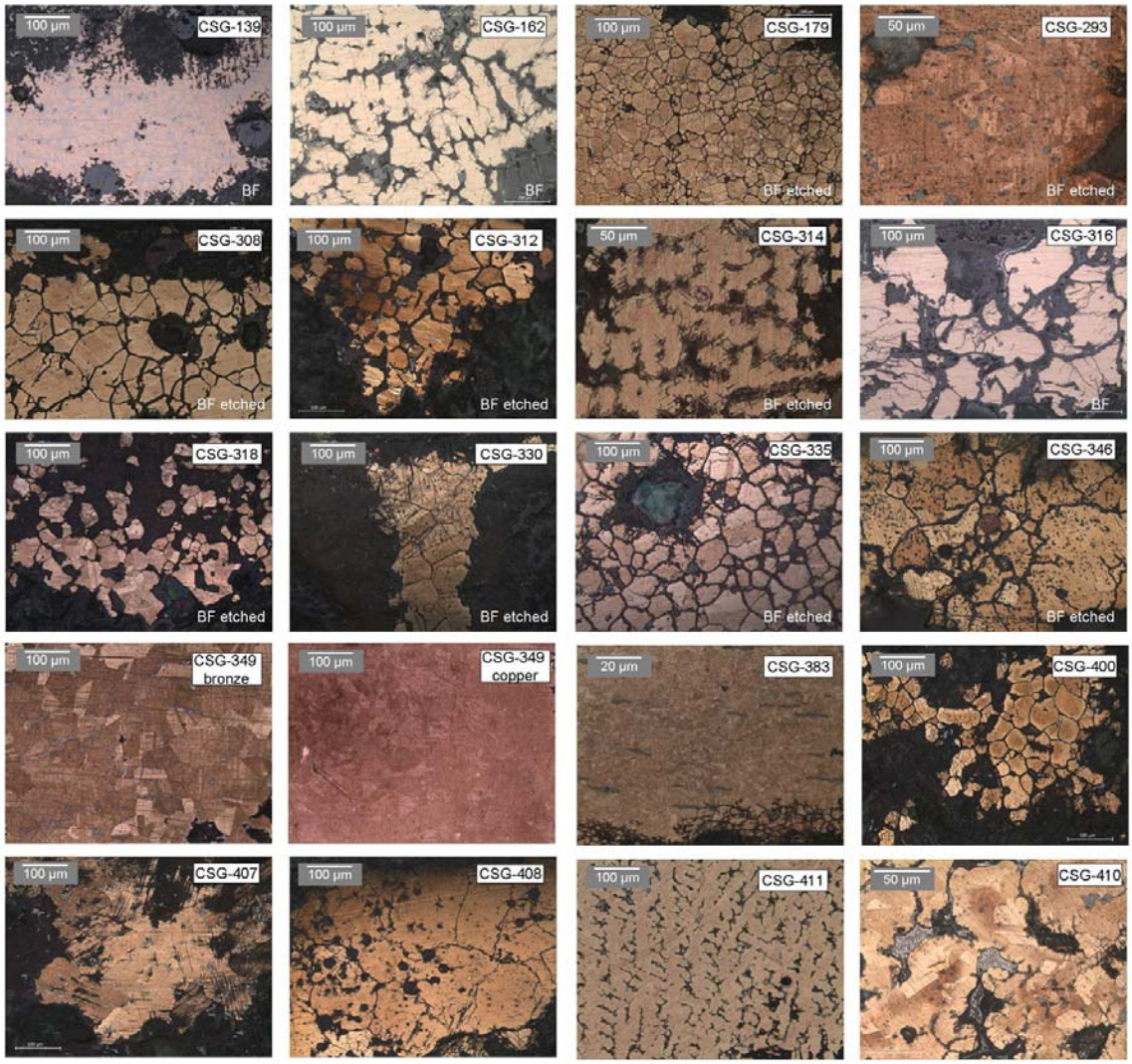

Fig. 3.47 Microstructures of the artefacts and fragments from *Baiões* (OM).

The microstructures of the heat-distorted blade fragments CSG-318 and CSG-335 and the sickle fragment CSG-400 show equiaxed α-grains, with varying (although low) amount of twinning and low amount of (α+δ) eutectoid taking into account the Sn contents. These features represent a typical recrystallized microstructure, indicating a post-casting work, which suggests that they were not faulty castings. If they were faulty castings a dendritic structure composed by α-cored dendrites with interdendritic (α+δ) eutectoid would be expected. They are most likely artefacts that suffered high temperatures, perhaps during a recycling operation interrupted at an initial stage or during a fire involving the settlement. The latest, however, does not seem so appropriate since there is absence of artefacts in the collection with microstructures that show a final heat treatment, as well as there is a relatively small number or artefacts showing heat-distorted shapes. Thus, these artefacts do rather point out to some intentional metallurgical operation, such as a recycling operation.

The amalgam of four bar fragments, CSG-312, joined by corrosion products or partially melted together, also suggests recycling operations at the site since they appear to be scrap fragments gathered for melt. Microstructures of two analysed bar fragments are similar to the sickle (CSG-400).

The microstructures of the artefact fragments CSG-314 and CSG-316, scabbard chape fragment CSG-346, buckle element CSG-407 and bracelet fragment CSG-408 show absence of high deformations. They have a dendritic (CSG-314) or an annealed microstructure with large grains (CSG-316, 346, 407 and 408), without annealing twins, and presenting various amounts of (α+δ) eutectoid. They have only been subjected to a annealing and/or to a slight final cold deformation - evidenced by corrosion along slip bands (CSG-314 and 407). Their shapes were most probably obtained by cast, with some posterior mechanical work applied for surface finishing.

The unifacial palstave butt fragment CSG-308 has a microstructure composed by large equiaxed grains with a small amount of twinning. Its primary shape was most likely obtained by cast (a mould to produce such a palstave was found at the site). Its microstructure suggests that after casting it was subjected to some cycles of deformation and annealing, possibly for the cutting of the casting sprue and finishing of the surface.

The two spatula fragments CSG-179 and CSG-330 and the double spatula CSG-383 are those which show the most pronounced thermo-mechanical processed microstructures. They are composed by equiaxed grains totally twinned and CSG-383 show clear elongated Cu-S inclusions. They also have slip bands indicative of a final cold work, probably performed to provide a strain hardening effect. The shape and microstructure of these artefacts is thus consistent with a cast bar fragment that was subject to thermo-mechanical cycles until its final shape.

The microstructural examinations made on the weights show that they have been subjected to different manufacturing sequences (these weights were previously presented in the metrological study in section 2.3.4). The bitroncoconic 9.08 g weight shows a dendritic microstructure with a secondary dendrite arm spacing (DAS) of ~25 μm, typical of an as-cast bronze object. The sphere 6.22 g weight shows a recrystallized grain structure, typical of an object that has been subjected to thermo-mechanical processing after casting. This suggests that a more severe final work (involving deformation and heat treatments) could be required on the sphere shaped weight to produce a “perfect” spherical shape.

The CSG-349 item is probably a fragment of a vessel or cauldron, and is composed by two sheets of bronze joined by a rivet of copper (**Fig. 3.48**). Composite objects made by joining different metals and dated to BA are known, however they are not very usual. Bronze artefacts with copper rivets are one of the most common examples (Northover and Anheuser, 2000). Other Iberian copper rivets dating to LBA were found in the *Ria de Huelva* hoard, however not connected to any artefact (Rovira, 1995).

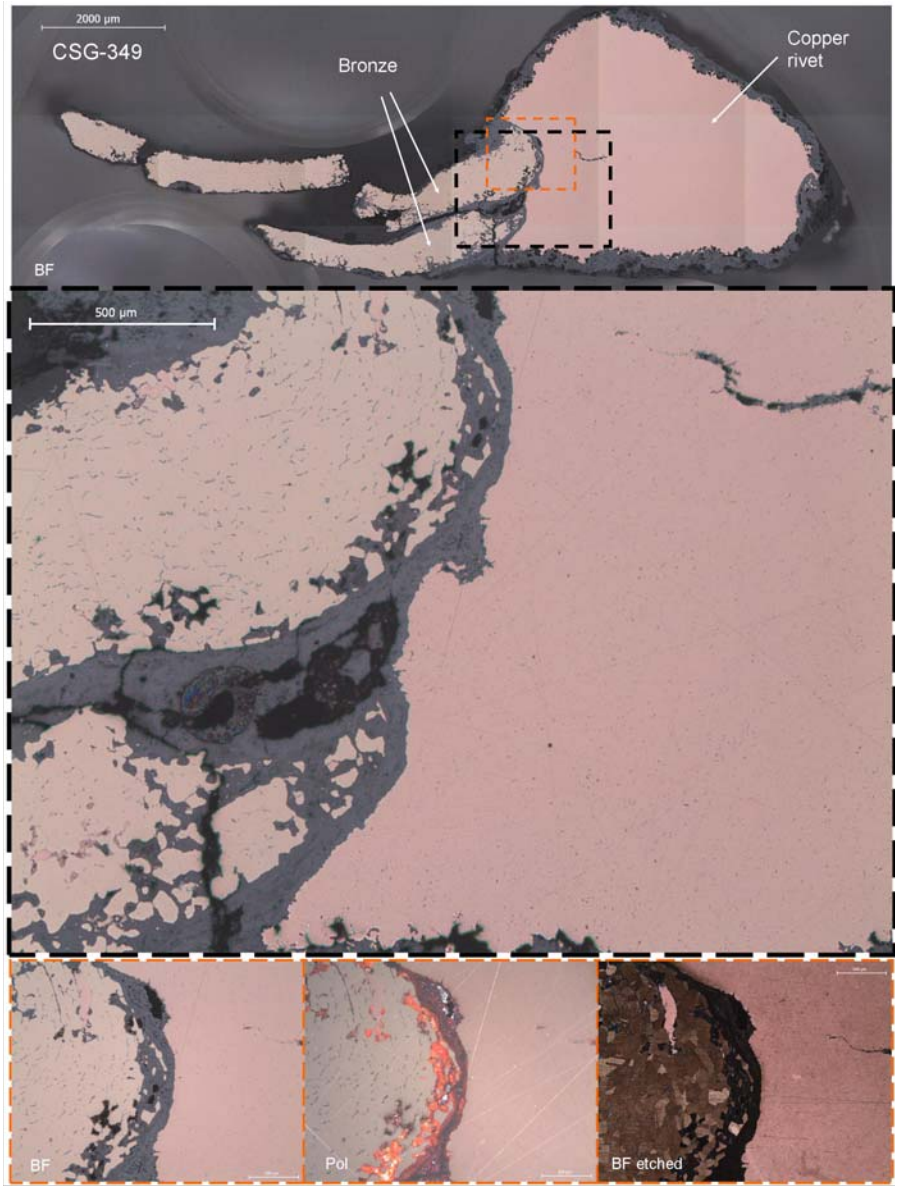

Fig. 3.48 Microstructure of the composite artefact (CSG-349) from *Baiões* (OM).

The sampling of this particular item allowed a detailed observation of both bronze sheets and copper rivet microstructures, as well as an appraisal of the joining technique. The bronze sheets have a thickness of ~500-800 µm, obtained by working the bronze through thermo-mechanical cycles, as demonstrated by its microstructure presenting equiaxed grains totally twinned and clear elongated Cu-S inclusions. The copper rivet has a twinned small size grain microstructure with some small inclusions, with the grains showing some deformation due to a last mechanical work. This last mechanical operation was most likely the shaping of the rivet in place, by placing it through the hole and hammering against a flat surface with a tool that left a conical shape on the outside for ornamental reasons. It can be observed that this tool also deformed the two bronze sheets next to the rivet, provoking strain deformations that later facilitated the break and corrosion of the outer sheet. Rivets with shaped heads (sometimes with remarkable modern looking) have previously been described for cauldrons in the British Isles (Coghlan, 1975).

The rivet seems to be made with a slightly purer copper than the bar CSG-293. This, however, does not exclude the possibility of the bar to serve for producing items as this one; actually, it supports the need for unalloyed copper availability for producing specific items at the site/region/period (other unalloyed copper artefacts are going to be presented later, in sections 3.3.3.4 and 3.4.1.2).

In respect to the Sn contents among the various items studied it can be shown that there is no clear difference between the artefacts, nodules, and even the bronze used to make the relatively thin sheets in the composite artefact (**Fig. 3.49**). The use of a ~9-15% Sn bronze on almost all the items suggests that its optimum mechanical properties were appreciated, and that some "control" in the bronze composition was accomplished. Moreover, the absence of low tin bronzes suggests that the site had a good and constant access to the materials needed for bronze production, particularly tin or cassiterite.

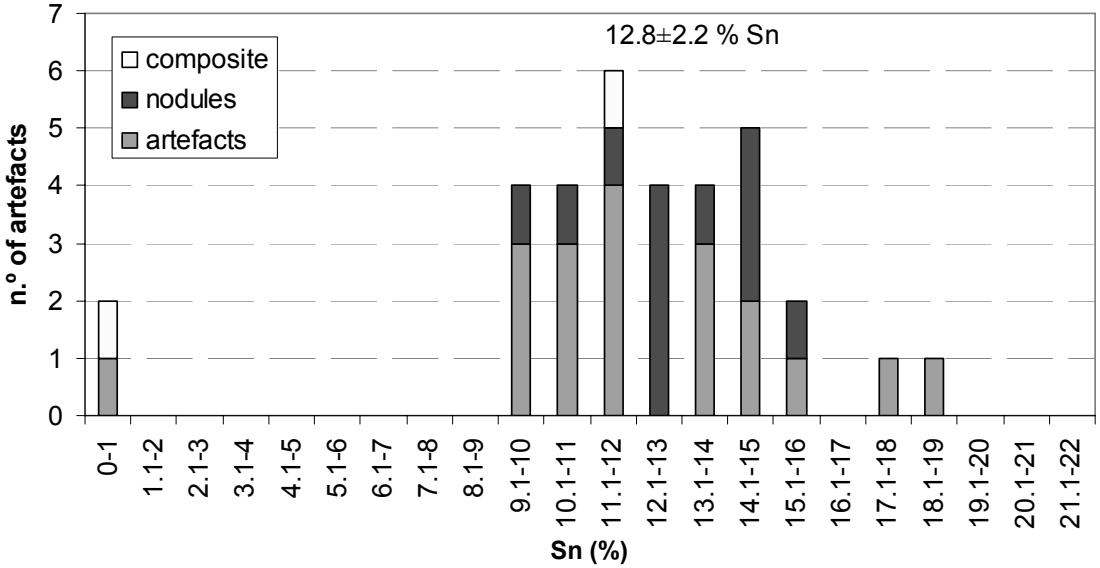

Fig. 3.49 Histogram of Sn content in the studied items from *Baiões* (average and one standard deviation annotated for the bronze artefacts – unalloyed copper excluded).

3.3.3.2 *Santa Luzia*[11]

The *Santa Luzia* archaeological site is placed on a hilltop some 20 km Southwest of *Baiões*. Four Radiocarbon dates were obtained for the site, pointing out to the sites earliest occupation between 1270-1030 cal BC (Senna-Martinez, 2000). At the site various bronze artefacts have been found, as well as fragments of scrap and a mould for casting chisels with a near-square section.

For the present study the following items have been chosen for analysis: six scrap bars with similar sizes but different sections; one weight (sphere shape with 4.34 g); two fibula fragments; and one awl (**Fig. 3.50**). Among the scrap bars three have a square section, two a circular section, and one an oval section. Their original functionality is unknown, but their shape can relate them with items such as

[11] The content of this section has adaptations from the following published work:

- E. Figueiredo, M.F. Araújo, R. Silva, F.M. Braz Fernades, J.C. Senna-Martinez, J.L. Inês Vaz (2006) Metallographic studies of copper based scraps from the Late Bronze Age Santa Luzia archaeological site (Viseu, Portugal). In: R. Fort, M. Alvarez de Buergo, M. Gomez-Heras, C. Vazquez-Calvo (Eds.), *Heritage, Weathering and Conservation*, Taylor and Francis, London, Vol. I, pp. 143-149.

chisels, awls or bracelets. The weight has a similar shape as the previous studied weights from *Baiões* and *Pragança* and was formerly presented in the metrological study in section 2.3.4. The last three items (two fibula fragments and an awl) have previously been published as fragments of a gilded fibula (e.g. Vilaça, 2008), however the detailed observation for the present study made the current typological attribution seem more adequate.

Fig. 3.50 Items studied from *Santa Luzia*.

All items were analysed by EDXRF and micro-EDXRF in prepared surfaces (the bars and small piece of the fibula fragment SL-622-I (b) were mounted in resin without sampling) and micro-EDXRF analysis were also performed over the gold-like surfaces of the awl and fibula fragments. Also, microstructural observations by OM were performed on prepared surfaces. Exception was made for the weight that was only analysed by non-invasive EDXRF. Results are presented in **Table 3.14**.

Table 3.14 Summary of the experimental results on the bronze items from *Santa Luzia* (EDXRF results are given in a semi-quantitative way; composition is given by average of three micro-EDXRF analyses ± one standard deviation)

No.	Item (section)	Composition (wt.%) Cu	Sn	Pb	As	Sb	Fe	Ni	Method of fabrication	Phases present
SL-61	Bar frag (oval 5×4 mm)	++ 87.8±2.2	++ 11.8±2.1	vest. 0.13±0.02	vest. 0.10±0.02	vest. -	vest. <0.05	n.d. 0.26±0.00	C+D↓+T	α
SL-70	Bar frag (square 3×3 mm)	++ 87.9±1.9	+++ 11.8±1.9	+ 0.24±0.04	vest. <0.1	vest. -	vest. <0.05	n.d. n.d.	C+D+T+D↓	α, δ↓
SL-259-II	Bar frag (square 5×5mm)	++ 88.6±1.1	++ 10.3±1.0	vest. 0.1±0.04	+ 0.64±0.09	+ -	+ <0.05	vest. 0.37±0.04	C	α, δ
SL-58	Bar frag (circular 5mm∅)	++ 86.6±1.1	+++ 13.2±1.0	vest. <0.1	vest. 0.19±0.07	n.d. -	vest. <0.05	n.d. n.d.	C+D+T+D↓	α, δ
SL-266-I	Bar frag (circular 5mm∅)	++ 91.2±0.5	++ 8.7±0.5	n.d. n.d.	vest. <0.1	n.d. -	vest. <0.05	vest. n.d.	C+D+T+D	α
SL-283-I	Bar frag (square 3×3mm)	++ 87.1±0.4	+++ 12.8±0.3	vest. <0.1	n.d. <0.1	n.d. -	+ <0.05	n.d. n.d.	C+D+T	α, δ↓
SL-596-I	Weight 4.34 g (sphere)	+++	++	vest.	vest.	n.d.	vest.	n.d.		
SL-622-I	Fibula frag	++ 86.9±0.1	+++ 13.1±0.1	n.d. n.d.	vest. n.d.	n.d. -	vest. <0.05	n.d. n.d.	C+D+T+D↓	α
SL-454-I	Fibula frag	+++ 85.5±2.0	++ 13.9±1.4	vest. 0.49±0.53	n.d. <0.1	vest. -	vest. <0.05	n.d. n.d.	C+D+T+D↓	α, δ↓
SL-524-I	Awl	+++ 87.5±1.4	++ 12.5±1.4	n.d. n.d.	n.d. n.d.	n.d. -	vest. <0.05	n.d. n.d.	C+D+T+D	α

+++ >50%; ++ 10-50%; + 1-10%; vest. (Vestiges) <1%; n.d. not detected

C cast; D deformation/forged; T heat treatment/annealed; ↓ low amount

The results show that all the artefacts are made of bronze, frequently with small amounts of Pb, As and Sb. Their Sn content is between ~8-14%, with an average and standard deviation of 12.0±1.6% (Sn content in the weight was not determined). The analyses show that the Sn content is not significantly different among the different typologies, although the bar fragments show a higher Sn content range – most likely a result of their higher representativity among the small sample studied (**Fig. 3.51**). Generally, the bronze composition of the artefacts is similar to the bronze from *Baiões*, both in Sn contents and in the low impurity pattern.

In the present study no indication for a gilded surface in the awl and fibula fragments was found. Both superficial EDXRF analysis and micro-EDXRF analysis made over the surfaces with the gold-like colour detected only the main Cu and Sn elements. The observation of the cross-section of the fibula fragment SL-622-I (b) did show that the gold-like colour surfaces in these items are, in fact, uncorroded bronze. The exposure of uncorroded bronze in the surfaces of these items is only explainable by an inadequate conservation treatment, as an over-mechanical cleaning (Degrigny, 2007). Also, detailed observation of the awl surface showed a layer of a green colour paint covering many parts of the uncorroded bronze, as to re-coate recently exposed metal, supporting an previous intervention on these items.

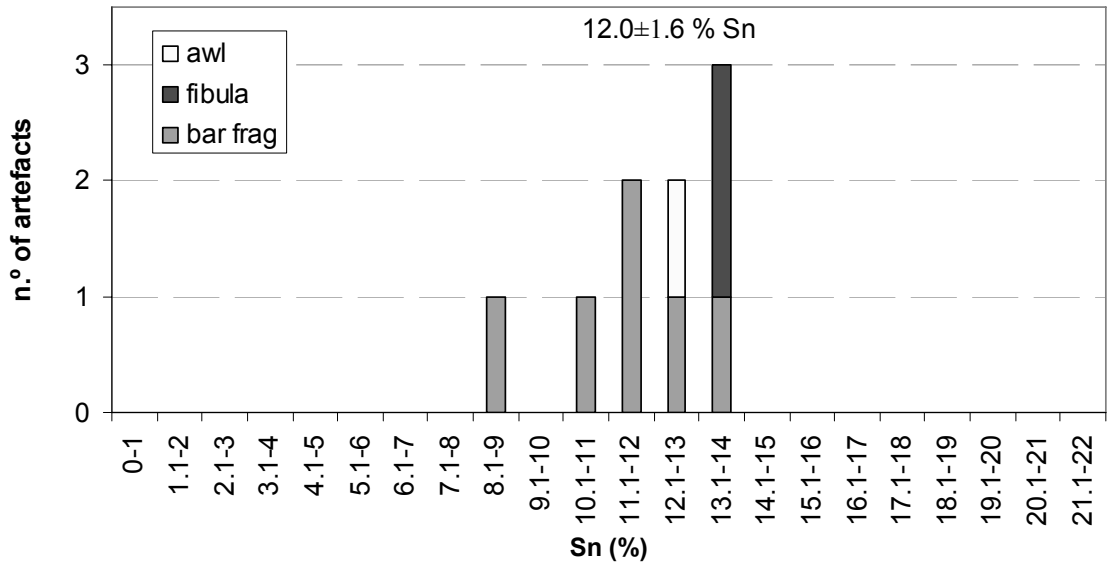

Fig. 3.51 Histogram of Sn content among the studied artefacts from *Santa Luzia* (average and one standard deviation annotated).

Microstructural observations of the artefacts showed that most of them have heavily worked microstructures, with the presence of twinned grains and a general presence of Cu-S inclusions (**Fig. 3.52**). Only the square bar SL-259-II does not show any feature related to cold work and the oval shaped bar SL-61 shows a few twinned grains near the surface indicating minor superficial mechanical works previously to an annealing, which were not enough to reduce significantly the pores that are of similar size as the as-cast SL-259-II square bar.

Among the square bar shaped items the SL-259-II bar is also the one with the largest cross-section. This may indicate that the other two square bars could have been shaped from bars with cross-sections similar to the SL-259-II bar (i.e. circa 2 mm larger). Both the circular bars show heavy worked microstructures, which may also indicate the shaping of near-square cross-section bars (besides the mould found in *Santa Luzia* to cast such near-square bars/chisels, see the mould presented in section 3.3.4).

The fact that none of the bars showed a final deformation can have different interpretations: they might be fragments of artefacts that where not subjected to any final cold work; or they might be "raw material" that would later be used to produce specific items.

The shaping of the awl and the fibula was most likely also performed through thermo-mechanical processing of a cast bar. This seems to have been the most simple and likely way to manufacture all the bar-shaped artefacts (as the ones studied in this section) during this period.

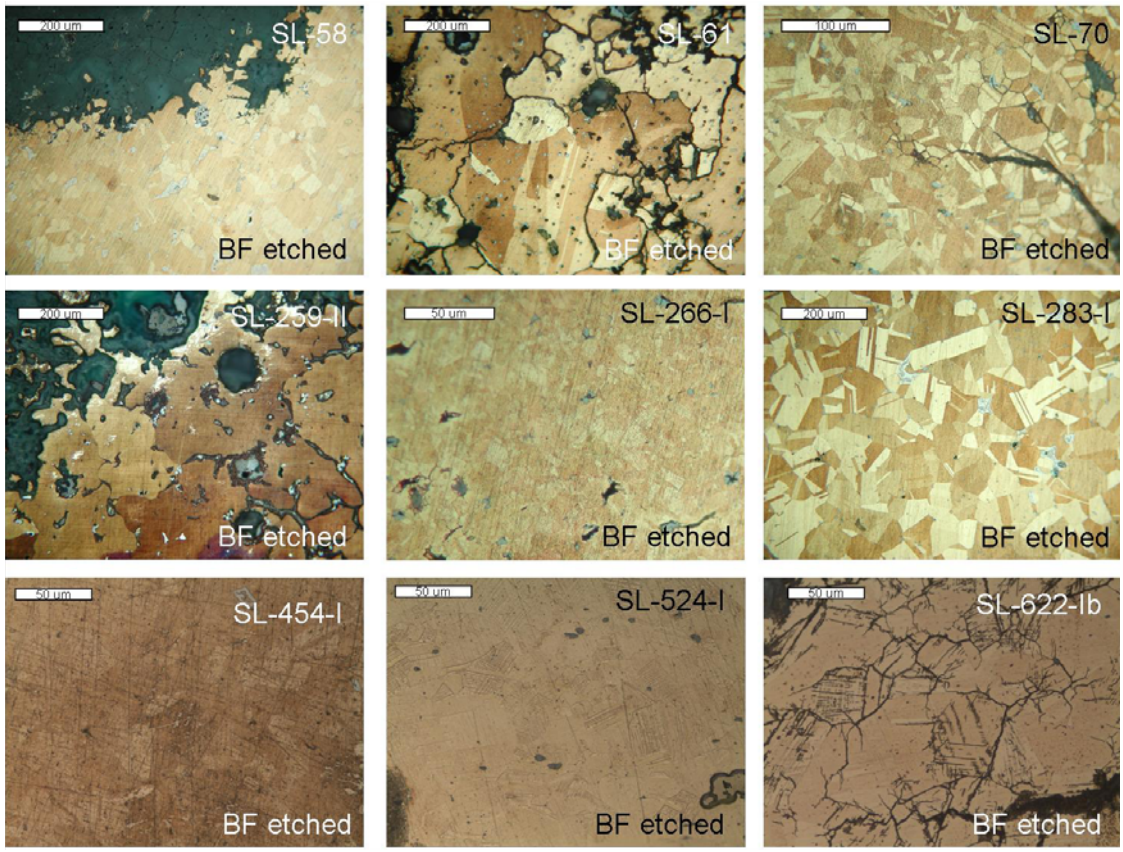

Fig. 3.52 Microstructures of the artefacts from *Santa Luzia* (OM).

3.3.3.3 *Figueiredo das Donas*

During the first half of the XX century, six exceptional nails, a dagger and a sickle (**Fig. 3.53**) were found in *Figueiredo das Donas* (Vouzela), located between *Baiões* and *Santa Luzia* sites. Since their finding, the items have been described as belonging to a deposit. More recently, during a reappraisal of BA deposits in the Portuguese territory Vilaça (2006b) has proposed the existence of an habitat at the place, based on the evidences found in the surroundings (e.g. remains of constructions) and the materials found together with the metal artefacts (e.g. worked stones, millstones, ceramics, charcoal, etc.).

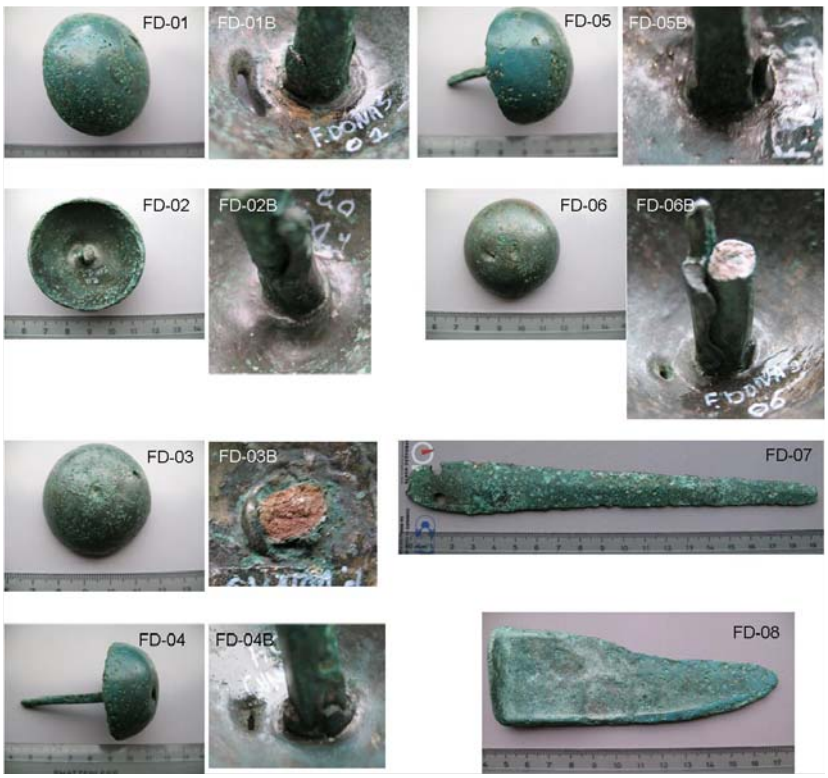

Fig. 3.53 Artefacts studied from *Figueiredo das Donas*: nails (FD-01-06); dagger (FD-07); and sickle (FD-08). For each nail a detailed image of the head and pin junction area is shown (FD-01B-06B).

The nails are unique in the Iberian territory; their size has no parallels among other nails found, and scarce parallels among similar items, as buttons (Coffyn, 1985). Their large size indicate that they where used in heavy structures, and a suggestion has been made by J.C. Senna-Martinez (personal communication) that they could have been shield nails, as those represented in warrior stelae, which have been found dispersed in South-West IP and are attributed to a period of time that ranges from LBA to 1st IA (Celestino Pérez, 2001; Ruiz-Gálvez, 2008; Sanjuán, 2006). If this is the case, the metallic nails must have had a strong decorative function, since the shields were most likely made of leather (Ruiz-Gálvez, 2008) and/or wood similarly to others found in European areas (Celestino Pérez, 2008) (note that there is absence of shields in the archaeological records of the IP, making one suppose that these must have been manufactured in an easy decaying material).

Detailed observations on the reverse side of the nails (**Fig. 3.53**, FD-01B to 06B) suggest that the nails are made of two independent pieces, the head and the pin, joined during the manufacture.

Daggers were widely used during LBA, and many have been found in LBA Iberian contexts (Coffyn, 1985). The dagger (FD-07) is almost complete; it was joined to a hilt by the means of rivets (now missing), a frequent joining technique at the time (an example from *Baiões* site was studied previously in section 3.3.3.1).

The sickle (FD-08) is complete and belongs to the Rocannes type, a typology found mainly in LBA contexts of the Portuguese territory (outside the Iberian territory only two were found in Sardinia) (Giardino, 1995) and from which moulds are known, namely in *Casal de Rocanes* (Cacém, Central

Portugal) (Fontes, 1916). This item appears to have been used in past due to the worn condition of the cutting edge.

In the study of these items only non-invasive procedures were performed. EDXRF analyses were performed on all the artefacts in two different areas. Regarding the nails it allowed the evaluation of special features such as a composite character (i.e. among the head and pin and eventually some superficial treatment on the head). Micro-EDXRF was performed on one of the nails on (1) a fracture on the pin and (2) over a small area free of the most superficial corrosion products on the head, to obtain the metal composition. Finally, a radiograph was performed with the nails on different positions, in order to search for metal heterogeneities and to investigate the manufacturing/joining process.

The EDXRF analyses of the **dagger** (FD-07) and **sickle** (FD-08) showed that they were made of bronze (Cu-Sn) with irregular impurities of As, Pb and Sb (**Fig. 3.54**). Low Fe contents were detected on some of the analyses and are most probably due to the incorporation of soil particles in the corrosion layers.

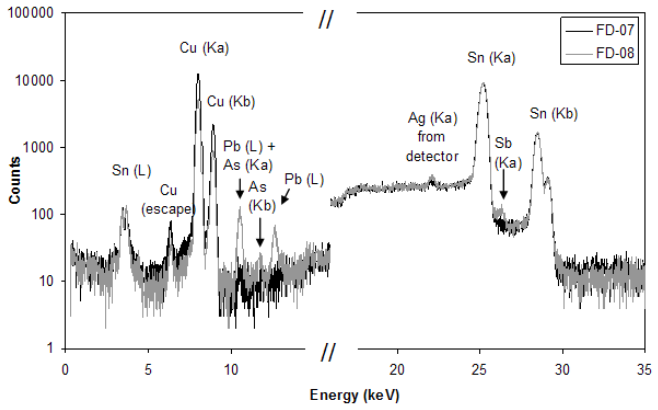

Fig. 3.54 EDXRF spectra of dagger (FD-07) and sickle (FD-08).

The EDXRF analyses made on the **nails**, over the pins (when existent), and over the convex side of the heads, resulted in spectra with the same elements detected previously for the dagger and sickle – major Cu and Sn and minor As, Pb and Sb – with alike relative intensities (**Fig. 3.55**). These results show that both head and pin of the nails were made of bronze, probably of a similar composition. The analyses made on the convex and concave sides of the heads of those nails with broken pins, did also resulted in the same elements with alike relative intensities, giving no evidence of the use of a solder – a solder is a low melting temperature alloy, usually lead and/or tin rich (Coghlan, 1975) – for the joining of the pin to the head or a superficial treatment on the outer convex side of the head, such as tinning (**Fig. 3.56**).

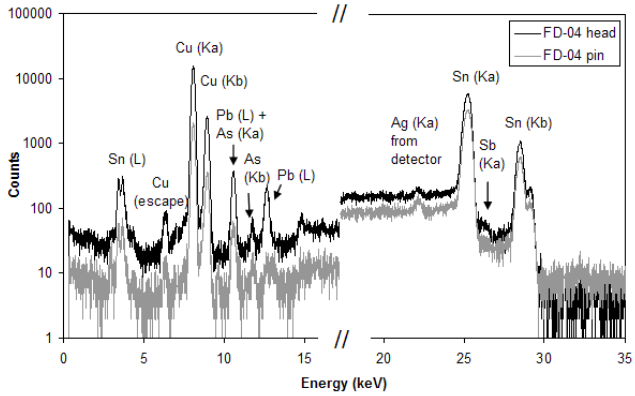

Fig. 3.55 EDXRF spectra of the nail FD-04 performed over the convex side of the head and over the pin (different intensities are due to the differences in the analysed areas due to the different size of the pieces).

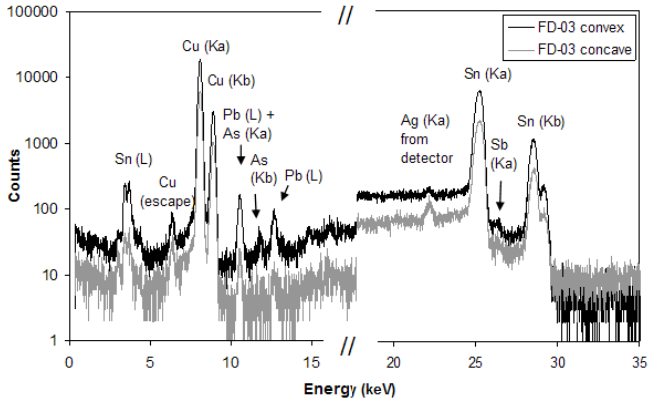

Fig. 3.56 EDXRF spectra of the head of the nail FD-03 performed over the convex and concave sides (different intensities are due to geometrical factors caused by the different surface shapes).

The results of the micro-EDXRF analyses made on the nail FD-01 are shown in **Table 3.15**. These show, as indicated previously by the EDXRF analyses, that both head and pin are made of a bronze with a similar composition, ~11 wt.% Sn and vestiges of Pb and As (Sb is below the detection limit <0.15 wt.%). The higher Fe content in the head is most likely due to some contamination from corrosion.

Table 3.15 Results of micro-EDXRF analyses performed on nail FD-01(wt.%, normalized)

	Cu	Sn	Pb	As	Fe	Ni
Head	88.5	10.9	0.11	<0.1	0.11	n.d.
Pin	88.4	11.4	0.14	<0.1	<0.05	n.d.

This binary bronze – with ~11% Sn in the case of the nail FD-01 – with As, Pb and Sb as impurities can be related to the metallurgical tradition studied previously for the *Baiões* and *Santa Luzia* sites. A bronze with ~11% Sn has optimal mechanical properties, being much harder than pure copper after cold work, and has a gold-like colour, that was probably also appreciated. The absence of a supposedly less valuable metal, such as copper, to manufacture less visible pieces, such as the pin in the nails, may be related to the bronze higher mechanical properties, very relevant to attach and sustain

the nail in place, or to the general availability of bronze in relation to copper (see section 3.5 – Archaeometallurgical final discussion and conclusions).

The radiographic image obtained of the six nails is shown in **Fig. 3.57**. The image has been processed so that the darker areas refer to higher densities and the lighter areas to lower densities.

The radiograph shows no apparent fixing system joining the pin to the head. In those nails whose front view was examined, FD-01, FD-02, FD-03 and FD-06, it can be observed some small bright regions around the junction of pin and head (dot-like light areas) and a nearby larger bright region (near the top of the heads) that in some cases is actually a hole (FD-01 and FD-06; FD-04 does also have a hole that is not visible in the radiographic image but can be observed in **Fig. 3.53**, FD-04B). In those nails where this region is not a hole (FD-02 and FD-03), visual observations clearly indicate that this region is constituted by thinner metal than the surrounding regions. This is also true for FD-05 (not visible in the radiograph due to its positioning). These observations exclude the presence of a closed void (e.g. large pore), and do not point out to metal composition heterogeneity.

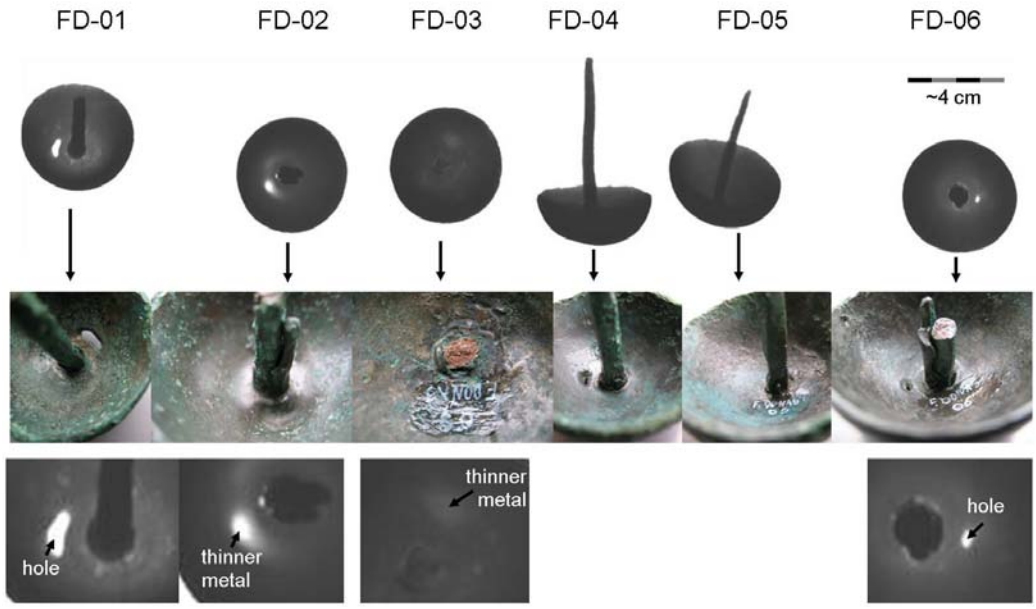

Fig. 3.57 Radiograph of the six nails from *Figueiredo das Donas*. At top the general radiograph image; at the middle a photograph of the joining area; and at bottom a detailed radiographic image of the region around the junction of pin and head of FD-01, FD-02, FD-03 and FD-06.

Both the smaller dot-like bright regions and the larger bright region can be related with the manufacturing process. The small dot-like regions around the junction of pin and head suggests either the presence of gas bubbles entrapped in the contact zone of the two metallic parts, or the development of some corrosion along that contact zone. This supports the visual examination that suggested that the nails were manufactured by two independent pieces, joined during manufacturing, in contrast to one single piece, as would have resulted from a one-stage casting operation.

The holes (in FD-01, FD-04 and FD-06) and the thinner metal regions (in FD-02, FD-03 and FD-05) near the top of the heads are probably a result of a gas bubble entrapped in the mould, showing a difficulty in a proper escape of gas and a difficulty in a free flow of metal to all parts of the work.

It is interesting to note that the heads of the nails are exactly of the same size and shape, and present quite smooth surfaces. If the lost-wax casting was employed in the manufacture of the heads, the use of a spinning wheel to shape each model in bees-wax could be one explanation to the homogeneity and control of the shapes. The use of these techniques (lost-wax casting and spinning wheel) during LBA in the IP has been suggested by Perea and Ambruster (2008) in the manufacture of gold cylindrical shape items, as the bracelets from *Villena/Estremoz*, with perfect symmetries. Otherwise, the heads of the six items could have been manufactured in the same mould resulting in identical shapes – a bivalve metal or stone mould could resist to multiple castings in comparison to the one-piece ceramic mould used in the lost-wax casting technique, which was fragmented to recover the metallic object. This process would probably better explain the recurrent region of metal lack next to the top of the nail heads (a hole in some cases). If different moulds were used to manufacture each nail (as would be necessary in the case of lost-wax casting technique) defects would most likely be avoided by improving the procedure each time.

The detailed visual observation of the contact surfaces of the pin and head shows that in all the nails a small portion of metal frequently in the form of a run-off (droplet) extending from the head along the pin surface is present. One of them, in FD-06, was analysed by micro-EDXRF and the spectrum showed that it was of bronze. In some of the nails these droplets have been broken. In those pins that have a near-quadrangular cross-section, the droplet follows the plain surfaces rather than the edges. These portions of metal appear to be a result of a leaking occurrence (see a good example in **Fig. 3.53**, FD-06B). A run of metal has also been observed in a radiograph made over a cast hilt of a BA dagger from Italy made of bronze (Cu-Sn, traces of As and Pb), and has been explained as possibly resulting from an ancient repair (Sestieri et al., 2007).

Ancient repairs were frequently made by the casting-on technique, that consisted in casting a new piece of metal to a pre-existing one. This technique was known by BA (Coghlan, 1975) and was most certainly in use by the LBA metallurgists of the Central Portuguese Beiras (Ambruster, 2002-2003). Although it has been mostly associated to repairs, the casting-on technique seems to also have been used in the manufacture of artefacts, as evidenced by a composite artefact from the site of *Baiões*, a dagger with a blade made of iron and a handle made of bronze (one of the first iron items from the IP attributed to LBA) (Vilaça, 2006a). The employ of this technique would explain the droplets in the nails, which would have formed during the pouring of the metal to make the head through a space between the mould and the pre-existing pin. Furthermore, the direction of the running droplets indicates that the pouring would have been performed with the mould of the head above the pin. This may relate to the lack of metal found near the top of the heads, as resulting from the last part to fill in the mould. Analysis of the shapes of several casting sprues from BA artefacts have shown that the

pouring was frequently performed with the mould in an angle that could reach 30 degrees (Coghlan, 1975). In **Fig. 3.58** a scheme illustrating the possible joining of the head to the pin by the casting-on technique is shown, and the pouring has been illustrated with the mould in an angle that can be related to the lack of metal next to the top of the nails head.

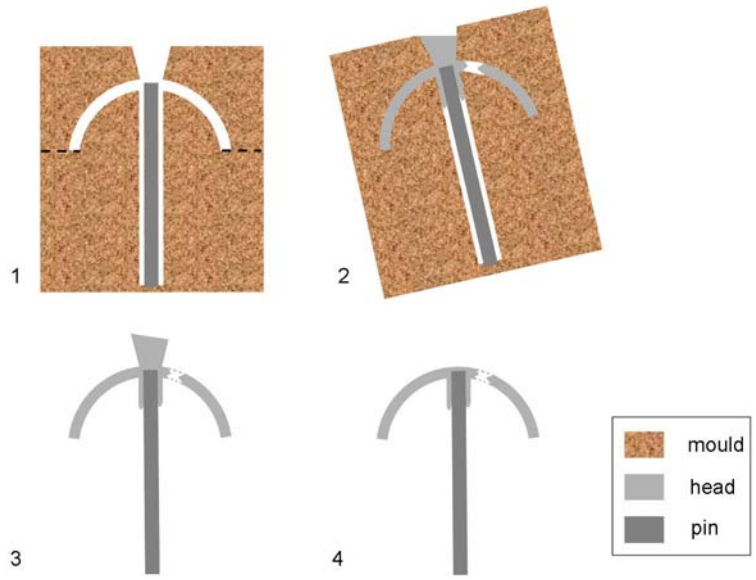

Fig. 3.58 Scheme illustrating the possible manufacture of the nails by the casting-on technique: (1) mould positioned above the metallic pin; the mould could be composed by one single piece, if lost wax technique was used, or it could be composed by two pieces, of stone or metal, with a possible union in the broken line; (2) pouring of the metal to make the head of the pin with some leaking in the pin-mould junction and incomplete fill of the mould on the most top area; (3) appearance of the nail after the mould has been taken off; (4) final appearance, after a final surface finishing (metal lack is represented).

The manufacture of the head and pin pieces of the nails in a bronze with similar composition is probably related to (1) the generalization of this alloy at LBA period in the region, (2) absence of leaded bronzes among the *Baiões/Santa Luzia* group that, if existent, could have been preferred to manufacture the head due to its better casting properties (increased fluidity and lower liquidus/solidus temperature) probably avoiding the casting defect observed at the top of the heads, (3) the mechanical and aesthetical properties of this particular bronze composition when compared to others (as low tin bronzes) or to pure copper.

3.3.3.4 *Crasto de São Romão*[12]

Cabeço do Castro de São Romão is located near Seia, Southeast to the previous sites. The site has been excavated during the 1980's and a set of metallic artefacts and metallurgical debris were found in a layer that has been Radiocarbon dated to a period ranging from 1270 to 1060 cal BC (2σ

[12] The content of this section has adaptations from the following published work:

- E. Figueiredo, R.J.C. Silva, M.F. Araújo, J.C. Senna-Martinez (2010) Identification of ancient gilding technology and Late Bronze Age metallurgy by EDXRF, Micro-EDXRF, SEM-EDS and metallographic techniques. *Microchimica Acta* 168, 283-291.

probability), and thus perfectly incorporated in the LBA period (Senna-Martinez, 2000). The entire set of metallic artefacts has been analysed by EDXRF with no surface preparation in the late 80's, in a preliminary study by Gil et al. (1989). Analytical results made over the patinated surfaces showed that all artefacts were made of bronze with varying vestiges of As, Ag, Sb and Pb except for a decorative nail, which was made of copper. Beside the different bulk composition, the decorative nail also presented unusual vestiges of Au.

For the present study, the copper nail (CRS-3000), some bronze artefacts – a spear-head fragment (CSR-7003), an awl fragment (CSR-3169) and a bar fragment (CSR-4660) – and a crucible fragment (CSR-7003) and a vitrified material that could be related to metallurgy (CSR-7007) were selected for analyses (**Fig. 3.59**).

Fig. 3.59 Items studied from *Crasto de São Romão*.

Conventional EDXRF analyses were performed, at a first stage, on all the items over different areas. Regarding the metallic items it allowed the evaluation of any special features such as the presence of composite objects. In the case of the crucible fragment and the vitrified fragment, it allowed an evaluation of their use in ancient metallurgical operations.

Small samples, representative of the cross-section, were taken from the awl and bar fragments for metallographic preparation. On the spear-head no sample was taken due to its stronger aesthetical feature, but a small area at a border was prepared for metallographic observation. Elemental composition was obtained through micro-EDXRF analyses over the previous prepared areas. Various micro-EDXRF analyses were also performed on the decorative nail without surface preparation. Additionally, a small area (at an edge) was cleaned from the most superficial corrosion and was grinded (manually, using no water) for examination under a SEM-EDS without a conductive coating.

The EDXRF analyses made on the metallic items showed, as the previous ones performed by Gil et al. (1989), that the nail was made of copper and the other three artefacts were made of binary bronze with minor impurities. In the present work, due to particularities found in the copper nail, its detailed study will be presented first, followed by the bronzes. At last the results on the other metallurgical remains (i.e. crucible fragment and vitrified fragments) will be shown.

Results of the EDXRF analyses made on both sides of the decorative **nail** (CSR-3000), the front and reverse surfaces, showed the presence of Cu as major element, vestiges of Pb, Sn, Ag in both sides, and the presence of Au just on the front side (**Fig. 3.60**). Other elements were detected, such as Fe and Ca, and their presence is probably due to the incorporation of soil particles in corrosion during burial.

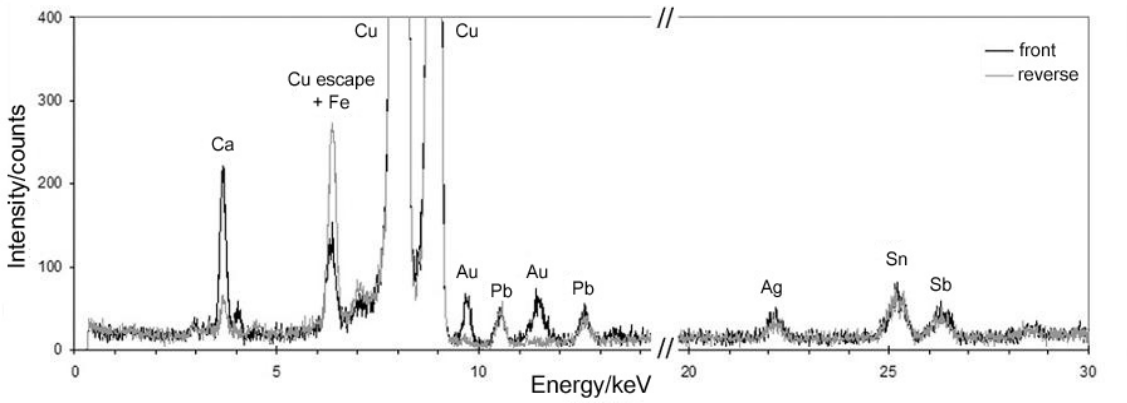

Fig. 3.60 EDXRF spectra of the front and the reverse sides of the decorative copper nail (CSR-3000).

Since Au was only detected in the front side, the results suggest that the nail is made of copper (with Pb, Ag, Sn and Sb impurities) with a deliberate gilded surface only on the visible side (front).

Composite objects made by joining different metals and dated to BA are known, however they are not very usual. Gold attached to other metals is particularly rare in European areas and from the IP one can report the hilt of the MBA sword from *Guadalajara* (Spain) which is covered with embossed gold sheet (Rovira, 2002b).

The use of a copper substrate on the decorative nail instead of a bronze one suggests that it was either an economic choice – copper could be less valuable than bronze – or an intentional technological decision.

The application of a gold layer to the surface of a less noble metal, a process known as **gilding**, came into favour from about the 3rd millennium BC in the Middle East (Oddy, 1981, 2000). It gave the appearance of solid gold (Gänsicke and Newman, 2000) allowing a greater use of the limited gold available. The first techniques involved mechanical attachment of relatively thick sheets of gold foil into a metallic surface by riveting or by cutting grooves into the surface of the base metal. Other procedures emerged as gold refining techniques developed, probably early in the 2nd millennium BC (Oddy, 2000). The use of very pure gold allowed a significant reduction in the gold sheet thickness by hammering (Nicholson, 1979; Oddy, 2000) resulting in savings in the amount of gold required. In fact, in Egypt the beating of gold was depicted on tomb paintings and was mentioned in a funerary papyrus

from the fourteenth century BC decorated with thin gold leaf pointing out to a specialised craft (Oddy, 2000). One of the emerging techniques was the attachment of a thin sheet of gold to the substrate, that could be metal or some intermediate ground layer such as calcite or gypsum, using an organic adhesive (Oddy, 1981). Another technique was diffusion bonding. This seems to have been the most common gilding technique for metallic objects in the Ancient World before the invention of mercury amalgam gilding around the second century BC (Gänsicke and Newman, 2000).

Diffusion bonding was employed from at least as early as ca. 1200 BC (Oddy, 2000) and involved burnishing the gold directly to a scrupulously cleaned metal base and then heating it gently to cause interdiffusion among the two metals (Oddy, 1981). Unlike a mechanically gilded metal surface, a diffusion-gilded surface could be further worked and shaped with less risk of detachment of the coating (Gänsicke and Newman, 2000). Additionally, the very strong bonding among the two metals made it more resistant to wear and tear (Oddy, 2000). This technique revealed good results on a silver or pure copper substrate but not on a bronze alloy when the use of a burnishing tool was necessary (Healy, 1999).

The front surface of the nail is covered with a dark corrosion that exhibits a few particular small areas with a gold shine. In the most exposed regions, this dark corrosion has been lost, revealing a red-brownish colour. Presuming that an Au gold layer was still preserved in some areas of the front surface, micro-EDXRF analyses were conducted on various spots in order to evaluate the extension of the gold layer. Au was detected in the analyses performed over the dark corrosion and over the metallic shine areas, not in the red-brownish regions (**Fig. 3.61**). This suggests that the gold layer has been lost in most exposed areas, probably due to a deep corrosion development and its detachment.

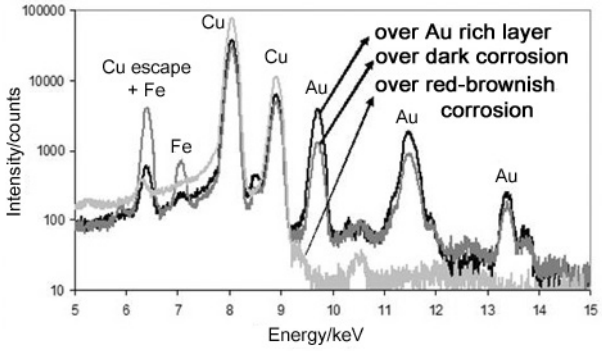

Fig. 3.61 Representative spectra of the Micro-EDXRF analyses performed over the three areas identified in the nails front surface (CSR-3000).

The SEM examination was conducted in the next stage at an edge of the head of the nail – representative of a cross-section – where the dark corrosion layer was still preserved. Low BSE magnification observations and EDS analyses showed a distinct layer of gold between the copper base metal that was partially oxidized and the corrosion layer that reached frequently >200 μm in thickness and was composed by C, O, Al, Si, P, K, Ca and Fe, besides Cu. This corrosion layer, which represents the dark areas observed on the front surface of the head of the nail, can be interpreted as a

mixture of soil particles and copper salts that were leached out from the nail body during corrosion processes. Generally, the cohesion between the gilding and the copper substrate is very good (only few regions have the Au layer damaged) (**Fig. 3.62**), suggesting either the use of a quite durable adhesive or that some diffusion among the metals has taken place. Any mechanical attachment would most likely lead to the formation of a strong corrosion among the two metals, in the same way as the use of a less durable organic adhesive that would easily decay under burial (Selwyn, 2000; Strahan and Maines, 2000).

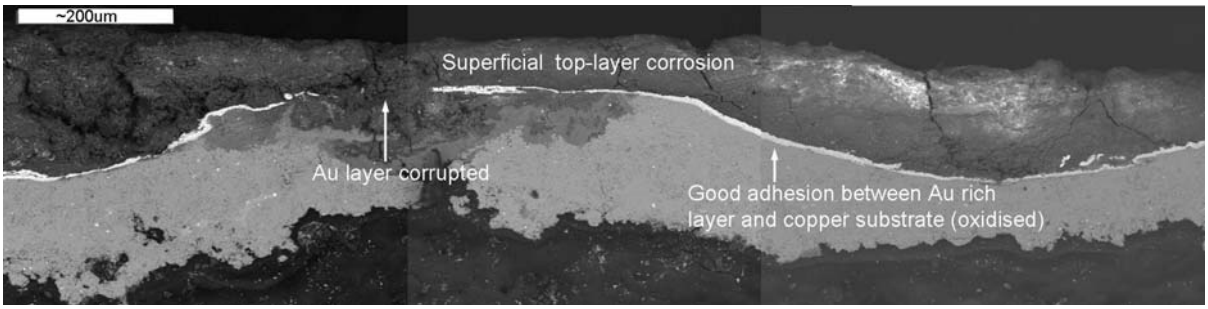

Fig. 3.62 SEM (BSE) image of a general view of a region of the prepared area in the nail (CSR-3000).

Detailed examination of the gold layer showed that it was quite thin, ranging 5-8 μm in thickness – **Fig. 3.63** reports to the main results of the gold layer features. In some particular areas more than one layer was visible suggesting folding of individual sheets or detachment of top regions of the gold rich layer, like ”flaking”, probably as a result of damage provoked by corrosion (some “flaking” is also observed in **Fig. 3.62**, at the right). The EDS analyses made on various spots of the gold layer only detected the presence of Au and Cu metallic elements (**Fig. 3.63**a, second spectrum) with Cu regularly in contents >50 wt.%. The absence of Ag suggests the use of refined gold since this element is commonly present in native gold (electrum); native gold may attain silver concentrations up to 40%, copper up to 1% and iron up to 5% (Guerra and Calligaro, 2003). The high amount of copper present in the gold layer suggests that it is not likely to be original or deliberately added to the gold since it would not facilitate the hammering of the gold sheet. Its presence suggests in-situ incorporation, either due to: corrosion of the copper substrate (i.e. with diffusion of soluble copper species); technological features (e.g. diffusion bonding); or a combination of both.

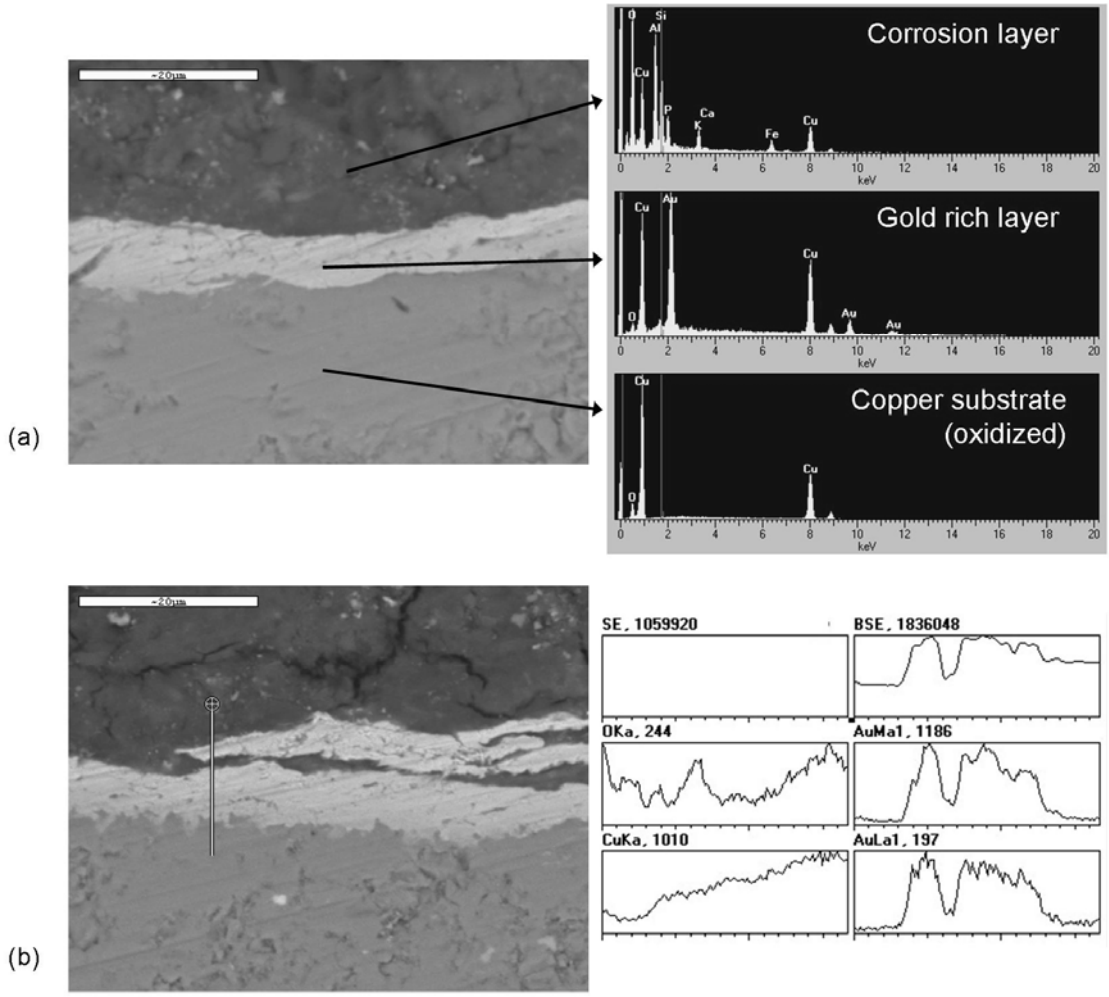

Fig. 3.63 (a) SEM (BSE) image of the gold rich layer in the nail (CSR-3000) and EDS spectra of corrosion layer, gold rich layer and copper substrate. (b) SEM (BSE) image on another area of the gold rich layer and EDS line scan with oxygen (O Ka), copper (Cu Ka) and gold (Au Ma and Au La) distribution.

When a durable adhesive has been used it has occasionally been detected in SEM-EDS analyses (Griffin, 2000). In the present case no area below the gold layer has particular features detected by EDS, such as carbon-rich. Instead, the gold/copper interface is regularly characterized by the presence of more or less pronounced gold rich extensions penetrating into the copper metal, visible in BSE images (**Fig. 3.63**). This feature, commonly called "fingers" in literature, has been reported as typical in objects gilded by diffusion bonding (Gänsicke and Newman, 2000; Griffin, 2000). It has been explained as a result of preferential diffusion of gold along grain boundaries of the substrate metal, enhanced in BSE contrast image due to the oxidation of the substrate (Gänsicke and Newman, 2000).

Another feature occasionally reported as a criterion for identifying a diffusion bonding technique is a compositional gradient across the gilding layer in a cross-section (Gänsicke and Newman, 2000). Diffusion is temperature (and time) dependent and processed in two-way. The higher the temperature and the time involved, larger is the diffusion zone. In ancient objects, these have been reported to range from only a few micrometers to more than fifty micrometers (Gänsicke and Newman, 2000). In the present case, since the EDS spatial resolution (1-2 μm) is close to the thickness of the gold rich

layer, a compositional gradient through an EDS line-scan cannot be considered as conclusive (**Fig. 3.63**b).

Detailed observations of the copper body showed some dispersed inclusions. SEM-EDS analyses made on some of them identified various associations of the Sb, As, Pb and Ag elements (**Fig. 3.64**). Most of these elements had previously been detected in the EDXRF analyses, and have also been detected earlier in the unalloyed copper bar of *Baiões* (section 3.3.3.1).

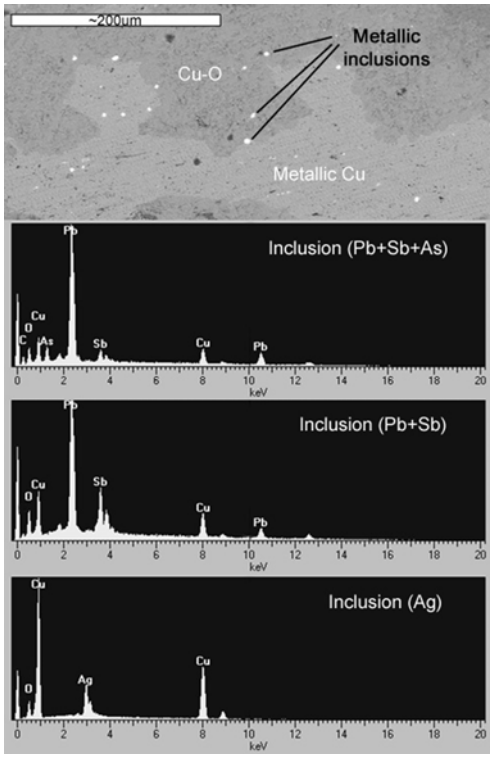

Fig. 3.64 SEM (BSE) image of the bulk of the copper base metal in the nail (CSR-3000) and EDS spectra of some metallic inclusions.

Taking into consideration all the experimental results, a bonding through diffusion seems to be the most probable technique used. It would explain: (1) the use of copper to produce the base metal in a period and region where nearly all the metallic artefacts were produced in bronze (see also next section 3.3.4 Others); (2) the good cohesion between the gold and copper substrate in most areas; (3) the morphology of gold/copper interface in these areas; and (4) the high amount of copper in the gold layer.

The EDXRF analyses showed, as the previous ones performed by Gil et al. (1989), that the spear-head, the awl and the bar fragments are made of binary **bronze** with minor impurities. The micro-EDXRF analyses made on the prepared areas showed that the bronze alloy has 9-15% Sn, being the bar fragment CSG-4660 the one with the highest content – **Table 3.16** summarizes the experimental results. Generally, the bronze composition of the artefacts is among the general range of the bronzes from *Baiões*, *Santa Luzia* and *Figueiredo das Donas*, both in Sn contents and in the low impurity pattern.

Table 3.16 Summary of the experimental results on the bronze items from *Crasto de São Romão* (EDXRF results are given in a semi-quantitative way; composition is given by average of three micro-EDXRF analyses ± one standard deviation)

No.	Item (section)	Composition (wt.%)							Method of fabrication	Phases present
		Cu	Sn	Pb	As	Sb	Fe	Ni		
CSR-3169	Awl frag (sub-rectangular ~2x3 mm)	+++	++	n.d.	n.d.	n.d.	n.d.	n.d.	C+D+T+D↑	α
		90.9±0.1	9.0±0.1	n.d.	n.d.	-	<0.05	n.d.		
CSR-4660	Bar frag (sub-square ~4x4 mm)	+++	++	vest.	vest.	n.d.	vest.	n.d.	C+D↓+T+D↓	α, δ↓
		84.4±1.0	15.4±1.0	n.d.	0.12±0.0	-	<0.05	n.d.		
CSR-7003	Spear-head frag	+++	++	vest.	n.d.	n.d.	vest.	n.d.	C+D↓+T+D↓	α
		87.8±0.2	12.2±0.2	n.d.	n.d.	-	<0.05	n.d.		

+++ >50%; ++ 10-50%; + 1-10%; vest. (Vestiges) <1%; n.d. not detected

C cast; D deformation/forged; T heat treatment/annealed; ↓ low amount; ↑ high amount

In **Fig. 3.65** some images related to the metallographic observations made under the OM are shown. The CSR-3169 **awl** fragment has been extensively worked to shape and has a completely recrystallized twinned grain structure. Most of the twinned crystals exhibit a high concentration of slip bands. These are probably a result from a severe final cold work of the item. Furthermore, there are many Cu-S inclusions which are flattened and elongated, corroborating the extensive work done during the items manufacture. The manufacture of the awl was probably done through the shaping of a cast bar since moulds for bar production have been found in CSR site as well as in other LBA *Baiões/Santa Luzia* habitat sites (Senna-Marinez, 2000) (see also section 3.3.3.2 – *Santa Luzia* and section 3.3.4 – Others).

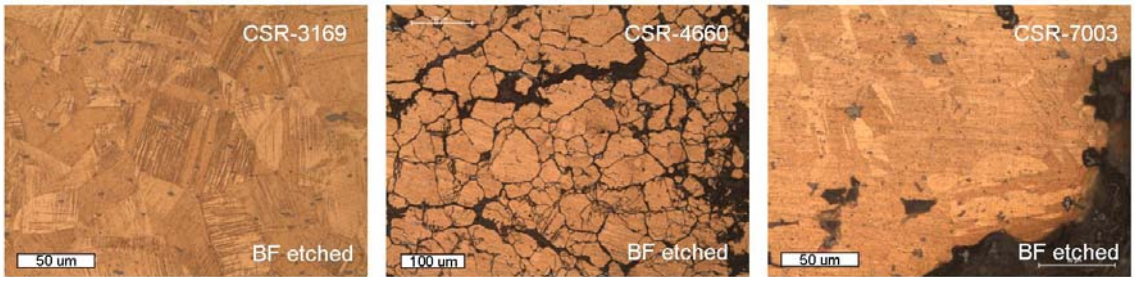

Fig. 3.65 Microstructures of the awl fragment (CSR-3169), bar fragment (CSR-4660) and spear-head fragment (CSR-7003) (OM).

The CRS-4660 **bar** fragment is composed of primary α grains and a few α+δ eutectoid structures. Some inclusions of Cu-S are also visible in intergranular regions. Extensive intergranular corrosion has occurred outlining most of the grain boundaries. Some transgranular corrosion is also observed, that in some areas follow crystallographic planes suggesting that the bronze must have suffered some plastic deformation during manufacturing or use.

The CSR-7003 **spear-head** fragment has a recrystallized grain structure composed by single α phase twinned grains. This indicates that after casting (moulds for casting spear-heads are known in the region, e.g. see section 3.3.4, and a fragment was found at CSR) the item was subjected to some cycles of hammering and annealing. Still, no major change in shape has occurred since the numerous blue-grey Cu-S inclusions still detain the irregular shapes they obtained in the interstitial interdendritic

regions during solidification. Furthermore, many of the twin lines are bent indicating that a post-annealing deformation has occurred. This deformation may be a result of the last stage in the manufacturing process (as hammering) or other posterior actions, as those involving its use or break.

Likely, the awl and bar fragment have been shaped from similar cast bars, since the awl is the one with the smallest cross-section and also the one with the most worked microstructure. The deeper intergranular corrosion on the bar fragment comparatively with the awl is probably due to a less homogenized structure, as a result of a smaller amount of thermo-mechanical actions.

Non-invasive EDXRF analyses were performed on five areas of the **crucible** fragment (CSR-7006). Although the absence of visible metallic prills in the surface, all analysis showed the present of two elements related with ancient metallurgy: Cu and Sn. Other elements such as Fe, Rb, Sr, Y and Zr were also detected and are a result from the crucible raw material (geological origin – clay). In **Fig. 3.66** one of the EDXRF spectra is represented. This analysis demonstrates that the crucible has been used in binary bronze metallurgy. The kind of metallurgical operation performed, i.e. smelting or melting, is not possible to achieve with only this analysis; nevertheless, this remain gives support to a local metallurgical production of bronzes such as those analysed here and in agreement with the metallurgical tradition of the region (see the other bronze compositions of *Baiões/Santa Luzia* sites, section 3.3.3).

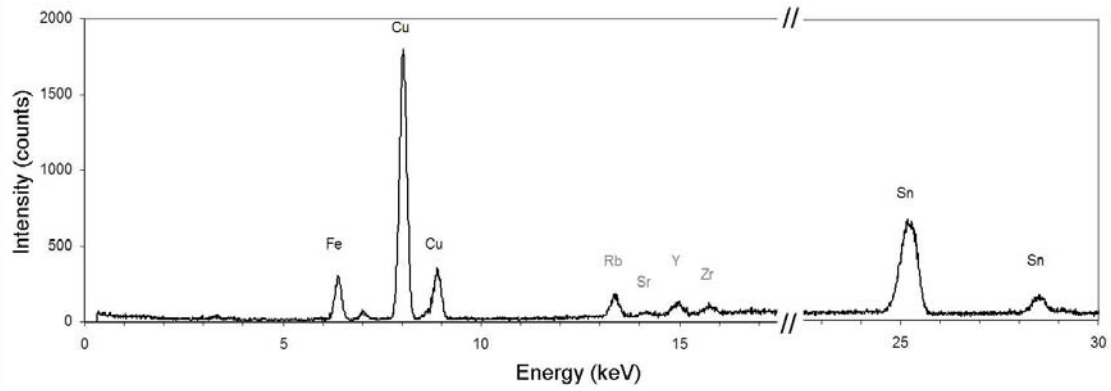

Fig. 3.66 EDXRF spectrum of the crucible fragment (CSR-7006).

The EDXRF analysis made on the **vitrified fragment** showed no peaks related to ancient metallurgy: the most intense peak was of Fe, and others are Mn, Zn, Rb, Sr, Zr and Cu in such small content that is perfectly explainable by geological/clay constituents. If this material was part of any metallurgical processes, one could expect it to be part of some structure, e.g. base of a small furnace (?).

3.3.4 Others

Studies were performed in other metallic artefacts (**Fig. 3.67**) and a mould (**Fig. 3.68**) from Central Portugal, namely: a fragment of a sickle of Roccannes type (as the FD-08 sickle, section 3.3.3.3) from *Cabeço do Couço* (CC), (Vouzela); a bar fragment, two fragments of a fibula and a stone mould to produce spear-heads from *Cabeço do Cucão*, *Pedra Calveira* (CCPC) (Silgueiros, Viseu); a ring

fragment from *Castro do Outeiro dos Castelos de Beijós* (COCB) (Carregal do Sal); a spear-head from *Sernancelhe*; and a spear-head from *Penela*.

All the artefacts are from the *Baiões/Santa Luzia* region except for the *Penela* spear-head, which was found in a cave, *Gruta do Algarinho*, in Beira Litoral region (not far from *Medronhal*).

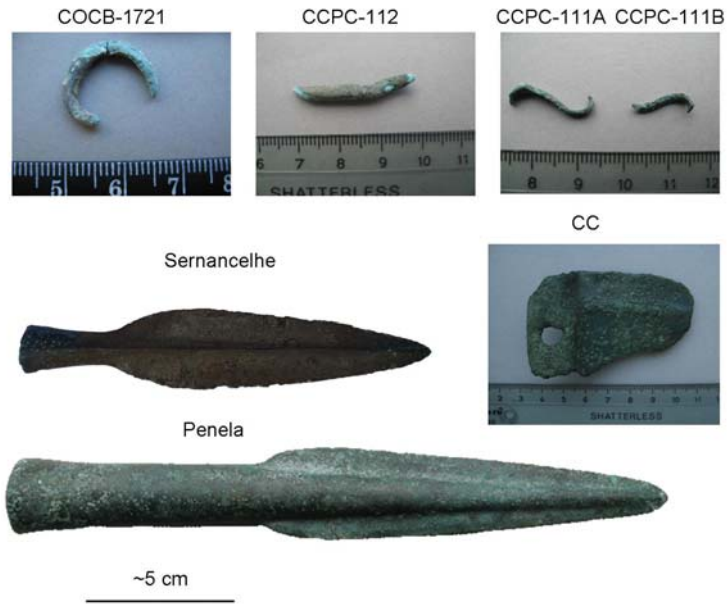

Fig. 3.67 Metallic items studied from other sites in Central Portugal.

Fig. 3.68 Different views of the sandstone mould fragments (CCPC-110). The blue arrow indicates the entrance of metal during pouring for the spear-head production.

All the artefacts were analysed by EDXRF. The metallic artefacts were also analysed by micro-EDXRF in a small prepared area, except for the *Sernancelhe* spear-head that was analysed in a small area on the socket that had lost the most superficial corrosion products, without any further cleaning. *Penela* spear-head was analysed in two different prepared areas, one in the socket and another in the blade, to attain the alloy homogeneity and search for different thermo-mechanical treatments among the socket and the blade. The microstructural investigations were done by the OM examination. The main results on the composition and microstructural analysis are exposed in **Table 3.17**.

Table 3.17 Summary of the experimental results on the bronze items from various other sites in Central Portugal (EDXRF results are given in a semi-quantitative way; composition is given by average of three micro-EDXRF analyses ± one standard deviation)

No.	Item	Composition (wt.%)							Method of fabrication	Phases present
		Cu	Sn	Pb	As	Sb	Fe	Ni		
CC	Sickle	+++	++	vest.	vest.	vest.	vest.	vest.	C+T?+D	α, δ
		86.9±2.6	12.9±2.5	n.d.	0.19±0.04	-	<0.05	n.d.		
CCPC-111A	Fibula frag	+++	++	n.d.	n.d.	n.d.	vest.	n.d.		
CCPC-111B	Fibula frag	+++	++	n.d.	n.d.	n.d.	vest.	n.d.	C+D+T	α
		87.4±1.3	12.4±1.3	n.d.	n.d.	-	<0.05	n.d.		
CCPC-112	Bar frag	+++	++	vest.	vest.	vest.	vest.	n.d.	C+D↓+T	α
		88.5±0.2	11.4±0.2	n.d.	0.1±0.0	-	<0.05	n.d.		
COCB-1721	Ring frag	+++	++	+	n.d.	n.d.	+	n.d.	C+D↓+T	α
		87.3±1.5	12.5±1.4	0.23±0.13	<0.1	-	<0.05	n.d.		
Penela	Spearhead	+++	++	n.d.	vest.	vest.	vest.	vest.		
	(blade)	88.4±1.4	10.6±1.4	n.d.	0.49±0.04	-	<0.05	0.46±0.01	C+D↓+T+D↓	α
	(socket)	88.3±1.3	10.8±1.2	n.d.	0.47±0.05	-	<0.05	0.43±0.01	C+D↓+T+D↓	α
Sernancelhe	Spearhead*	+++	++	+	n.d.	n.d.	+	n.d.		
		89.3±0.88	8.7±1.2	1.82±0.37	n.d.	-	0.14±0.04	n.d.		

+++ >50%; ++ 10-50%; + 1-10%; vest. (Vestiges) <1%; n.d. not detected

C cast; D deformation/forged; T heat treatment/annealed; ↓ low amount; ↑ high amount

* EDXRF result from Senna-Martinez et al. (2004)

The EDXRF elemental analyses show that all the **metallic artefacts** are made of bronze. The analysis of the fibula fragments CCPC-111A and CCPC-111B showed similar results: a bronze with neither Pb, As and Sb detected, showing that they are most likely fragments of the same artefact, as suggested previously by their shapes. Thus, only one of the fragments was subjected to the following invasive micro-EDXRF and microstructural study.

The micro-EDXRF analyses confirm that all are made of a bronze alloy, with 10-13% Sn and low impurity pattern, except for the *Sernacelhe* spear-head that shows slightly lower Sn and slightly higher Pb contents (**Fig. 3.69**). The *Sernacelhe* spear-head does also show slightly higher Fe content than the other items, most likely due to the analysis being made in an area recently free of the most superficial corrosion and not metallographically prepared, and thus still preserving some external contaminations (analogous situation can be observed in the *Figueiredo das Donas* head FD-01 in section 3.3.3.3, and in the FC shelter artefacts FC-181 and FC-188 in section 3.4.1.2). The two analyses made on the *Penela* spear-head, one on the blade and another on the socket, resulted in very similar elemental contents, indicating that although the relative large size of the cast object, the alloy is very homogeneous all over the item.

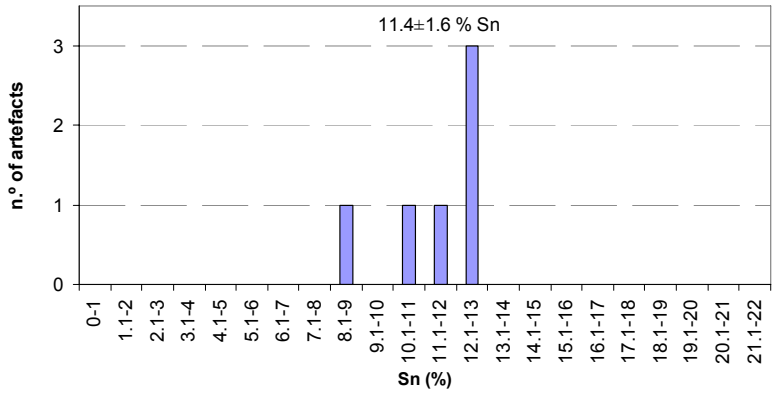

Fig. 3.69 Histogram of Sn content among the studied artefacts from various other sites in Central Portugal (average and one standard deviation annotated).

Microstructural observations of the artefacts showed that most of them have twinned grains and a general presence of Cu-S inclusions (**Fig. 3.70**). Only the sickle has a coarse dendritic microstructure, possibly obtained in a pre-heated mould, with strain bands formed as a result of a final cold deformation.

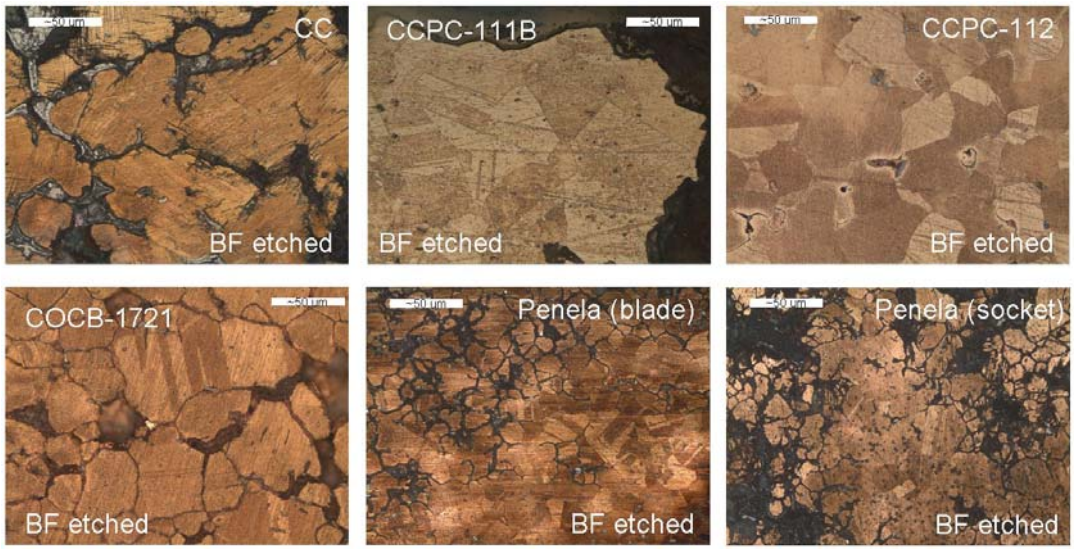

Fig. 3.70 Microstructures of the artefacts from various other sites in central Portugal (OM).

Analysis on the blade and socket of the *Penela* spear-head showed very similar microstructures, with the presence of equiaxed twinned grains, and some slip bands. No significant difference was found among these two areas, suggesting that thermo-mechanical operations were performed all over the item to provide the finishing of the surfaces after casting, rather than to improve local mechanical properties.

The fibula, ring and bar fragments were most likely produced thought the shaping of a cast bar (as the one that was being cast in the mould CCPC-110) through thermo-mechanical processes. Possibly, they were left in an annealed state, to be able to bend them into final shape.

The EDXRF analysis made over the stone **mould** showed no peaks related with ancient metallurgy. This mould was probably never used, as also suggested by the clean surfaces. Possibly, it broke before use, during its manufacture or heating previously to a casting.

The choice of sandstone to produce the mould shows that the metallurgists were aware of the materials soft properties, adequate to carving and producing very fine finishing surfaces. In the British Isles numerous MBA two-piece sandstone moulds for casting socketed spear-heads have been found (Tylecote, 1962). There, a more recurrent use of stone moulds in MBA than later in LBA has been recorded. This can be related to the need of carefully heating the stone moulds previously to any casting to avoid cracking due to thermal shock, and since accidents happen, the LBA metallurgists possibly discarded stone and preferably used the more expendable clay moulds. Also, the effort of finding the right type of stone and the enormous amount of work in carving the stone mould (where any mistake could not be corrected), did also contribute to the change in moulds manufacturing technology.

The CCPC-110 mould could produce spear-heads ~21 cm long and ~3.5 cm wide in the bottom part of blades, and a metal bar ~14 cm long with a near-square section of less than 1×1 cm^2 (considering metal shrinkage during solidification). The spear-head produced in the mould would be very similar to the *Penela* spear-head, supporting the production of the latest in the Central Portuguese territory. The main difference would be the size of the blades: *Penela* spear-head has shorter blades and thus a longer socket (**Fig. 3.71**).

Fig. 3.71 Mould from *Cabeço do Cucão* and spear-head from *Penela*.

Detailed observation of the mould suggests that the filling of the spear-head was made through gates around the core (this being presumably of clay). Also, the fitting of the two halves of the mould was probably done by tying them together, as suggested by shallow scratches on the outside surface and deep scratches on the top outside surfaces (the latest are easily visualised in the middle bottom image in **Fig. 3.68**) (note that the studied half is not complete and the other half has not been found). In the British Isles this way of fitting together the mould halves was more common during MBA than LBA, when most moulds were fitted together by means of dowels (Tylecote, 1962).

The precise chronological period to which this mould (and *Penela* spear-head?) is attributed is not possible to attain with this study (MBA or LBA?). Although the studies of moulds from the British Isles suggest that this could be a MBA mould, the type of spear-head it produced is normally attributable to LBA in the studied region (e.g. see the only two published studies with the *Penela* spear-head: Pessoa (2002) and Vilaça (2006b)). Additionally, the use of stone moulds to produce artefacts during LBA in the region has been recorded, e.g. the mould found in *Santa Luzia* to produce chisels (Senna-Martinez, 2000).

3.4 Northern Portugal – Trás-os-Montes region

3.4.1 *Fraga dos Corvos* – two Bronze Ages

Fraga dos Corvos archaeological site is located in a hilltop of the North-Western versant of Serra de Bornes, Eastern Trás-os-Montes (Macedo de Cavaleiros, Bragança). The site has been known as an IA fortified settlement; however, in 2003, agricultural works on its Northern platform revealed BA levels. Those levels where subjected to recent archaeological interventions (Senna-Martinez et al., 2005). The excavations were done in the Northern platform and in a rock shelter in the Western versant of the site. The works in the Northern platform showed the existence of a 1st BA habitat place (FC settlement) with metallurgical vestiges. The works in the rock shelter documented a later occupation moment, attributed to a late stage of LBA (contemporaneous of the 1st IA-Orientalising period in South of the IP), with a number of metal artefacts found in disturbed layers of the entrance of the shelter.

3.4.1.1 FC Settlement – 1st BA[13]

The settlement has been under archaeological excavations since 2003, and so far its occupation has been attributed to the second quarter of the 2nd millennium BC based on the cultural environment documented, namely the manual pottery industry – some decorated with a mixture of motifs of epi-bell-beaker geometric comb-stamped type and carinated bowls of "Cogeces" or "Protocogotas type" decoration (Senna-Martinez et al., 2007). During the first year of excavations, a negative structure of oval configuration inside a relatively large hut (Hut 4) was found, filled with blackened sand

[13] Part of the content of this section has been published in the following work:

- F. Geirinhas, M.Gaspar, J.C. Senna-Martinez, E. Figueiredo, M.F. Araújo, R.J.C. Silva, Copper isotopes on artifacts from Fraga dos Corvos First Bronze Age habitat site and nearby Cu occurrences: an approach on metal provenance. In: Proceedings V Congresso Internacional - Mineração e Metalurgia Históricas no Sudoeste Europeu, León, Spain (Jun 2008), *in press.*

containing ashes and delimited by a ring of small stones (Senna-Martinez et al., 2007) (**Fig. 3.72**). The responsible archaeologist (J.C. Senna-Martinez) interpreted this structure as a sand box, similarly to a structure that has been found in *Zambujal* site (Chalcolithic site in Central Portuguese Estremadura region), where moulds could be filled with the molten metal. In the surroundings of this structure and at the general excavated areas vestiges of metallurgical operations and some metallic artefacts were found.

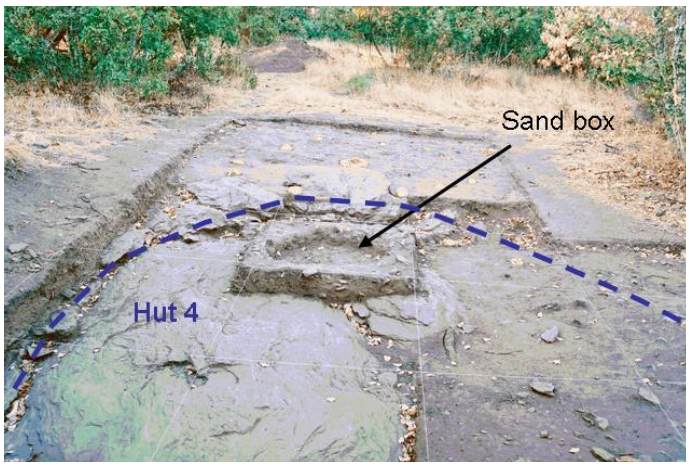

Fig. 3.72 Excavated area of *Fraga dos Corvos* settlement where a sand box was found (photo taken in 2007, facing South).

In the present study, three metallic nodules, five metallic fragments of artefacts and two crucible fragments are going to be discussed (**Fig. 3.72**). Several vitrified fragments of small size were also found and were analysed by EDXRF. These analyses showed absence of elements related with ancient metallurgical activities (as Cu, Sn or Pb). Among these, a selected cut sample was analysed by SEM-EDS and confirmed the absence of any Cu, Sn or Pb metallic prills. These analyses excluded the possibility of these fragments being ancient slag fragments; instead, they can be remains of some fire place structure.

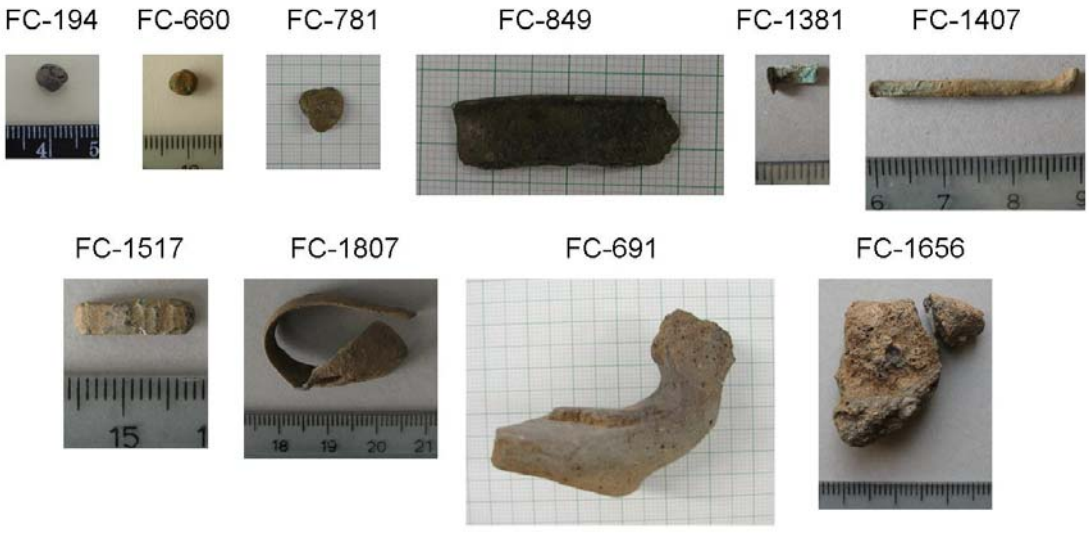

Fig. 3.73 Items studied from *Fraga dos Corvos* settlement.

Among the metallic items studied, the three metallic nodules (FC-194, FC-660 and FC-781) can be smelting nodules, melting nodules, or small fragments of artefacts, as reported before for the *Baiões* nodules (section 3.3.3.1), and the microstructural study can help answering this question. The fragments of artefacts are composed by: a relatively thin sheet (FC-849) fractured in three areas bearing intact only a thicker border, and thus resembling a fragment of a container (an vessel/cauldron?); a very fragile, totally corroded bar (FC-1381), that resembles a rivet; a bar fragment (FC-1407) with a circular cross-section; a very particular bar fragment (FC-1517) with an irregular rectangular cross-section bearing hammering marks in one of the surfaces (visible in **Fig. 3.73**) - the marks resemble those made with an chisel-like instrument, probably to shape it thinner; and a relatively thin bent plate (FC-1807), with no recognizable function or typology.

Among the crucible fragments, the FC-691 is composed by part of a flat bottom, the wall and the border. The border is more vitrified, and the ceramic has a dark colour in the internal side and border and a reddish colour in the external side of the bottom. These evidences point out to a heating from above and inside the crucible (dark areas correspond to a firing in a more reducing atmosphere than the reddish areas). The other crucible fragment (FC-1656) is much smaller, and is only composed by part of a wall and border which show vitrification evidences. J.C. Senna-Martinez has suggested that this fragment could correspond to a reaction vessel such as the large open shapes used in some primitive sites to smelt copper (Rovira, 2002). Although the vitrified borders, none of the two fragments show visible metallic prills.

All items were analysed by EDXRF and the metallic items were also analysed by micro-EDXRF in prepared surfaces, except for the FC-1381 item due to its strong corrosion. Most of the artefacts were sampled, except for the nodules (due to their small size) and the FC-1807 item. Microstructural observations were performed on prepared surfaces by OM. Results are presented in **Table 3.18**.

Table 3.18 Summary of the experimental results on the copper-base metallic items from *Fraga dos Corvos* settlement (copper artefact in grey) (EDXRF results are given in a semi-quantitative way; composition is given by average of three micro-EDXRF analyses ± one standard deviation)

No.	Item	Composition (wt.%)							Method of fabrication	Phases present
		Cu	Sn	Pb	As	Sb	Fe	Ni		
FC-194	Metallic nodule*	+++	++	vest.	n.d.	n.d.	+	n.d.		α, δ↓
		86.0±9.2	13.9±9.1	0.18±0.05	n.d.	-	<0.05	n.d.		
FC-660	Metallic nodule	+++	++	+	n.d.	vest.	+	n.d.		α
		88.9±0.7	10.8±0.7	0.25±0.02	<0.1	-	<0.05	n.d.		
FC-781	Metallic nodule	+++	++	vest.	n.d.	vest.	+	n.d.		α, δ↓
		88.2±2.1	11.6±2.1	0.18±0.05	n.d.	-	<0.05	n.d.		
FC-849	Container frag(?)	+++	++	+	n.d.	vest.	+	n.d.	C+D+T+D↓	α
		90.3±0.3	9.1±0.3	0.62±0.14	n.d.	-	<0.05	n.d.		
FC-1381	Rivet(?)	+++	++	n.d.	vest.	n.d.	+	n.d.		
FC-1407	Bar frag (circular section)	+++	+	vest.	+	vest.	+	n.d.	C+D+T	α-copper
		98.7±0.7	1.3±0.2	n.d.	0.50±0.03	-	<0.05	n.d.		
FC-1517	Bar frag	++	++	++	n.d.	vest.	+	n.d.	C+D+T+D↑	α
		84.4±2.7	13.9±2.4	1.6±0.6	n.d.	-	<0.05	n.d.		
FC-1807	Thin bent plate	++	++	++	n.d.	vest.	++	n.d.	C+D+T+D	α

+++ >50%; ++ 10-50%; + 1-10%; vest. (Vestiges) <1%; n.d. not detected

C cast; D deformation/forged; T heat treatment/annealed; ↓ low amount; ↑ high amount

* EDXRF analysis of FC-194 performed by P. Valério.

Due to aggregated earth in the items the Fe contents in the EDXRF analysis were constantly high (note that these artefacts were brought to analysis previously to any cleaning or other conservation intervention). The elemental analyses showed that all except for one item are made of bronze. Only the bar fragment with a circular section (FC-1407) is made of **copper** with Sn as minor element (~1%). The **bronze** artefacts show an Sn content among 9-14%, and have regularly vestiges of Sb, rarely As, and have Pb in contents <2%. The spatula FC-1807 showed a strong intergranular corrosion in the prepared surface that prevented the determination of the alloy elemental contents. Nevertheless, the EDXRF analysis suggests that this artefact might have more Pb than the previous ones. The presence of Pb content up to 2% is frequently related to ore contamination, and not a sign of intentional addition of Pb to the alloy, being only higher values normally considered as intentional additions or as a result of the recycling of various metals. The presence of these Pb contents in artefacts that are possibly from the 1st BA period can only suggest a different metal or ore supply than the one occurring during the later period (LBA) in Central Portugal, where most bronzes had a very low impurity pattern, as previously demonstrated (section 3.3).

Metallographic observations (**Fig. 3.74**) on the four items FC-849, FC-1407, FC-1517 and FC-1807 showed that all suffered thermo-mechanical cycles. All show equiaxed twinned grains, and some of them do also show strain lines. This suggests that they were either a part of a bigger artefact, part of a composite artefact, or that they were small metal pieces which were being worked to their final shape at the site.

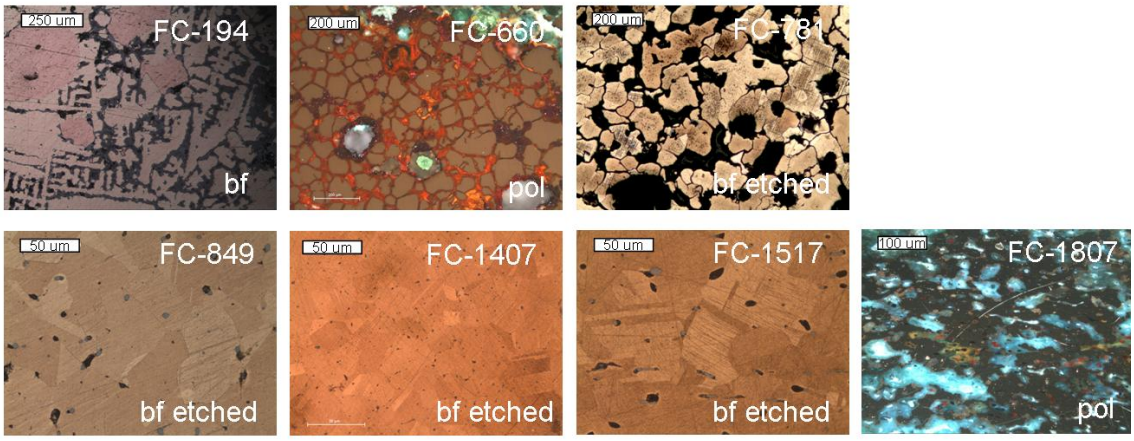

Fig. 3.74 Microstructures of the items form *Fraga dos Corvos* settlement (OM).

The three metallic nodules show deep intergranular corrosion. FC-660 and FC-781 show large and coarse grains, and FC-194 show a dendritic structure (DAS ~30 µm). The presence of large globules of redeposited copper in the FC-194 nodule resulted in a high standard deviation of the three micro-EDXRF analyses. The deeper intergranular corrosion observed in these nodules when compared to the other metallic items is most likely related to a less homogenised microstructure, a result of absence of thermo-mechanical processing. Some of these nodules, as the FC-660 and FC-781 can be smelting nodules due to their coarse microstructure that developed under slow cooling rates. However, as previously brought up by the study of the nodules from *Baiões*, one has to question their Sn content

that does not show dispersed values as expected from nodules resulting from a primitive smelting operation such as a co-smelting one. Instead, the elemental results show that the three metallic nodules have Sn contents in the range of the metal artefacts and fragments analysed (**Fig. 3.75**).

If these artefacts are from the second quarter of the 2nd millennium BC, then, a bronze alloy with the Sn content around the optimal quantity was already at use, showing differences from other early Iberian bronzes, as those from *El Argar* (S Spain), where bronzes had various Sn contents (see section 3.1 – Archaeometallurgical Introduction).

The EDXRF analyses made on the crucible fragments FC-691 and FC-1656 showed strong peaks of Cu, Pb and Sn, indicating that they were used for metallurgical activities (in **Fig. 3.76** the spectra of FC-691 is shown). A semi-quantification on the FC-691 showed a relationship among the three elements of approximately 2Cu:1Sn:3Pb (wt.%) which is not close to the composition of the analysed metallic items. This different ratio must be a result of different chemical affinities of these elements to the material of the crucible during the firing operation and the different leaching degrees during burial. It has previously been shown that some elements are enhanced in moulds comparing to the metal that was poured, particularly Pb (Kearns et al., 2007).

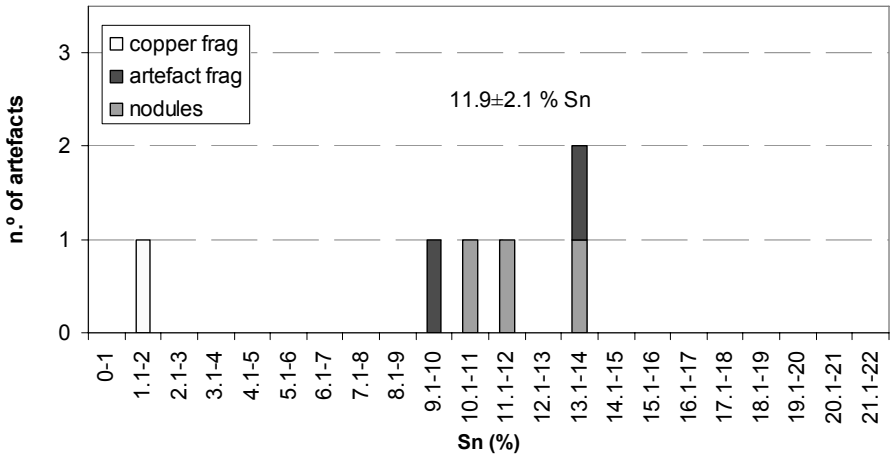

Fig. 3.75 Histogram of Sn content in the studied artefacts from *Fraga dos Corvos* settlement (average and one standard deviation annotated for bronze artefacts – copper frag. excluded).

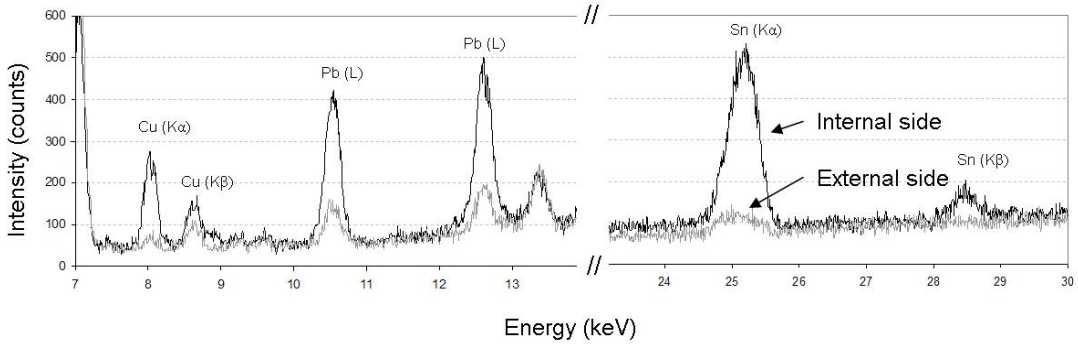

Fig. 3.76 EDXRF spectra of the FC-691 crucible fragment.

In relation to the CSR-crucible (section 3.3.3.4) these fragments have higher intensities of the Pb (L) lines. This is most probably a direct result of the metal that was being worked at the site, which had a higher Pb content than the one worked in the Central Portuguese Beiras, as shown by the elemental analysis of the artefacts.

Based on the materials found at the site and on the present analyses it is not possible to state which kind of metallurgical activities were performed (i.e. smelting or melting). The presence of possible smelting nodules, alone (slag and other evidences as minerals are lacking), does not prove smelting at the site, since nodules could be traded and exchanged as raw material. Possibly, future studies and new uncovered materials from the site will give further clues.

3.4.1.2 Rock shelter – LBA/1stIA[14]

During the archaeological excavations of the rock shelter at *Fraga dos Corvos* site (2005-2006), fourteen metallic items were found, some of them with an Orientalising typology. These latest comprise a double resort fibula, two needles, a cosmetic spatula, and a flat pendant decorated on both sides with star-shape motif, that appears to have been performed by punching the surface with a chisel-like instrument. The others items are eight bar-shaped fragments (comprising possibly fragments of a bracelet and a ring) and one metallic nodule (**Fig. 3.77**).

Fig. 3.77 Artefacts studied from *Fraga dos Corvos* shelter.

[14] The content of this section has adaptations from the following published work:

- E. Figueiredo, J.C. Senna-Martinez, R.J.C. Silva, M.F. Araújo (2009) Orientalizing Artifacts from Fraga dos Corvos Rock Shelter in North Portugal. *Materials and Manufacturing Processes* 24, 949-954.

Typologically, the group of artefacts has a Mediterranean character which suggests a Phoenician origin or, at least, a strong influence from the Southern areas of the IP, e.g. the decoration of the pendant finds close parallels in the Orientalising graffiti on the grey ware of *Medellín* (Almagro-Gorbea, 2004). Although the items were found in disturbed layers, the typology of the objects suggests that they are all part of one set of artefacts, possibly composing a funerary deposit from a late period of the LBA, contemporary with 1st IA in Southern IP (Senna-Martinez et al., 2005).

All items were analysed by EDXRF to identify the type of metal. Subsequently, small samples were taken for metallographic examination from three bar fragments (FC-206, FC-208 and FC-215), the ring fragment (FC-120), the bracelet(?) fragment (FC-362) and from the metallic nodule (FC-474). All samples were mounted in epoxide resin and surfaces were prepared following the usual procedure. On three other artefacts (needle FC-457, cosmetic spatula FC-361, and Tartessian belt hook fragment FC-473) a small area of the surface was cleaned from superficial corrosion and polished without sampling. All items were examined by OM for microstructural study and micro-EDXRF analyses were conducted on all prepared surfaces for determination of the alloy composition.

Additionally, micro-EDXRF analyses were also conducted on the needle (FC-188) and the fibula (FC-181) in an area with a recent fracture with no further cleaning. A selected sample, bar fragment (FC-206), was also observed under SEM-EDS for the identification of Cu-S inclusions and lead rich-phase globules. The pendant (FC-252) was only analysed by EDXRF. The main results on the elemental and microstructural analysis are exposed in **Table 3.19**.

The EDXRF analyses showed that all items, with exception of the Tartessian belt hook fragment (FC-473), are made of bronze with some Pb; that among the bronzes the nodule (FC-474) seems to have a higher Pb content than the other bronze artefacts; and that the Tartessian belt hook fragment FC-473 is made of copper with some impurities.

The micro-EDXRF analysis showed that most of the items have 8–13% Sn and Pb <2% (average 10.1 ± 1.5% Sn and 1.1 ± 0.6% Pb) (**Fig. 3.78**). The needle (FC-457) seems to have a heterogeneous Pb distribution (high standard deviation) probably related to the strong intergranular corrosion in the area analysed (see below microstructural examination), which did not allow the determination of the Pb content with accuracy. The higher standard deviation determined for the tin contents in the needle (FC-188) and fibula (FC-181) items is probably also related to some internal corrosion, as the micro-EDXRF analyses were performed over recent fractures. This may also explain the higher Fe contents in these artefacts, as a result of the absence of totally cleaned and metallographically prepared surfaces. As previously suggested by the EDXRF analyses, the metallic nodule (FC-474) is made of a different alloy, with a higher Pb and a lower Sn content, distinct from all the other bronzes.

Table 3.19 Summary of the experimental results on the copper-base metallic items from *Fraga dos Corvos* shelter (copper artefact in dark grey) (EDXRF results are given in a semi-quantitative way; composition is given by average of three micro-EDXRF analyses ± one standard deviation)

No.	Item	Composition (wt.%) Cu	Sn	Pb	As	Sb	Fe	Ni	Method of fabrication	Phases present
FC-474	Nodule	++	++	++	n.d.	n.d.	+	n.d.	(dendr)	α, δ
		88.3±0.78	5.5±0.4	6.1±0.7	n.d.	-	<0.05	n.d.		
FC-120	Ring frag.	+++	++	+	n.d.	vest.	+	n.d.	C+D+T+D	α
		87.1±0.5	11.8±0.5	0.86±0.22	<0.1	-	0.05±0.04	n.d.		
FC-181	Fibula	+++	++	+	n.d.	n.d.	+	n.d.		
		87.4±4.1	11.2±3.9	0.65±0.24	<0.1	-	0.57±0.14	n.d.		
FC-188	Needle	++	++	++	n.d.	vest.	+	vest.		
		87.4±1.7	11.1±1.5	1.1±0.3	0.1±0.0	-	0.09±0.03	n.d.		
FC-206	Bar frag.	+++	++	++	n.d.	vest.	+	n.d.	C+D↓+T+D↓	α
		89.2±0.5	8.6±0.5	2.0±0.3	n.d.	-	<0.05	n.d.		
FC-208	Bar frag.	++	+++	++	n.d.	vest.	+	n.d.	C+D↑+T+D↓	α
		88.4±0.4	10.1±0.5	1.3±0.1	<0.1	-	0.05	n.d.		
FC-215	Bar frag.	++	++	++	n.d.	vest.	+	vest.	C+D↓+T+D	α
		89.7±0.6	8.1±0.2	1.7±0.64	<0.1	-	<0.05	n.d.		
FC-252	Pendant	+++	++	+	n.d.	vest.	vest.	n.d.		
FC-361	Cosmetic spatula	++	++	++	n.d.	vest.	+	vest.	(worked)	α
		89.9±0.8	8.9±0.9	1.2±0.2	n.d.	-	0.05	n.d.		
FC-362	Bracelet frag. (?)	+++	++	n.d.	vest.	n.d.	+	vest.	C+D+T+D	α, δ↓
		89.4±0.1	10.5±0.15	n.d.	n.d.	-	<0.05	n.d.		
FC-364	Bracelet frag. (?)	+++	++	n.d.	vest.	n.d.	+	n.d.		
FC-457	Needle	++	++	++	n.d.	vest.	+	n.d.	C+D+T+D	α
		82.8±4.6	12.2±0.8	4.9±4.1	0.1±0.0	-	<0.05	n.d.		
FC-473	Tartessian belt hook frag.	+++	+	+	vest.	vest.	+	vest.	C+D+T+D↓	α-copper
		98.4±0.1	0.73±0.14	0.36±0.07	0.20±0.0	-	0.11±0.03	0.28		
FC-475	Metal plate	++	++	++	n.d.	vest.	+	vest.	(worked)	α (corroded)

+++ >50%; ++ 10-50%; + 1-10%; vest. (Vestiges) <1%; n.d. not detected

C cast; D deformation/forged; T heat treatment/annealed; ↓ low amount; ↑ high amount

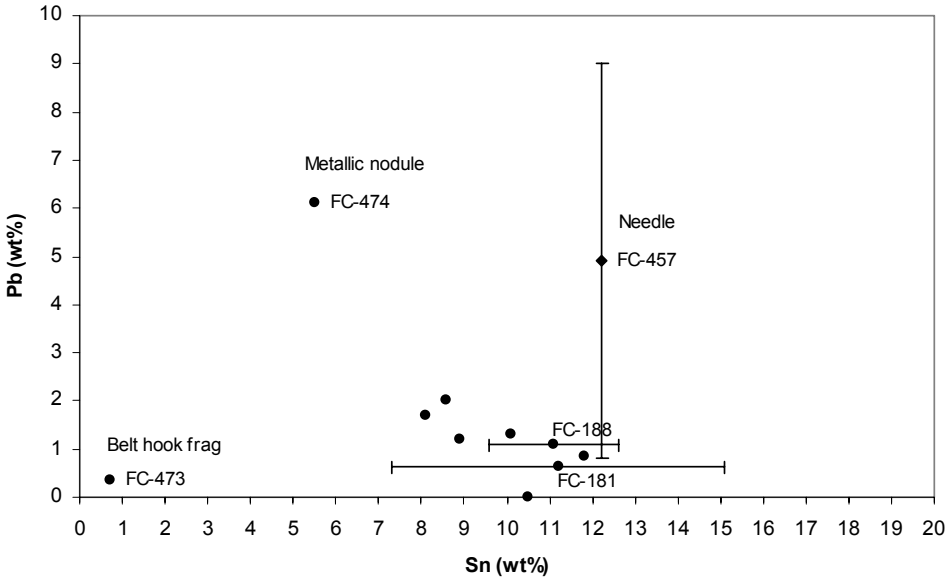

Fig. 3.78 Plot of the Sn and Pb average contents among artefacts from *Fraga dos Corvos* shelter (one standard deviation >1 illustrated).

The Tartessian belt hook fragment (FC-473) can be considered as an unalloyed copper with various impurities (Sn, Pb, As, Sb and Ni). Its higher Fe content is also different from the other bronzes (higher Fe contents in FC-188 and FC-181 are due to incomplete prepared surfaces, see discussion above). A similar object was found in *Canedotes* (part of the *Baiões/Santa Luzia* cultural group) and analysis by Valério et al. (2007a) show that it is also made of unalloyed copper, but with a slightly different impurity pattern: traces of Sn (0.85%) and As (0.53%) and less than 0.05% Fe. The higher impurity pattern in the FC-473 can be due to a different origin of ores, a different supply of metal, or, given the typological features of the assemblage and the higher Fe content, it can be an indication of a new and more efficient smelting process incorporated during the Orientalising period in places better related with the Phoenicians (see section 3.1 – Archaeometallurgical Introduction).

Considering the complete set of artefacts, the metal composition shows closer associations with the metallurgical tradition of the Orientalising sites of *Medellín* and *El Palomar*, where the binary bronzes (<2% Pb) are in the highest proportion, followed by leaded bronzes and unalloyed copper, than with the "indigenous" LBA bronzes from the Central Portuguese Beiras, namely the *Baiões/Santa Luzia* cultural group (section 3.3.3), where generalized lower Pb and higher Sn contents are present. Also, the typological features of the artefacts find closer matches among the objects from *El Palomar* and *Medellín*, supporting this interpretation.

Metallographic examinations revealed that with the exception of the metallic nodule (FC-474), all items have recrystallized α-grains (twinned) and absence of (α+δ) eutectoid (only FC-362 has very scarce δ phase present) (**Fig. 3.79**). The absence of (α+δ) eutectoid shows that the annealing treatment was long enough to homogenize the alloy and solubilize any remains of the δ phase, resulting in a decrease of brittleness and in an increase of tenacity of the metal. The microstructure of the cosmetic spatula (FC-361) was difficult to examine due to geometry factors (complex positioning for OM observations), nevertheless, clear elongated Cu-S inclusions were observed among the α-matrix, which revealed that this item has been worked to shape.

On some items, such as bar fragment (FC-215), ring fragment (FC-120), bracelet(?) fragment (FC-362), and needle (FC-457), slip bands were also observed, probably as a result of some cold work in the final stage of metalwork.

All microstructures reveal the presence of pores, in various number and sizes, as well as the presence of sulphide inclusions (Cu–S). Generally, the artefacts with the thinnest sections were also those with the smallest pores and the most distorted sulphide inclusions.

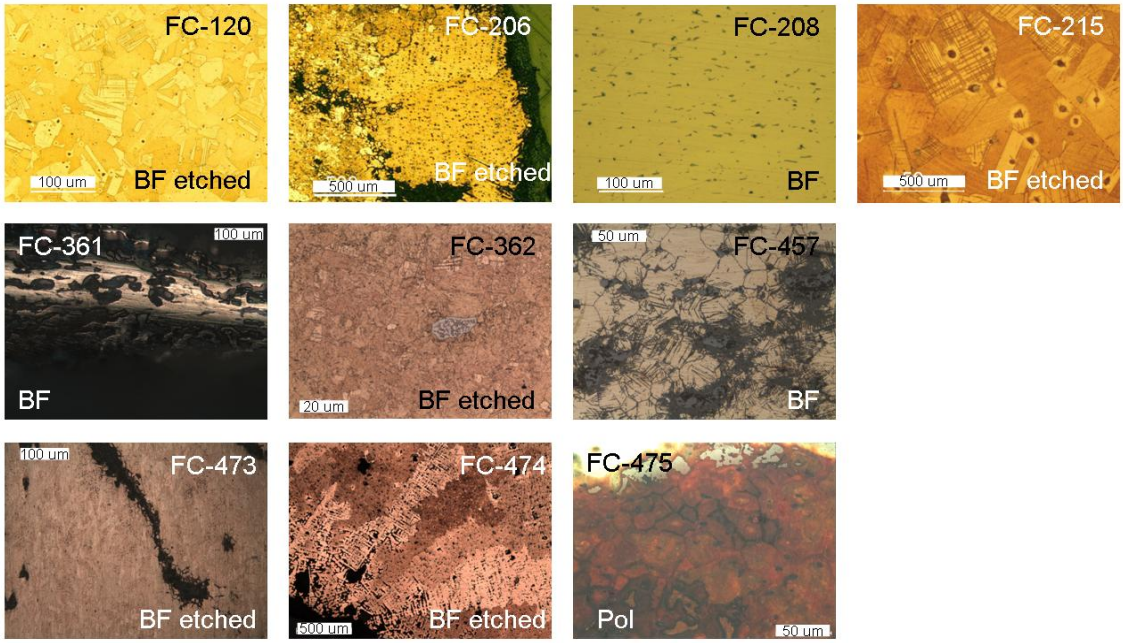

Fig. 3.79 Microstructures of the artefacts from *Fraga dos Corvos* shelter (OM).

The bar fragment (FC-206) is the one with the largest cross-section among the bar-shaped items and is also the one with the largest pores (∅ >100 µm). This item is also the only one that still shows some remains of the as-cast microstructure morphology, as the aligned lead globules and sulphide inclusions, which clearly indicate the dendrite structure that grew during the solidification of the alloy, which in turn allows an estimation of the (secondary) dendritic arms spacing (DAS ~23µm) (**Fig. 3.80**). It also shows a heterogeneous recrystallization (with grains of different sizes), which can be a result of a previous heterogeneous deformation. All these features are in agreement with a bar with the largest cross-section, considering that bar-shaped items could have been worked from similar size cast bars.

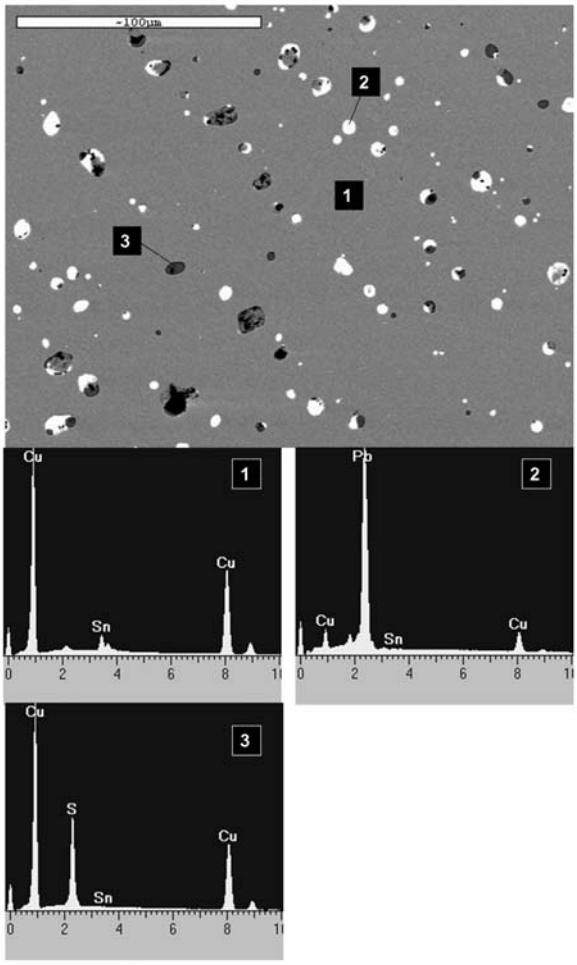

Fig. 3.80 SEM (BSE) image of bar fragment FC-206 and EDS analyses that have been performed over: (1) matrix composed by α-phase; (2) lead globules; (3) sulphur inclusions.

The microstructure of the FC-474 metallic nodule is composed by dendrites with a DAS of ~25 µm, a small amount of interdendritic eutectoid and some shrinkage cavities (Pb is not clearly visible in the OM observations). Its microstructure does not indicate if it is a result of a melting or smelting operation; however, it's distinctive composition (different from all the other bronzes analysed) suggests that it can be a smelting nodule.

As a final note, one can point out to the typologies of the FC shelter Orientalising artefacts, which show some parallels with some items represented on LBA/1st IA warrior stelae (distributed mainly in SW IP, and dispersed in an N-S corridor linking the Northern tin rich areas to the Southern Iberian areas). Among these, there are regularly representations of fibulae, mirrors, which have frequently a similar shape to that of the pendant, and small circular items, that have been suggested to be weights (Celestino Pérez, 2001) but which could also be metallic nodules that were traded as raw material (as a pre-monetary form?). This could somewhow explain the presence of the FC-474 nodule among the other artefacts.

3.5 Final discussion and conclusions

The archaeometallurgical study has provided a general picture of the **metallic materials** used to fabricate the artefacts among the various sites, representing various regions at different pre and proto-historic periods. In **Fig. 3.81** the number of different metals and alloys analysed from each site is shown. It can be observed that most of the analysed artefacts are made of binary bronze (considered here with <2% Pb), followed by unalloyed copper. Also, it is shown that *Pragança* is the site with the highest diversity in types of metal, with copper, bronze, lead and iron artefacts, most likely a reflection of its long diachrony.

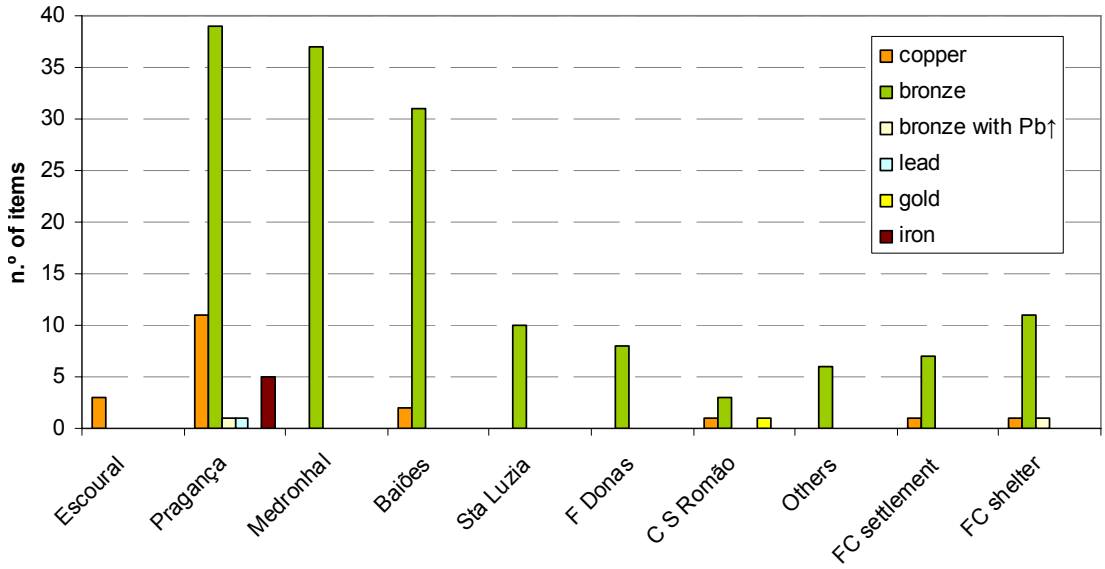

Fig. 3.81 Histogram with the metallic materials studied from each site (based on EDXRF and micro-EDXRF analysis). A clear domain of bronze (<2% Pb content) can be observed (in green).

In **Fig. 3.82** a diachronic view of the metallic materials used from Chalcolithic to 2nd IA based on the present analysis is shown. During Chalcolithic a clear domain of copper is observed (copper with relatively high As contents is not presented independently since the intentionality of As addition was not discussed), and by BA and 1st IA binary bronze takes over, although unalloyed copper is still used to manufacture some particular items. During 2nd IA a diversification in the types of metals occur, with the introduction of lead and iron.

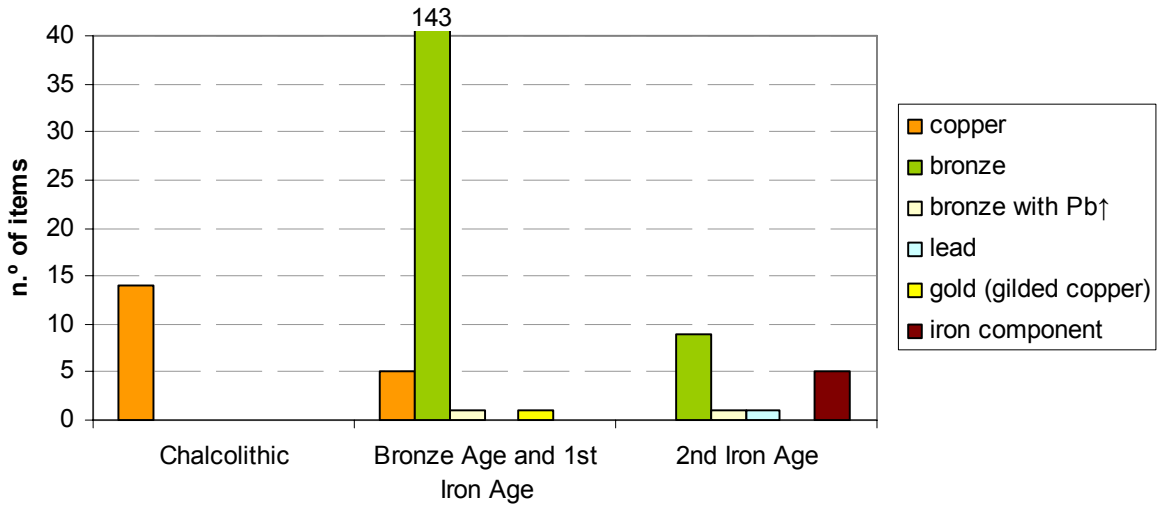

Fig. 3.82 Histogram with a diachronic view of the metallic materials studied over the different chronological periods (based on EDXRF and micro-EDXRF analysis) (the relative small number of non copper-based metals is a result of the primary selection of copper-based artefacts for the present study).

Most of the artefacts analysed are made of the copper-based alloy **bronze**. In **Fig. 3.83** a histogram with the Sn contents among all the studied artefacts from BA and 1st IA is shown. It can be observed a general lack of low tin bronzes (only the leaded bronze nodule from FC shelter has <8% Sn), and that the distribution of tin content in the bronzes is close to a normal distribution with ~12.4±2.0% Sn.

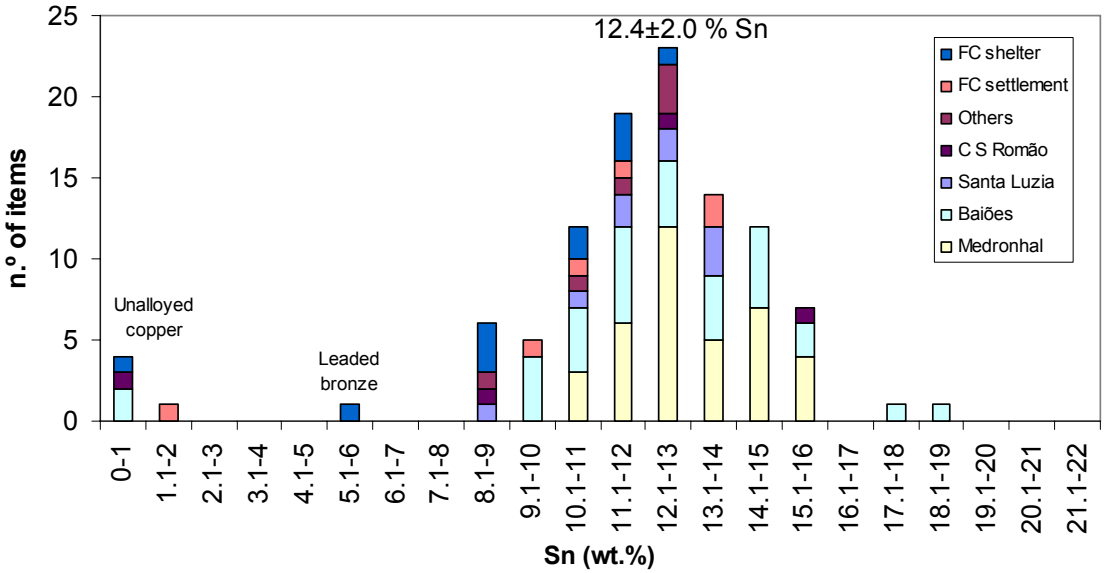

Fig. 3.83 Tin content among the studied artefacts from BA and 1st IA (based on the micro-EDXRF analysis) (average and one standard deviation is depicted for the bronze artefacts – unalloyed coppers and leaded bronze excluded).

During the study, no correlation was found among different artefact typologies and Sn (or Pb) contents. However, it has been observed that the latest bronzes, the LBA/1st IA FC-shelter ones, are those that show the lowest Sn contents and the highest Pb contents. In **Fig. 3.84** the average of **Sn**

contents in the bronze artefacts is shown for each site. It can be observed that all stand between 10-13% Sn (average) and that the FC-shelter bronzes have an average of ~10% Sn. In **Fig. 3.85** a histogram with the **Pb content** among the bronze artefacts for each site is shown. In all sites most of the bronzes have <0.5% Pb, except for the bronzes from FC shelter, that show mainly >0.5% Pb. A note can also be drawn for the FC settlement bronzes, where 2/5 do also show >0.5% Pb, which can be considered as a tendency to higher amounts of Pb in this site. Taking into account the different cultural contexts of these two sites in respect to the other sites (1st BA and LBA/1st IA vs. LBA), as well as their different location (Northern Portugal vs. Central Portugal) one can explain this higher Pb content as a regional variation (different ores or metal supply for this area?), or as a reflection of different chronological periods (e.g. could the first bronzes be imported?).

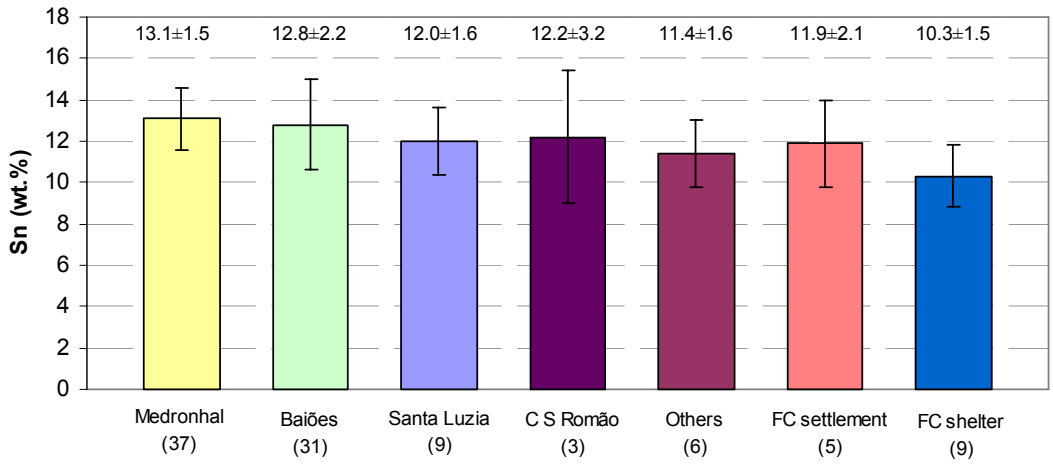

Fig. 3.84 Sn contents in BA-1st IA bronze items from the different sites studied (number of artefacts annotated as well as average and one standard deviation) (note that leaded nodule from FC shelter excluded).

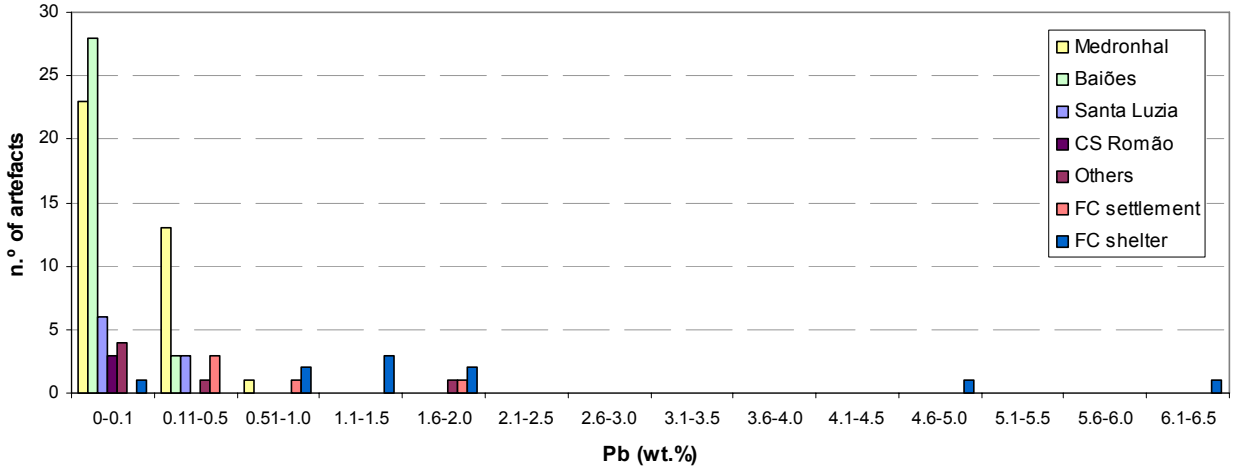

Fig. 3.85 Histogram of Pb content in bronzes from the various sites studied.

In the FC shelter bronzes, it can be observed that a rise in the Pb content is also followed by a general decrease in the Sn content (**Fig. 3.86**). These slightly higher Pb contents and lower Sn contents are typically found among Orientalising bronzes from Southern IP, and can thus be a clear indication of

the different cultural context of these bronzes in comparison with the LBA bronzes analysed from Central Portugal. Additionally, the composition of the *Pragança* fibula, dated to IA, finds more similarities with the FC shelter bronzes than with the LBA bronzes from Central Portugal. This can be an evidence for the spread of an alloy with relatively higher Pb contents and lower Sn contents from the Orientalising period (1st IA) to the 2nd IA.

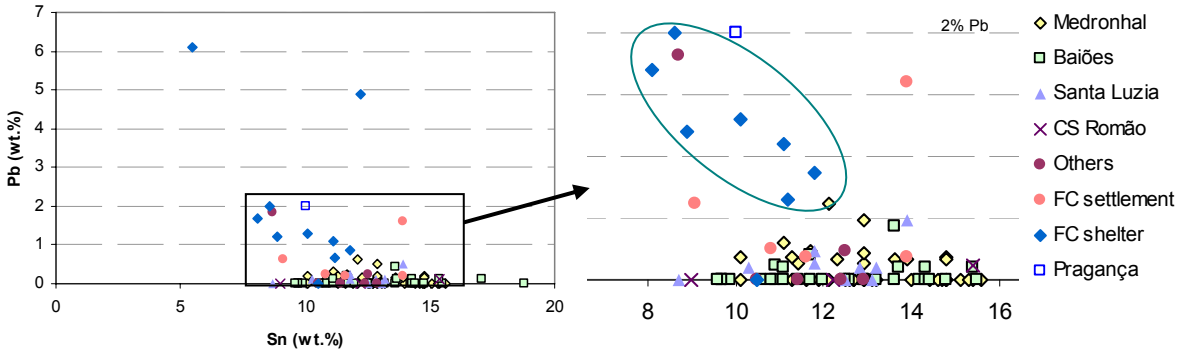

Fig. 3.86 Plot with Sn and Pb contents in bronzes from the various sites studied. FC shelter artefacts are depicted due to higher Pb contents and slightly lower Sn contents.

In **Fig. 3.87** the bronzes have been organized regarding their chronologies and cultural contexts. Although the small number of artefacts attributed to 1st BA and the Orientalising period, it is suggested that the **Sn content** in the early bronzes from the Northern areas became rapidly around the optimal quantities. In respect to the bronzes from the LBA "indigenous" cultural contexts, the Sn content follows a unimodal, tight and normal distribution, which might reflect a consistent and well organized tin supply. The relatively high Sn content (12.7±1.9%) may even indicate that there was no lack of tin, possibly due to the exploration of local cassiterite.

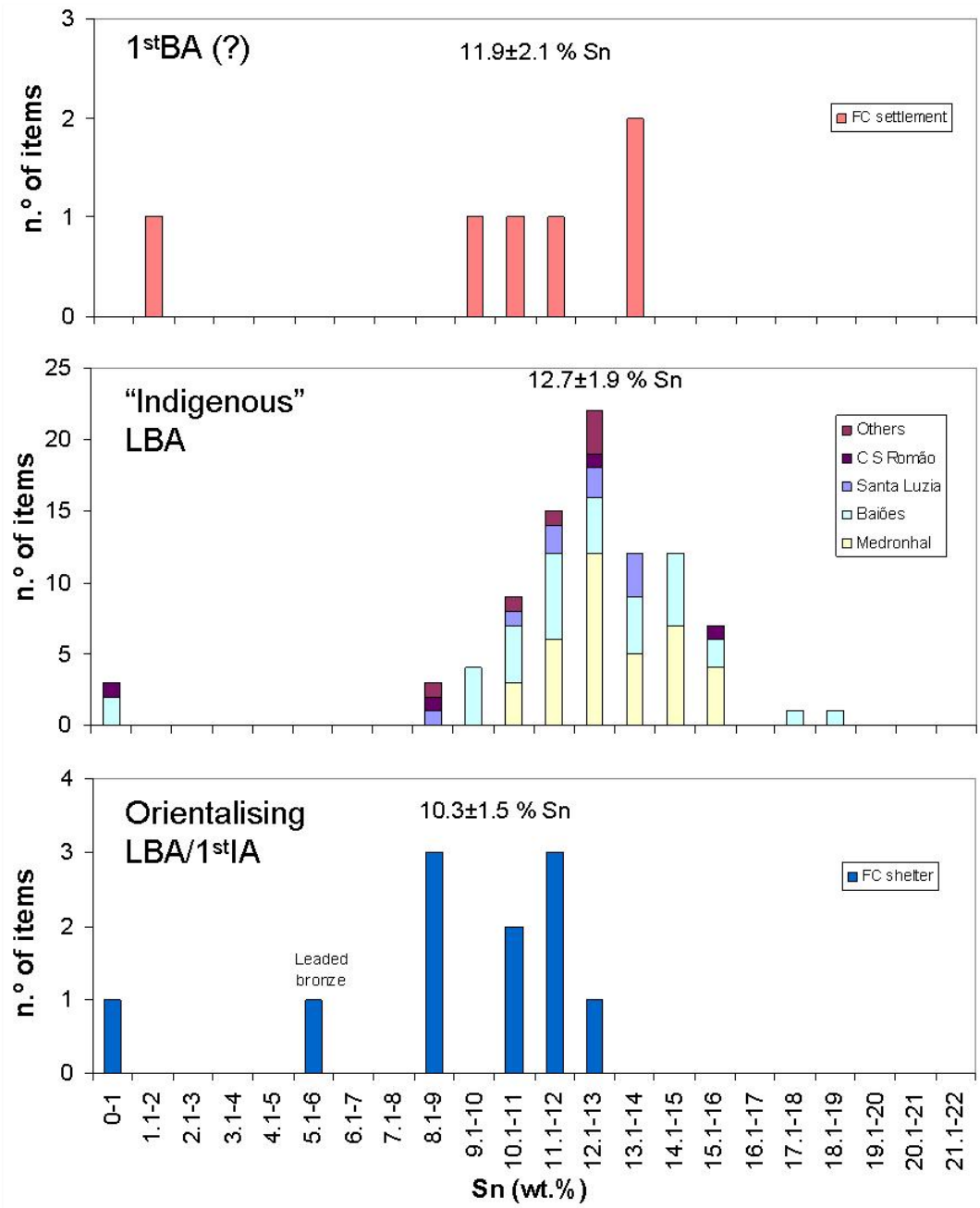

Fig. 3.87 Diachronic view of Sn contents in bronzes.

When comparing the Sn contents of the studied LBA bronzes with other bronzes from the Western IP (**Fig. 3.88**), one can observe that there are similarities among the group of bronzes from Beira Alta and Beira Litoral regions and those from *Ria de Huelva*. Only the bronzes from *Castro dos Ratinhos* show a smaller mean Sn content, possibly explained by some Orientalising influences that the site experienced.

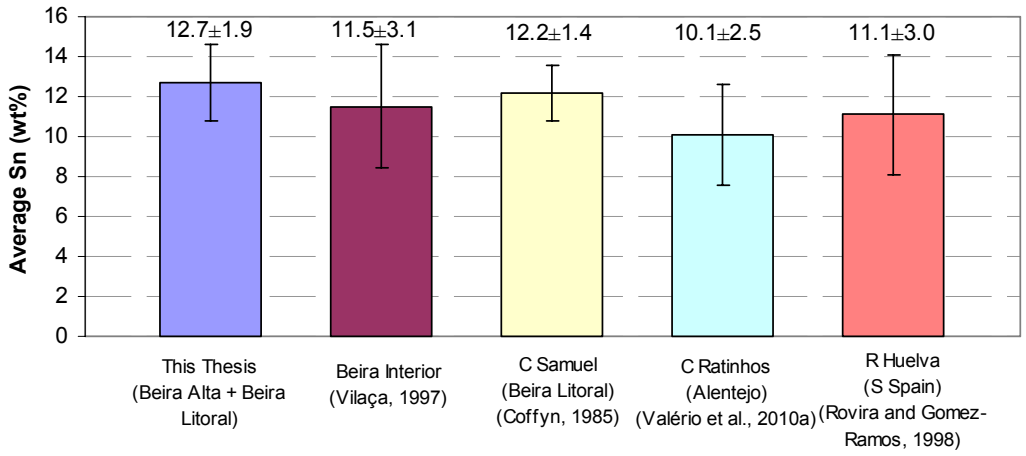

Fig. 3.88 Average Sn contents in bronzes from various LBA sites/regions in the Western IP (different analytical techniques have been used to obtain the Sn contents in other works that can account for some differences, however, general trends should be those exposed here).

Among the **unalloyed coppers** the study shows that a significant increase in the impurities, namely Pb, happens from the earlier period (CA) to the later ones (BA and IA) (**Fig. 3.89**). This doesn't seem to be a result of regional particularities, as can be demonstrated for the *Pragança* site – that has both CA, BA and IA occupations – where Pb impurities are only detected among the bronzes (**Fig. 3.90**). Instead, this may indicate that with the beginning of bronze metallurgy different copper sources or different copper ores began to be explored. Also, the regular presence of Cu-S inclusions in the bronzes (and the LBA copper bar CSG-293 from *Baiões*) and their absence in the earlier copper artefacts from *Escoural* can point out to similar changes. Following the suggestion made by Craddock (1995), possibly by LBA deeper mineralizations were worked, those more sulphur rich, contrasting with the more oxidized top mineralization that were explored and probably exhausted in earlier periods. On the other hand, the Fe content in the metals from CA and LBA is always very low (<0.05%, exception for the Tartessian belt brooch fragment FC-473 found in the later Orientalising context) indicating some continuity in extraction technologies, as would be the case of the reducing conditions.

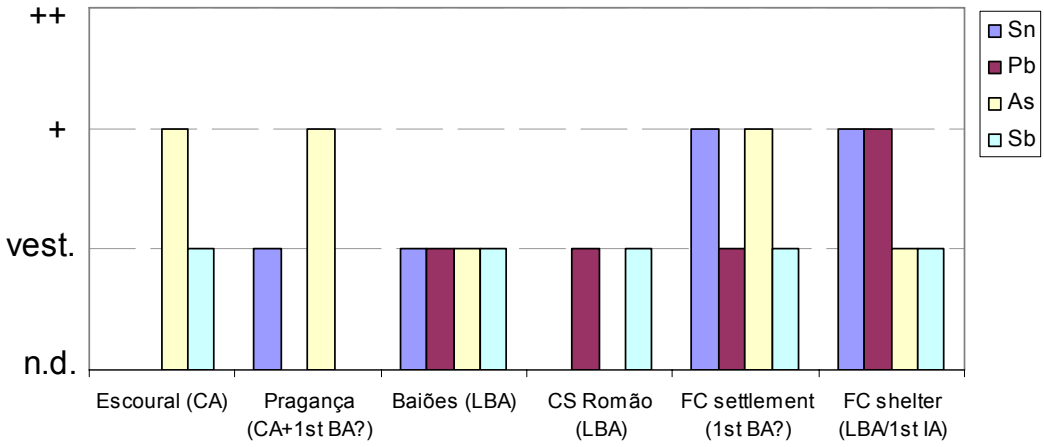

Fig. 3.89 Impurity patterns in unalloyed copper artefacts from various sites studied (maximum values for each site are given) (based on EDXRF analysis).

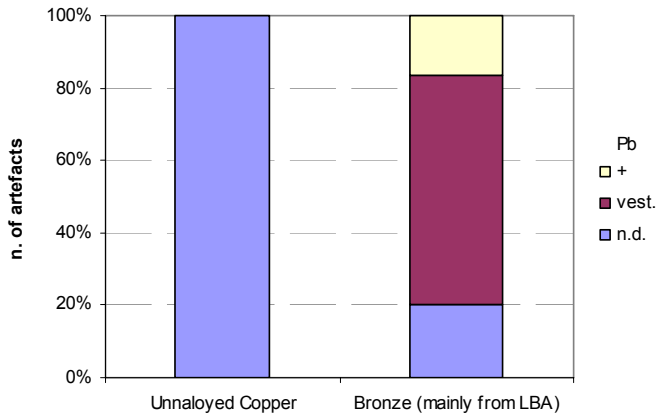

Fig. 3.90 Pb impurity pattern in unalloyed copper and bronze artefacts from *Pragança* site (based on EDXRF analysis).

Another hypothesis for the "sudden" Pb impurity pattern could be the importation of extra-peninsular bronzes, which were recycled to produce local types of items. But then the high Sn contents, as well as the normal distribution of the Sn content among the studied artefacts does not indicate a permanent loss in Sn due to recycling processes. Also, the absence of a significant dispersion among the Sn contents do not point out to a dependence on external sources that could result in alloy composition fluctuations. Additionally, the high Pb contents that by LBA some items in the most Atlantic areas show (areas that also have tin resources), does not seem to have had a strong repercussion in the Iberian bronzes, pointing out to an absence of major importations of bronze from those areas. The introduction of **leaded bronzes** in the IP has been associated to the presence of some leaded palstaves/axes in the Northern regions which have been attributed to LBA. However Bettencourt (2001) argues that these leaded artefacts should be attributed to the IA period, and not LBA as frequently suggested. Also, the LBA bronzes studied in this work point out to the absence of leaded bronzes during LBA in the Portuguese studied regions. Excluding some importations that could occur among the Atlantic areas resulting in the presence of some leaded bronzes, the local productions seem to have been exclusively of binary bronze. Thus, so far, ternary bronzes seem to better fit IA productions (beginning with the Orientalising period) than LBA local "indigenous" productions.

The study of the **metallurgical remains** showed that regardless the chronological periods, metallurgy seems to have been a common and widespread practice inside the settlements, as previously proposed for other Iberian regions. Despite the increase in metal demand during LBA, the needs of the local populations seem to have been easily answered with the numerous local workshops. As proposed by Senna-Martinez and Pedro (2000) for the Beiras regions, instead of one large production centre distribution for a large region, the pattern in the studied area might have been of several small workshops providing metal for the local and nearby areas. The exchange network, where minerals and metals could have travelled, is a very interesting matter, and likely a subject for further studies. Also, the complete spectrum of metallurgical operations that were performed inside the settlements is so far an unanswered question, particularly in respect to the smelting/melting issue. The conduction of melting operations is not questioned, as the various moulds, crucibles and unfinished artefacts

suggested, from Chalcolithic to LBA sites. However, the conduction of smelting operations is much more difficult to demonstrate, principally for bronze production.

The only bronze slag analysed in this work was a small piece, collected in the site of *Baiões*. Despite the difficulty in distinguishing melting from smelting slags (see discussion in section 3.3.3.1), the analysis suggest that the slag is a product of a smelting operation. Nevertheless, more evidences and exhaustive analysis, as to more slags and crucibles would be needed, to fully understand the nature of the metallurgical operations performed at the site/region.

Also, the presence of bronze nodules with roundish shapes and microstructures that indicate a slow cooling in sites as FC settlement and *Baiões* suggests the presence of smelting nodules. The formation of such metallic nodules, or prills, can only be explained by a relatively primitive smelting process, where the liquid metal was trapped in the slag. This, together with the low Fe content in the artefacts (<0.05%), can be an evidence for the production of bronze in primitive smelting processes. Consequently, it might not be strange that large "cakes" of slag have not been found in these Iberian contexts. Nevertheless, their rather narrow Sn range, close to the Sn content in the associated artefacts, is not expectable for "lost" smelting nodules, which should show higher Sn content dispersion (the only nodule that shows an Sn value different form the associated artefacts is the nodule from FC shelter, also the only one that was not found in an habitat place with metallurgical evidences). This issue clearly remains an open question: could the analysed nodules be selected nodules that were collected/traded for melting together and producing bronze artefacts with the "right" Sn content?

The "right" Sn content could easily be perceived by the colour (and hardness?) of the metals; the Sn content range of ~10-15% (most of the artefacts) produces a metal with a yellowish gold-like colour that was probably appreciated (remember the colour of the uncorroded bronze surfaces in the SL "gilded fibula", section 3.3.3.2), besides its good thermo-mechanical properties.

Most probably, among these LBA communities "**control**" over the Sn content was achieved by an empirical deep understanding of the materials behaviours and characteristics. This can somewhat be reflected in (1) the composition of the bronze metals, since (1a) α-Cu phase can be substantially hardened by the solid solution of tin at concentrations above ~10 wt.% (Lechtman, 1996), and (1b) optimal thermo-mechanical properties can be achieved for alloys with <15 wt.% Sn, from where the hard and brittle δ phase can be totally removed by appropriate annealing operations; and in (2) the various thermo-mechanical processes that were applied to the artefacts regarding their shapes. Long cycles of forging and annealing were more evident in the small bar-like objects (e.g. chisels, awls, fibulae, various bar fragments) that frequently showed very elongated Cu-S inclusions. Others, of larger size and more complex shapes (e.g. spear-heads, scabbard chape, buckle element), could need just some final adjustments after their shape was obtained in the mould (**Fig. 3.91**).[15] Also, the

[15] In fact, the mould studied from *Cabeço do Cucão* (Viseu) made for casting a spear-head and a bar is the perfect example of the manufacture of bronze artefacts. The larger, more complex shaped artefacts were shaped

properties of copper in respect to bronze must have been well understood, as observed in the following **composite artefacts:** the use of copper to produce a rivet to join two bronze sheets (CSG-349); the use of copper to fabricate the substrate of the gilded nail (CSR-3000). Later, during IA, the use of iron to produce the fibulae axles does also suggest that iron could have been appreciated by its mechanical properties.

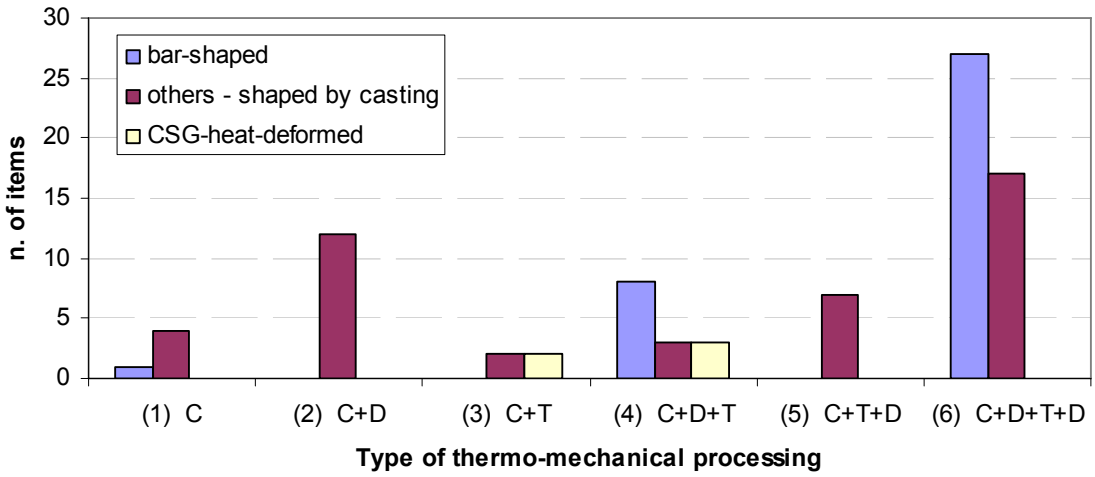

Fig. 3.91 Histogram with the types of thermo-mechanical processing performed in the various artefacts studied: (in blue) chisels, awls, early fibulae, rivets, open rings, etc. that were produced by working pre-defined forms as cast bars; (in violet) all the other artefacts, that include closed rings, spear-heads, axes, and other items of larger or more complex shape that were shaped by moulding; and (in white) the heat-deformed artefacts from *Baiões*.

In respect to specific metal works, this study has allowed the identification of different **joining techniques**: riveting (CSG-349), casting-on (FD nails) and gilding by diffusion (CSR-3000). All these techniques have been identified in artefacts dated to LBA, and show that by this period various solutions were in practice (riveting was already at use in earlier times). The adoption of new technological solutions during LBA happened in general all over the Western European areas, and is probably a result of major interactions among distant populations and cultures, as has been pointed out by Kristiansen and Larsson (2005). In the present study, this has also been previously suggested in the metrological study of the LBA weights (section 2.3.4), demonstrating that these "indigenous" populations were not culturally isolated, and could, in fact, have had some active role in long-distance trade routes.

in the mould, being needed just some final works. In contrast, the small section artefacts, as chisels, awls, early simple fibulae, rivets, (open) rings, etc., were produced by working pre-defined forms, such as cast bars.

General Conclusions

The present work has given, for the first time to the Portuguese territory, a wide scope picture of ancient metallurgy, from Chalcolithic to Iron Ages. Most of the studies were done on Late Bronze Age metalwork, filling a gap that existed among the more traditional typological and archaeological studies. Also, it has provided vital data on long-term corrosion of copper-based alloys, essential for future studies on ancient metals and for proper conservation treatments.

The **analytical and methodological design** that was set up to study the various artefacts has shown to be very adequate to reach the aims proposed at the beginning of the study, i.e. to perform an elemental and microstructural study with minimum chemical and physical intervention/damage on the artefacts, giving valuable contributions to both long-term corrosion studies and to a better understanding of ancient metallurgical technologies. Regarding the **EDXRF** analysis, although only providing a semi-quantitative result in corroded artefacts, this technique has shown to be very useful, since: (1) it allowed a first general distinction among different types of metals by a complete non-invasive mean; (2) provided useful information in the detection of composite artefacts, even if the surfaces were totally corroded; (3) and provided a useful first evaluation of the use of non-metallic items, such as crucibles, moulds and vitrified materials in metallurgical operations, by the detection of elements related to ancient metallurgy. The **micro-EDXRF** analysis has proven to be very useful in the elemental analysis of small, cleaned and prepared surfaces of metallic artefacts, providing quantitative data of the metal composition. This has been mostly useful in the study of the Sn content in bronzes, and in the evaluation of some impurities contents, as Pb, As and Fe. This analytical technique has also been very valuable in the analysis of small metallic inclusions in crucibles, as well as in the study of different superficial corrosion layers. The **OM** examination of metallographically prepared areas has allowed a detail study of the microstructure of the artefacts as well as of corrosion features. The small metallographically prepared areas by a manual polishing have been essential to the work, allowing a large amount of artefacts to be studied with a minimum invasive procedure. The adoption of this methodology has only been possible due to the specific features of the microscope used, as its inverted lenses allowing large artefacts to be analysed, and the computer program that allows the collection of digital images at different z-positions combining them into one single sharp composite image. The use of the **SEM-EDS** has allowed the study of detailed features related to microstructural heterogeneities of the alloys and corrosion. The different imaging modes, particularly the BSE one, and the possibility to detect oxygen and carbon in the EDS analysis, has been fundamental to the identification of different copper compounds in corrosion and also different inclusions in the metal matrixes. The adaptations made to analyse small items without the need of sampling or performing a sputtered conductive coating has been much profitable, resulting in a higher number of artefacts that could be analysed by this technique. The adaptations performed, as the use of different conductive tapes bridging the analysed surface to the ground and enclosing the rest of the artefact, has brought such

good results, that future analysis on other metallic cultural items will certainly benefit from this previous experiences. Additionally, other techniques used in the work, as XRD and Digital Radiography, have shown to be adequate complementary techniques. In general, the experimental design used in this work has shown to be very adequate to the type of study performed, so that future studies on ancient metals will most likely strongly rely on this previous experience.

Regarding the **Corrosion Study**, this work has provided a general revision on bronze corrosion and some detailed descriptions of specific corrosion features. For the first time, a detailed description of preferential corrosion of δ phase in more internal regions and its passivation in the most external regions has been described for archaeological artefacts, as a probable result of different oxygen contents. Also, the study has provided detailed information on other corrosion patterns, as the intergranular corrosion along different symmetry planes in bar fragments (a common item) regarding the microstructure heterogeneities. It has also allowed the identification of redeposited copper with various morphologies, regularly found in the most internal corrosion regions as a probable result of long-term corrosion processes. It was also demonstrated that both decuprification and destannification can occur in archaeological bronzes, and wherever it is one or the other that occurs might depend strongly upon the presence of chlorides and the environmental conditions of the burial. Generally, a decuprification phenomenon was found to be the most common among the studied items, accounting probably for the general burial conditions occurring in archaeological sites from Southern to Northern Portuguese regions. Although it was not possible to study further the destannification phenomena on the *Medronhal* items, it is suggested that this phenomena is related to the presence of high Cl concentrations. This is probably a result of the burial in the *Medronhal* cave, which created rather reducing and low pH conditions, and thus favoured the formation of tin chloride species instead of oxide ones, which are water soluble and thus readily removed from the corrosion layers. The study has also provided valuable information on the influence that corrosion has in the superficial elemental analysis adopted in this work, demonstrating that alloying elements such as Sn, can be enhaced into values ~5 times higher than those on the uncorroded alloy due to decuprification, and that relatively small Pb amounts can be enhanced into values ~9 times higher than those in the uncorroded metal. Finally, this study has allowed a general evaluation of the conservation state of the analysed items, showing that some items have copper chlorines in the most internal corrosion layers, and thus an active corrosion can take place if the most internal corrosion layers are exposed to moisture in air. This is valuable information to be taken into consideration at the time of the devolution of the items to their primary holders.

Regarding the **Archaeometallurgical Study**, this work has provided a first general picture on the types of metal used during various periods in a large area of the Portuguese territory, as well as specific descriptions on thermo-mechanical processes performed to shape various types of artefacts. The study has shown an increase in the variety of metallic materials from Chalcolithic to Iron Ages, being one of the most interesting results the demonstration of the general use of binary bronze, with relatively low impurity patterns and relatively high Sn contents (12.7±1.9%Sn) during LBA,

contrasting with other Atlantic territories. Also, the absence of low Sn bronzes, and the lack of high tin bronzes (that can be very brittle) do seem to show a relative control over the Sn content in the alloy, as well as a constant tin supply. The study of various metallurgical remains as crucibles, nodules and slags, suggests that metallurgy must have been a common activity, performed inside the settlements from Chalcolithic to pre-Roman times. The microstructural study suggests that the manufacture of small and simple items, as some fibulae, open rings, cosmetic spatula, belt hooks, chisels and awls, was carried out by working pre-defined forms, such as bars cast previously in a mould, by forging and annealing operations. Only the heavier and more complex shape items, as spear-heads, axes, among others, were shaped in a mould, being needed just some final works.

Ultimately, a correct **interaction among the corrosion and the archaeometallurgical studies** has shown to be very profitable, leading to very interesting observations and proposals. Some specific cases are for example the metrological study of the bronze weights and the study of the SL "gilded fibula". In the first case, a correct understanding of corrosion processes allowed an estimation of the loss in mass of the relatively small weights, providing valuable data to the attribution of each weight into an ancient measuring system. This had very profitable results, since it could be demonstrated that most weights are part of a ~9.5 g unit base metrical system that was at use in Eastern Mediterranean regions (as the Syria-Palestinian coasts and Cyprus), suggesting that by LBA some kind of interaction existed between these opposite Mediterranean territories. In the second case, the archaeometallurgical study on the SL "gilded fibula" has shown that due to improper conservation conducts, this item has been misinterpreted. Over-mechanical cleaning has exposed the uncorroded bronze, making three independent fragments of artefacts appear to belong to one unique artefact with a singular feature, i.e. a "gilded" surface.

Also, the present study has demonstrated the importance of conducting scientific studies using proper analytical techniques, to aid the historical and material interpretation and provide a solid base for adequate conservation conducts. A specific case was the detailed study of the CSR copper nail, which allowed the discovery of a gilded surface, a vital finding for a correct archaeological and historical interpretation of the item, as well as for any future conservation treatments. Considering that any artefact raises specific conservation issues, with this work it can be concluded that the establishment of these specific issues can perfectly be done during an archaeometallurgical study, preventing mass treatments which can conduct to side effects as flaking and destruction of associated information.

In the end, with this first general study on ancient metals from the Portuguese territory, some key guide lines were placed. However, it is clear that many questions remain unanswered, and that many others have been raised along the study. **Future corrosion studies** should focus on the application of other methodologies to characterise some of the corrosion products, namely those involved in the destannification process and in the corrosion/passivation of the δ phase in the two-phase bronze artefacts. Also, collection and analysis of soil samples from burial environments could be an interesting and exciting investigation to be undertaken to associate certain corrosion features to

specific burial conditions. **Future archaeometallurgical investigations** should involve more detailed studies on crucibles to better understand their use (i.e. for smelting or melting), and on vitrified fragments and other metallurgical remains that may still be stored in museum collections. The question of the melting vs. smelting activities is still lacking responses, particularly in relation to bronze metallurgy. To help in these questions, it also seems mandatory an awareness of the archaeologists/excavators to materials which are not easily perceived in the archaeographic records, such as some metallic minerals (cassiterite can be hardly perceptible due to its dark colour), that are currently missing from the general archaeometallurgical picture. Such materials can also give important information on the metallurgical technologies, namely in the issue alloying/partial smelting/co-smelting to produce bronze. Moreover, more field investigation, as to identify ancient mining explorations would be very useful to support the exploration of local minerals and to study the relation of the ancient populations with their territory, giving a new awareness of the value that each region could have had in ancient economies. Studies should also be focused in artefacts from recently excavated sites with well documented stratigraphies, to better trace a local metallurgical evolution. This could be very important to detect important technological incorporations, as the first bronzes, from the Northern to the Southern territory. All in all, future studies performed in the framework of the Archaeometallurgical working group that has been recently established in the Portuguese territory shall profit by applying and improving the minimum-invasive methodology developed along this work. Additionally, some new investigation lines ought to appear, as provenance studies, based on appropriate isotope analysis. Finally, many of the exposed issues will be focused in due course, since along the development of this archaeometallurgical work other projects have been submitted for funding, and are due to begin.

References

Adriens, A. 1995. Non-destructive analysis and testing of museum objects: An overview of 5 years of research. *Spectrochimica Acta B* 60, 1503-1516.

Adriaens, A., Yener, K.A., Adams, F. 1999. An analytical study using electron and ion microscopy of thin-walled crucibles from Göltepe, Turkey. *Journal of Archaeological Science* 26, 1069-1073.

Alberti, M.E., Ascalone, E., Parise N., Peyronel L. 2006. Weights in context. Current approaches to the study of the ancient weight systems. In: Alberti M. E., Ascalone, E., Peyronel, L. (Eds.), *Weights in Context*, Instituto Italiano di Numismatica, Roma, 1-8.

Allen, I.M., Britton, D., Coghlan, H.H. 1970. Metallurgical reports on British and Irish Bronze Age Implements and Weapons in the Pitt Rivers Museum. In: Penniman, T.K., Blackwood, B.M. (Eds.), *Occasional Papers on Technology* 10, University Press, Oxford.

Almagro-Gorbea, M. 2004. Inscripciones y grafitos tartésicos de la necrópolis orientalizante de Medellín, *Palaeohispanica* 4, 13-44.

Almagro-Gorbea, M. (Dir.) 2008. *La Necrópolis de Medellín: II Estudio de los hallazgos*, Real Academia de la Historia, Madrid.

Ambruster, B. 2002-2003. A metalurgia da Idade do Bronze Final Atlântico do castro de Nossa Senhora da Guia, de Baiões (S. Pedro do Sul, Viseu). *Estudos Pré-Históricos* 10-11, 145-155.

Ambruster, B. 2004. Tradition atlantique et innovation méditerranéenne à la fin de l'Âge du Bronze. Le complexe de Baiões (Viseu, Portugal). In: Lehoerff, A. (Ed.), *L'Artisant Métallurgique dans les Sociétés Anciennes en Méditerranée Occidentale*, École Française de Rome, Rome, 45-65.

Araújo, M.F., Alves, L.C., Cabral, J.M.P. 1993. Comparison of EDXRF and PIXE in the analysis of ancient gold coins. *Nuclear Instruments and Methods in Physics Research B: Beam Interactions with Materials and Atoms*, 75 (1), 450-453.

Araújo, M.F., Barros, L., Teixeira, A.C., Melo, A.A. 2004. EDXRF study of prehistoric artefacts from Quinta do Almaraz (Cacilhas, Portugal). *Nuclear Instruments and Methods in Physics Research B* 213, 741-746.

Artoli, G. 2007. Crystallographic texture analysis of archaeological metals: interpretation of manufacturing techniques. *Appl Phys A* 89, 899-908.

Ascalone, E., Peyronel, L. 2006. Balance weights from Tell Mardikh-Ebla and the weighing systems in the Levant during the Middle Bronze Age. In: Alberti M. E., Ascalone, E., Peyronel, L. (Eds.), *Weights in Context*, Instituto Italiano di Numismatica, Roma, 127-59.

Barros, L., Soares, A.M. 2004. Cronologia absoluta para a ocupação orientalizante da Quinta do Almaraz, no estuário do Tejo (Almada, Portugal). *O Arqueólogo Português* 22, 333-52.

Bauer, I., Northover, J.P. 1988. Zug-Sumpf: and extensive approach to the analysis of a single site and the development of sampling strategies for other sites. In: Mordant, C., Pernot, M., Rychner, V. (Eds.), *L'Atelier du Bronzier en Europe du XXe au VIIIe Siècle avant notre Ère*, CTHS, Paris, 137-151.

Bettencourt, A.M. 2001. Aspectos da metalurgia do bronze durante a Proto-história do Entre Douro e Minho. *Arqueologia* 26, Porto, 13-40.

Blot, M.L.P., 2002. *Os portos na origem dos centros urbanos: contributo para a arqueologia das cidades marítimas e flúvio-marítimas em Portugal*, Trabalhos de Arqueologia 28, Instituto Português de Arqueologia, Lisboa.

Bosi, C., Garagnani, L., Imbeni, V., Martini, C., Mazzeo, R., Poli, G. 2002. Unalloyed copper inclusions in ancient bronze artefacts. *Journal of Materials Science* 37, 4285-4298.

Briard, J., Bourhis, J.R., Vivet, J.B. 1998. Nouvelles séries d'analyses spectrographiques sur les bronzes Armoricains: Tréboul et Haches à douille. In: Mordant, C., Pernot, M., Rychner, V. (Eds.), *L'Atelier du Bronzier en Europe du XXe au VIIIe Siècle avant notre Ère*, CTHS, Paris, 91-100.

Bronk, H., Rohrs, S., Bjeoumikhov, A., Langhoff, N., Schmalz, J., Wedell, R., Gorny, H.E., Herold, A., Waldschlager, U. 2001. ArtTAX – a new mobile spectrometer for energy-dispersive micro X-ray fluorescence spectrometry on art and archaeological objects. *Fresenius Journal of Analytical Chemistry* 371, 2001, 307-316.

Burger, E., Bourgarit, D., Rostan, P., Carozza, L., Artioli, G. 2007. The mystery of Plattenshlacke in Protohistoric copper smelting: early evidence at the Early Bronze Age site of Saint-Véran, French Alps in Western Europe. In: Proceedings of 2nd International Conference of Archaeometallurgy in Europe, Associazione Italiana di Metallurgia, Milano (CD-ROM).

Cabral, J.M.P., Possolo, A., Marques, M.G. 1979. Non-destructive analysis of reais and fortes of Dom Fernando of Portugal by x-ray spectrometry. *Archaeometry* 21, 211-231.

Celestino Pérez, S. 2001. *Estelas de Guerrero y Estelas Diademadas*, Bellaterra, Barcelona.

Celestino Pérez, S. 2008. La precolonización a través de los símbolos. In: Celestino, S., Rafel, N., Armada, X.-L. (Eds.), *Contacto cultural entre el Mediterráneo y el Atlántico (siglos XII-VIII ane)*, CSIC, Madrid, 107-119.

Celestino, S., Rafael, N., Armada, X.-L. (Eds.) 2008. *Contacto cultural entre el Mediterrâneo y el Atlântico (siglos XII-VIII ane) La precolonización a debate*, CSIC, Madrid.

Coffyn, A. 1985. *Le Bronze Final Atlantique dans la Péninsule Ibérique*, Centre Pierre Paris, Bordeaux.

Coghlan, H.H. 1975. *Notes on the Prehistoric Metallurgy of Copper and Bronze in the Old World*, Occasional Papers on Technology, University Press, Oxford.

Correia, A., Silva, C.T., Vaz, J.I. 1979. Catálogo da colecção arqueológica Dr. José Coelho. *Beira Alta* 38, 605-638.

Craddock, P.T. 1995. *Early Metal Mining and Production*, Smithsonian Institution Press, Washington D.C.

Craddock, P.T. 2007. Evidences of the earliest smelting process in Western Europe. In: Proceedings of 2nd International Conference of Archaeometallurgy in Europe, Associazione Italiana di Metallurgia, Milano (CD-ROM).

Creagh, D.C. 2005. The characterization of artefacts of cultural heritage significance using physical techniques. *Radiation Physics and Chemistry* 74, 426-442.

Davy, J. 1826. Observations on the changes which have taken place in some ancient alloys of copper. *Philosophical Transactions of the Royal Society of London* 116, 55-59.

De Ryck, I., Adriaens, A., Adams, F. 2005. An overview of Mesopotamian bronze metallurgy during the 3rd millennium BC. *Journal of Cultural Heritage* 6, 261-268.

De Ryck, I., Adriaens, A., Pantos, E., Adams, F. 2003. A comparision of microbeam techniques for the analysis of corroded ancient bronze objects. *Analyst* 128, 1104-1109.

Degrigny, C. 2007. Examination and conservation of historical and archaeological metal artefacts: a European overview. In: Dillmann, P., Béranger, G., Piccardo, P., Matthiesen, H. (eds.), *Corrosion of metallic heritage artefacts*. Woodhead Publishing Limited, Cambridge, 1-17.

Delibes de Castro, G., Fernández Manzano, J., Herrán Martínez, J.I. 1998. La métallurgie de L'Âge du cuivre dans le Nord du plateau Espagnol: caractéristiques des coulées et systèmes de production. In: Mordant, C., Pernot, M., Rychner, V. (Eds.), *L'Atelier du Bronzier en Europe du XXe au VIIIe Siècle avant notre Ère*, CTHS, Paris, 63-79.

Doménech-Carbó, A., Doménech-Carbó, M.T., Martínez-Lázaro, I. 2008. Electrochemical identification of bronze corrosion products in archaeological artefacts. A case study. *Microchimica Acta* 162, 351-359.

Dungworth, D. 2000. Serendipity in the foundry? Tin oxide inclusions in copper and copper alloys as an indicator of production process. *Bulletin of the Metals Museum* 32, 1-5.

Fernández-Miranda, M., Montero Ruíz, I., Rovira Llorens, S. 1995. Los primeros objetos de bronce en el Occidente de Europa. *Trabajos de Prehistoria* 52(1), 57-69.

Ferrer Eres, M.A., Valle-Algarra, M., Gimeno Adelantado, J.V., Peris-Pricente, J., Soriano Piñol, M.D., Mateo-Castro, R. 2008. Archaeometric study on polymetallic remains from the

archeological dig in Lixus (Larache, Morocco) by scanning electron microscopy and metallographic techniques. *Microchimica Acta* 162, 341-349.

Figueiredo, E., Melo, A.A., Araújo, M.F. 2007. Artefactos metálicos do Castro de Pragança: um estudo preliminar de algumas ligas de cobre por Espectrometria de Fluorescência de Raios X. *O Arqueólogo Português* 25, 195-215.

Fontes, J. 1916. Sur un moule pour faucilles de bronze provenant du Casal de Rocanes, *O Archeologo Português* I 21, 337-342.

Galán, E., Ruiz-Gálvez, M. 1996. Divisa, dinero y moneda. *Complutum* 6, 151-65.

Gänsicke, S., Newman, R. 2000. Gilded silver from Ancient Nubia. In: Drayman-Weisser T (Ed.), *Gilded Metal – History, Technology and Conservation*, Archtype and The American Institute for Conservation of Historic and Artistic Works, London, 73-96.

Garcia, F. (Ed.) 1963. *Minas concedidas no continente desde Agosto de 1836 a Dezembro de 1962*, Direcção Geral de Minas e Serviços Geológicos, Lisboa.

Giardino, C. 1995. *The western Mediterranean between the 14th and the 8th centuries B.C.* BAR international Series 612, Oxford.

Gettens, R.J. 1951. The corrosion products of an ancient Chinese bronze. *Journal of Chemical Education* 28, 67-71.

Gil, F.B., Senna-Martinez, J.C., Guerra, M.F., Seruya, A.I., Fabião, C. 1989. Produções metalúrgicas do Bronze Final do Cabeço do Crasto de São Romão, Seia: uma primeira análise. Actas do I Colóquio Arqueológico de Viseu, Colecção Ser e Estar, n.2, 235-248.

Gimeno Adelantado, J.V., Ferrer Eres, M.A., Valle Algarra, F.M., Peris Vicente, J., Bosch Reig, F. 2003. Application of SEM/EDX and metallographic techniques to the diachronic study (6th-18th century) of metallurgical materials found in archaeological excavations on the island of Ibiza (Spain). *Analitical and Bioanalytical Chemistry* 375, 1161-1168.

Giot, P.-R., Lulzac, Y. 1998. Datation à l'Âge du bronze d'une exploitation de cassiterite dans le Finistère. *Bulletin de la Société Préhistorique Française* 95(4), 598-600.

Giumlia-Mair, A. 2005. On surface analysis and archaeometallurgy. *Nuclear Instruments and Methods B* 239, 35-43.

Gomes, M.V. 1991. Corniformes e figuras associadas de dois santuários do Sul de Portugal. Cronologia e interpretação, *Almansor* 9, 17-34.

Gomes, R.V., Gomes, M.V., SANTOS, M.F. 1983. O santuário exterior do Escoural - Sector NE (Montemor-o-Novo), *Zephyrus* 36, 287-307.

Gomes, M.V., Gomes, R.V. Santos, M.F. 1994. O Santuário exterior do Escoural - Sector SE (Montemor-o-Novo, Évora), *Actas das V Jornadas Arqueológicas* 2, Lisboa, 93-108.

Gómez Ramos, P. 1993. Tipología de lingotes de metal y su hallazgo en los depósitos del Bronze Final de la Península Ibérica. *CuPAUAM* 20, 73–105.

Gómez Ramos, P. 1999. *Obtención de metales en la Prehistoria de la Península Ibérica*. BAR International Series 753, Oxford.

Gonçalves, V.S., Valério, P., Araújo, M.F. 2005. The copper archaeometallurgy at Monte Novo dos Albardeiros (Regengos de Monsaraz, Évora). *O Arqueólogo Português* 23, 231-255.

Griffin, P.S. 2000. The selective use of gilding on Egyptian Polychromed Bronzes. In: Drayman-Weisser T (ed), *Gilded Metal – History, Technology and Conservation*, Archtype and The American Institute for Conservation of Historic and Artistic Works, London, 49-72.

Grolimund, D., Senn, M., Trottmann, M., Janousch, M., Bonhoure, I., Scheidegger, A.M., Marcus, M. 2004. Shedding new light on historical metal samples using micro-focused synchrotron X-ray fluorescence and spectroscopy. *Spectrochimica Acta B* 59, 1627-1635.

Guerra, M.F., 1995. Elemental analysis of coins and glasses. *Applied Radiation and Isotopes* 46, 583-588.

Guerra, M.F., Calligaro, T. 2003. Gold cultural heritage objects: a review of studies of provenance and manufacturing technologies, *Measurement Science and Technology* 14, 1527–1537.

Haarer, P. 2001. Problematising the transition from bronze to iron. In: Shortland, A.J. (Ed.) *The social context of technological change: Egypt and the Near East 1650-1550 BC*, Oxbow Books, Oxford, 255-273.

Hauptmann, A. 2007. *The Archaeometallurgy of Copper*. Springer, Berlin.

Healy, J.F. 1999. *Pliny the Elder on Science and Technology*, Oxford University Press, New York.

Huth, C. 2000. Metal circulation, communication and traditions of craftsmanship in Late Bronze Age and Early Iron Age Europe. In: Pare, C.F.E. (Ed.) *Metals make the world go round: The supply and circulation of metals in Bronze Age Europe*, Oxbow Books, Oxford, 176-193.

Hunt Ortiz, M.A. 2003. Prehistoric mining and metallurgy in south west Iberian Peninsula, BAR IS 1188, Archaeopress, Oxford.

Ingo, G.M., De Caro, T., Riccucci, C. 2006. Large scale investigation of chemical composition, structure and corrosion mechanism of bronze archaeological artefacts from Mediterranean basin. *Applied Physics A* 83, 513-520.

IUPAC 1978. Nomenclature, symbols, units and their usage in spectrochemical analysis – II. Data interpretation. *Spectrochimica Acta B* 33, 242-245.

Janssens, K., Vittiglio, G., Deraedt, I., Aerts, A., Vekmans, B., Vincze, L., Wei, F., De Ryck, I., Schalm, O., Adams, F., Rindby, A., Knöchel, A., Simionovici, A., Snigirev, A. 2000. Use of

microscopic XRF for non-destructive analyses in art and archaeometry. *X-Ray Spectrometry* 29, 73-91.

Jorge, V.O., Cardoso, J.M., Vale, A.M., Velho, G.L., Pereira, L.S. 2006-2007. Problemática suscitada pelas escavações do sítio pré-histórico do Castanheiro do Vento (Horta do Douro, Vila Nova de Foz Côa), sobretudo após a campanha de 2005. *Ciências e Técnicas do Património* V-VI, Revista da Faculdade de Letras, Porto, 241-277.

Junghans, S., Sangmeister, E., Schröder, M. 1960. *Metallanalysen kupferzeitlicher und frühbronzezeitlicher Bondenfunde aus Europa*, Studien zu den Anfängen der Metallurgie 1, Gerb. Mann Verlag, Berlin.

Junghans, S., Sangmeister, E., Schröder, M. 1968. *Kupper und Bronze in der frühen Metallzeit Europas*, Studien zu den Anfängen der Metallurgie 2/1-3, Gerb. Mann Verlag, Berlin.

Junghans, S., Sangmeister, E., Schröder, M. 1974. *Kupper und Bronze in der frühen Metallzeit Europas*, Studien zu den Anfängen der Metallurgie 2/4, Gerb. Mann Verlag, Berlin.

Kalb, P., 1995. Produção local e relações a longa distância na Idade do Bronze Atlântico do Oeste da Península Ibérica. In: Jorge, S.O. (Ed.), *Existe uma Idade do Bronze Atlântica?*, IPA, Lisboa, 157-165.

Kearns, T., Martinón-Torres, M., Rehren, T. 2007. Metal to mould – an experimental study of casting moulds using ED-XRF. Poster presented in Archaeometallurgy in Europe 2007, Aquileia, Italy.

Kienlin, T.L., Bischoff, E., Opielka, H. 2006. Copper and bronze during the eneolithic and early bronze age: a metallographic examination of axes from the northalpine region. *Archaeometry* 48, 453-468.

Klein, S., Hauptmann, A. 1999. Iron Age leaded tin bronzes from Khirbet Edh-Dharih, Jordan. *Journal of Archaeological Science* 26, 1075-1082.

Kristansen, K., Larsson, T.B. 2005. *The rise of Bronze Age Society: travels, transmissions and transformations*. Cambridge University Press, Cambridge.

Lago, M., Duarte, C., Valera, A., Albergaria, J., Almeida, F., Carvalho, A.F. 1997. Povoado dos Perdigões (Reguengos de Monsaraz): dados preliminares dos trabalhos arqueológicos realizados em 1997. *Revista Portuguesa de Arqueologia* 1, 45-152.

Larssen, H. 2000. Introduction to weight systems in the Bronze Age East Mediterranean: the case of Kalavasos-Ayios Dhimitrios. In: Pare C. (Ed.) *Metals make the world go round: The supply and circulation of metals in Bronze Age Europe*, Oxbow Books, Oxford, 233-246.

Lechtman, H. 1996. Bronze: Dirty copper or chosen alloy? A view from the Americas. *Journal of Field Archaeology* 23, 477-514.

Liversage, D., Northover, J.P. 1998. Prehistoric trade monopolies and bronze supply in northern Europe. In: Mordant, C., Pernot, M., Rychner, V. (Eds.), *L'Atelier du Bronzier en Europe du XXe au VIIIe Siècle avant notre Ère*, CTHS, Paris, 137-151.

Lorrio, A.J. 2008. *Qurénima: El Bronce Final del Sureste de la Peninsula Ibérica*, Real Academia de la Historia, Madrid.

Mantler, M., Schreiner, M. 2001. X-ray analysis of objects of art and archaeology. *Journal of Radioanalytical and Nuclear Chemistry* 247, 635-644.

Meeks, N.D. 1986. Tin-rich surfaces on bronze – some experimental and archaeological considerations. *Archaeometry* 28, 133-162.

Melo, A.A. 2000. Armas, utensílios e esconderijos. Alguns aspectos da metalurgia do Bronze Final: o depósito do Casal dos Fiéis de Deus. *Revista Portuguesa de Arqueologia* 3(1), 15-119.

Melo, A.A., Alves, H., Araújo, M.F. 2002. The bronze palstave from the Quarta Feira Copper Mine, Central Portugal. In: Ottaway, B.S., Wagner, E.C. (Eds.), *Metals and Society*, BAR IS 1061, British Archaeological Reports, Oxford, 109-113.

Merideth, C. 1998. *An archaeometallurgical survey for ancient tin mines and smelting sites in Spain and Portugal*, BAR International Series 714, Oxford.

Michailidou, A. 2006. Stone balance weights? The evidence from Akrotiri. In: Alberti M. E., Ascalone, E., Peyronel, L. (Eds.), *Weights in Context*, Instituto Italiano di Numismatica, Roma, 233-263.

Mohen, J. -P. 1990. *Métallurgie Préhistorique – Introduction à la paléométallurgie*, Collection Préhistoire, Masson, Paris.

Montero Ruiz, I. 2008. Ajuares metálicos y aspectos tecnológicos en la metalurgia del Bronce Final-Hierro en el sudeste de la Península Ibérica. In: Lorrio, A.J. *Qurénima: El Bronce Final del Sureste de la Península Ibérica*. Real Academia de la Historia, Madrid, 499-516.

Montero Ruiz, I., Gómez Ramos, P., Rovira Llórens, S. 2003. Aspectos de la metalurgia orientalizante en Cancho Roano. In: *Cancho Roano IX. Los Materiales Arqueológicos II*, Instituto de Historia, Madrid, 195-210.

Müller, R., Cardoso, J.L. 2008. The origin and use of copper at the Chalcolithic fortification of Leceia, Portugal. *Madrider Mitteilungen* 49, 64-93.

Müller, R., Goldenberg, G., Bartelheim, M., Kunst, M., Pernicka, E. 2007. Zambujal and the beginnings of metallurgy in southern Portugal. In: LaNiece, S., Hook, D., Craddock, P. (Eds.) *Metals and Mines, Studies in Archaeometallurgy*, Oxford, 15-26.

Müller, R., Pernicka, E. 2009. Chemical analyses in archaeometallurgy: a view on the Iberian Península. In: Kienlin, T.L., Roberts, B (Eds.) *Metals and Society – Studies in honour of Barbara S. Ottaway*, Verlag Dr. Rudolf Habelt GMBH, Bonn, 296-306.

Müller, R., Soares, A.M.M. 2008. Traces of early copper production at the Chalcolithic fortification of Vila Nova de São Pedro, Portugal. *Madrider Mitteilungen* 49, 94-114.

Needham, S.P., Leese, M.N., Hook, D.R., Huges, H.J. 1989. Developments in the Early Bronze Age metallurgy of southern Britain*. World Archaeology* 20(3), 283-402.

Nicholson, E.D. 1979. The ancient craft of gold beating. *Gold Bulletin* 12, 161-166.

Nocete, F., Queipo, G., Sáez, R., Nieto, J.M., Inácio, N., Bayona, M.R., Peramo, A., Vargas, J.M., Cruz-Auñón, R., Gil- Ibarguchi, J.I., Santos, J.F. 2008. The smelting quarter of Valencia de la Concepción (Seville, Spain): the specialised copper industry in a political centre of the Guadalquivir Valley during the Third millennium BC (2750-2500 BC). *Journal of Archaeological Science* 35, 717-732.

Northover, P., Anheuser, K. 2000. Gilding in Britain: Celtic, Roman and Saxon. In: Drayman-Weisser, T. (Ed.) *Gilded Metal: History, Technology and Conservation*, Archtype and The American Institute for Conservation of Historic and Artistic Works, London, 109–121.

Oddy, A. 1981. Gilding through the Ages. *Gold Bulletin* 14, 75-79.

Oddy, A. 2000. A History of Gilding with particular reference to statuary. In: Drayman-Weisser T (Ed.), *Gilded Metal – History, Technology and Conservation*, Archtype and The American Institute for Conservation of Historic and Artistic Works, London, 1-19.

Organ, R.M. 1963. Aspects of bronze patina and its treatment. *Studies in Conservation* 8, 1-9.

Ottaway, B.S., Roberts, B. 2008. The emergence of metalworking, In: Jones, A. (Ed.) *Prehistoric Europe: Theory and Practice*, Wiley-Blackwell, 193-224.

Paço, A. 1955. Castro de Vila Nova de San Pedro (VII). Considerações sobre o problema da Metalurgia (1). *Zephyrus* 6, 27–40.

Pare, C. 2000. Bronze and Bronze Age. In: Pare C. (Ed.) *Metals make the world go round: The supply and circulation of metals in Bronze Age Europe*, Oxbow Books, Oxford, 1-38.

Perea, A., Armbruster, B. 2008. Tradición, cambio y rupture generacional. La producción orfebre de la fachada Atlántica durante la transición Bronce-Hierro de la Península Ibérica. In: Celestino, S., Rafel, N., Armada, X.-L. (Eds.), *Contacto cultural entre el Mediterráneo y el Atlántico (siglos XII-VIII ane)*, CSIC, Madrid, 509-520.

Pérez, J.A., Rivera, T., Romero, E. 2002. Crisoles-horno en el Bronce del suroeste. *Boskan* 19, 65-73.

Pessoa, M. 2002. Uma ponta de lança do Bronze Final: Gruta do Algarinho/Sistema do Dueça, Penela, Portugal. In: Actas do IV Congresso Nacional de Espeleologia, 5ª secção, Leiria, 124-127.

Petruso, K.M. a. In: http://www.uta.edu/anthropology/petruso/metrology.1.html (Sep 2008).

Petruso, K. M. 1984. Prolegomena to Late Cypriot Weight Metrology. *American Journal of Archaeology* 88, 293-304.

Petruso, K. M. 2006. Ancient Metrology and Modern Globalisation: Notes on a Bronze Age World System, Pre-conference manuscript, First Conference on Early Economic Developments, Department of Economics, University of Copenhagen, previously available online in: http://www.econ.ku.dk/eed (2006).

Piccardo, P., Mille, B., Robbiola, L. 2007. Tin and copper oxides in corroded archaeological bronzes. In: Dillmann, P., Béranger, G., Piccardo, P., Matthiesen, H. (Eds.), *Corrosion of metallic heritage artefacts*, Woodhead Publishing Limited, Cambridge, 239-262.

Pinasco, M.R., Ienco, M.G., Piccardo, P., Pellati, G., Stagno, E. 2007. Metallographic approach to the investigation of metallic archaeological objects. *Annali di Chimica-Rome* 97, 553-574.

Ponte, S. 2006a. *Corpus Signorum das Fíbulas Proto-Históricas e Romanas de Portugal*, Caleidoscópio, Coimbra.

Ponte, S. 2006b. A metalurgia do ferro e os artefactos da Pré-história Recente. In: Proceedings 3º Simpósio sobre Mineração e Metalurgia Históricas no Sudoeste Europeu, Sociedad Española para la Defensa del Património Geológico y Minero and IPPAR, Porto, Portugal, 95-124.

Primas, M., Wanner, B., Boll, P.O. 1998. The interpretation of metal analysis: a case study based on the silver spiral from Sion (Valais, Switzerland). In: Mordant, C., Pernot, M., Rychner, V. (Eds.), *L'Atelier du Bronzier en Europe du XXe au VIIIe Siècle avant notre Ère*, CTHS, Paris, 53-61.

Pulak, C. 2000. The balance weights from the Late Bronze Age shipwreck at Uluburun. In: Pare, C.F.E. (Ed.) *Metals make the world go round: The supply and circulation of metals in Bronze Age Europe*. Oxbow Books, Oxford, 247-266.

Pulak, C. 2006. The Balance weights from the Uluburun and Cape Gelidonya shipwrecks. In: Alberti M. E., Ascalone, E., Peyronel, L. (Eds.), *Weights in Context*, Instituto Italiano di Numismatica, Roma, 47-48.

Rahmstorf, L. 2006. In search of the earliest balance weights, scales and weighting systems from the East Mediterranean, the Near and Midlle East, In: Alberti M. E., Ascalone, E., Peyronel, L. (Eds.), *Weights in Context*, Instituto Italiano di Numismatica, Roma, 9-45.

Reimer, P.J., Baillie, M.G.L., Bard, E., Bayliss, A., Beck, J.W., Bertrand, C.J.H., Blackwell, P.G., Buck, C.E., Burr, G.S., Cutler, K.B., Damon, P.E., Edwards, R.L., Fairbanks, R., Friedrich, M., Guilderson, T.P., Hogg, A.G., Hughen, K..A., Kromer, B., McCormac, G.,

Manning, S., Ramsey, C.B., Reimer, R.W., Remmele, S., Southon, J.R., Stuiver, M., Talamo, S., Taylor, F.W., Van Der Plicht, J., Weyhenmeyer, C.E. 2004. IntCal04 Terrestrial Radiocarbon Age Calibration, 0-26 cal Kyr BP. *Radiocarbon* 46, 1029-58.

Renfrew, C., Bahn, P. 1991. *Archaeology: Theories, Methods and Practice*, Thames and Hudson, London.

Robbiola, L., Blengino, J.-M., Fiaud, C. 1998. Morphology and mechanisms of formation of natural patinas on archaeological Cu-Sn alloys. *Corrosion Science* 40, 2083-2111.

Rosenfeld, A., Ilani, S., Dvorachek, M. 1997. Bronze Alloys from Canaan during the Middle Bronze Age. *Journal of Archaeological Science* 24, 857-864.

Rodríguez Diaz, A., Pavón Soldevila, I., Merideth, C., Tresserras, J.J.I. 2001. *El Cerro de San Cristobal, Logrosan, Extremadura, Spain*. BAR IS 922, Archaeopress, Oxford.

Rothenberg, B. 1985. Copper smelting Furnaces in the Arabah, Israel: the archaeological evidence. In: Craddock, P.T., Hughes, M.J. (Eds.), *Furnaces and Smelting Technology in Antiquity*, British Museum Occasional Papers 48, London, 123-135.

Rovira, S. 1995. Estudio Arqueometalúrgico del depósito de la Ria de Huelva. In: Ruiz-Gálvez, M. (Ed.), *Ritos de paso y puntos de paso La Ria de Huelva en el mundo del Bronce Final Europeo*, Complutum Extra 5, Universidade Complutense, Madrid, 33-57.

Rovira, S. 2002. Metallurgy and Society in Prehistoric Spain. In: Ottaway, B.S., Wagner, E.C. (Eds.), *Metals and Society*, BAR International Series 1061, British Archaeological Reports, Oxford, 5-20.

Rovira, S. 2004. Tecnología metalúrgica y cambio cultural en la prehistoria de la Península Ibérica. *Norba. Revista de Historia* 17, 9-40.

Rovira, S. 2005. Tinned surface in Spanish Late Bronze Age swords. *Surface Engineering* 21, 368-372.

Rovira, S. 2007. La produccíon de bronces en la Prehistoria. In: Marimon, J., Silva, J., Grabulosa, P., Cara, T. (Eds.), *Avances en Arqueometría*, Universitat de Girona I Futur, Girona, 21-35.

Rovira, S., Gómez-Ramos, P. 1998. The Ria de Huelva hoard and the Late Bronze Age metalwork: a statistical approach. In: Mordant, C., Pernot, M., Rychner, V. (Eds.), *L'Atelier du Bronzier en Europe du XXe au VIIIe Siècle avant notre Ère*, CTHS, Paris, 81-90.

Rovira, S., Gómez Ramos, P. 2003. *Las primeras etapas metalúrgicas en la Península Ibérica, III. Estudios Metalográficos*, Imprenta Taravilla, Madrid.

Rovira, S., Montero, I. 2003. Natural tin-bronze alloy in Iberian Peninsula metallurgy: potentiality and reality. In: Giumlia-Mair, A., Lo Shiavo, F. (Eds.), *Le problème de l'étain à l'origine de la métallurgie,* BAR International Series 1199, British Archaeological Reports, Oxford, 15-22.

Rovira, S., Montero, I., Ortega, J., Ávila, J.J. 2005. Bronce y trabajo del bronce en el poblado orientalizante de "El Palomar" (Oliva de Mérida, Badajoz). *Anejos de AEspA* XXXV, 1231-1240.

Rovira, S., Montero-Ruiz, I., Renzi, M. 2009. Experimental Co-smelting to Copper-tin Alloys. In: Kienlin, T.L., Roberts, B (Eds.) *Metals and Society – Studies in honour of Barbara S. Ottaway*, Verlag Dr. Rudolf Habelt GMBH, Bonn, 407-414.

Ruiz-Gálvez, M. 1993. El Occidente de la Peninsula Iberica, punto de encontro entre el Mediterraneo y el Atlantico a fines de la Edad del Bronce. *Complutum* 4, 41-68.

Ruiz-Gálvez, M. 1998. *La Europa Atlántica en la Edade del Bronce*, Crítica, Barcelona.

Ruiz-Gálvez, M. 2000. Weight systems and exchange networks in Bronze Age Europe. In: Pare, C.F.E. (Ed.) *Metals make the world go round: The supply and circulation of metals in Bronze Age Europe*, Oxbow Books, Oxford, 267-279.

Ruiz-Gálvez, M., 2003. Investigating weight systems in Nuragic Sardinia. In: Giumlia-Mair, A., Lo Shiavo, F. (Eds.), *Le problème de l'étain à l'origine de la métallurgie,* BAR International Series 1199, British Archaeological Reports, Oxford, 149-57.

Ruiz-Gálvez, M. 2008. Writing, counting, self-awareness, experiencing distant worlds. Identity process and free-lance trade in the Bronze Age/Iron Age transition. In: Celestino, S., Rafel, N., Armada, X.-L. (Eds.), *Contacto cultural entre el Mediterráneo y el Atlántico (siglos XII-VIII ane)*, CSIC, Madrid, 27-40.

Ruiz-Taboada, A., Montero-Ruiz, I. 1999. The oldest metallurgy in Western Europe. *Antiquity* 73, 897-902.

Sáez, R., Nocete, F., Nieto, J.M., Capitán, M.A., Rovira, S. 2003. The extractive metallurgy of copper from Cabezo Juré, Huelva, Spain: Chemical and mineralogical study of slags dated to the third millennium B.C. *The Canadian Mineralogist* 41, 627-638.

Sangmeister, E. 2005. Les débutes de la métallurgie dans le sud-ouest de l'Europe: l'apport de l'étude des analyses métallographiques. In: Ambert, P., Vaquer, J. (Eds.) *La première métallurgie en France et dans les pays limitrophes*, Mémoire XXXVII, Société Préhistorique Française, 19-25.

Sanjuán, L.G. 2006. The warrior stelae of the Iberian South-west. Symbols of power in ancestral landscapes. Available from: http://www.scribd.com/doc/15691934/GarciaSanjuan-etal-2006-bronze-age-warrior-stelae-in-Southern-Spain-en.

Scott, D.A. 1985. Periodic corrosion phenomena in bronze antiquities. *Studies in Conservation* 30, 49-57.

Scott, D.A. 1990. Bronze disease: a review of some chemical problems and the role of relative humidity. *Journal of the American Institute for Conservation* 29, 193-206.

Scott, D.A. 1994. An examination of the patina and corrosion morphology of some Roman bronzes. *Journal of the American Institute for Conservation* 33, 1-23.

Selwyn, L. 2000. Corrosion chemistry of gilded silver and copper. In: Drayman-Weisser T (ed), *Gilded Metal – History, Technology and Conservation*, Archtype and The American Institute for Conservation of Historic and Artistic Works, London, 21-47.

Senna-Martinez, J.C. 1994. Subsídios para o estudo do Bronze Pleno na Estremadura Atlântica: (1) Albarda de tipo "Atlântico" do Habitat das Baútas (Amadora). *Zephyrus* XLVI, 161-182.

Senna-Martinez, J.C. 1995. Entre Atlântico e Mediterrâneo: algumas reflexões sobre o Grupo Baiões/Santa Luzia e o desenvolvimento do Bronze Final Peninsular. In: AAVV, *A Idade do Bronze em Portugal - Discursos de poder*, Secretaria de Estado da Cultura e Instituto Português de Museus, Lisboa, 118-122.

Senna-Martinez, J.C. 1998. Produção, ostentação e redistribuição: estrutura social e economia política no Grupo Baiões/Santa Luzia. In: Jorge S.O. (Ed.), *Existe uma Idade do Bronze Atlântica?*, IPA, Lisboa, 218-230.

Senna-Martinez, J.C. 2000. O "Grupo Baiões/Santa Luzia" no Quadro do Bronze Final de Centro de Portugal. In: Senna-Martinez, J.C., Pedro, I. (Eds.), *Por Terras de Viriato - Arqueologia da Região de Viseu*, Governo Civil do Distrito de Viseu e Museu Nacional de Arqueologia, Viseu, 117-146.

Senna-Martinez, J.C., Araújo, M.F., Valério, P., Peixoto, H. 2004. Estudos sobre a arqueometalurgia do grupo Baiões/Santa Luzia: (1) ponta de lança do Castro da Senhora das Necessidades (Sernancelhe). *O Arqueólogo Português* 22, 319-332.

Senna-Martinez, J.C., Figueiredo, E., Valério, P., Araújo, M.F., Ventura, J.M.Q., Carvalho, H. 2007. Bronze melting and symbolic of power: the foundry area of Fraga dos Corvos Bronze Age Habitat site (Macedo de Cavaleiros, North-Eastern Portugal). In: Proceedings of 2nd International Conference of Archaeometallurgy in Europe, Associazione Italiana di Metallurgia, Milano (CD-ROM).

Senna-Martinez, J.C., Pedro, I. 2000. Between Myth and Reality: the foundry area of Senhora da Guia de Baiões and Baiões/Santa Luzia Metallurgy, *Trabalhos de Arqueologia da EAM* 6, 61-77.

Senna-Martinez, J.C., Ventura, J.M.Q., Carvalho, H.A., Figueiredo, E. 2005. A Fraga dos Corvos(Macedo de Cavaleiros): Um sítio de habitat da primeira Idade do Bronze em Trás-os-Montes Oriental, A Campanha 3. *Caderno Terras Quentes* 3, 61-85.

Seruya, A.I., Carreira, J.R.. 1994. Análise não destrutiva por Fluorescência de raios X do espólio metálico do Abrigo de Bocas (Rio Maior). *Trabalhos de Arqueologia da E.A.M.*, 135-143.

Sestieri, A.M.B., Macnamara, E., Hook, D. 2007. *Prehistoric metal artefacts from Italy (3500-720 BC) in the British Museum*, British Museum Research Publications 159, The Trustees of the British Museum, London.

Silva, R.J.C., Figueiredo, E., Araújo, M.F., Pereira, F., Braz Fernandes, F.M. 2008. Microstructure Interpretation of Copper and Bronze Archaeological Artefacts from Portugal. *Materials Science Forum* 587-588, 365-369.

Simpson, D.R., Fisher, R., Libsch, K. 1964. Thermal stability of azurite and malachite. *The American Mineralogist* 49, 1111–1114.

Soares, A.M.M. 2005. A metalurgia de Vila Nova de S. Pedro. Algumas reflexões. In: Arnaud, J.M., Fernandes, C. (Eds.) *Construindo a memória. As colecções do Museu Arqueológico do Carmo*, Associação dos Arqueólogos Portugueses e Museu Arqueológico do Carmo, Lisboa, 179-118.

Soares, A.M.M., Araújo, M.F., Alves, L., Ferraz, M.T. 1996. Vestígios Metalúrgicos em contextos do Calcolítico e da Idade do Bronze no sul de Portugal. In: *Miscellanea em homenagem ao professor Bairrão Oleiro*, Edições Colibri, Lisboa, 553-579.

Soares, A.M..M., Araújo, M.F., Cabral, J.M.P. 1994. Vestígios da prática de metalurgia em povoados Calcolíticos da bacia do Guadiana, entre o Ardila e o Chanca. *Arqueología en el entorno del Bajo Guadiana*, Huelva, 165-200.

Spratling, M. G. 1980. Weighing of gold in prehistoric Europe. In: Oddy, W. A. (Ed.), *Aspects of Early Metallurgy*, British Museum Occasional Papers 17, Trustees of the British Museum, London, 179-183.

Strahan, D.K., Maines, C.A. 2000. Lacquer as an adhesive for gilding on copper alloy sculpture in southeast Asia. In: Drayman-Weisser T (Ed.), *Gilded Metal – History, Technology and Conservation*, Archtype and The American Institute for Conservation of Historic and Artistic Works, London, 185-201.

Taylor, R.J., MacLeod, I.D. 1985. Corrosion of bronzes on shipwrecks: a comparison of corrosion rates deduced from shipwreck material and from electrochemical methods. *Corrosion* (NACE) 41, 100-104.

Théry-Parisot, I. 2002. Fuel management (bone and wood) during the Lower Aurignacian in the Pataud rock shelter (Lower Palaeolithic, Les Eyzies de Tayac, Dordogne, France): contribution of experimentation. *Journal of Archaeological Science* 29, 1415–1421.

Thornton, C., Lamberg-Karlovsky, C.C., Liezers, M., Young, S.M.M. 2002. On pins and needles: tracing the evolution of copper-base alloying at Tepe Yahya, Iran, via ICP-MS analysis of common-place items. *Journal of Archaeological Science* 29, 1451-1460.

Timberlake, S. 2007. The use of experimental archaeology (archaeometallurgy for the understanding and reconstruction of Early Bronze Age mining and smelting technologies). In: La Niece, S., Hook, D., Craddock, P. (Eds.), *Metals and Mines*, Archetype Publications and The British Museum, London, 27–36.

Tylecote, R.F. 1962. *Metallurgy in Archaeology: A Prehistory of Metallurgy in the British Isles*, Edward Arnold, London.

Tylecote, R.F. 1979. The effect of soil conditions on the long-term corrosion of buried tin-bronzes and copper. *Journal of Archaeological Science* 6, 345-368.

Tylecote, R.F. 1983. The behaviour of lead as a corrosion resistant medium undersea and in soils. *Journal of Archaeological Science* 10, 397-409.

Valério, P., Araújo, M.F., Canha, A. 2007a. EDXRF and micro-EDXRF studies of Late Bronze Age metallurgical productions from Canedotes (Portugal). *Nuclear Instruments and Methods in Physics Research B* 263, 477-482.

Valério, P., Araújo, M.F., Senna-Martinez, J.C., Vaz, J.L.I. 2006. Caracterização química de produções metalúrgicas do Castro da Senhora da Guia de Baiões. *O Arqueólogo Português* 24, 289-319.

Valério, P., Silva, R.J.C., Monge Soares, A.M., Araújo, M.F., Braz Fernandes, F.B., Silva, A., Berrocal-Rangel, L. 2010a. Technological continuity in Early Iron Age bronze metallurgy at the South-Western Iberian Península – a sight from Castro dos Ratinhos. *Journal of Archaeological Science* 37, 1811-1819.

Valério, P., Silva, R.J.C., Araújo, M.F., Soares, A.M.M., Braz Fernandes, F.M. 2010b. Microstructural signatures of bronze archaeological artifacts from the Southwestern Iberian Peninsula. *Materials Science Forum* 636-637, 597-604.

Valério, P., Soares, A.M.M., Araújo, M.F., Silva, C.T., Soares, J. 2007b. Vestígios arqueometalúrgicos do povoado calcolítico fortificado do Porto das Carretas (Mourão). *O Arqueólogo Português* 25, 177-194.

Van Grieken, R.E., Markowicz, A.A. 1993. *Handbook of X-Ray Spectrometry*, Marcel Dekker, USA.

Vandkilde, H. 1998. Denmark and Europe: Typochronology, metal composition and sócio-economic change in the Early Bronze Age. In: Mordant, C., Pernot, M., Rychner, V. (Eds.), *L'Atelier du Bronzier en Europe du XXe au VIIIe Siècle avant notre Ère*, CTHS, Paris, 119-134.

Vilaça, R. 1995. *Aspectos do povoamento da Beira Interior (Centro e Sul) nos finais da Idade do Bronze*, Trabalhos de Arqueologia 9, IPPAR, Lisboa.

Vilaça, R. 1997. Metalurgia do Bronze Final da Beira Interior: revisão dos dados à luz de novos resultados. *Estudos Pré-Históricos* V, 123-154.

Vilaça, R. 2003. Acerca da existência de ponderais em contextos do Bronze Final/Ferro Inicial no território português. *O Arqueólogo Português* 21, 245-88.

Vilaça, R., 2004. Metalurgia no Bronze Final no entre Douro e Tejo português: contextos de produção, uso e deposição. In: Perea, A. (Ed.), Actas del congresso: Âmbitos tecnológicos, Âmbitos de poder. La transición Bronze Final-Hierro en la Península Ibérica, Madrid, 1-12.

Vilaça, R. 2006a. Iron artefacts in contexts of the Late Bronze age in the Portuguese territory. *Complutum* 17, 81-101.

Vilaça, R., 2006b. Depósitos de Bronze do Território Português – Um debate em aberto. *O Arqueólogo Português* 24, 9-150.

Vilaça, R. 2008. Reflexões em torno da "Presença Mediterrânea" no centro do território Português, na charneira do Bronze Pleno para o Ferro. In: Celestino, C., Rafael, N., Armada X.-L. (Eds.) *Contacto cultural entre el Mediterráneo y el Atlántico (siglos XII-VIII ane): La precolonización a debate*, CSIC, Madrid, 371-400.

Walker, P.L., Miller, K.W.P., Richmann, R. 2008. Time, temperature, and oxygen availability: an experimental study of the effects of environmental conditions on the color and organic content of cremated bone. In: Schmidt, C.W., Symes S.A. (Ed.) *The analysis of burned human remains*, Academic Press, London, 129-135.

Wang, Q., Merkel, J.F. 2001. Studies on the redeposition of copper in Jin Bronzes from Tianma-Qucun, Shanxi, China. *Studies in Conservation* 46, 242-250.

Wang, Q., Ottaway, B.S. 2004. *Casting experiments and microstrucutre of archaeologically relevant bronzes*, BAR IS 1331, Archaeopress, Oxford.

Williamson, R.A., Nickens, P.R. (Eds.) 2000. *Science and technology in historic preservation*. Advances in Archaeological and Museum Science, Klumer Academic/Plenum Publishers, New York, Vol. 4.

Zhou, G., Yang, J.C. 2003. Temperature effect on the Cu_2O oxide morphology created by oxidation of Cu(001) as investigated by in situ UHV TEM. *Applied Surface Science* 210, 165-170.

Postscript – Promoting Science&Heritage

The OM images obtained in this work were since a very early stage valued by their artistic character, besides their scientific value.

In 2006, in the context of the Scientific Photography competition *Laboratório de Imagens – A Ciência em Fotografia* (Image Lab - Science in Photography), one image evidencing the internal corrosion of the SL-58 bar fragment reached a finalist position and made part of an exposition in *Centro Cultural de Belém* (CCB, Lisbon). The image was also printed as a postcard in a collection edited and sold during the event (**Fig. i**). Additionally, the reproduction exposed in the CCB was purchased in an auction by a private collector.

Fig. i Picture of the OM image in the collection of postcards edited for the CCB exhibition.

More recently, some OM images were selected to be the basis of the creation of a fashion collection by the designer Alexandra Moura[16] (**Fig. ii**). Images enhancing corrosion patterns were printed in different fabrics, which in turn were worked creating different textures and colours, resulting in the Spring/Summer 2011 collection "MICRObservation", to be presented in the 35º Lisbon Fashion Week event (Oct. 2010). The fashion show is divulgated by diverse means reaching different audiences, as world wide thought the Fashion TV channel and nationally through public television channels in varied programs. Also, focused editorials on the designer and the creation of the collection can be published in more general Art magazines and particular items can be selected for fashion editorials published in renowned fashion magazines as Vogue, Elle, among others. Presently, the fashion collection is in permanent exhibition at the Alexandra Moura atelier/show room in Principe Real (Lisbon) for press and buyers, and will be available for private purchase in the next 2011 summer season at the Alexandra Moura store in Principe Real.

[16] A. Moura is the only Portuguese designer selected to be part of the international edition of *Atlas of Fashion Designers* (2008) by Laura Eceiza, Rockport Publishers, EUA, where the main fashion centres and the most promising and influent fashion designers of the world are presented.

Fig. ii Pictures of the creation process concerning the production of the Spring/Summer 2011 collection "MICRObservation" by Alexandra Moura, involving the fabrics produced with printed OM images.

As an additional wide-range conclusion, with this work it is shown the potential of interactions among *a priori* independent and unrelated spheres of knowledge and creation. This gives the general sense that more and more multi and interdisciplinary works can emerge as an essential and profitable global trend, anticipating exciting and fascinating new associations.

Finally, for the present work, the products of these interactions are a viable way of divulgating the variety of scientific studies involving cultural heritage, targeting publics that would in other ways never know about this particular working field. It is also a way of sensitizing a broad community to conservation and archaeometric studies, contributing to the enhancement of the value of cultural heritage, and by this, also promoting new scientific studies.

Appendix I Glossary

Due to the interdisciplinary character of the present work a glossary has been included. Adaptations have been made after: Goffer, Z. (1980) *Archaeological Chemistry*, John Wiley & Son, New York; Scott, D.A. (1991) *Metallography and microstructure of ancient and historic metals*, The Getty Conservation Institute, The J. Paul Getty Museum in association with Archetype Books, Los Angeles; and Tylecote, R.F. (1992) *A History of Metallurgy*, Institute of Materials, Minerals and Mining, London.

1st Bronze Age – the chronological period that embraces Early Bronze Age (q.v.) and Middle Bronze Age. Applied to regions where there is an absence of a clear archaeographic distinction between the two different moments (cultural continuity).

Accuracy – agreement between the measured concentration and the "true value". Calculated as ((certificated content-obtained content)/certificated content) × 100.

Alloy – mixture of two or more elements in solid solution in which the major component is a metal. Combining different ratios modifies the properties of pure metals to produce desirable characteristics.

Annealing – heating a metal, keeping it at a given temperature, and then cooling at a suitable rate. Annealing results in more stable structures. Thus, frequently the aim of annealing is to reduce hardness, facilitate cold work, and obtain desirable mechanical and physical properties.

Annealing twins – crystallographic defect formed as a consequence of grow accidents during the recrystallization of the formed face centred cubic metals such as α-copper. Faults in crystals wich show that the structure has once been strained, mostly by hammering of bending.

As-cast – an artefact that has been shaped by mould; normally used in relation to microstructure observations; opposite to wrought (q.v.).

Bell Beaker period – generally known as the last phase of the Chalcolithic period, which marks the transition to the Early Bronze Age; name given due to the use of a type of flat-bottomed clay vessel with a wide distribution; chronologically it can regard to the last half of the 3rd millennium BC, and in some regions (e.g. N Portugal) it can extend until the first half of the 2nd millennium BC, already during the Early Bronze Age. The work of Cardoso and Monge Soares (1990-1992)[17] suggests that at least for the Estremadura region, Bell Beaker goes back to the first quarter of the 2nd millennium BC.

Beneficiation – crushing and separating ore into valuable substances or waste; ore processing; enrichment of a metal ore by separation and removal of gangue (q.v.).

[17] Cardoso, J.L., Monge Soares, A.M. 1990-1992. Cronologia absoluta para o Campaniforme da Estremadura e do Sudoeste de Portugal. *O Arqueólogo Português* IV 8/10, 203-228.

Bronze Age –chronological period that goes from the beginning of the 2nd millennium BC until the middle of the 1st millennium BC in most parts of the Portuguese territory (mainly centre and north); it can go until VIII century BC in the south and V century BC in centre and north of Western Iberian Peninsula. It can be divided into 1st Bronze Age (q.v.) (~2000-1200 BC) and Late Bronze Age (q.v.). The Late Bronze Age begins by the last quarter of the 2nd millennium BC.

Bronze disease – corrosion phenomena related to the contamination with chlorides, that in humid weather leads to the oxidation and hydrolysis of cuprous chloride to basic cupric chloride.

Casting – process of pouring molten metal into a prepared mould, where it is allowed to solidify and form an object of desired shape. In the present work three techniques have been mentioned: (1) open mould casting; (2) two-piece mould casting; and (3) lost wax casting.

Cold working – the plastic deformation of a metal, as bending, piercing, and forging, carried out below its temperature of recrystallization. Cold working brings about the hardening and strengthening of copper based metals, which can be eliminated by subsequent annealing (q.v.).

Copper Age – chronological period that begins at the end of the 4th millennium BC and extents during most of the 3rd millennium BC.

Core – piece of a mould inserted in such a way as to give a hollow in the final casting.

Coring/Cored – term used to describe the segregation which accurs during solidification of metallic crystals in an alloy melt. The melt has a uniform composition in the liquid state but segregation (q.v.) often occurs during cooling, resulting in a clearly visible structure under the microscope.

Chalcolithic – same as Copper Age (q.v.)

Decuprification – the corrosion of copper-tin alloys resulting in the preferential loss of copper.

Dendrites – a fern- or leaf-like growth formed by a solid metal or constituent growing from the liquid. Many pure metals and alloys solidify in this way, as do some constituints of slag.

Destannification – the corrosion of copper-tin alloys resulting in the preferential loss of tin.

Ductility – the degree to which a metal is able to undergo plastic deformation without fracturing.

Early Bronze Age – the first of three moments in which Bronze Age can be divided to: Early Bronze Age; Middle Bronze Age and Late Bronze Age. Due to the continuity of Early and Middle Bronze Age in many regions of the Portuguese territory, 1st Bronze Age (q.v.), relating to the first two periods, is normally employed.

Electrum – a natural alloy of gold containing a moderate proportion of silver (circa 20 wt.%).

Equiaxed – term applied to crystals which are rougly as broad as they are long.

Etching – developing the structure of a metal by attacking it with acid or other solutions.

Eutectic – triphasic equilibrium that during cooling result in $A(l) \leftrightarrow B(s)+C(s)$.

Eutectoid – same as for eutectic (q.v.) but involve only solid phases, $A(s) \leftrightarrow B(s)+C(s)$.

Extraction process – the process of obtaining something from a mixture or compound by chemical, physical or mechanical means; smelting (q.v.).

Flux – a material added to metallurgical furnace charges to react with the non-metallic components of ores to form slags; lime or other material added to the smelting charge to render a slag easy-flowing.

Forging – the working of metal by hammering.

Gangue – the valueless minerals found in ores; unwanted mineral.

Gilding – the forming of an adherent layer of metal on the surface of an object made from another metal.

Hammering – beating a metal sheet into a desired shape.

Hardening – increasing the hardness of metals by suitable treatment. In copper-based alloys by forging or hammering.

Heat treatment – the controlled heating and cooling of metals to alter their structure and thus their mechanical properties. Basic heat treatment consists of three main steps (1) heating the object to a predetermined temperature, (2) maintaining the object at the given temperature until the metal structure becomes uniform throughout, and (3) cooling at a predetermined rate to cause the formation or retention of desirable structural properties within the metal.

Iron Age – chronological period that can be divided into the 1st Iron Age (or Early Iron Age) and 2nd Iron Age. The 1st Iron Age begins by the VIII century BC in Southern parts of the Portuguese territory. The 2nd Iron Age begins by the V century BC, and affects all the Portuguese territory.

Late Bronze Age – the third of three moments in which Bronze Age can be divided. For most regions this period embraces the last quarter of the 2nd millennium BC and the first centuries of 1st millennium BC.

Lost-wax casting – casting from a wax model. The object to be made is shaped in wax and is covered in a clay mould. When the wax is molten out, the space can be filled with molten metal.

Malleability – the capacity of metals and alloys to undergo plastic deformation under compression (e.g. by hammering) without rupture.

Metal – an element, compound, or alloy characterized by high electrical conductivity. In a metal, atoms readily lose electrons to form positive ions (cations). Those ions are surrounded by delocalized electrons which are responsible for the conductivity.

Metallography – the study of constitution and microstructure of metals and alloys by optical means (unaided eye, magnifying glass, microscope, electron microscope).

Oxidation – a chemical reaction in which there is positive increase in valence; the loss of electrons. Metals are oxidized, e.g. Cu loses two electrons, and its charge goes from 0 to +2.

Phase – a homogeneous chemical composition and structurally uniform material, describing one constituent in a thermodynamic system.

Positive structures – in archaeological records it can be walls, or other structures; opposed to negative structures, as those carved in the rock or soil.

Prills – in the extraction (q.v.) of copper from primitive smelts, the metal is produced as small droplets or particles in a slaggy matrix. These small metallic particles are called prills and were often extracted by breaking up the smelted product and sorting the metal.

Pseudomorphic corrosion – the replacement during corrosion process of a material with another that mimics the shape of the former one.

Reduction – a chemical reaction in which there is an increase in negative valence; gain of electrons. Non metals are reduced, e.g. Cl gains one electron and goes from oxidation number 0 to -1.

Seam – casting seam; is a thin irregular ridge of metal on the outer faces of casting, resulting from the seepage of the molten metal into the joint between the separate components of the mould used in its manufacture.

Segregation – compositional/constitutional gradient that occurs in various forms in alloys: *micro-segregation* (nonuniform distribution of the alloying elements within a volume characteristic of the solidification microstrucutre); *normal segregation* (the alloy elements and impurities are concentrated towards the inner region of the cast); *inverse segregation* (the alloy elements and impurities are concentrated towards the outer cast surfaces); and gravitic segregation (higher density phases are concentrated towards the bottom of the cast).

Slag – waste product of smelting resulting from the combination of non-metallic components. In primitive smelting operations there isn't a proper separation of metal and slag.

Slip bands – face centred cubic metals can show a series of lines in two intersecting directions upon deformation of the metal.

Smelting – the reduction of ores to crude metals at high temperatures; extraction process (q.v.).

Solder – an alloy used for joining metals (e.g. 50/70Pb-30/50Sn alloy) usually with a lower liquidus temperature than the metals to be joined.

Sprue – is the passage through which molten metal is introduced into a mould; also refers to the excess material which solidifies in the sprue passage. Bronze in particular has a high shrinkage rate during cooling; a sprue can continue to provide molten metal to the casting (provided it is large enough to retain its heat and stay liquid).

Tinning – coating metal with a very thin layer of molten tin-rich metal.

Tin pest – a change occurring in tin at very low ambient temperatures, whereby the metal changes its crystalline state and falls into a coarse grey powder. Tin pest is often confused with tin corrosion.

Wrought – an artefact shaped by thermo-mechanical processes.

Appendix II Phase diagrams

Next, some binary phase diagrams relevant to the present study are presented. The phase diagrams are adaptations from: AMS (1972) *Metals Handbook 7: Atlas of Microstructures of Industrial Alloys*, Metals Park, OH, American Society for Metals International; and AMS (1973) *Metals Handbook 8: Metallography, Structures and Phase Diagrams*, Metals Park, OH, American Society for Metals International, except when indicated.

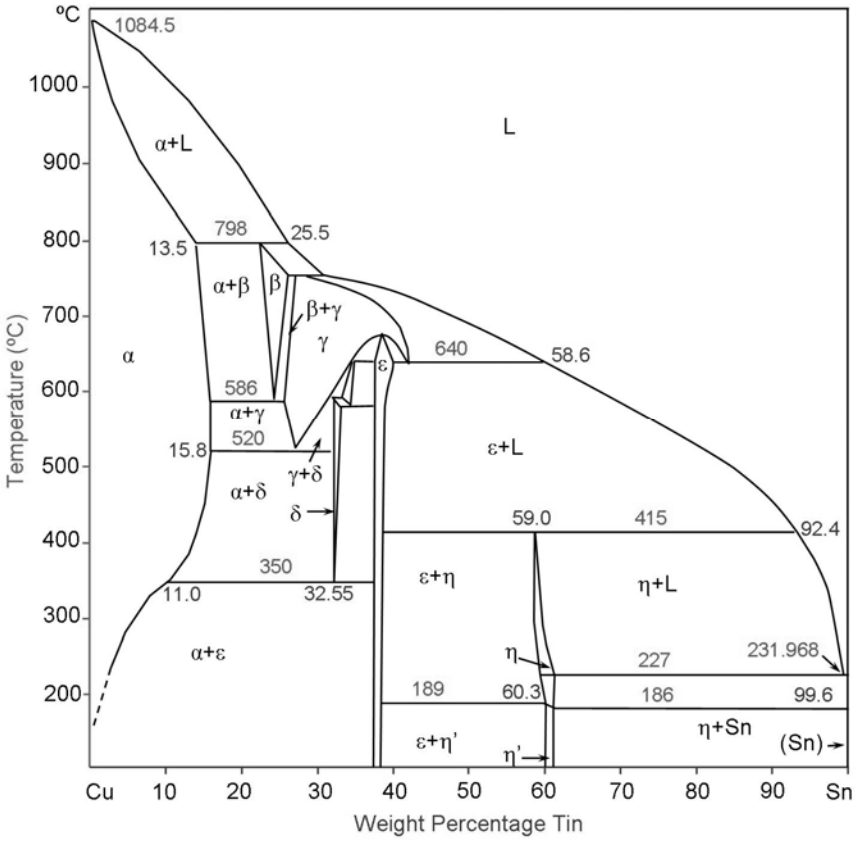

Fig. II.1 Equilibrium phase diagram for Cu-Sn system.

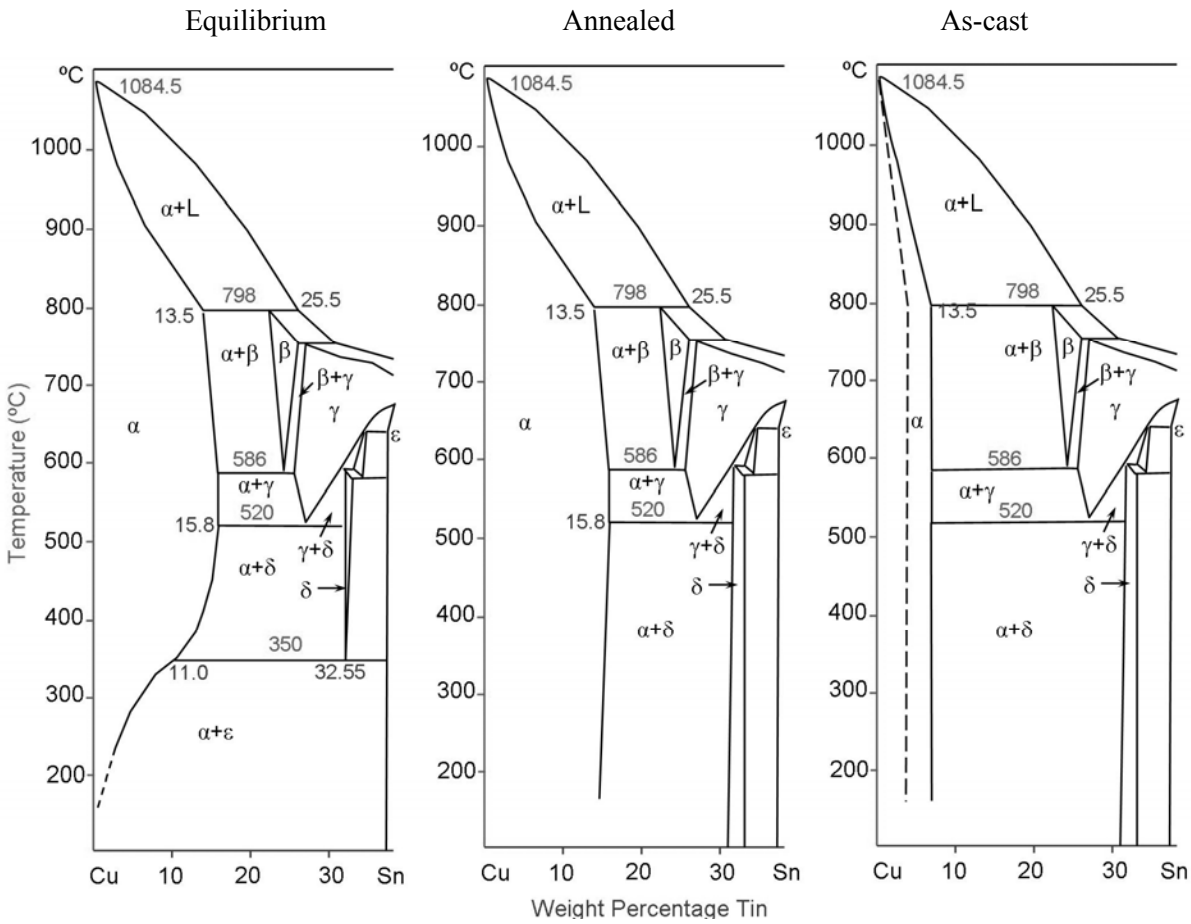

Fig. II.2 Equilibrium and metastable phase diagrams for Cu-Sn system after Centre Technique des Industries de la Fonderie (1967) *Atlas Métallographique des Alliages Cuivreux*, Éditions des Industries de la Fonderie, Paris.

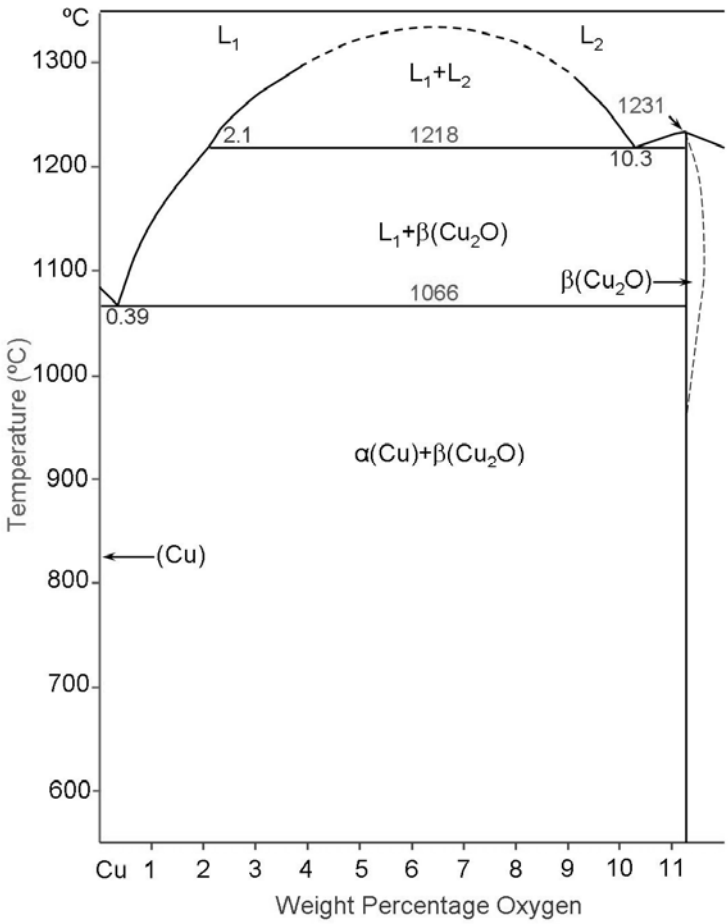

Fig. II.3 Equilibrium phase diagram for Cu-O system.

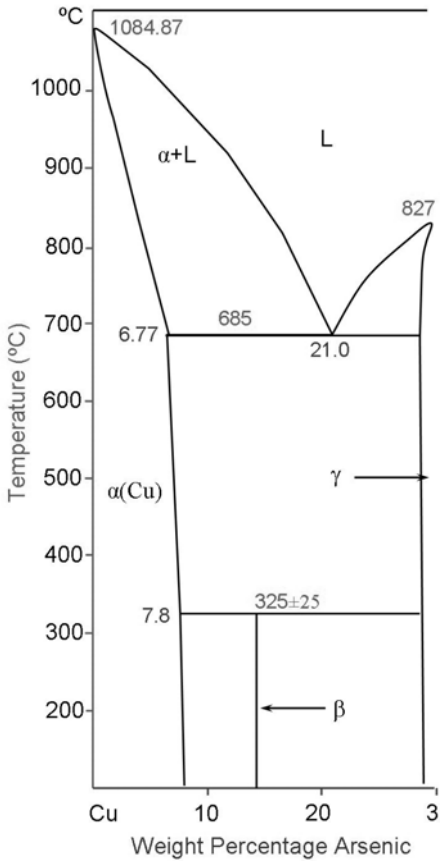

Fig. II.4 Equilibrium phase diagram for Cu-As system.

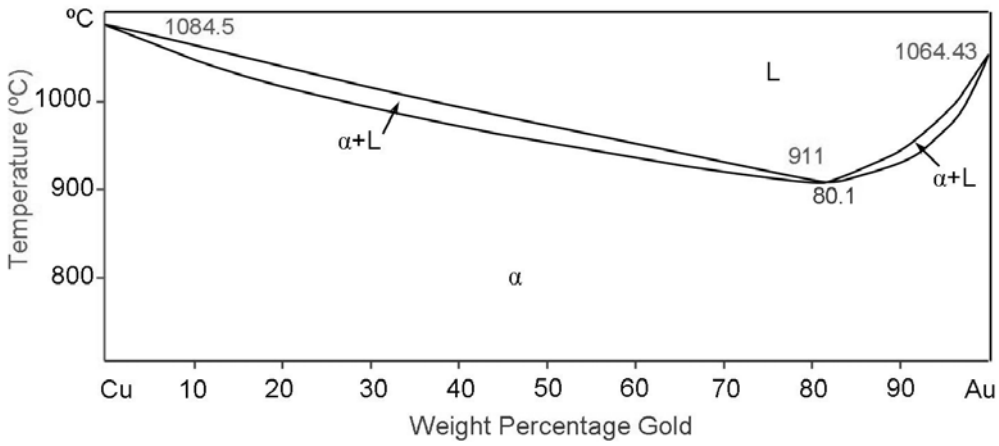

Fig. II.5 Equilibrium phase diagram for Cu-Au system.

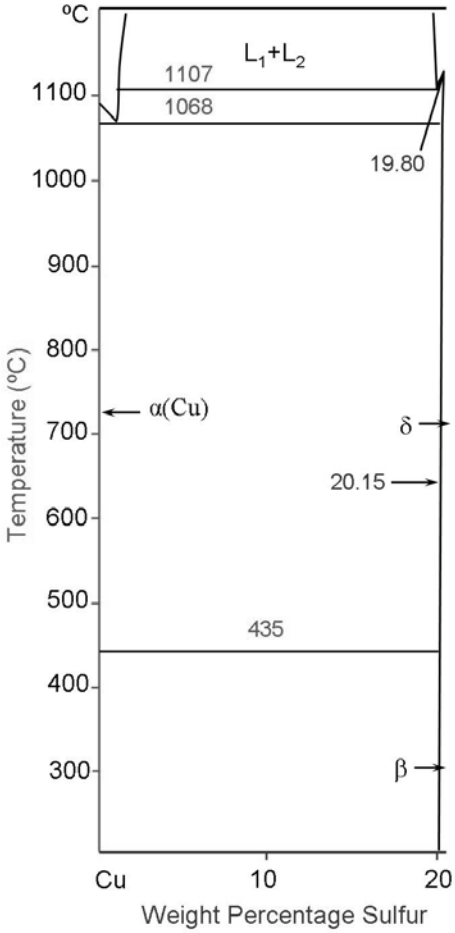

Fig. II.6 Equilibrium phase diagram for Cu-S system.

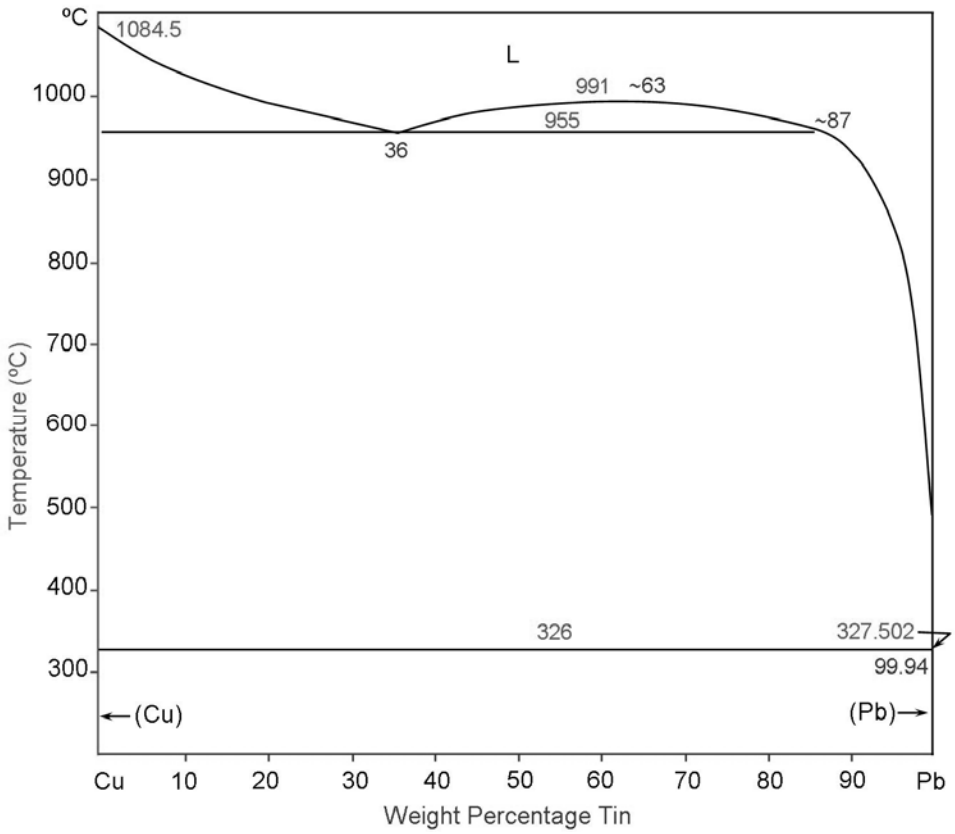

Fig. II.7 Equilibrium phase diagram for Cu-Pb system.

Appendix III Standard reduction potentials

Next, some standard reduction potentials in aqueous solution at 25ºC are presented based on Lide, D.R. (Ed.) (1991-1992) *Handbook of Chemistry and Physics*, Chemical Rubber Company, USA, 72nd Edition.

Table III.1 Some standard reduction potentials

Half-reaction			Eº(V)
$F_2(g) + 2e^-$	→	$2F^-$	2.87
$O_3(g) + 2H^+ + 2e^-$	→	$O_2(g) + H_2O(l)$	2.07
$Co^{3+} + e^-$	→	Co^{2+}	1.82
$H_2O_2 + 2H^+ + 2e^-$	→	$2H_2O$	1.77
$Au^{3+} + 3e^-$	→	$Au(s)$	1.50
$Cl_2\ (g) + 2e^-$	→	$2Cl^-$	1.36
$O_2(g) + 4H^+ + 4e^-$	→	$2H_2O(l)$	1.23
$Br_2(l) + 2e^-$	→	$2Br^-$	1.07
$2Hg^{2+} + 2e^-$	→	Hg_2^{2+}	0.92
$Hg^{2+} + 2e^-$	→	$Hg(l)$	0.85
$Ag^+ + e^-$	→	$Ag(s)$	0.80
$Hg_2^{2+} + 2e^-$	→	$2Hg(l)$	0.79
$Fe^{3+} + e^-$	→	Fe^{2+}	0.77
$O_2(g) + 2H^+ + 2e^-$	→	H_2O_2	0.68
$I_2\ (s) + 2e^-$	→	$2I^-$	0.53
$Cu^+ + e^-$	→	$Cu(s)$	0.52
$O_2(g) + 2H_2O + 4e^-$	→	$4OH^-$	0.40
$Cu^{2+} + 2e^-$	→	$Cu(s)$	0.34
$Cu^{2+} + e^-$	→	Cu^+	0.15
$Sn^{4+} + 2e^-$	→	Sn^{2+}	0.15
$S\ (s) + 2H^+ + 2e^-$	→	$H_2S(g)$	0.14
$2H^+ + 2e^-$	→	**$H_2(g)$**	**0.00**
$Pb^{2+} + 2e^-$	→	$Pb(s)$	-0.13
$Sn^{2+} + 2e^-$	→	$Sn(s)$	-0.14
$Ni^{2+} + 2e^-$	→	$Ni(s)$	-0.25
$Co^{2+} + 2e^-$	→	$Co(s)$	-0.28
$Tl^+ + e^-$	→	$Tl(s)$	-0.34
$Cd^{2+} + 2e^-$	→	$Cd(s)$	-0.40
$Cr^{3+} + e^-$	→	Cr^{2+}	-0.41
$Fe^{2+} + 2e^-$	→	$Fe(s)$	-0.44
$Cr^{3+} + 3e^-$	→	$Cr(s)$	-0.74
$Zn^{2+} + 2e^-$	→	$Zn(s)$	-0.76
$2H_2O + 2e^-$	→	$H_2(g) + 2OH^-$	-0.83
$Mn^{2+} + 2e^-$	→	$Mn(s)$	-1.18
$Al^{3+} + 3e^-$	→	$Al(s)$	-1.66
$Be^{2+} + 2e^-$	→	$Be(s)$	-1.70
$Mg^{2+} + 2e^-$	→	$Mg(s)$	-2.37
$Na^+ + e^-$	→	$Na(s)$	-2.71
$Ca^{2+} + 2e^-$	→	$Ca(s)$	-2.87
$Sr^{2+} + 2e^-$	→	$Sr(s)$	-2.89
$Ba^{2+} + 2e^-$	→	$Ba(s)$	-2.90
$Rb^+ + e^-$	→	$Rb(s)$	-2.92
$K^+ + e^-$	→	$K(s)$	-2.92
$Cs^+ + e^-$	→	$Cs(s)$	-2.92
$Li^+ + e^-$	→	$Li(s)$	-3.05

Appendix IV Potential-pH (Pourbaix) diagrams

The Pourbaix diagrams indicate stable forms of ions and compounds in a solution (aqueous or other more complex media with anions others than OH^- considered) as a function of pH and electrode potential. Natural environments have generally a pH value between 4.5 and 9 and an oxidation-reduction potential Eh between -0.3 and 0.5 V (NHE). This pH-Eh domain corresponds to the stability domains of copper- and tin-containing protective compounds such as cuprous oxide, cupric hydroxycompounds or tin oxide in the absence of complexing agents (Robbiola, L., Blengino, J.-M., Fiaud, C. (1998) Morphology and mechanisms of formation of natural patinas on archaeological Cu-Sn alloys. *Corrosion Science* 40, 2083-2111).

Next, some Pourbaix diagrams are going to be presented based on Pourbaix, M. (1966) *Atlas of Electrochemical Equilibria in Aqueous Solutions*, Pergamon, New York.

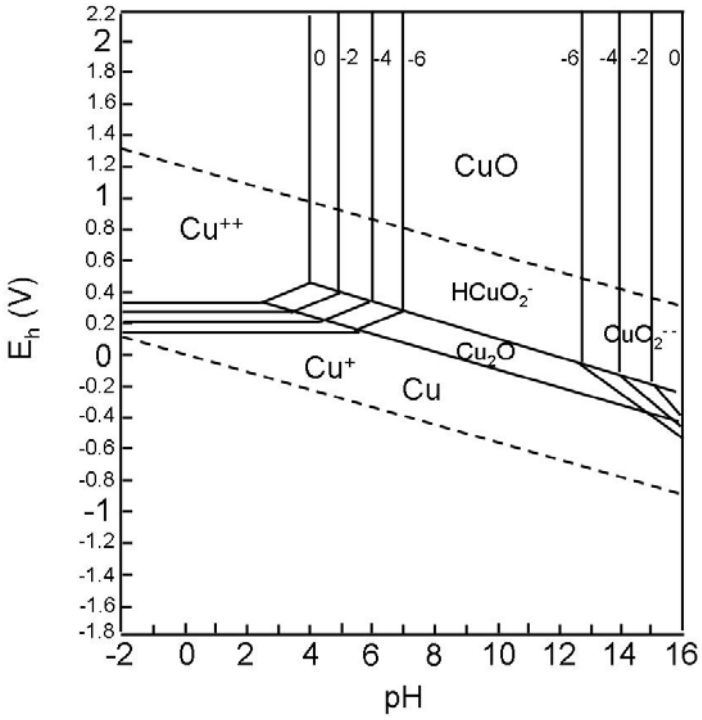

Fig. IV.1 Pourbaix diagram for Cu-H_2O system at 25ºC.

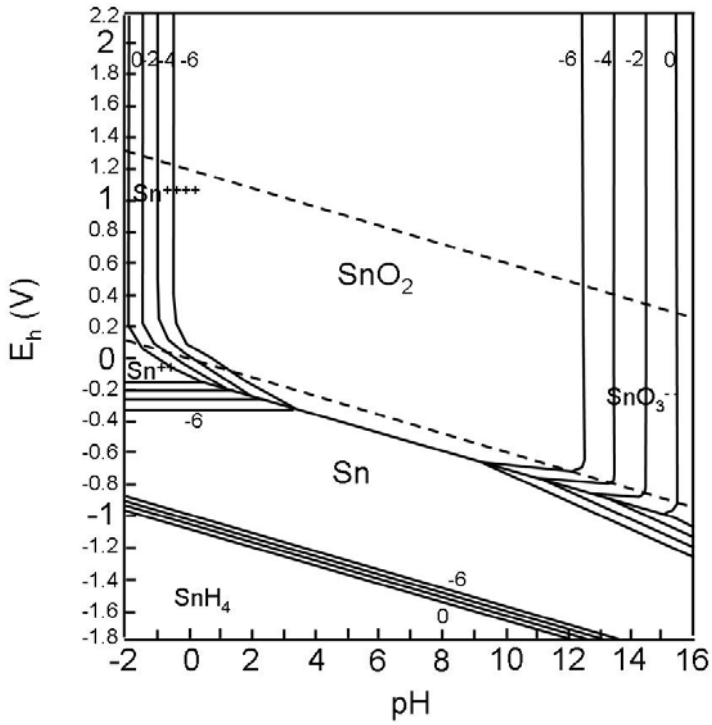

Fig. IV.2 Pourbaix diagram for Sn-H_2O system at 25ºC.

Appendix V Some reactions and mechanisms of corrosion formation

Since the XIX century that various chemical reactions have been suggested to explain the formation of the several mineral products contained in the layered structures of ancient corroded bronzes. Next, some of the most relevant are shown, based on Robbiola L., Blengino, J.-M., Fiaud, C. (1998) Morphology and mechanisms of formation of natural patinas on archaeological Cu-Sn alloys. *Corrosion Science* 40, 2083-2111.

General oxidation of bronze metal (for the sake of simplicity, tin and copper primary oxidation compounds are assumed to be only SnO_2 and Cu_2O)

$$Sn + 2H_2O \rightarrow \mathbf{SnO_2} + 4H^+ + 4e^- \quad (1)$$

$$Cu + \frac{\alpha}{2} H_2O \rightarrow \frac{\alpha}{2} \mathbf{Cu_2O} + (1-\alpha)Cu^+ + H^+ + e^- \quad (2)$$

$$\mathbf{Cu_2O} + \frac{1}{2} O_2 = 2CuO \quad (3)$$

$$Cu^+ \rightarrow Cu^{2+} + e^- \quad (4)$$

In these equations, α is identical to $1\text{-}f_{Cu}$ (with f_{Cu} copper dissolution factor introduced in eq. (8)). Equations (1)+(2) give the global oxidation reaction of the alloy:

$$Sn + \chi Cu + (2+\frac{\chi\alpha}{2}) H_2O \rightarrow \mathbf{SnO_2} + \frac{\chi\alpha}{2} \mathbf{Cu_2O} + \chi(1-\alpha)Cu^+ + (4+\alpha\chi)H^+ + (4+\chi)\, e^- \quad (5)$$

with χ the atomic ratio $(Cu/Sn)_a$ in the alloy.

A part of the oxidised copper (α in reaction eq. (2)) remains under the original limit of the surface, as cuprous species such as Cu_2O, which can be later oxidized to cupric compounds (in eq. (3) CuO is the result of the presence of just oxygen, if CO_2 was also present, basic copper compounds would also be formed). The other part $(1-\alpha)$ is dissolved into the environment (eq. (4)) and can precipitate to the surface as cupric compounds (e.g. hydroxycarbonates).

Involving the presence of Cl species - in Type II corrosion or the so-called *bronze disease*

$$Cu^o + Cl^- \rightarrow \mathbf{CuCl} + e^- \quad (6)$$

$$\mathbf{CuCl} + \chi O^{2-} \rightarrow \chi \mathbf{Cu_2O} + Cl^- + (1-2\chi)Cu^+ \quad (7)$$

The accumulation of chloride ions can be interpreted as an autocatalytic process. The formation of chloride-containing compounds, less stable than oxygen-containing ones, facilitates the extraction of copper cations.

Copper selective dissolution from the alloy, i.e. decuprification

Decuprification has been proposed as the general corrosion behaviour for ancient bronzes from several historical periods and exposed to different water-containing environments, in poorly to moderately aggressive conditions – in respect to outer passive layers of Type I corrosion. Soil and minor alloying elements do not play a major role in the selective dissolution of copper.

$$f_{Cu} = 1 - \frac{\left(\frac{X_{Cu,p}}{X_{Sn,p}}\right)}{\left(\frac{X_{Cu,a}}{X_{Sn,a}}\right)} \tag{8}$$

f_{Cu} – dissolution factor of copper

p – outer passive layer

a – alloy

X – atomic content

(assuming that $X_{Sn,a} + X_{Cu,a} = X_{Sn,p} + X_{Cu,p} + X_{Sn,l} + X_{Cu,l} = 1$, where l is the leaching fractions)

From eq. (8) it shows that when Cu/Sn ratio of the alloy is conserved within the patina $f_{Cu} = 0$; on the contrary, when copper has totally vanished from the corrosion layers $f_{Cu} = 1$. For single α-phase bronzes a typical value is $f_{Cu} = 0.94 \pm 0.04$.

Appendix VI Some properties of elements and compounds

Next, some tables with selected properties of elements and compounds relevant to the present study are presented based on: Lide, D.R. (Ed.) (1991-1992) *Handbook of Chemistry and Physics*, Chemical Rubber Company, USA, 72nd Edition; and Scott, D.A. (1991) *Metallography and microstructure of ancient and historic metals*, The Getty Conservation Institute, The J. Paul Getty Museum in association with Archetype Books, Los Angeles.

Table VI.1 Some properties of relevant elements to the study

		Cu (metallic)	Sn (metallic)	Pb (metallic)	As (metalloid)	Au (metallic)
Atomic number		29	50	82	33	79
Atomic weight		63.546	118.69	207.2	74.922	197.967
Valence		1, 2	2, 4	2, 4	-3, 0, 3, 5	1, 3
Melting point (ºC)		1084.5	231.9	327.5	817	1064.4
Density (g/cm^3)		8.96	7.28	11.34	5.73	19.3
Colour		Copper, reddish metallic	Silvery lustrous grey	Bluish white	Metallic grey	Gold yellow
Colour in Optical Microscope examinations	BF	Pink		Very dark		
	DF	Black		Black		
	Pol	Black		Black		

Table VI.2 Some properties of phases and inclusions in bronze alloys

		Cu-Sn alloy α phase	δ phase (intermetallic $Cu_{31}Sn_8$)	Inclusions Cu-S (Cu_2S)	Cu-O (Cu_2O)
Colour in Optical Microscope examinations	BF	Pink to pale yellow	Blue grey	Grey	Grey
	DF	Black	Black	Dark grey	Reddish
	Pol	Dark grey	Dark grey	Dark grey	Reddish

Table VI.3 Some properties of corrosion products relevant to the study

		Cu_2O (cuprite)	$Cu_2(CO_3)(OH)_2$ (malaquite)	SnO_2 (cassiterite)	SnO (romarchite)
Oxidation state		Cu [I]	Cu[II]	Sn[IV]	Sn[II]
Melting point (ºC)		1244	164	1630	1080
Density (g/cm^3)		6.14	4	6.9	6.5
Colour		Red, dark red	Bright green, dark green	Black, brownish black; white (powder)	Black
Colour in Optical Microscope examinations	BF	Grey	Dark grey		Black(?)
	DF	Reddish	Green		Black(?)
	Pol	Reddish	Green		Black(?)

Appendix VII Some common corrosion products

Depending on the burial environment, the copper (II) salts are frequently malachite ($Cu_2(CO_3)(OH)_2$) in soil corrosion, brochantite ($CuSO_4.3Cu(OH)_3$) in atmosphere corrosion and atacamite ($CuCl_2.3Cu(OH)_2$) in seawater corrosion (Hassairi, H., Bousselmi, L., Khosrof, S., Triki, E. (2008) Characterization of archaeological bronze and evaluation of the benzotriazole efficiency in alkali medium. *Materials and Corrosion* 59, 32-40). A list of the most common corrosion products found in bronze artefacts is listed below, based on Scott D.A. (2002) *Copper and Bronze in Art, Corrosion, Colorants, Conservation*, Getty Publications, Los Angeles.

Table VII.1 Some common bronze corrosion products

Oxides	Cuprite	Cu_2O	Red-brown
	Tenorite	CuO	Dark-black
	Cassiterite	SnO_2	Dark-black-brown-grey
Sulphides	Calcocite	Cu_2S	Dark-black-blue
	Covelite	CuS	Dark brown to black
	Calcopirite	$(CuFe)S_2$	Brown to yellow
Chlorides	Atacamite	$Cu_2Cl(OH)_3$	Green-yellowinsh
	Paratacamite	$Cu_2Cl(OH)_3$	Pale green
	Nantoquite	$CuCl$	Pale white
Sulphates	Antlerite	$Cu_3(SO_4)(OH)_4$	Emerald green-dark green
	Brochantite	$Cu_4(SO_4)(OH)_6$	Green-yellowish
Carbonates	Malaquite	$Cu_2(CO_3)(OH)_2$	Dark green
	Azurite	$Cu_3(CO_3)_2(OH)_2$	Blue
Nitrates	Gerhardtite	$Cu_2(NO3)(OH)_3$	Green

Appendix VIII Absorption of X-ray in matter: attenuation of X-rays

When a radiation penetrates the matter, it is absorbed along its path. Next, an approach on the attenuation of X-rays in matter is exposed based on Jenkins, R., Gould, R.W., Gedcke, D. (1981) *Quantitative X-ray Spectrometry*, Marcel Dekker, New York.

If a mono-energetic X-ray beam, of intensity I_0 (in photons per unit time) passes through a given homogeneous material of thickness ×, its intensity is reduced to I due to absorption and scattering phenomena. This attenuation process obeys the Lambert-Beer law:

$$I = I_0 e^{-\mu m \rho \times}$$

where **e** is the base of a napierian logarithm; $\boldsymbol{\mu_m}$ is the mass attenuation coefficient (cm^2g^{-1}) and **ρ** the material density (g/cm^3).

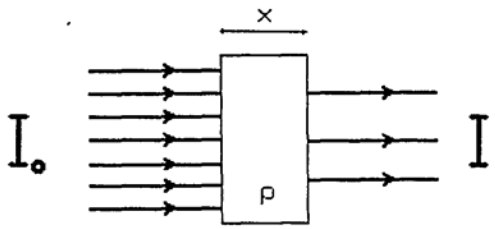

Fig. VIII.1 Absorption of a radiation of intensity I_0 when passing through matter of ρ density and × thickness.

The mass attenuation coefficient represents the reduction on the x-ray intensity, and varies with the chemical composition of the matter, and for the same matter it varies also with the energy of the radiation, E, and the physical state of the matter.

The μ_m of a chemical compound, as an alloy, can be calculated adding the mass attenuation coefficient of each element (μ_{mi}) times their fractions in weight (W_i):

$$\mu_m(\text{compound}) = \Sigma (\mu_{mi} W_i)$$

In a sample of infinite thickness the travel distance of an x-ray radiation depends on the energy of the radiation and on the composition of the sample.

The penetration (×) of a monochromatic x-ray beam in a matter of infinite thickness can be estimated in a simple way, through the Lambert-Beer law, if considered that $I/I_0 = 0.01$ (corresponding to the thickness the beam has travelled until 99% of attenuation):

$$\ln (0.01) = \ln (-\mu_m \rho \times)$$